THE UNIVERSITY *of* EDINBURGH

Targeting a custom-engineered flavonoid to the mitochondria protects against acute oxidative stress

Nicola J. Drummond

Thesis submitted for the degree of Doctor of Philosophy
The University of Edinburgh
2014

Declaration

I declare that the work in this thesis is my own, unless otherwise stated. This thesis has been composed by myself and has not been previously submitted for any other degree or professional qualification, except where stated.

Nicola J. Drummond
December 2014

Acknowledgements

Here I would like to thank those people who without which this thesis would not have been written. Firstly, I would like to thank my supervisor Dr. Tilo Kunath for giving me the opportunity to do a PhD in his lab, for his support, enthusiasm and motivation throughout my PhD and especially in the last few months. Additionally, Dr. Donald McPhail and Graeme Cook from Antoxis Limited who provided me with AO-1-530 and helped me especially in the early stages. I am grateful to Dr. Keisuke Kaji for providing me with the cloning plasmids. In addition, I thank my committee members, Dr. Sally Lowell and Dr. Anna Williams for their guidance during the project. This studentship was funded by BBSRC and SULSA with financial contribution from Antoxis Limited.

I am also grateful to Kunath lab members and other members of the ISCR/SCRM past and present for their scientific discussions, help with lab work, friendship and support with writing up. A special thanks to, Ratsuda for getting me through some of the toughest times; Fatima for her help with cloning and her continued support; Maurice and Amy for their advice and motivation with thesis writing; Karamjit for scientific discussions and Fella for allowing me to use some of her and Xing's results in this thesis and for her guidance through thesis writing. I also want to thank Rachel for training me in slice cultures and Amy Pegg for her help and motivation throughout writing this thesis. Hopefully I can do the same for you!

The core facility staff at the ISCR/SCRM have been fundamental for this work. Thank you to Helen and Marilyn for keeping the cell culture facility running smoothly. In addition, I would like to thank Dr. Valeria Berno for her microscopy training and patience.

The EPR experiments, most of which do not feature in this thesis, would not have been possible without the help and patience of Dr. Janet Lovett and Dr. Mark Miller.

Finally, my deepest appreciation goes to my parents, family, friends and Paco. Thank you to my parents, my brother and sister for their love, support and encouragement throughout. Thank you to my friends who have motivated me to complete my PhD. Lastly, thank you to Paco for putting up with me, for letting me use his computer and for being there when I needed him. I promise Spanish next!

Thank You.

Lay Summary

The main symptoms experienced by Parkinson's disease patients are motor symptoms, which are caused by the loss of nerve cells in the brain. A possible cause of this nerve cell death is oxidative stress. Oxidative stress is an imbalance between reactive molecules containing oxygen, which cause damage to components of the cell, and antioxidants, which prevent this damage. This damage can build up over time eventually resulting in cell death. Post-mortem analysis of Parkinson's disease patients' brains show evidence of damage caused by oxidative stress. In addition, these brains have clumps of the protein α-synuclein, which have also been implicated in nerve cell death. It is possible that reactive molecules containing oxygen may damage the α-synuclein protein enhancing it's clumping, however, this has not been proven. Therefore the aim of this thesis was to produce a cell model of Parkinson's disease that would allow investigation of the link between oxidative stress, α-synuclein clumping and cell death. As part of such a model, better tools are needed to assess the involvement of oxidative stress; therefore the potential of a novel synthetic antioxidant was investigated.

A doubling in the levels of the α-synuclein protein in humans causes Parkinson's disease. Therefore the levels of the α-synuclein protein were increased in cells to try to model Parkinson's disease. However, this increase in the protein level failed to show toxicity in the cells used. This may be due to the length of time the protein was in the cells, the levels of the protein or the type of cells used. Further experiments are needed to produce a cell model of Parkinson's disease.

One possible tool to examine the involvement of oxidative stress in disease models is the compound AO-1-530, which was synthesised by Antoxis Limited. The chemical composition of AO-1-530 is based on a group of natural antioxidants found in plants known as flavonoids. AO-1-530 was shown to maintain the antioxidant ability of flavonoids and was found to enter cells quickly, where it unexpectedly becomes enriched in a part of the cell known as the mitochondria. A toxin induced oxidative stress cell model showed AO-1-530 was protective and it out-performed the other antioxidants tested. This protective potential was due to its ability to enter cells and remove damaging reactive molecules. Therefore, AO-1-530 is a synthetic antioxidant that may be a powerful novel tool to study the involvement of oxidative stress in disease models.

Abstract

Oxidative stress is caused when there are more reactive oxygen species (ROS), than antioxidants to scavenge them, resulting in damage to cellular components. It has been implicated as a major player at multiple points in the disease process of Parkinson's disease (PD) and many other conditions. For example, evidence suggests oxidative damage to the α-synuclein protein may affect its aggregation propensity. In addition, α-synuclein may increase ROS production. However, how this oxidative stress relates to neurodegeneration is not known. Therefore, there is a need for models of α-synucleinopathies and tools to assess the involvement of oxidative stress in the disease process.

In order to model α-synucleinopathies, overexpression of the α-synuclein protein was used. A BacMam viral expression system containing human α-synuclein was generated and used to assess toxicity. α-Synuclein overexpression in undifferentiated or differentiated SH-SY5Y cells failed to show toxicity. However, the stability of α-synuclein protein expression and the cell line used may have influenced in the lack of toxicity. The current work provides important guidance for future experimental design.

Flavonoids are found in plants and have antioxidant capability. AO-1-530 is a synthetic compound with a flavonoid head group and a long hydrocarbon tail. It is highly cell permeable and localises to the mitochondria. In order to investigate its protective properties, toxin-induced oxidative stress cell assays were established. AO-1-530, in the low micromolar range, was protective against high doses of *tert*-butyl hydroperoxide (tBHP), whereas natural antioxidants, such as myricetin and quercetin, showed limited protection or required at least 10-fold higher concentrations to achieve similar protection.

The ability of AO-1-530 to directly scavenge radicals was assessed cell-free in solution and in a cell-based assay. In solution the mechanism of action was investigated by electron paramagnetic resonance (EPR) spectroscopy. AO-1-530 had similar scavenging ability to myricetin, but was a slightly stronger scavenger than quercetin. The intracellular scavenging ability was quantified by CellROX® Deep Red live imaging. Although the compounds had similar cell-free scavenging abilities, AO-1-530 significantly out-performed both myricetin and quercetin in the intracellular assay, suggesting the mitochondrial localisation is critical to its highly protective properties. AO-1-530 is a powerful, novel tool to study the involvement of oxidative stress in diverse disease models.

Table of Contents

List of Figures

List of Tables

List of Abbreviations

4-HNE	4-hydroxynonenal
8-OHdG	8-hydroxy-2-deoxyguanosine
ALS	Amyotrophic lateral sclerosis
ANOVA	Analysis of variance
ARE	Antioxidant response element
ATP	Adenosine triphosphate
au	Arbitrary units
BSA	Bovine serum albumin
CHAT	Choline acetyl transferase
Cul3	Cullin 3
DAPI	4',6-Diamidino-2-Phenylindole
DBH	Dopamine β-hydroxylase
DCF	2',7'-Dichlorofluorescein
DHE	Dihydroethidium
Drp1	Dyanmin-related protein 1
DLB	Dementia with Lewy bodies
DMPO	5,5-Dimethyl-1-pyrroline N-oxide
DMSO	Dimethyl sulphoxide
Dmt	2,6-Dimethyltyrosine
EPR	Electron paramagnetic resonance
FACS	Fluorescence activated cell sorting
FBS	Fetal bovine serum
FCCP	Trifluorocarbonylcyanide phenylhydrazone
GCIs	Glial cytoplasmic inclusions
GFP	Green fluorescent protein
GPx	Glutathione peroxidase
GSH	Glutathione/reduced glutathione
GSSG	Glutathione disulphide/oxidised glutathione
GST	Glutathione S-transferase
H_2O_2	Hydrogen peroxide
HBSS	Hank's balanced salt solution
HPLC	High-performance liquid chromatography
IRES	Internal ribosome entry sequence
Keap1	Kelch-like ECH-associated protein 1
LBs	Lewy Bodies
LDH	Lactate dehydrogenase
MAP2	Microtubule associated protein 2
MPP+	1-methyl-4-phenylpyridinium
MPTP	1-methyl-4-phenyl-1,2,3,6-tetrahydropyridine
mRNA	messenger Ribonucleic acid
MSA	Multiple system atrophy
MSR	Methionine sulphoxide reductase

mtGFP	mitochondrial targeted GFP
mtGFP-SNCA	Mitochondrial targeted GFP with α-synuclein
NADPH	Nicotinamide adenine dinucleotide phosphate
NEB	New England Biolabs
NFE2L2 or Nrf2	Nuclear factor-erythroid 2 (NF-E2)-related factor 2
NGFβ	Nerve growth factor β
NOX	NADPH oxidase
NS-1	Neuroscreen™-1
PD	Parkinson's disease
PFA	Paraformaldehyde
PI	Propidium iodide
PINK1	PTEN-induced putative kinase 1
PMS	Phenazine methosulphate
qRT-PCR	Quantitative reverse transcription PCR
ROS	Reactive oxygen species
SEM	Standard error of mean
SNPs	Single-nucleotide polymorphisms
SNpc	Substantia nigra pars compacta
SOD	Superoxide dismutase
tBHP	*tert*-Butyl hydroperoxide
TBP	TATA-binding protein
TH	Tyrosine hydroxylase
TPP	Triphosphonium ion
UPL	Universal probe library
VMAT2	Vesicular monoamine transporter 2

Chapter 1 – Introduction

1.1. General Introduction

Oxygen is present in the air and is required by aerobic cells to produce sufficient amounts of energy. However, exposure of cells to oxygen can result in the production of reactive derivatives of oxygen known as reactive oxygen species (ROS) (Gerschman *et al*, 1954). To protect themselves, aerobic cells have developed antioxidant defences that remove these reactive species (McCord *et al*, 1971). Within healthy cells there is usually a balance between the production of reactive species and their removal by antioxidants. However, if there is a reduction in antioxidants or an increase in reactive species, then oxidative stress occurs and the reactive species are free to react with cellular components, causing oxidative damage. The oxidative stress theory of aging, which remains controversial, stipulates that the build up of oxidative damage over time causes aging (Finkel & Holbrook, 2000). Therefore, in diseases, such as Parkinson's, where age is a significant risk factor, oxidative stress has been implicated as a potential cause (Surmeier *et al*, 2011; Jenner *et al*, 1992). In addition, mitochondrial dysfunction has been implicated in Parkinson's and may be closely related to the oxidative stress observed (Schapira *et al*, 1990; Surmeier *et al*, 2011). It is important to be able to model the disease accurately in order to determine the relationship between oxidative stress and neurodegeneration. This understanding of the disease process will allow the rationale design of targeted treatments for people with Parkinson's disease (PD).

1.2 α-Synuclein and Neurodegeneration

PD is part of a larger family of neurodegenerative diseases that are now known collectively as α-synucleinopathies.

1.2.1 α-Synucleinopathies

α-Synucleinopathies are neurodegenerative diseases that have symptoms of Parkinsonism and have some form of α-synuclein protein inclusions. These protein inclusions, known as Lewy bodies (LBs), Lewy neurites or glial cytoplasmic inclusions (GCIs), are mainly composed of the protein α-synuclein, but also contain a large number of other protein constituents (Spillantini *et al*, 1997; Wakabayashi *et al*, 1998). The Parkinsonism symptoms experienced, including tremor, rigidity, akinesia and postural instability, are caused by the loss of dopaminergic neurons in substantia nigra pars compacta (SNpc) (Langston *et al*, 1999; Parent & Parent, 2010). The most common α-synucleinopathies are PD, dementia with Lewy bodies (DLB) and multiple system atrophy (MSA). These diseases differ in the cell

types that contain the α-synuclein protein inclusions and the subsequent brain areas that are affected.

Some evidence suggests these are not separate diseases but rather a spectrum of diseases with differing symptom severity. PD would be the mildest form with degeneration of neurons in the substantia nigra, locus coeruleus and raphe nucleus. Surviving neurons in these areas contain α-synuclein-rich LBs and Lewy neurites (Braak *et al*, 2003). A more severe form of α-synucleinopathies is DLB, where patients experience Parkinsonism as well as psychiatric symptoms, including visual hallucinations. In addition, neurodegeneration and LBs are more widespread throughout the brain (McKeith *et al*, 1996). Another α-synucleinopathy more severe than PD is MSA. MSA symptoms include Parkinsonism, autonomic failure and cerebellar ataxia, including urinary incontinence and slurred speech (Gilman *et al*, 2008). In MSA the α-synuclein protein inclusions are found in oligodendrocytes throughout the white matter of the cerebellum and cerebrum, known as GCIs. Post-mortem analysis shows neurodegeneration in the cerebellum and pons (Gilman *et al*, 2008). The presence of α-synuclein protein inclusions in surviving cells of the brain implicates α-synuclein in the disease process.

Further evidence that implicates α-synuclein as a cause of neurodegeneration was the discovery of mutations and multiplications of the α-synuclein gene, which encode protein modifications, in familial cases of Parkinsonism (Table 1.1). The first α-synuclein mutation discovered was an autosomal dominant single amino acid change, A53T (Polymeropoulos *et al*, 1997). Compared to sporadic PD patients, patients with this mutation experience an earlier onset of symptoms, faster progression and some develop late onset dementia (Golbe *et al*, 1990). Subsequently, the A30P mutation was reported, which caused milder symptoms than A53T, with later onset and slower progression more representative of sporadic PD (Krüger *et al*, 1998; Seidel *et al*, 2010). Next to be found was the E56K mutation, which showed symptoms more representative of DLB including hallucinations and dementia (Zarranz *et al*, 2004). More recently two further mutations have been discovered G51D and H50Q. The G51D mutation showed a much earlier age of onset than sporadic PD, as young as 19 years, and patients had symptoms of PD, DLB and MSA. Post-mortem analysis showed LBs and GCIs throughout the brain with substantial cell loss in the SNpc, hippocampus and cerebellum (Kiely *et al*, 2013; Lesage *et al*, 2013). The H50Q mutation resulted in milder symptoms with later disease onset of 60 years with dementia (Appel-Cresswell *et al*, 2013). These mutations suggest that an alteration in the α-synuclein protein can cause the major types of α-synucleinopathies.

There is also evidence that indicates the level of α-synuclein protein is influential in neurodegeneration. α-Synuclein gene triplication patients have twice as much α-synuclein protein than control patients (Singleton, AB *et al*, 2003; Farrer *et al*, 2004), therefore from the gene dosage, duplication patients are expected to have 1.5 times more protein than controls (Chartier-Harlin *et al*, 2004). The affected family members in these kindreds show the higher the α-synuclein protein level the earlier the average age of disease onset and the more severe the symptoms experienced (Table 1.1) (Nishioka *et al*, 2006; Chartier-Harlin *et al*, 2004). One report documented an average age of onset of 33 years for triplication patients compared to 50 years for duplication patients (Shin *et al*, 2010). Triplication patients often experience hallucinations and dementia, but this is rarely found in duplication patients (Shin *et al*, 2010; Gwinn *et al*, 2011; Ibáñez *et al*, 2004; Nishioka *et al*, 2006). In addition, a number of so far asymptomatic duplication carriers have been found through affected family members (Ahn *et al*, 2008). This suggests that simply increasing the α-synuclein protein level may result in more aggressive neurodegeneration and earlier onset of disease symptoms. However, α-synuclein multiplications and mutations are rare (Lesage & Brice, 2009). A number of genome-wide association studies comparing sporadic PD patients and unaffected controls have shown single-nucleotide polymorphisms (SNPs) in the SNCA gene were associated with sporadic PD (Edwards, 2010). These variations in the SNCA gene may be capable of influencing α-synuclein protein expression levels.

How α-synuclein causes toxicity is unknown but recent progress in the field suggests α-synuclein acts in a prion-like manner, with toxic oligomeric α-synuclein species spreading between interconnected neurons within the nervous system. The causes of the initial oligomer formation is unknown but there is evidence to indicate once formed they can spread between neurons. The first piece of evidence came from studies performed by Braak and colleagues. They examined the α-synuclein pathology in 168 brains of sporadic PD patients, LB and Lewy neurite containing brains and non-LB or Lewy neurite containing brains. This analysis suggested α-synuclein pathology starts in specific regions of the brain and spreads through connected neurons in a predictable way (Braak *et al*, 2004; 2003). Further evidence to support the spread of α-synuclein came from post-mortem analysis of PD patients who had received fetal transplants 11-14 years earlier to reduce PD motor symptoms. The grafted neurons contained α-synuclein positive LBs, indicating that α-synuclein could spread from affected neurons. However, another possible explanation was the environment the grafts were injected into could induce α-synuclein pathology (Chu & Kordower, 2010; Kordower *et al*, 2008; Li *et al*, 2008). Evidence for the spreading of α-synuclein came from *in vitro* studies where α-synuclein was aggregated in solution to form

pre-formed fibrils. These fibrils were then sonicated to produce oligomeric fragments (Volpicelli-Daley *et al*, 2011). When these oligomeric fragments were incubated with mouse primary neurons, they were taken up and seeded endogenous cellular α-synuclein. These seeded aggregates, like LBs contained phosphorylated α-synuclein and were positive for ubiquitin. In addition, the oligomeric fragments induced toxicity in neurons two weeks after addition; suggesting α-synuclein oligomers are the toxic form of α-synuclein (Volpicelli-Daley *et al*, 2011). This aggregation and toxicity was only seen in neurons that contained endogenous α-synuclein and the more α-synuclein present the quicker aggregates developed (Volpicelli-Daley *et al*, 2011). Sonicated pre-formed fibrils have also been injected into α-synuclein containing mice brains (Luk *et al*, 2012). They were taken up into neurons, spread to interconnected neurons and caused neuronal toxicity. The neuronal toxicity resulted in impaired balance and motor coordination (Luk *et al*, 2012). Therefore oligomeric α-synuclein may be the toxic species that can spread from one neuron to another interconnected neuron causing α-synuclein toxicity. The rate of this toxicity is dependant on the endogenous α-synuclein levels.

Mutation	Age at onset	Phenotype	Associated disorders	Frequency	References
A53T	20-85	PD; late onset dementia		~15 families reported	Polymeropoulos *et al*, 1997; Golbe *et al* 1990; Papadimitriou *et al* 1999; Markopoulou *et al* 1999; Spira *et al* 2001; Bostantjopoulou *et al* 2001; Berg *et al* 2005; Ki *et al* 2007; Puschmann *et al* 2009
A30P	54-76	PD		1 family reported	Krüger *et al*, 1998
E46K	50-69	PD, dementia, hallucinations	Demetia with Lewy Bodies	1 family reported	Zarranz *et al*, 2004
H50Q	60-71	PD, dementia	Dementia with Lewy Bodies	1 family reported	Appel-Cresswell *et al*, 2013; Proukakis *et al* 2013
G51D	19-60	PD, pyramidal signs, psychiatric symptoms	Multiple systems atrophy, Dementia with Lewy Bodies	2 families reported	Kiely *et al*, 2013; Lesage *et al*, 2013
Duplication	31-77	PD		0.2-0.7%; ~22 familial or sporadic cases reported	Chartier-Harlin *et al* 2004; Ibáñez *et al* 2004; Nishioka *et al* 2006; Fuchs *et al* 2007; Ahn *et al* 2008; Ikeuchi *et al* 2008;Sironi *et al* 2010; Uchiyama *et al* 2008; Brueggemann *et al* 2008; Troiano *et al* 2008; Nuytemans *et al* 2009; Nishioka *et al* 2009;Shin *et al* 2010; Garraux *et al* 2012; Itokawa *et al* 2012; Elia *et al* 2013; Darvish *et al* 2013
Triplication	20-50	PD, dementia, hallucinations	Dementia with Lewy Bodies; multiple system atrophy	~5 families reported	Singleton, AB *et al*, 2003; Farrer *et al*, 2004; Keyser *et al* 2009; Sekine *et al* 2010; Kojovic *et al* 2013

Table 1.1- Mutations and multiplications of the α-synuclein gene.

1.2.2 α-Synuclein and Oxidative Stress

There is evidence to suggest oxidative stress may be involved in the toxicity of α-synuclein. Oxidative damage to the α-synuclein protein itself may increase its aggregation propensity, producing toxic oligomers. Alternatively, α-synuclein aggregates may induce a state of oxidative stress within cells.

Exposure of α-synuclein to oxidative insults, including rotenone and dopamine, can result in modification of the methionine and tyrosine residues (Figure 1.1) (Mirzaei *et al*, 2006; Leong *et al*, 2009). Oxidation of the methionine sulphur atom produces methionine sulphoxide and further sulphur oxidation produces methionine sulphone (Figure 1.1b) (Mirzaei *et al*, 2006). It is suggested the oxidation of the methionine residue to methionine sulphoxide is an antioxidant function because there is a family of methionine sulphoxide reductase (MSR) enzymes in the cell that are capable of reducing the sulphoxide to produce methionine (Figure 1.1b) (Maltsev *et al*, 2013; Liu *et al*, 2008). Methionine oxidation in the α-synuclein protein results in reduced membrane binding affinity and produces soluble seemingly non-toxic stable globular oligomers that are unable to produce fibrils (Maltsev *et al*, 2013; Zhou *et al*, 2010).

Oxidative damage to the tyrosine residues in the α-synuclein protein results in nitration and phosphorylation (Figure 1.1) (Mirzaei *et al*, 2006; Souza *et al*, 2000; Hodara *et al*, 2004). LBs examined on post-mortem analysis of α-synucleinopathy patients contain nitrated α-synuclein (Giasson *et al*, 2000). This nitration is capable of producing α-synuclein oligomers, which are heat stable due to the covalent dityrosine bonds that form between monomers (Souza *et al*, 2000; Schildknecht *et al*, 2011). These nitrated products are degraded more slowly, show reduced lipid binding and are capable of fibril formation in the presence of non-nitrated α-synuclein (Martinez-Vicente *et al*, 2008; Hodara *et al*, 2004; Sevcsik *et al*, 2011).

The α-synuclein protein can also be modified by the addition of a product of lipid peroxidation, 4-hydroxynonenal (4-HNE), to the lysine or histidine residues. This can result in β-sheet α-synuclein aggregates that may seed aggregation and result in increased cellular α-synuclein release (Bae *et al*, 2013). Most of these studies were not performed in cells; therefore how the protein modifications relate to cellular toxicity needs to be investigated.

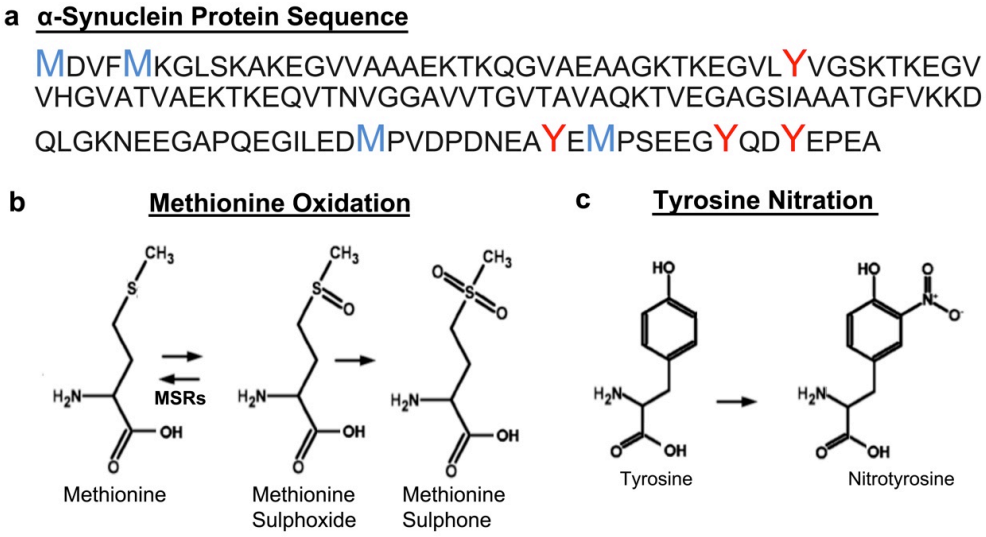

Figure 1.1 - Oxidative modification of the α-synuclein protein. (a) The α-synuclein amino acid sequence with residues susceptible to oxidative modification highlighted, methionine (blue) and tyrosine (red). (b) Methionine undergoes oxidation to methionine sulphoxide and then methionine sulphone. The methionine sulphoxide can be reduced back to methionine by the family of enzymes known as methionine sulphoxide reductases (MSRs). (c) Tyrosine undergoes nitration to produce nitrotyrosine (Figure adapted from Mirzaei *et al*, 2006).

There are some studies that indicate α-synuclein protein aggregates are capable of increasing the levels of oxidative stress in cells. α-Synuclein fibrils that have been sonicated to produce smaller fibril fragments are capable of inducing toxicity in mouse hippocampal neurons after 14 days (Volpicelli-Daley *et al*, 2011). If these fibril fragments are incubated with mesencephalic mouse neurons for 14 days there is an increase in cytosolic and mitochondrial oxidation. This increase in oxidation was prevented by the antioxidant N-acetyl cysteine and by apocynin, a nicotinamide adenine dinucleotide phosphate (NADPH) oxidase (NOX) inhibitor, which both act to reduce the levels of ROS (Dryanovski *et al*, 2013). In another study, α-synuclein oligomers, fibrils and monomers were all taken up into rat primary neurons. However, analysis of the rate of ROS production using dihydroethidium (DHE) showed that only the oligomeric forms of α-synuclein increased cellular production of ROS (Cremades *et al*, 2012).

These studies suggest oxidative damage to the α-synuclein protein can produce oligomers that could be toxic. In addition, α-synuclein oligomers may result in an increase in the production of ROS. Therefore, this implicates oxidative stress at multiple points within the disease process of α-synucleinopathies.

1.3 Oxidative Stress and Neurodegeneration in Parkinson's Disease

PD patients also implicate oxidative stress in the degeneration of neurons through post-mortem analysis of PD patients and genes involved in recessive PD. In addition, the midbrain SNpc neurons severely affected in Parkinsonism appear to be particularly susceptible to oxidative stress.

1.3.1 Post-Mortem Analyses of Parkinson's Disease Brains

Post-mortem analyses of PD brains show evidence of mitochondrial dysfunction and oxidative stress. The substantia nigra has an increase in lipid oxidative damage and some forms of DNA oxidative modifications (Dexter *et al*, 1989; Alam *et al*, 1997). In addition, protein oxidative damage to mitochondrial complex I may result in its reduced activity (Schapira *et al*, 1990; Keeney *et al*, 2006). The levels of the antioxidant glutathione (GSH) are also reduced and iron ions that can enhance production of damaging ROS, are increased (Sofic *et al*, 1988; 1992). This indicates oxidative stress is involved at some stage of the disease. However, post-mortem analyses are performed at the end-stage in the disease process so it is unclear whether oxidative stress acts as a cause or just a by-product of neurodegeneration.

1.3.2 Recessive Parkinson's Disease

DJ-1, PTEN-induced putative kinase 1 (PINK1) and parkin are involved in damaged mitochondrial removal and mitochondrial ROS scavenging. Mutations in the genes encoding these proteins cause recessively inherited PD, implicating mitochondrial dysfunction and oxidative stress as a cause for PD. Patients with recessively inherited PD show symptoms of Parkinsonism and psychiatric disturbances often before the age of 40, with a good response to L-3,4-dihydroxyphenylalanine (L-DOPA) treatment (Bonifati *et al*, 2003; Valente *et al*, 2004a; 2004b; Kitada *et al*, 1998). In addition, recent studies suggest some recessive PD patients have LBs in surviving neurons (Kitada *et al*, 1998; Farrer *et al*, 2001a; Pramstaller *et al*, 2005; Samaranch *et al*, 2010).

The first autosomal recessive inherited mutation to be discovered was in the *PARK2* gene, which encodes parkin (Kitada *et al*, 1998). Parkin is an E3 ubiquitin ligase that degrades other proteins and itself through the ubiquitin degradation pathway (Zhang *et al*, 2000). It is found in the brain and many other tissues including skeletal muscle and blood (Serdaroglu *et al*, 2005; Kasap *et al*, 2009). In cells it is located in the cytoplasm and on the outer mitochondrial membrane (Darios *et al*, 2003; Kitada *et al*, 1998). *PARK2* knockout mice have nigrostriatal dysfunction but no degeneration (Goldberg *et al*, 2003). They have normal mitochondrial morphology but a reduction in the mitochondrial electron transport

chain function, reduced antioxidant capacity and more oxidative damage (Palacino *et al*, 2004). In contrast, its absence in *Drosophila* does cause dopaminergic neurodegeneration over time, which can be reduced by increased antioxidant gene expression (Whitworth *et al*, 2005).

Mutations in *PINK1* also cause autosomal recessive inherited Parkinsonism (Valente *et al*, 2004a). PINK1 is a mitochondrial targeted serine/threonine protein kinase (Unoki & Nakamura, 2001; Valente *et al*, 2004a). In *Drosophila* knockdown of PINK1 caused a reduction in lifespan and abnormal flight muscles. The number of mitochondria was reduced and those that were present were swollen with disintegrated cristae, and adenosine triphosphate (ATP) production was significantly reduced (Yang *et al*, 2006). The flies also showed dopaminergic neurodegeneration similar to parkin null *Drosophila*. This loss was rescued by human *PINK1* or *PARK2* overexpression (Yang *et al*, 2006). This indicated PINK1 and parkin likely act together or in the same pathway. Further experiments showed cellular mitochondrial depolarisation could stabilise PINK1 in the mitochondria. This increase in PINK1 caused phosphorylation of mitofusin-2 (Mfn2), which attracts parkin to the mitochondria and binds it (Chen & Dorn, 2013). Parkin then ubiquitinates a protein on the mitochondria and promotes mitochondrial degradation. Mutations in the *PARK2* gene, associated with Parkinsonism in patients, interfere with this mitochondrial degradation by preventing parkin binding to the mitochondria or by preventing mitochondrial protein ubiquitination (Geisler *et al*, 2010).

Mutations in the *DJ-1* gene were also found to be responsible for cases of autosomal recessive inherited early onset Parkinsonism (Bonifati *et al*, 2003). DJ-1 is expressed in most tissues in a number of subcellular compartments including the mitochondria (Zhang *et al*, 2005). It is an atypical peroxiredoxin-like peroxidase that directly scavenges hydrogen peroxide (H_2O_2) and other peroxides (Andres-Mateos *et al*, 2007). Its absence in mice does not lead to substantia nigra neurodegeneration, but there is an increase in mitochondrial H_2O_2 levels and an increase in neuronal susceptibility to oxidative insults (Andres-Mateos *et al*, 2007; Kim *et al*, 2005).

These autosomal recessive mutations are involved in the removal of damaged mitochondria or the protection of mitochondria from oxidative insults. Therefore, they implicate oxidative stress and mitochondrial dysfunction as central to the etiology of Parkinsonism.

1.3.3 Midbrain Substantia Nigra Dopaminergic Neuron Susceptibility to Oxidative Stress

The loss of the midbrain SNpc dopaminergic neurons causes the motor symptoms of Parkinsonism. There are several pieces of evidence to suggest they are more susceptible to oxidative stress than other neurons of the brain, further suggesting increased oxidative stress could be critical to their degeneration.

One piece of evidence comes from their susceptibility to oxidative stress related toxins. Drug addicts that took heroin containing the impurity 1-methyl-4-phenyl-1,2,3,6-tetrahydropyridine (MPTP) showed a relatively selective loss of SNpc neurons, indicating these neurons were more susceptible to the MPTP toxin (Langston *et al*, 1999). Its toxicity was found to be due to 1-methyl-4-phenylpyridinium (MPP+), which was produced after MPTP metabolism by monoamine oxidase B (Langston *et al*, 1984; Markey *et al*, 1984). MPP+ is specifically taken up into catecholaminergic neurons and inhibits complex I of the mitochondrial electron transport chain, resulting in cell death (Javitch *et al*, 1985; Richardson *et al*, 2007). Therefore of all the catecholaminergic neurons in the brain, those of the SNpc were preferentially susceptible to MPP+ toxicity. Further evidence comes from intravenous rotenone injection of rats. Rotenone is also a mitochondrial electron transport chain inhibitor but is not specifically taken up into catecholaminergic neurons (Earley & Ragan, 1984; Lindahl & Oberg, 1960). These rats showed loss of SNpc neurons, as well as the catecholaminergic neurons of the locus coeruleus (Betarbet *et al*, 2000). This suggests that of all the neurons in the brain the SNpc neurons are more susceptible to death due to inhibition of complex I of the mitochondrial electron transport chain.

The reason for this increased susceptibility may be partly due to an observation made by Heiko Braak. He observed the neurons lost in PD have long thin axons and are either unmyelinated or poorly myelinated with extensive arborisation (Braak *et al*, 2004; Matsuda *et al*, 2009). These properties result in greater energy demands and would make them more susceptible to oxidative damage or inhibition of the mitochondrial electron transport chain.

Another related reason for their increased susceptibility might be due to their redox state. Mice expressing mitochondrial-targeted redox-sensitive green fluorescent protein (GFP) had a higher mitochondrial oxidation state in the SNpc neurons than in the neighbouring ventral tegmental area dopaminergic neurons. This higher oxidation state was shown to be due to the influx of calcium through L-type calcium channels during the pace-making activity of the SNpc neurons (Guzman *et al*, 2010). The SNpc neurons have lower levels of calcium buffering proteins and may therefore require more energy to remove

the calcium, putting a greater load on the mitochondria. L-type calcium channel blockers prevented the calcium influx, and significantly reduced the oxidation state of the SNpc neurons. This higher mitochondrial oxidation state was also present in the locus coeruleus and the dorsal motor nucleus of the vagus neurons, which are also lost early in PD (Goldberg *et al*, 2012; Sanchez-Padilla *et al*, 2014). Therefore this higher mitochondrial oxidation state may make it easier to shift the balance towards oxidative stress induced death than other neuronal cell types.

One more SNpc property that may make it more susceptible to oxidative stress is the presence of dopamine in these neurons. Dopamine and catecholamines can undergo auto-oxidation in the presence of metal ions or at neutral and basic pH to produce H_2O_2 (Klegeris *et al*, 1995; Rosenberg, 1988). This increase in ROS could shift the redox balance causing oxidative stress.

The SNpc neurons have properties that may make them more susceptible to oxidative insult, including thin, poorly myelinated neurons, an oxidised mitochondrial redox potential and the presence of dopamine. Therefore the SNpc and other select neurons that degenerate in early PD are more susceptible to oxidative insults than other neurons of the brain.

1.4 Oxidative Stress

Oxidative stress is an imbalance between reactive species and antioxidants. This imbalance results in reactive species that are free to react with cellular components, causing oxidative damage.

1.4.1 Reactive Species

ROS are formed by the reduction of the oxygen atom (Figure 1.2). These species are reactive or unstable, hence the name ROS (Kellogg & Fridovich, 1975). The reactivity of each species differs, with the hydroxyl radical being the most reactive (Sies, 1993). In addition to ROS, other atoms have reactive derivatives, including reactive nitrogen species. Some of the reactive species are free radicals with one or more unpaired electron, including diatomic oxygen, the superoxide radical and the hydroxyl radical.

Diatomic oxygen has two unpaired electrons that have parallel spins (Pauling, 1931). In order to react with another atom or molecule it too must have two unpaired electrons with parallel spins. However, this is rare so oxygen usually receives one electron at a time (Pauling, 1931; Halliwell & Gutteridge, 1984). Alternatively, energy can be provided to oxygen, which results in pairing up of the unpaired electrons. This produces singlet oxygen, which has no unpaired electrons and is therefore more reactive than diatomic oxygen

(Herzberg & Herzberg, 1947; Halliwell & Gutteridge, 1984). The addition of one electron to oxygen produces the superoxide radical, which has one unpaired electron (Figure 1.2) (Pauling, 1979; Neuman, 1934). Reduction of the superoxide radical by the addition of another electron produces the peroxide ion that becomes protonated to give H_2O_2 (Figure 1.2) (Halliwell & Gutteridge, 1984). H_2O_2 has no unpaired electrons but it has a weak bond between the oxygen atoms making it highly reactive (Halliwell & Gutteridge, 1984). The breakage of the bond between the oxygen atoms in H_2O_2 produces the hydroxyl radical, which has one unpaired electron. This reaction occurs in the presence of heat or radiation (Halliwell & Gutteridge, 1984; Gajewski *et al*, 1990). In addition, in the presence of metal ions the rate of this reaction is increased, and is known as the Fenton reaction (Figure 1.2) (Fenton, 1894). The addition of an electron and proton to the hydroxyl radical produces the more stable water molecule (Figure 1.2).

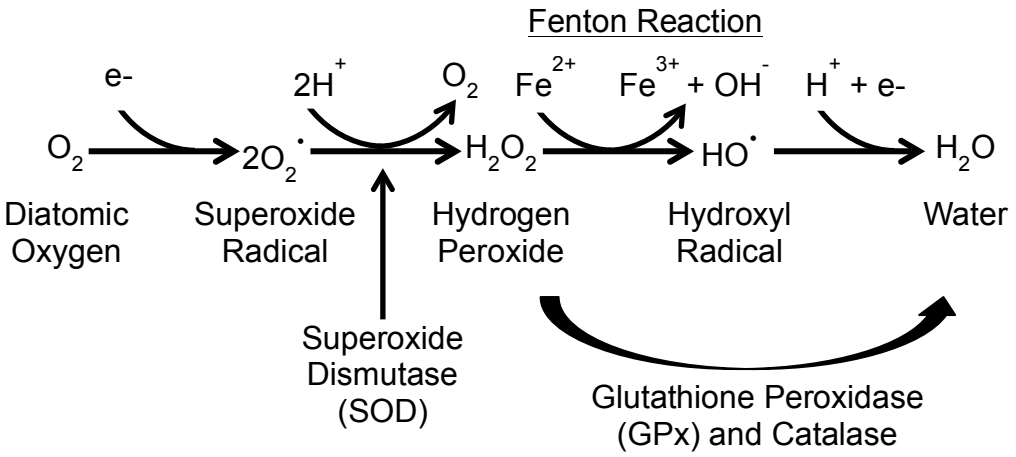

Figure 1.2 - Reduction of the oxygen atom to produce reactive oxygen species (ROS) and cellular antioxidant defence enzymes. The superoxide radical is produced by the one electron reduction of diatomic oxygen. In cells the superoxide dismutase (SOD) enzyme catalyses the removal of the superoxide radical to produce H_2O_2. A one-electron reduction of the superoxide radical produces H_2O_2, which is removed by glutathione peroxidase (GPx) and catalase to produce water and oxygen. The hydroxyl radical is produced by the one-electron reduction of H_2O_2, which iron or copper ions can catalyse, this is a Fenton reaction. There is no known cellular defence enzyme for the hydroxyl radical.

Other ROS exist that are produced from the reaction of ROS with lipids including the alkoxyl radical ($RO^{\bullet}$) and peroxyl radical ($ROO^{\bullet}$) (Bateman, 1954; Bolland, 1949; Girotti, 1985). In addition, ROS can react with other species to produce other reactive molecules. For example, the superoxide radical can react with nitric oxide to produce peroxynitrite, which is a reactive nitrogen species (Goldstein & Czapski, 1995).

1.4.2 Cellular Sources of Reactive Species

Reactive species are produced at a number of sites within the cell, including the endoplasmic reticulum, peroxisome, mitochondria and cytosol (Figure 1.3). The types of ROS produced at these sites vary and the mechanism of their production is different.

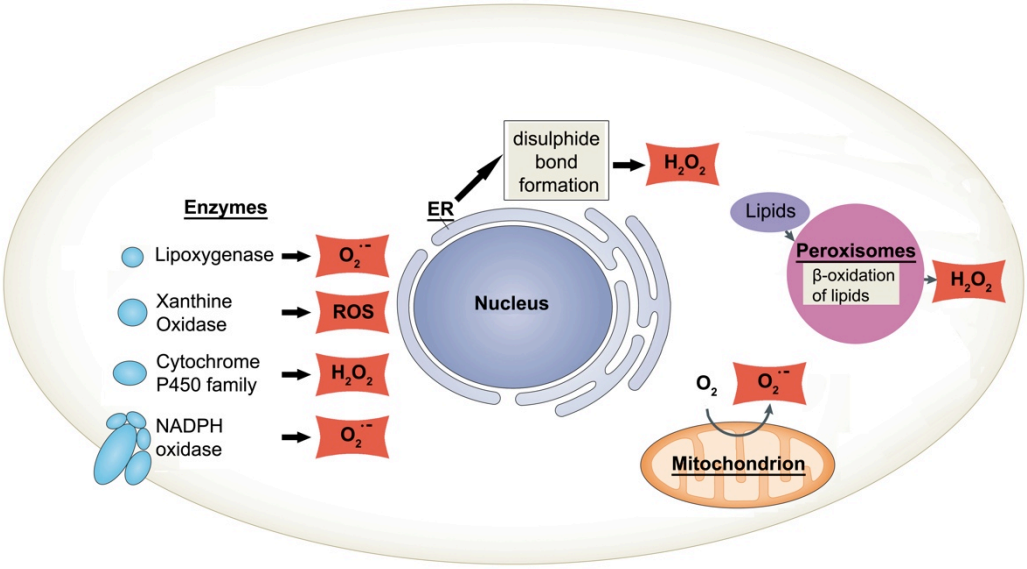

Figure 1.3 – Cellular sources of ROS. Within cells there are a number of sites known to produce ROS. Superoxide is produced in mitochondrion due to leakage of electrons from the mitochondiral electron transport chain. H_2O_2 is produced in peroxisomes by the break down of lipids and in the endoplasmic reticulum (ER) as a by-product of disulphide bond formation. The enzymes lipoxygenase, xanthine oxidase, cytochrome P450 and NADPH oxidase produce ROS either as by-products or to kill invading organisms (Adapted from Holmström & Finkel, 2014).

A major source of ROS production in cells is enzymatic activity. NOX enzymes are one of the most studied. NOX2, originally isolated from the membrane of phagocytes, produces superoxide radicals to kill invading organisms (Babior *et al*, 1973; 1975). The NOX2 enzyme is made up of a complex of subunits that upon activation form a functional enzyme, which catalyses the production of the superoxide radical from NADPH and oxygen (Clark *et al*, 1990). A defect in the NOX2 enzyme causes patients to develop chronic infections with a disease known as chronic granulomatous disease (Curnutte *et al*, 1974; 1975). Further studies have found isoforms of the NOX enzyme in other subcellular compartments, including the mitochondria and the endoplasmic reticulum; these isoforms may be involved in cell signalling (Chen *et al*, 2008).

Enzymes may also produce ROS as by-products of other cellular functions. For example, lipoxygenase produces the superoxide radical as a by-product of lipid breakdown (O'Donnell & Azzi, 1996). In addition, the enzyme xanthine oxidase involved in the breakdown of purines produces superoxide and H_2O_2 (Sanders *et al*, 1997; Harrison, 2002).

The cytochrome P450 family of enzymes in the endoplasmic reticulum also produce H_2O_2, as a by-product of xenobiotic breakdown (Gorsky *et al*, 1984; Zhukov & Ingelman-Sundberg, 1999; Szczesna-Skorupa & Kemper, 1993).

Another source of ROS production in cells is the mitochondria. In isolated mitochondria the major site of superoxide production is complex I of the mitochondrial electron transport chain (Loschen *et al*, 1974; Kussmaul & Hirst, 2006). Studies have shown the flavin mononucleotide of complex I, which can be found on the matrix side of the inner membrane, is the site of superoxide production (Kussmaul & Hirst, 2006; Kudin *et al*, 2004). The levels of superoxide production from complex I *in vivo* are unknown. Within the mitochondria there may be other sites of ROS production, such as the coenzyme Q pool and the mitochondrial electron transport chain complex III, but the major source is considered to be complex I (Murphy, 2009).

The endoplasmic reticulum and peroxisomes also produce H_2O_2 (Gorsky *et al*, 1984; Zhukov & Ingelman-Sundberg, 1999; Mueller *et al*, 2002; Boveris *et al*, 1972). In the endoplasmic reticulum a source of this H_2O_2 is the Ero1p enzyme, which is involved in disulphide bond formation, as well as the cytochrome P450 enzymes (Gross *et al*, 2006; Szczesna-Skorupa & Kemper, 1993). In the peroxisomes, H_2O_2 is produced by the metabolism of lipids and oxygen (Mueller *et al*, 2002; Boveris *et al*, 1972).

The mitochondria, endoplasmic reticulum, peroxisomes and cytosol are all potential sources of ROS production in cells (Boveris *et al*, 1972). Some of this production is intentional to kill invading organisms, some is produced to allow cell signalling and some is produced as a by-product of other cellular reactions. In addition, ROS can be found in cells as a consequence of environmental interactions, for example exposure to sun (Heck *et al*, 2003), exposure to toxins (Valavanidis *et al*, 2009) or as a result of trauma (Tyurin *et al*, 2000).

1.4.3 Oxidative Damage to Cellular Components

Low levels of reactive species are required for cell signalling (Reviewed Finkel, 2011). However, when higher levels are produced the reactive species can attack DNA, lipids and proteins in the cell to produce oxidative damage, which eventually results in cell death. H_2O_2, for example, is reported to become toxic above 0.7 μM (Antunes & Cadenas, 2001).

DNA oxidative damage is the result of reactive species attack on any of the 4 bases; guanine, adenine, cytosine or thymidine; or the DNA backbone (Balasubramanian *et al*, 1998; Jaruga & Dizdaroglu, 1996; Dizdaroglu *et al*, 1991). The most susceptible base to oxidation is guanine (Steenken & Jovanovic, 1997). In the presence of singlet oxygen or peroxyl radicals ($ROO^{\bullet}$) the guanine base was preferentially modified, whereas in the

presence of the hydroxyl radical all DNA bases were modified (Valentine *et al*, 1998; Prat *et al*, 1997). There are many DNA oxidative modifications that have been found after irradiation or hydroxyl radical exposure but 8-hydroxy-2-deoxyguanosine (8-OHdG) (Figure 1.4a) and thymine glycol are among the most commonly observed (Figure 1.4a) (Douki *et al*, 2006; Frelon *et al*, 2000; Pouget *et al*, 2002). DNA base modifications were also found in DNA not exposed to the hydroxyl radical, but the levels were much lower, indicating DNA bases may be oxidised under normal conditions (Gajewski *et al*, 1990). Therefore, cells have repair mechanisms that can removed oxidised DNA bases or prevent incorporation of oxidised bases into DNA (Jaruga & Dizdaroglu, 1996; Kasai *et al*, 1986; Hazra *et al*, 1998; Mo *et al*, 1992). Failure of these repair mechanisms to remove all oxidised bases can produce changes in DNA base pairing, resulting in DNA mutations that can alter gene expression and cause disease (Cheng *et al*, 1992; Tan *et al*, 1999; Harwood *et al*, 1991).

Cellular membranes are composed of phospholipids, which are another target for ROS attack (Gorter & Grendel, 1925). This oxidative damage to lipids produces lipid peroxidation (Figure 1.4b). Initiation of lipid peroxidation occurs due to the removal of hydrogen from a lipid (LH). This could be due to attack by a hydroxyl radical, alkoxyl radical ($RO^{\bullet}$), peroxyl radical ($ROO^{\bullet}$) or iron ion but not H_2O_2 or the superoxide radical (Fong *et al*, 1973; Catalá, 2010; Fridovich & Porter, 1981). A lipid alkyl radical ($L^{\bullet}$) is produced. This can then react with oxygen to produce a lipid peroxyl radical ($LOO^{\bullet}$), which removes hydrogen from another lipid to produce a lipid hydroperoxide (LOOH) and another alkyl radical ($L^{\bullet}$) (Bateman, 1954; Bolland, 1949; Girotti, 1985). Therefore creating a lipid peroxidation chain reaction. Further degradation of these lipid hydroperoxides produces toxic aldehydes, including 4-HNE and malondialdehyde (Mlakar & Spiteller, 1996). Lipid peroxidation can cause an increase in membrane fluidity, loss of cell membrane integrity and eventually cell death. Therefore, cells have mechanisms to remove these toxic lipid products: antioxidants can remove the alkyl radicals ($L^{\bullet}$); GPx can remove the lipid hydroperoxides and enzymes like glutathione S-transferase (GST) can remove the aldehydes produced.

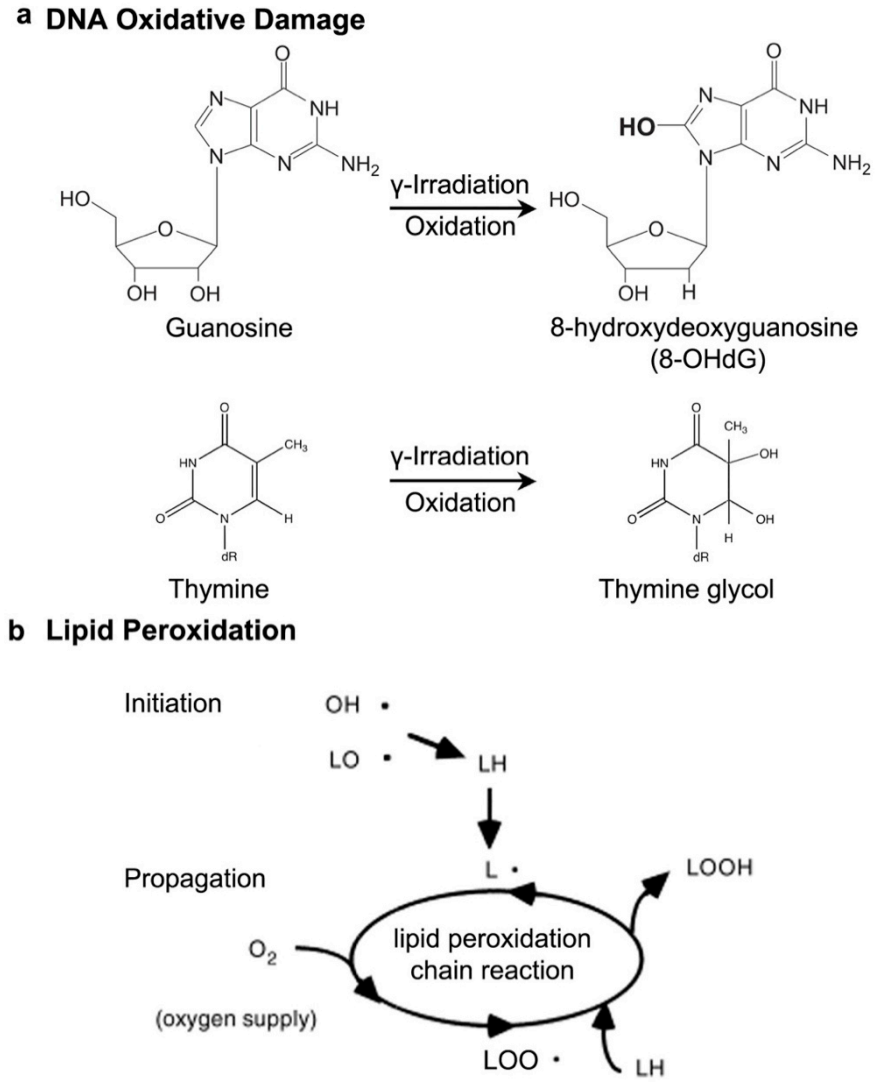

Figure 1.4- DNA and lipid oxidative damage. (a) Two commonly found ϒ–irradiation induced DNA base oxidative modifications - 8-hydroxy-2-deoxyguanosine (8-OHdG) and thymine glycol (Figure adapted from Aller *et al*, 2007 and Wu *et al*, 2004). (b) Lipid peroxidation is initiated by the removal of a hydrogen atom from a lipid to produce a lipid radical (L•). Propagation occurs when the lipid radical reacts with oxygen to produce a lipid peroxyl radical (LOO•). This lipid peroxyl radical propagates the reaction by removing a hydrogen atom from another lipid, producing a lipid hydroperoxide (LOOH) and another lipid radical (L•). This lipid radical can then react with oxygen to produce the lipid peroxyl radical and so on, creating a chain reaction (Figure adapted from Ishiyama *et al*, 1999).

Proteins can also be damaged through ROS attack of the amino acids or the peptide backbone (Garrison *et al*, 1962). Some amino acids are more susceptible to oxidative damage including histidine, tyrosine, tryptophan, cysteine and methionine (Alvarez *et al*, 1999; Davies *et al*, 1987; Proctor & Bhatia, 1953; Drake *et al*, 1957; Barron *et al*, 1955). Histidine is converted to 8-oxohistidine by the hydroxyl radical (Uchida & Kawakishi, 1993). Tyrosine exposure to nitric oxide produces 3-nitrotyrosine and subsequently dityrosine (Kikugawa *et al*, 1994), and H_2O_2 exposure produces the tyrosyl radical and then dityrosine (Heinecke *et al*, 1993). Tryptophan produces 5-nitroindole after nitric oxide

damage (Kikugawa *et al*, 1994). Cysteine produces sulphenic acid and then a disulphide bond on exposure to H_2O_2 (Carballal *et al*, 2003). Methionine is oxidised by peroxynitrite to methionine sulphoxide and then methinone sulphone (Figure 1.1) (Pryor *et al*, 1994). One repair mechanism that has been found is the family of MSR enzymes that reduce methionine sulphoxide to methionine (Ciorba *et al*, 1997; Moskovitz *et al*, 2001). In addition, the aldehydes produced during lipid peroxidation if not removed are capable of reacting with proteins at the histidine, lysine or cysteine residues, producing for example 4-HNE modified proteins (Uchida & Stadtman, 1993). Oxidative damage to proteins can prevent them from functioning, prevent their degradation or may be involved in cell signalling (Barron *et al*, 1955; Friguet *et al*, 1994).

The over production of ROS can result in damage to DNA, lipids and proteins, providing a measurable output of cellular oxidative stress. However, if this damage is left unrepaired it will eventually cause cell death and potentially initiate disease.

1.4.4 Tools to Measure Reactive Oxygen Species Production

One method to detect the presence of free radical ROS, with at least one unpaired electron, is electron paramagnetic resonance (EPR) spectroscopy. In addition, there are dyes available that are non-fluorescent but produce fluorescent products after reaction wth ROS, for example DHE and the CellROX® family of dyes. This provides a method to directly measure the levels of ROS production.

1.4.4.1 Electron Paramagnetic Resonance Spectroscopy

Free radicals possess at least one unpaired electron, which can be detected by a technique known as EPR spectroscopy. The unpaired electron acts as a magnet in the presence of a magnetic field, aligning either parallel or antiparallel to it, creating two energy levels. Application of electromagnetic radiation of the correct energy results in it being absorbed allowing the electron to move from the lower energy level to the higher energy level. This absorption of energy is measured and is presented as the first derivative, which is the rate of change in absorbance. The atoms surrounding the unpaired electron, for example hydrogen or nitrogen, can also act as magnets, creating additional energy levels and therefore additional energy absorptions. Therefore the spectrum produced from the absorbance of energy allows identification of the radicals produced. Most free radicals are highly reactive so chemical spin traps, like 5,5-dimethyl-1-pyrroline N-oxide (DMPO), are often employed to create radicals with longer half-lives that can be measured by EPR (Figure 1.5). For example the DMPO/•OH radical adduct has a half-life of hours rather than the nanosecond half-life of the hydroxyl radical (Figure 1.5) (Review: Hawkins & Davies, 2014).

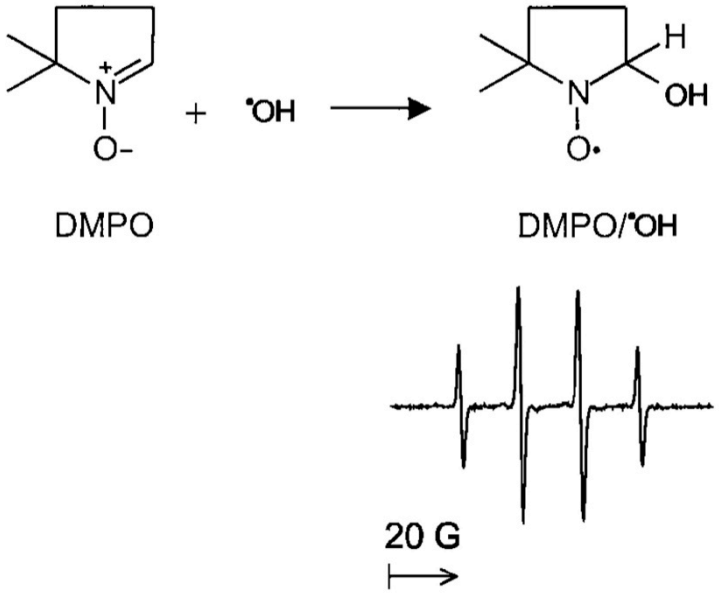

Figure 1.5 – The chemical spin trap DMPO and the EPR spectra produced after trapping the hydroxyl radical. The chemical structure of the spin trap DMPO is shown. DMPO can trap the hydroxyl radical to produce the DMPO/•OH radical adduct. The unpaired electron in this radical adduct can be detected by EPR. A 1:2:2:1 quartet spectrum is produced due to the surrounding nitrogen and hydrogen atoms. G stands for Gauss and is the strength of the magnetic field used (Figure adapted from Lawrence *et al*, 2003).

1.4.4.2 Dihydroethidium

DHE, also known as hydroethidine, is used to detect the production of superoxide and the presence of other oxidants in cells. It is easily taken up into cells and has a blue fluorescence in the reduced state (Bindokas *et al*, 1996). Once inside cells it can be oxidised to produce the red fluorescent products, ethidium and 2-hydroxyethidium, which bind to DNA (Bindokas *et al*, 1996). This oxidation is known to occur in the presence of the superoxide radical or cytochrome c, but not H_2O_2, singlet oxygen, hydroxyl radical, nitric oxide or peroxynitrite (Bindokas *et al*, 1996; Benov *et al*, 1998). However, other ROS may be involved in the oxidation of DHE to ethidium (Zielonka *et al*, 2006). Therefore ethidium and 2-hydroxyethidium productions, that is the red fluorescence at excitation 510 nm, does not solely report superoxide production. Further investigation into the reaction between the superoxide radical and DHE showed 2-hydroxyethidium was produced (Zhao *et al*, 2003). This product is unique to DHE oxidation by the superoxide radical and can be detected by high-performance liquid chromatography (HPLC). This method provides a way to solely detect superoxide radical production in cells (Zhao *et al*, 2003; Zielonka *et al*, 2009; 2006). Additional studies using a mitochondrial-targeted form of DHE, MitoSOX, showed it might be possible to distinguish between the 2-hydroxyethidium and ethidium fluorescence using excitation at 360 nm. This wavelength caused excitation of 2-hydroxyethidium, but not

ethidium, to give a semi-quantitative indication of superoxide levels (Robinson *et al*, 2006). In practice, DHE can be used to assess the presence of several oxidants in the cell by measuring amount of red fluorescence or rate of increase of red fluorescence over a short time-frame. Since ethidium binds DNA, nuclear fluorescence measurements are taken although the oxidation of DHE could have occurred elsewhere in the cell. Alternatively, when combined with HPLC or 360 nm excitation, DHE can be used to detect the production of superoxide radicals in cells.

1.4.4.3 CellROX® Family

The CellROX® family of dyes consists of three members; CellROX® Green, CellROX® Orange and CellROX® Deep Red, that are sold by Life Technologies. Each member is cell permeable with little or no fluorescence in the reduced state but on oxidation they become highly fluorescent. The reactivity of these dyes to different ROS differs according to Life Technologies. CellROX® Green and CellROX® Deep Red both react with hydroxyl and superoxide radicals, but not H_2O_2, nitric oxide or peroxynitrite. In contrast, CellROX® Orange reacts with all of these ROS. In addition, the dyes differ in their cellular localisation CellROX® Orange and CellROX® Deep Red are both cytoplasmic whereas CellROX® Green binds to DNA after oxidation and is therefore nuclear. A further difference is that CellROX® Green and Deep Red can undergo fixation, whereas CellROX® Orange cannot (Life Technologies, 2014).

These CellROX® dyes have been used in a number of papers to detect ROS production. Evidence from these papers that suggest they are suitable for ROS production detection come from their increase in fluorescence in the presence of toxins *tert*-butyl hydroperoxide (tBHP) and menadione, which result in an increase in ROS production (Yoon *et al*, 2014; Gemelli *et al*, 2014). In addition, if antioxidants are added to reduce these ROS the fluorescence increase is prevented (Yoon *et al*, 2014). This suggests CellROX® dyes are suitable for use in detecting an increase in ROS production, but cannot be used to distinguish the type of ROS produced.

1.4.5 Cellular Antioxidant Defences

The cellular antioxidant defence mechanisms include small molecules and enzymes with the ability to directly scavenge radicals as well as cellular responses that act to reduce oxidative stress. Cells have many endogenous antioxidant defence mechanisms only some of which are mentioned here. Here, the enzymatic antioxidant defences, the small antioxidant peptide GSH and the transcription factor Nuclear factor-erythroid 2 (NF-E2)-related factor 2 (NFE2L2 or Nrf2) that activates antioxidant gene transcription, will be covered. Further

antioxidant defences include other small molecules synthesised in the cell, small molecules that are absorbed from the diet, other transcription factors that activate gene expression of antioxidant genes and metal iron chelators.

1.4.5.1 Enzymatic Defences

Cellular enzymatic antioxidant defences act to remove ROS produced in cells, thereby preventing the formation of oxidative damage. This includes SOD, catalase, GPx (Figure 1.2) and peroxiredoxins.

SOD catalyses the removal of superoxide to produce H_2O_2 and oxygen (Figure 1.2) (McCord & Fridovich, 1969). It is present in a number of aerobes, but absent from many anaerobes, since anaerobes die in the presence of oxygen it was suggested that SOD was required for survival in the presence of oxygen (McCord *et al*, 1971). The original report isolated SOD with copper and zinc at the active site. Since then further SODs have been discovered with different metal ion cofactors, including, manganese, nickel and iron, at their active sites. In humans there are 3 forms of SOD. SOD1 or Cu/ZnSOD that is found in the cytosol, the mitochondrial intermembrane space and the nucleus (Weisiger & Fridovich, 1973; Crapo *et al*, 1992). SOD2 or MnSOD has manganese at its active site and is found in the mitochondrial matrix (Keele *et al*, 1970; Weisiger & Fridovich, 1973). SOD3 also known as extracellular SOD has copper and zinc at its active site but its amino acid composition and weight are different to SOD1 (Marklund, 1982). The most important of these appears to be MnSOD as *SOD2* knockout mice die 4-10 days after birth with impaired mitochondrial function (Li *et al*, 1995). SOD1 is also important, as SOD1 mutations have been found in patients with amyotrophic lateral sclerosis (ALS) (Rosen *et al*, 1993). When SOD1 is knocked out in mice they show a slightly earlier age of death than normal, an increase in oxidative damage, an increased susceptibility to toxins and impaired fertility (Ho *et al*, 1998; Elchuri *et al*, 2005; Reaume *et al*, 1996). This suggests SODs are important cellular antioxidant enzymes.

Another antioxidant enzyme is catalase, which catalyses the reduction of H_2O_2 to water in a two-step process using iron ions at its active site (Figure 1.2) (Loew, 1900; Putnam *et al*, 2000). Catalase has four subunits, with four iron ions at its active site and four NADPH molecules (Kirkman & Gaetani, 1984; Sumner & Dounce, 1937). In cells it is mainly located in peroxisomes and some other membranous particles, but is not abundant in the cytosol (Aikawa *et al*, 1991). The absence or low levels of catalase in humans produces acatalasemia, with mild symptoms of oral gangrene in childhood (Takahara *et al*, 1960). In catalase-null mice there is a delayed removal of H_2O_2 but no abnormalities were detected

(Ho *et al*, 2004). The reason for these mild phenotypes may be because cells have alternative mechanisms for the removal of H_2O_2, including GPx and peroxiredoxins.

Another enzyme capable of the removal of H_2O_2 and alkyl peroxides is the antioxidant protein peroxiredoxin (Chae *et al*, 1993). Some peroxiredoxin isoforms are also capable of peroxynitrite removal (Dubuisson *et al*, 2004). A cysteine residue in the peroxiredoxin proteins is evolutionarily conserved and is essential for their ability to reduce peroxides (Chae *et al*, 1994b). This cysteine residue is oxidised by peroxides, to remove them and then reduced by thioredoxin, to produce an active enzyme (Chae *et al*, 1994a). In mammals there are 6 isoforms that are split into 3 subclasses: 2-cysteine peroxiredoxins, 1-cysteine peroxiredoxin and the atypical 2-cysteine peroxiredoxin. These isoforms are located in different regions of the cell: cytosol, mitochondria, extracellular space and peroxisomes (Seo *et al*, 2000; Okado-Matsumoto *et al*, 2000; Kang *et al*, 1998; Reviewed by Rhee *et al*, 2005)

In summary, the cell has a number of important antioxidant defence enzymes that remove ROS and prevent them from producing oxidative damage to the cell. GPx is also involved in the removal of peroxides and will be discussed in the next section.

1.4.5.2 Glutathione Antioxidant

GSH is a tripeptide synthesised in cells containing cysteine, glycine and glutamic acid (Hopkins, 1929; Kosower & Kosower, 1978). A deficiency in GSH results in metabolic acidosis and neurological symptoms, possibly as a result of oxidative stress (Wellner *et al*, 1974). The presence of the thiol group in the cysteine residue allows GSH to act as an electron donor, or antioxidant. In cells GSH has been reported to have a number of diverse functions, but here the focus will be on its antioxidant function.

Direct radical scavenging of superoxide and hydroxyl radicals by GSH is possible but this would produce a thiyl radical (Eriksen & Fransson, 1988; Sjoberg *et al*, 1982; Wefers & Sies, 1983; Galano & Alvarez-Idaboy, 2011). This may then react with another thiyl radical to produce oxidised glutathione known as glutathione disulphide (GSSG). However, whether this scavenging occurs *in vivo* is unknown as other antioxidant mechanisms may be more competitive than GSH for the radicals (Jones *et al*, 2003). A known mechanism by which GSH acts as an antioxidant *in vivo* is by acting in conjunction with GST and GPx to remove toxic substrates.

GST acts as a xenobiotic or electrophilic substance detoxification enzyme by catalysing their conjugation to GSH (Booth *et al*, 1961; Combes & Stakelum, 1961; Baez *et al*, 1997; Cheng *et al*, 2001). These conjugates may be broken down further into mercapturic acids and excreted in the urine (Barnes *et al*, 1959; Stekol, 1941). There are 7 different GST

gene families with different amino acid sequences, giving them different xenobiotic substrate specificities (Mannervik & Jensson, 1982; Stockman *et al*, 1985). Soluble cytosolic GST forms were first discovered, and subsequently membrane-associated forms of GST were identified (Pemble *et al*, 1996). The cytosolic forms are dimers composed of the same monomer or monomers from the same family. Each monomer has a hydrophilic binding site for GSH and a hydrophobic binding site for the xenobiotic substance (Jakobson *et al*, 1979).

GPx is an enzyme involved in the removal of H_2O_2 and other peroxides, including tBHP and lipid hydroperoxides. The first GPx to be analysed was GPx1, which was isolated from the cytosol of cells. It contains four subunits with one selenium atom per subunit at the active site (Flohe *et al*, 1973; Lötscher *et al*, 1979). These selenium ions catalyse the reduction of peroxides to alcohol, using GSH as the hydrogen donor. GSH then becomes oxidised to GSSG (Little & O'Brien, 1968; Christophersen, 1969). GPx is not specific for the peroxides that it reduces, unlike catalase that has higher specificity for H_2O_2 (Little & O'Brien, 1968). The GSSG produced is then either released from cells or reduced to GSH by glutathione reductase, which uses NADPH as the hydrogen donor (Sies *et al*, 1972). The limiting step in this reduction is the NADPH levels (Sies *et al*, 1972).

A number of other GPxs have been discovered which catalyse the same reaction but are found in different tissues and have varied specificities for different peroxides. GPx2 and 3 are both tetramers containing selenium. However, GPx2 is mainly found in the liver and colon, therefore it is known as gastrointestinal GPx whereas GPx3 is found at higher levels in the plasma (Maddipati & Marnett, 1987; Chu *et al*, 1993; Akasaka *et al*, 1990). GPx4 is a monomeric enzyme with selenium at its active site and is mainly found in phospholipid bilayers, acting as a protector against lipid peroxidation (Ursini *et al*, 1985; Thomas *et al*, 1990). Mutations of GPx4 cause neonatal lethality in mice and humans with cardiac defects and nervous system abnormalities, illustrating its importance (Smith *et al*, 2014; Yant *et al*, 2003).

Four further GPx enzymes 5, 6, 7 and 8 have been identified but they are less well studied. Although, GPx 5, 7 and 8 do not have selenium at their active site, they are capable of catalysing the same reaction, possibly at a slower rate (Toppo *et al*, 2008). GPx6 does contain selenium and is expressed in the embryo and olfactory epitheium (Kryukov, 2003).

Both the GPx and GST enzymes require GSH to donate electrons, allowing removal of toxic compounds from cells. Therefore GSH is an important antioxidant in cells.

1.4.5.3 Nrf2

NFE2L2 or Nrf2 is a transcription factor transcribed by the gene *NFE2L2*. It is involved in the activation of antioxidant-associated gene expression in the presence of oxidative stress.

In Nrf2 knockout mice there is an inability to activate these genes therefore mice are more susceptible to toxins (Enomoto *et al*, 2001; Yoh *et al*, 2001).

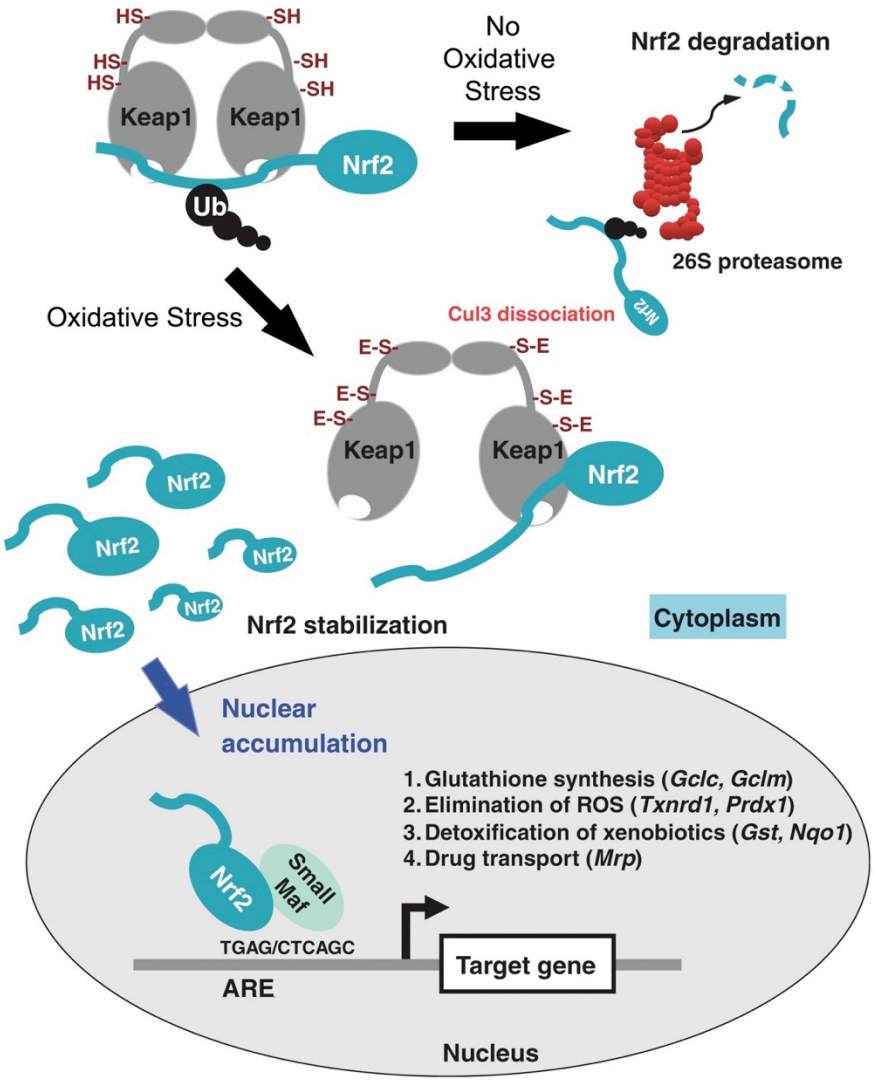

Figure 1.6 - Nrf2-Keap1 antioxidant response pathway. In the absence of stress Nrf2 is bound to a Keap1 dimer and targeted by ubiquitination for proteasomal degradation. In the presence of oxidative or electrophilic stress the cysteine sulphur atoms are altered changing the Keap1 secondary structure. This prevents Keap1 from associating with the E3 ubiquitin ligase Cul3 and reduces its association with Nrf2, preventing Nrf2 degradation. Therefore Nrf2 is stabilised and can accumulate in the nucleus. In the nucleus Nrf2 dimerises with small Maf proteins, which then bind to antioxidant response element (ARE) DNA sequences activating transcription of target genes, including those involved in GSH synthesis and removal of ROS (Figure adapted from Taguchi *et al*, 2011).

In the absence of oxidative stress Nrf2 binds to a dimer of Kelch-like ECH-associated protein 1 (Keap1) (Kobayashi *et al*, 2004; Tong *et al*, 2006; 2007). This Keap1 protein acts as an adaptor protein linking Nrf2 with Cullin 3 (Cul3), an E3 ubiquitin ligase (Wakabayashi *et al*, 2003). This results in Nrf2 lysine residues becoming

ubiquitinated, targeting it for proteasomal degradation (Figure 1.6) (Kobayashi *et al*, 2004; Furukawa & Xiong, 2005; Cullinan *et al*, 2004; Zhang *et al*, 2004).

In the presence of stress the Nrf2 protein levels are increased without a change in messenger ribonucleic acid (mRNA) expression levels (McMahon *et al*, 2003). This is due to oxidative stress attacking the cysteine residues of the Keap1 protein, altering its secondary structure, which prevents it binding to Cul3 and weakens its association with Nrf2 (Rachakonda *et al*, 2008; Eggler *et al*, 2005; Zhang *et al*, 2004; Kobayashi *et al*, 2006; Yamamoto *et al*, 2008). This prevents the ubiquitination of Nrf2, allowing it to accumulate and move to the nucleus where it forms a dimer with small Maf proteins (Figure 1.6) (Kobayashi *et al*, 2006; McMahon *et al*, 2003). This dimer can bind to a specific DNA sequence known as the antioxidant response element (ARE), activating gene transcription (Itoh *et al*, 1997). AREs are found in genes that counteract oxidative or electrophilic stress, including genes involved in GSH synthesis, removal of ROS and breakdown of xenobiotics (Figure 1.6) (Yates *et al*, 2009). Therefore stabilisation of the Nrf2 transcription factor mediates an antioxidant transcriptional response in cells.

1.4.6 Flavonoid Antioxidants

Flavonoids are a group of polyphenolic compounds found in plants with a similar backbone structure (Figure 1.7a). Their name, flavonoid, comes from the Latin word for yellow, which is their colour (Baier, 1955). In plants, the flavonoids are pigments that may be involved in attracting insects to allow pollination of plants (Brouillard *et al*, 1990; Iwashina, 2003). In addition, they are considered as protectants against harmful ultraviolet rays from light, as well as other functions (Skaltsa *et al*, 1994). There are now over 5000 natural flavonoids reported. These flavonoids can be split into six subclasses; flavones, flavonols, flavanones, flavanols (or catechins), anthocyanidins and isoflavones (Figure 1.7b). They are reported to have a wide range of functions including an antioxidant radical scavenging ability. This antioxidant ability comes from the donation of hydrogen atoms from the hydroxyl groups. These hydrogen atoms can be donated to a number of radicals, including the hydroxyl, peroxyl ($ROO^{\bullet}$) and superoxide radicals (Bors *et al*, 1990; van Acker *et al*, 1996; Rafat Husain *et al*, 1987; Arora *et al*, 1998; Torel *et al*, 1986). In addition, flavonoids are capable of chelating metal ions, thereby preventing their production of radicals (Fernandez *et al*, 2002). In studies examining the antioxidant ability of a number of flavonoids, it was found the flavonols, quercetin and myricetin were some of the best (Firuzi *et al*, 2005; Arora *et al*, 1998; van Acker *et al*, 1996; Bors *et al*, 1990; Yang *et al*, 2001).

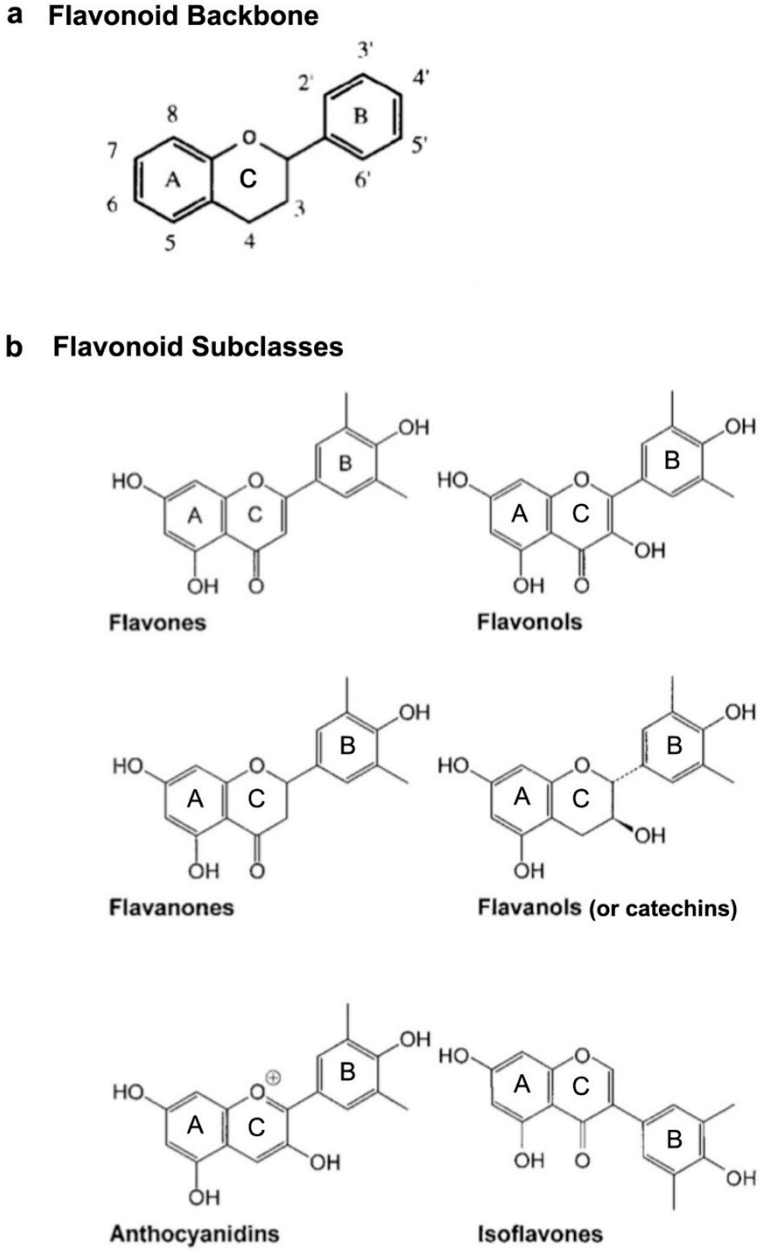

Figure 1.7 – Flavonoid backbone structure and the flavonoid subclasses. All flavonoids have a similar backbone structure composed of two phenyl rings A and B and a heterocyclic C ring containing oxygen (a). The six subclasses show variation on the hydroxyl and carbonyl groups attached to these rings and the position of the double bonds (b). In addition isoflavones show a different location of the B ring (Figures adapted from Hollman & Arts, 2000 and van Acker *et al*, 1996).

Flavonoids are found in fruits and vegetables with quercetin more abundant than myricetin (Bhagwat *et al*, 2014). In food, flavonoids usually have a sugar group attached, known as glycosides (Miean & Mohamed, 2001; Herrmann, 1988). Quercetin in the glycoside form was found to be absorbed through the diet more efficiently than without the

sugar attached (Hollman *et al*, 1995). However, it was estimated that around half of the quercetin glycoside eaten was not absorbed (Hollman *et al*, 1995). Further studies have shown the food source of quercetin is also influential in its absorption (de Vries *et al*, 1998). Therefore flavonoid antioxidants are potent radical scavengers that can be absorbed through the diet.

1.4.7 Synthetic Mitochondrial-Targeted Antioxidants

There are other antioxidants synthesised *in vivo* or absorbed from the diet but none of these natural antioxidants are known to locate to the mitochondria or other subcellular compartments involved in ROS production. Therefore research is being performed focussed on synthesising mitochondrial-targeted antioxidants. Since mitochondrial dysfunction and oxidative stress have been implicated in PD, mitochondrial targeted antioxidants may be suitable protective compounds (Schapira *et al*, 1990; Keeney *et al*, 2006). There are currently two published groups of mitochondrial-targeted antioxidants. One is the group of Mito compounds and the other is a group of small peptides, originally named the SS Peptides (Figure 1.8). Neither of these groups of compounds is available commercially for scientific use and both were due to undergo phase II clinical trials.

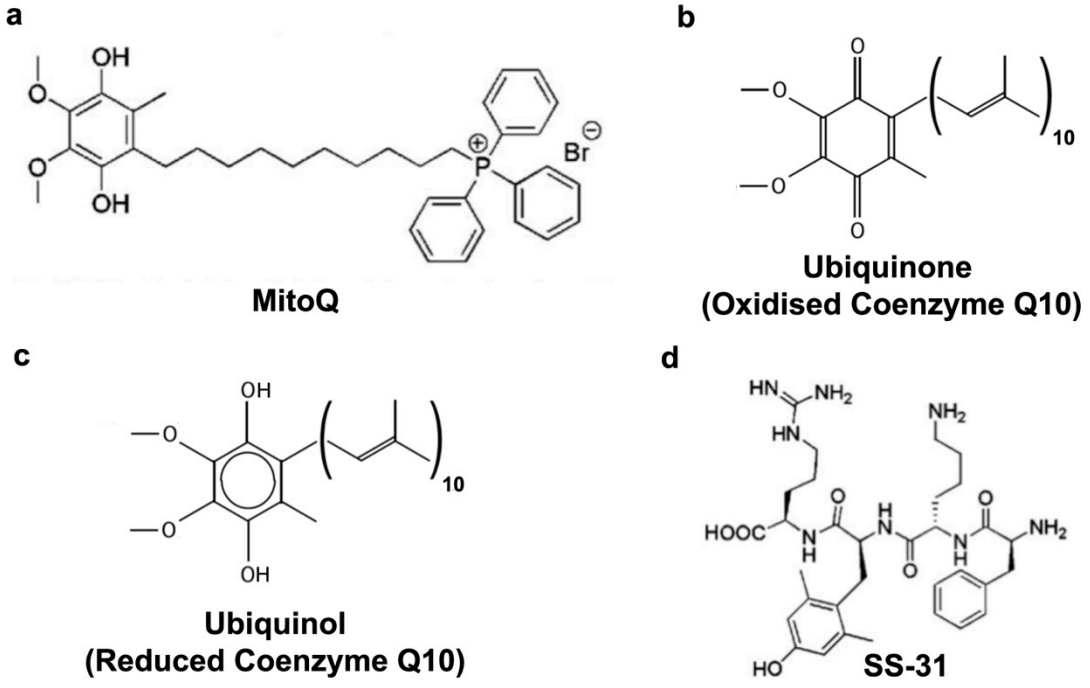

Figure 1.8 - Structure of mitochondrial-targeted antioxidants - MitoQ and SS-31. (a) MitoQ is based on coenzyme Q10 also known as ubiquinone (b) but a carbon chain has replaced the isoprenoid chain and the TPP ion is attached at the end of the carbon chain to attract MitoQ to the mitochondria. MitoQ is a mixture of oxidised, ubiquinone, and reduced, ubiquinol, forms of the coenzyme Q10 head group (b) and (c). (d) SS-31 is another mitochondrial-targeted antioxidant, which is a peptide, made up of D-arginine, dimethyltyrosine (Dmt), lysine and phenylalanine (Figure adapted from Sheu *et al*, 2006 and James *et al*, 2004)

1.4.7.1 Mito Compounds

Mito compounds are synthetic compounds that contain the triphosphonium ion (TPP). TPP has a positive charge, which is attracted to the negatively charged mitochondria. Therefore to create mitochondrial-targeted antioxidants this TPP has been attached to a number of known antioxidants. One of the first published was MitoVitE, which contained the antioxidant head group of Vitamin E with a two carbon chain and the TPP attached (Smith *et al*, 1999). It was taken up into cells and accumulated in the mitochondria, if the mitochondrial membrane potential was present. However, MitoVitE was less efficient than Vitamin E at protecting against lipid peroxidation, possibly due to its higher water solubility. In addition, as with other antioxidants it was toxic at high concentrations.

The second Mito antioxidant compound synthesised was MitoQ, which was based on coenzyme Q10, also known as ubiquinone, but the isoprenoid chain was changed to a carbon side chain and the TPP lipophilic cation was attached (Figure 1.8a). MitoQ contained both oxidised and reduced forms of the ubiquinone head group, known as ubiquinone and ubiquinol, respectively (Figure 1.8b and c). As with MitoVitE, MitoQ was taken up into the mitochondria, if the mitochondrial membrane potential was present and was capable of protecting against lipid peroxidation (Kelso *et al*, 2001). Further studies showed ubiquinol was the more active antioxidant form and that within the mitochondria the electron transport chain complex II continually reduced ubiquinone back to its ubiquinol form, recycling its antioxidant capability (Kelso *et al*, 2001; James *et al*, 2005). In addition, the length of the alkyl chain between the head group and the TPP ion was important. An increase in chain length increased the hydrophobicity of the compound, which in turn resulted in increased membrane binding and penetration. This increased antioxidant capacity against lipid peroxidation (Asin-Cayuela *et al*, 2004). MitoQ has been tested in Phase II clinical trials for its ability to delay the progression of PD. Newly diagnosed PD patients that had movement symptoms were given MitoQ or placebo for 12 months. However, no significant differences were found between MitoQ and the placebo in rate of disease progression (Snow *et al*, 2010). In addition, Antipodean Pharmaceuticals hoped to undertake Phase IIb clinical trial with MitoQ for its protection against non-alcoholic fatty acid disease. However, the trial was terminated due to low participant enrolment (ClinicalTrials.gov Identifier NCT01167088).

1.4.7.2 SS Peptides

Another group of mitochondrial-targeted antioxidants are the SS peptides, the most successful of which is SS-31 also known as Bendavia (Figure 1.8d). The SS peptides, which were named after their authors Hazel Szeto and Peter Schiller, are short peptide sequences of approximately 4 amino acids with a positive charge (Schiller *et al*, 2000; Zhao *et al*, 2004).

They were originally synthesised as opioid agonists but subsequent research showed they also had ROS scavenging capacity (Schiller *et al*, 2000; Zhao *et al*, 2004; Cho *et al*, 2007; Szeto, 2006). By altering the sequence of amino acids the opioid agonist action could be reduced while still maintaining the antioxidant ability (Petri *et al*, 2006). This antioxidant scavenging ability is due to the presence of the tyrosine derivative; 2,6-dimethyltyrosine (Dmt) (Zhao *et al*, 2004; Cho *et al*, 2007). However, whether the SS peptide's cellular protection is solely through its antioxidant scavenging is still controversial. In solution ROS scavenging appears to require much higher concentrations than in cells so they may be protecting cells through an alternative mechanism (Cho *et al*, 2007; Zhao *et al*, 2004).

The mitochondrial location of the SS peptides was suggested using radioactively labelled SS-02 and using a fluorescent derivative SS-19 (Zhao *et al*, 2004). However, a later study with radioactively labelled SS-31 suggested the mitochondrial uptake of SS-31 may be less than for other SS peptides (Zhao *et al*, 2005). These SS peptides, unlike MitoVitE, are not fully reliant on the mitochondrial membrane potential for their mitochondrial uptake (Zhao *et al*, 2004). Instead the mitochondrial uptake may be due to a combination of peptide lipophilicity and charge (Horton *et al*, 2008).

SOD1 mutations have been found in ALS patients therefore an ALS SOD1 mutation mouse model has been created that shows greater motor neuron susceptibility to toxins (Reaume *et al*, 1996). In this ALS mouse model SS-31 was found to slightly increase motor neuron survival and improve motor performance (Petri *et al*, 2006). In addition, SS-31 was able to reduce infarct size in rats after myocardial infarction (Cho *et al*, 2007). Therefore, SS-31, now named Bendavia is undergoing Phase II clinical trials with Stealth Peptides to assess its potential to reduce infarct size in myocardial infarction patients (Chakrabarti *et al*, 2013) (ClinicalTrials.gov Identifier: NCT01572909).

1.5 Hypothesis and Aims of this Thesis

As mentioned above, there is evidence to suggest oxidative stress, potentially from mitochondria, is involved in α-synucleinopathy neurodegeneration. For example post-mortem analysis of PD patients' brains suggest oxidative stress is involved at some stage in the disease process. Further evidence comes from recessive PD patients, which are known to have mutations in genes involved in antioxidant or mitochondrial function. In addition, the SNpc neurons lost in PD are sensitive to oxidative insults. It is possible that oxidative damage to the α-synuclein protein could increase its oligomerisation and thereby increase its toxicity. Alternatively, α-synuclein oligomers may increase the levels of oxidative stress resulting in toxicity. Therefore the hypothesis proposed is that oxidative stress is the cause of α-synuclein induced neurodegeneration. The lack of suitable models

has prevented investigation of how early in the disease process oxidative stress is involved and how influential it is in neuronal cell death. Therefore, there is a need for models that accurately represent the disease process. In addition, there is a need for commercially available potent synthetic antioxidants that can be used as tools to examine the involvement of oxidative stress in these models.

Therefore the aims of this project were to develop a model of α-synuclein-induced neuronal cell death and to determine the antioxidant scavenging potential of a synthetic flavonoid compound synthesised by Antoxis Limited. The specific aims were:

- to develop an α-synuclein induced toxicity cell model
- to develop a toxin-induced oxidative stress cell model
- to investigate the antioxidant ability of the synthetic compound, AO-1-530

Chapter 2- Materials and Methods

2.1 Cell Culture Materials

2.1.1 Cell Lines

The human neuroblastoma cell line, SH-SY5Y, was obtained from three different sources. A transgenic clone of SH-SY5Y with doxycycline inducible expression of α-synuclein was a kind gift from Dr. Kostas Vekrellis (Biomedical Research Foundation of the Academy of Athens, Greece) (Vekrellis *et al*, 2009). The second SH-SY5Y cell line was a kind gift from Dr. Mike Devine (Institute of Neurology, University College London). The third SH-SY5Y cell line was a kind gift from Professor David Porteous (Centre for Genomic and Experimental Medicine, University of Edinburgh).

The rat cell line Neuroscreen™-1 (NS-1) (Thermo Scientific, R04-0001-AP) is a subclonal derivative of the rat adrenal pheochromocytoma cell line PC-12, which was derived for use in high-throughput screening (Radio *et al*, 2008).

2.1.2 Cell Culture Media

2.1.2.1 Greece SH-SY5Y Cell Culture Medium

Since the SH-SY5Y clone from Greece carried a number of transgenes that expressed two drug-selectable markers, G418 and Hygromycin B, they were included in the medium. The α-synuclein transgene was repressed by doxycycline (Vekrellis *et al*, 2009). Therefore, the culture medium was composed of basal RPMI 1640 medium (Life Technologies, 11875) supplemented with 10% fetal bovine serum (FBS) (Life Technologies, 10270), 2 mM L-glutamine (Life Technologies, 25030), 200 µg/ml G418 (PAA Laboratories, P27-011), 50 µg/ml Hygromycin B (Roche, 843 555) and 2 µg/ml doxycycline (Sigma, D9891).

2.1.2.2 London and Edinburgh SH-SY5Y Cell Culture Medium

The SH-SY5Y cell lines from London and Edinburgh were cultured in DMEM basal medium (Life Technologies, 41965-039) supplemented with 10% FBS, 2 mM glutamine and 1 mM sodium pyruvate (Life Technologies, 11360-039).

2.1.2.3 Neuroscreen™-1 Cell Culture Medium

NS-1 cells were cultured in RPMI 1640 basal medium (Hyclone, SH30027) supplemented with 10% horse serum (Life Technologies, 26050-088), 5% FBS and 2 mM L-glutamine.

2.1.2.4 N2 Medium

In order to differentiate SH-SY5Y cells N2 medium was used. The basal medium for N2 consisted of 50% DMEM:F12 medium (Life Technologies, 21331-020) and 50% Neurobasal medium (Life Technologies, 21103). This was supplemented with an N2 supplement (200x) and L-glutamine to give a final medium concentration of 12.5 µg/ml insulin (Sigma, I-1882), 50 µg/ml apo-transferrin (Sigma, T-1147), 37.5 µg/ml bovine serum albumin (BSA) (Life Technologies, 15260-037), 9.9 ng/ml progesterone (Sigma, P8783), 8 µg/ml putrescine (Sigma, P5780), 15 nM sodium selenite (Sigma, S5261) and 2 mM L-glutamine.

2.1.2.5 Cell Freezing Medium

SH-SY5Y and NS-1 cells were frozen in cell freezing medium consisting of 50% cell culture media, 40% FBS and 10% dimethyl sulphoxide (DMSO) (VWR International, 23500.260), which was ice cold.

2.1.3 Antioxidants and Toxins

In the antioxidant protection against tBHP assays (Section 2.2.6.1-2.2.6.4) a number of antioxidants and toxins, which are listed, below were used. They were provided as powder or solution and stock solutions were made in DMSO, ethanol or media as stated below.

AO-1-530 (Antoxis Limited)	Stock 10 mM in DMSO
Myricetin (Sigma, 72576)	Stock 30 mM in DMSO
Quercetin (Sigma, Q4951)	Stock 30 mM in DMSO
Vitamin E ((+)-α-tocopherol, Sigma, T1539)	Stock 1.6 mM in ethanol (Fisher)
Idebenone (Antoxis Limited)	Stock 10 mM in DMSO
Coenzyme Q10 (Sigma, C9538)	Stock 1 mM in ethanol
tBHP (Sigma, 19990)	Stock 10 mM in media

2.2 Cell Culture Methods

2.2.1 Routine Cell Culture

2.2.1.1 SH-SY5Y Cell Culture

SH-SY5Y cells were thawed and cultured in the appropriate medium. Medium was changed every 2-3 days. When cells were 70-80% confluent they were passaged using trypsin (Life Technologies, 15090) 1 in 5 or counted and seeded for experiments at 1.25×10^5 cells/cm^2, unless otherwise stated. Cells were cultured at 37°C in a humidified atmosphere of 5% CO_2.

2.2.1.2 Neuroscreen™-1 Cell Culture

NS-1 cells were thawed and routinely passaged on cell culture dishes coated in collagen type I or pre-coated collagen type I T75 flasks (Beckton Dickinson, 356485) with NS-1 medium. In order to coat dishes or coverslips collagen type I (6 μg/cm^2, Sigma, C3867) was added and incubated overnight at 4°C or at 37°C for several hours. NS-1 cells were cultured until 70-80% confluent when they were lifted using trypsin/EDTA (Life Technologies, 25200) and passaged 1 in 5 or seeded for differentiation (Section 2.2.4.3). Cells were cultured at 37°C in a humidified atmosphere of 5% CO_2.

2.2.2 Cell Freezing

SH-SY5Y and NS-1 cells were frozen at 70-80% confluency. They were lifted and counted using a haemocytometer. SH-SY5Y cells were re-suspended to 8x10^6 cells/ml in freezing medium and NS-1 cells were frozen at 4x10^6 cells/ml in freezing medium. 0.5 ml aliquots of cells in freezing medium were added to cryovials and stored at -80°C for a couple of days before being transferred to liquid nitrogen for long term storage.

2.2.3 Coverslip Preparation

To prepare coverslips for collagen coating or for cell seeding 13 mm (VWR International, 631-0149) or 25 mm (VWR International, 631-0171) coverslips were washed in ethanol and baked at 180°C for at least 2 hours.

2.2.4 Cellular Differentiation

2.2.4.1 SH-SY5Y Differentiation (10% FBS with retinoic acid)

All three SH-SY5Y cell lines were seeded at 11.5x10^3 cells/cm^2 on cell culture treated plastic. The next day SH-SY5Y Greece cell culture medium (Section 2.1.2.1, without Hygromycin B, G418 and doxycycline) with 10 μM retinoic acid (Sigma, R2625) was added to begin differentiation. The medium was changed every 2 days until day 6, when cells were fixed in 4% paraformaldehyde (PFA) (Sigma, 158127) for immunocytochemistry (Section 2.4.6.1).

2.2.4.2 SH-SY5Y Differentiation (N2 medium with retinoic acid)

The Edinburgh SH-SY5Y cells were seeded at 11.8x10^3 cells/cm^2 on cell culture plastic or 30 μg/cm^2 poly-L-ornithine (Sigma, P4957) coated sterile glass coverslips (Section 2.2.3). Cells were left to attach and proliferate for 48 hours. The medium was then changed to N2 medium supplemented with 10 μM retinoic acid to begin differentiation. Medium was replaced every 2-3 days and cells were cultured until the desired end point when cells were

fixed in 4% PFA for immunocytochemistry (Section 2.4.6.1), lifted for RNA extraction and subsequent quantitative reverse transcription PCR (qRT-PCR) (Section 2.4.2- 2.4.4) or used for an MTS assay (Section 2.2.6.1.1 and Section 2.2.5.2).

2.2.4.3 Neuroscreen™-1 Differentiation

NS-1 cells were seeded at $3.125x10^4$ cells/cm^2, unless otherwise stated, on 6 μg/cm^2 collagen I coated dishes or coverslips. The following day medium was replaced with a 1 in 10 dilution of NS-1 medium in RPMI 1640 basal medium with 50 ng/ml nerve growth factor β (NGFβ) (Sigma, N2513). Medium was replaced on day 2. On day 3 cells were fixed in 4% PFA for immunocytochemistry (Section 2.4.6.1), lifted for RNA extraction and subsequent qRT-PCR (Section 2.4.2- 2.4.4) or cells were used for an MTS assay (Section 2.2.6.1.1).

2.2.5 Transfection and Transduction of SH-SY5Y Cells

2.2.5.1 Transfection by Liposomes

SH-SY5Y cells at 70-80% confluency were transfected using Lipofectamine® 2000 Reagent (Life Technologies, 11668027). 3.5% Lipofectamine® 2000 in Optimem® medium (Life Technologies, 31985) was mixed with 500 ng PB-CAG-mtGFP-SNCA plasmid DNA (Figure 4.2c) in Optimem® medium at a ratio of 1 to 1 and incubated at room temperature for 5 minutes. This Lipofectamine mix was then added to cells and incubated for 24 hours when cells were fixed in 4% PFA for immunocytochemistry using the α-synuclein primary antibody (Section 2.4.6.1).

2.2.5.2 BacMam Transduction

The two BacMam reagents, mitochondrial targeted GFP (mtGFP) (Life Technologies, C10600) and the generated mtGFP with α-synuclein (mtGFP-SNCA) (Figure 4.1), were used in the same way. The appropriate volume of BacMam viral solution was added to cells in culture. The volume added per 100,000 undifferentiated SH-SY5Y cells is stated in the figures and figure legends. In differentiated SH-SY5Y cells the volume added to 100 μl of media in a 96-well plate is shown, as the number of cells is unknown. Cells were incubated for the lengths of time shown below; with a 50% media change every 2 days.

- 24 hours after BacMam addition to cells they were lifted for fluorescence activated cell-sorting (FACS) analysis (Section 2.4.7). Post-acquisition analysis was performed with FlowJo X to exclude dead cells and to graph the GFP fluorescence.
- 24 and 48 hours after BacMam addition to cells they were fixed in 4% PFA for immunocytochemistry using the α-synuclein primary antibody (Section 2.4.6.1).

- 24 hours after BacMam addition protein was extracted from cells to perform a western blot (Section 2.4.5).
- 4 days after BacMam addition the MTS assay was performed (Section 2.2.6.1.2).
- 24 hours after BacMam addition, 25-250 nM rotenone (1 mM stock in DMSO, Sigma, R8875) was added for 4 days when the MTS assay was performed (Section 2.2.6.1.2).
- BacMam was added to 12 day differentiated SH-SY5Y cells and was topped up every 7 days until the desired end point of 2 weeks or 4 weeks when the MTS assay (Section 2.2.6.1.2) or α-synuclein immunocytochemistry (Section 2.4.6.1) was performed.
- 24, 48 and 72 hours after BacMam addition mitochondrial fragmentation was assessed (Section 2.2.7.8).
- 3 and 7 days after BacMam addition the DHE assay was performed (Section 2.2.7.9).

2.2.6 Cell Viability Assays

2.2.6.1 MTS Assay Experiments

2.2.6.1.1 Cell Treatments for MTS Assay

A number of cell treatments were performed where the MTS assay was used as a measure of cell viability; including SH-SY5Y and differentiated NS-1 cell number optimisation, tBHP-induced toxicity, antioxidant toxicity, antioxidant protection against tBHP-induced toxicity, intracellular AO-1-530 protection, and pre and post toxin antioxidant protection.

Initially, the cell number of SH-SY5Y and differentiated NS-1 cells was optimised for use with the MTS assay. SH-SY5Y cells (1-7 $x10^4$ cells per well) were seeded and incubated for 24 hours when the MTS assay was performed. In addition, NS-1 cells were seeded at different densities (1- 20 $x10^3$ cells per well) and differentiated for 3 days when the MTS assay was performed.

Secondly, the concentration of tBHP to use for toxicity in each cell line was assessed. SH-SY5Y cells were seeded at $1.25x10^5$ cells/cm^2 and incubated for 24 hours when tBHP was added. 5 hours later the MTS assay was performed. The NS-1 cells were differentiated for 3 days when tBHP was added for 16 hours. After this time the MTS assay was performed.

Thirdly, the antioxidant toxicity was examined. SH-SY5Y cells were seeded as above and incubated for 24 hours or NS-1 cell were differentiated for 3 days, when antioxidants were added for 16 hours or 48 hours, as stated in the figures. After this time the MTS assay was performed.

Fourthly, the antioxidant protection against tBHP-induced toxicity was assessed. SH-SY5Y cells were seeded as above and incubated for 24 hours. The cells were then pre-incubated with antioxidants (Section 2.1.3) for 30 minutes when 400 µM tBHP was added to the antioxidants for the length of time stated in the figure legends, usually 5 or 16 hours. Then the MTS assay was performed. 14-day differentiated SH-SY5Y cells (Section 2.2.4.2) were pre-incubated with antioxidant for 30 minutes when 400 µM tBHP was added for 8 hours when the MTS assay was performed. NS-1 cells were differentiated for 3 days, when antioxidants were added for 30 minutes. 200 µM tBHP was added to the antioxidants for 15 hours prior to performing the MTS assay.

Fifthly, the intracellular AO-1-530 protection was determined. SH-SY5Y cells were seeded and incubated for 24 hours, when AO-1-530 was added for 30 minutes. AO-1-530 was then removed and 400 µM tBHP was added for 5 hours when the MTS assay was performed.

Finally, the ability of AO-1-530 and quercetin to protect after tBHP addition was assessed. SH-SY5Y cells were seeded and incubated for 24 hours. Then groups of cells were treated in 3 ways: pre-incubated with antioxidant for 30 minutes before addition of tBHP; co-incubated with antioxidant and tBHP or treated with tBHP and subsequently antioxidants were added. 5 hours after 400 µM tBHP addition the MTS assay was performed.

In addition, the MTS assay was performed after BacMam treatment (as stated in section 2.2.5.2).

2.2.6.1.2 MTS Assay

The MTS assay was performed using the Promega CellTiter 96® Aqueous MTS Reagent Powder (Promega, G1112) with phenazine methosulphate (PMS) (Sigma, P9625) as the electron coupler. MTS was prepared at 2 mg/ml in dPBS, filter sterilised using a 0.22 µm filter, aliquotted and stored at -20°C. PMS was prepared at 0.92 mg/ml in dPBS, filter sterilised, aliquotted and stored at -20°C. Immediately before the MTS assay, 100 µl of PMS was added to 2 ml of MTS. 20 µl of the MTS/PMS mixture was added to each well of a 96-well plate containing 100 µl of media. The plate was incubated at 37°C/5% CO_2 for 1 hour. Then the absorbance at 490 nm and reference wavelength of 650 nm was measured using the FLUOstar OMEGA (BMG LabTech) plate reader. Subtraction of the 650 nm reference absorbance from the 490 nm absorbance gave the well absorbance. The background absorbance from the media incubated with MTS/PMS was subtracted from the well absorbance to give the sample absorbance. The percentage of the sample absorbance relative to control treated cells absorbance gave the % metabolic activity.

2.2.6.2 Lactate dehydrogenase (LDH) Assay

The Source Bioscience LDH-Cytotoxicity Assay Kit II (ABE2423) was used to perform the LDH Assay. The LDH assay was used to assess the antioxidant protection against tBHP-induced toxicity. SH-SY5Y cells were seeded at $1.25x10^5$ cells/cm^2 and incubated for 24 hours. The cells were then pre-incubated with antioxidants for 30 minutes when 400 μM tBHP was added to the antioxidants for 5 or 16 hours, as stated in the figure legends. Thirty minutes before the end of tBHP treatment cell lysis buffer was added to the high control wells. At the end of tBHP treatment the 96-well plate was gently mixed to distribute the LDH in the media. The plate was then centrifuged at 600g for 10 minutes to precipitate cells and debris. 10 μl of media from each well was moved to a new 96-well plate and 100 μl of LDH reaction mix was added to each well. The plate was then incubated at room temperature for 30-60 minutes when absorbance was read using the FLUOstar OMEGA (BMG LabTech) plate reader. The 650 nm reference absorbance was subtracted from the 450 nm absorbance reading to give the well absorbance. The background absorbance was subtracted from the well absorbance to give the sample absorbance. The sample absorbance was subtracted from control-cultured cells (low control) and divided by the cells that had been lysed (high control) minus the control cells (low control) to give the % cytotoxicity.

2.2.6.3 Propidium Iodide (PI) Assay

The PI assay was performed to assess AO-1-530 protection against tBHP-induced toxicity. SH-SY5Y cells were seeded at $1.25x10^5$ cells/cm^2 and incubated for 24 hours. The cells were then pre-incubated with AO-1-530 (1 or 10 μM) for 30 minutes when 400 μM tBHP was added for 6 or 16 hours. Then the media was collected and cells were lifted using trypsin, washed in PBS with 2% FBS and resuspended in 100 μl PBS with 2% FBS. This cell solution was filtered and incubated with PI (1 μg/ml) at room temperature for 10 minutes. Then 300 μl PBS with 2% FBS was added to dilute the cells. Cells were kept on ice until FACS analysis data was collected using the FACS Calibur and post-acquisition analysis was performed using FlowJo X. The unstained sample was used to create gates to determine PI positive cells and the percentage of PI positive and negative cells was calculated.

2.2.6.4 Images and Videos of Antioxidant Protection

Images and videos were created to show the cellular morphology after antioxidant protection against tBHP-induced toxicity. SH-SY5Y cells were seeded at $1.25x10^5$ cells/cm^2 and incubated for 24 hours. The cells were then pre-incubated with antioxidants for 30 minutes when 400 μM tBHP was added to the antioxidants. 5 hours after the addition of tBHP the

morphology of the cells was imaged in 96-well plates, using an Olympus IX51 inverted microscope.

Videos were created with cells in 12-well plates using the Zeiss Axio Observer. Immediately after tBHP addition the microscope was prepared to image every 30 minutes for 12 hours. Videos begin one hour after tBHP addition and end 13 hours after tBHP addition.

2.2.7 Other Cell Assays

2.2.7.1 Antioxidant Subcellular Localisation

SH-SY5Y cells were seeded $1.25x10^5$ cells/cm^2 on coverslips. 24 hours later the following antioxidants were added for 2 hours; 10 µM AO-1-530, 100 µM quercetin, 100 µM myricetin or DMSO as a control. Then cells were fixed in 4% PFA and counterstained with 4',6-Diamidino-2-phenylindole (DAPI) for 10 minutes. Coverslips were washed in MilliQ water and mounted onto slides using Vectashield (Vector Laboratories, H1000). Images were taken using the 63x objective of the Leica TCS SPE confocal microscope. The 488 nm laser was used to excite the antioxidants and emission was measured between 496-595 nm. DAPI was imaged using the 405 nm excitation laser.

2.2.7.2 AO-1-530 Mitochondrial Localisation

SH-SY5Y cells on coverslips (as above) were loaded with 100 nM Mitotracker Deep Red (Life Technologies, M22426) for 20 minutes before the addition of 10 µM AO-1-530 for 2 hours. The cells were then fixed in 4% PFA and processed as described above. The 635 nm laser was used to excite Mitotracker Deep Red.

2.2.7.3 Intracellular Antioxidant Fluorescence (FACS)

SH-SY5Y cells were seeded at $1.25x10^5$ cells/cm^2 and treated as above for antioxidant localisation but 2 hours after antioxidant addition cells were lifted using trypsin, washed in PBS with 2% FBS and resuspended in 100 µl PBS with 2% FBS. The cell solution was then filtered and cells were incubated with PI (1 µg/ml) on ice. 300 µl PBS with 2% FBS was added. Cells were kept on ice until fluorescence was analysed using the FACS Calibur. Post-acquisition analysis using FlowJo X was used to exclude PI positive cells and to graph the cells positive for green, FL-1, fluorescence.

2.2.7.4 CellROX® Deep Red Assay

SH-SY5Y cells were seeded at $6.25x10^4$ cells/cm^2 on 13 mm coverslips. 24 hours later cells were incubated with 10 µM CellROX® Deep Red (Life Technologies, C10422) and 2.8 µg/ml Hoechst 33342 (Fluka, 14533) for 30 minutes. CellROX® and Hoechst 33342 were

removed and cells were washed three times with complete medium. Antioxidant or DMSO vehicle was added for 30 minutes, and then 400 μM tBHP was added. One hour after tBHP addition, 13 mm coverslips were placed onto a 25 mm coverslip inside an Attofluor® Cell Chamber (Life Technologies, A-7816) holder and washed with Hank's balanced salt solution (HBSS) with calcium and magnesium. Images were taken of phase contrast, CellROX® Deep Red and Hoechst 33342 fluorescence. Multiple areas (5-6) of each coverslip were imaged. Post-acquisition analysis was performed using Volocity. A small area around each apparent cell nuclei was selected in all images and the mean fluorescence in arbitrary units (au) in these areas was calculated. The mean and standard error of mean (SEM) were calculated from the fluorescence value of each image.

2.2.7.5 Ratio of Oxidised and Reduced Glutathione

The GSH/GSSG Ratio Assay Kit from Merck Millipore (371757) was used with metaphosphoric acid (Sigma, 04103). Cells were incubated as previously with AO-1-530 or DMSO vehicle control for 30 minutes before the addition of 400 μM tBHP for 2 hours. Cells were then washed in ice cold PBS, scraped from the cell culture plates and placed on ice. After centrifugation at 300g for 5 minutes pellets were resuspended in 5% metaphosphoric acid and lysed using a 25-gauge needle. Immediately a sample was moved to 1-methyl-2-vinylpyridinium trifluoromethanesulphonate (M2VP) to scavenge the GSH leaving the GSSG. Samples were then centrifuged to remove debris and the supernatant was moved to a fresh 1.5-ml microfuge tube. Samples were then diluted 1:61 for GSH and 1:15 for GSSG in the appropriate assay buffer. 50 μl sample, blank or standard was loaded into a 96-well plate in duplicate. To this 50 μl chromagen and 50 μl enzyme was added. The plate was mixed gently and incubated at room temperature for 5 minutes. Then 50 μl NADPH was added and the change in absorbance 412 nm was measured every 15-30 seconds for 3 minutes using a FLUOstar OMEGA (BMG LabTech) plate reader. The slopes were calculated, the blank sample was subtracted and concentration was determined relative to the standard curve for GSH. From this the percentage GSH and GSSG were determined.

2.2.7.6 Nrf2 Experiment

SH-SY5Y cells were seeded at $1.25x10^5$ cells/cm^2 on coverslips and incubated for 24 hours when AO-1-530 or DMSO as a control was added for 30 minutes. Then 400 μM tBHP was added for 4.5 hours when cells were fixed in 4% PFA for Nrf2 immunocytochemistry (Section 2.4.6.1) or lifted for RNA extraction and subsequent qRT-PCR (Sections 2.4.2-2.4.4). After immunocytochemistry Nrf2 images were quantified using ImageJ. The z-stack images were flattened and a mask was created using the DAPI channel. This mask was then

used to calculate the nuclear red fluorescence intensity. The mean fluorescence from each image (2-4 images) and from each coverslip was calculated.

2.2.7.7 8-Hydroxy-2-deoxyguanosine (8-OHdG) Experiment

SH-SY5Y cells were seeded at $1.25x10^5$ cells/cm^2 on coverslips and incubated for 24 hours when AO-1-530 or vehicle control, DMSO, was added for 30 minutes. Then 400 μM tBHP was added for 4.5 hours when cells were fixed in 4% PFA for 8-OHdG immunocytochemistry (Section 2.4.6.1). The 8-OHdG images were quantified using ImageJ. The z-stack images were flattened and a mask was created using the DAPI channel, this mask included the nuclei and the area surrounding the nuclei by reducing the threshold. This mask was then used to calculate the nuclear green fluorescence intensity. The mean fluorescence from each image was calculated.

2.2.7.8 Mitochondrial Fragmentation

SH-SY5Y cells were seeded onto 25 mm coverslips at $2.5 x10^4$ cells/cm^2. The next day the appropriate volume of BacMam was added (as stated in Figure 4.13). Mitochondrial morphology was analysed 24, 48 and 72 hours after transduction. To analyse mitochondrial morphology coverslips were placed into the Attofluor® Cell Chamber with medium. This coverslip holder was loaded onto an inverted confocal Leica TCS SP2 microscope with an environmental chamber to keep the temperature at 37°C and CO_2 at 5%. The GFP was excited using the 488 nm laser and z-stack images were acquired. Subsequently the images were randomised and analysed blind using ImageJ. The axis of the mitochondria in each cell was calculated by dividing the length of the mitochondria by the width. Cells which contained mitochondria with an axis of >10 μm were classified as tubular, those with an axis of <3 μm were classified as fragmented and cells which contained both types of mitochondria were classified as intermediate. Excel was used to calculate and plot the percentage of cells at each time-point with each type of mitochondrial morphology.

2.2.7.9 Dihydroethidium (DHE) ROS Production Assay

DHE (Life Technologies, D11347) was dissolved in DMSO to a concentration of 5 mM. This compound is oxidised to ethidium and 2-hydroxyethidium, and upon binding to DNA, it fluoresces strongly in the red channel (excitation/emission, 518 nm/ 605nm). To perform the DHE assay, 25 mm coverslips with BacMam-treated adherent SH-SY5Y cells (Section 2.2.5.2) were placed into an Attofluor® Cell Chamber. This coverslip holder was placed onto the Zeiss Axio Observer microscope stage and an appropriate area containing cells was selected. DHE (5 μM) in HBSS was added to the cells and time-lapse images with the

appropriate filter to detect ethidium and 2-hydroxyethidium (605 nm emission) were taken every 8 seconds for 15 minutes. Subsequently, areas within the cell nuclei were selected using Volocity and the average red fluorescence intensity for each image was measured over time. The red fluorescence intensity was plotted against time using Excel and linear regression was performed to calculate the slope. The slope was a measure the rate of ROS production.

2.3 Mouse Brain Stem Slice Cultures

2.3.1 Mouse Brain Slice Culture Medium

The basal medium for mouse brain slice cultures contained 50% MEM with Earle's salts (Life Technologies, 32360-026) and 25% Earle's balanced salt solution (Life Technologies, 24010-043). This was supplemented with 25% heat-inactivated horse serum (Life Technologies, 26050-088), 10 U/ml Penicillin, 10 µg/ml Streptomycin (Life Technologies, 15140-122), 2 mM Glutamax (Life Technologies, 35050-038), 6.5 mg/ml glucose (Sigma, G8769), 1.25 µg/ml Fungizone (Life Technologies, 15290-018). The complete medium was then sterile-filtered using 0.22 µm filter (EMD Millipore).

2.3.2 Mouse Brain Stem Slices

All animal procedures were performed according to the Animal Scientific Procedures Act, UK, 1986. Mouse brain stem slices were performed as in Zhang *et al*, 2011. Briefly, P0-P2 mice pups were decapitated and the hindbrain was dissected into L15 medium (Sigma, L5520). Sagittal sections (300 µm) of the hindbrain were cut using a McIllwain Tissue Chopper. Sections were then separated in slice culture medium and placed onto Millicell CM organotypic culture inserts (EMD Millipore, PICM0RG50) in 6-well plates. They were cultured for 8 days with a medium change every 2 days and fixed in 4% PFA for 45 minutes when colourimetric immunohistochemistry (Section 2.4.6.2) or immunocytochemistry for α-synuclein, TuJ-1 and Synapsin I (Section 2.4.6.1) was performed.

2.4 Molecular Biology

2.4.1 DNA Cloning Techniques

2.4.1.1 Plasmids

Three DNA plasmids were used for the DNA cloning in this thesis. One was the GeneArt Construct, which was synthesised by Life Technologies from the DNA sequence of mtGFP-SNCA that we provided (Figure 4.1a). The second was pENTR2B2, which is a Life Technologies Gateway Entry Vector (Figure 4.1c) and was a kind gift from Dr. Keisuke Kaji

(MRC Centre for Regenerative Medicine, University of Edinburgh). This entry clone was required to insert mtGFP-SNCA so Life Technologies could synthesise the BacMam construct. The third plasmid was a destination vector for Gateway Cloning, PB-CAG (Figure 4.2b), which was a kind gift from Dr. Keisuke Kaji (MRC Centre for Regenerative Medicine, University of Edinburgh). After mtGFP-SNCA insertion into PB-CAG by Gateway Cloning the mtGFP-SNCA would be under the control of the pCAG promoter. Lipofection of this into cells would allow the expression of mtGFP-SNCA to be tested.

2.4.1.2 Restriction Enzyme Digestion

Restriction enzymes were used to produce plasmid fragments for ligation and as a diagnostic test to confirm the plasmid produced contains the insert. To produce fragments for ligation the GeneArt construct and the Gateway Entry Clone pENTR2B2 were digested. 3 µg of the GeneArt construct containing mtGFP-SNCA was digested with BamHI (10 units, New England Biolabs (NEB), R0136) and EcoRI (10 units, NEB, R0101) in a 30 µl reaction, containing buffer number 3 and BSA (Figure 4.1a). 2 µg of the Gateway Entry Vector pENTR2B2 (Figure 4.1c) was digested using BamHI (10 units) and EcoRI (10 units) in a 20 µl reaction, containing buffer number 3 and BSA. For diagnostic testing of the ligated plasmid pENTR2B2-mtGFP-SNCA (Figure 4.1e) the restriction enzymes EcoRV (NEB, R0195S) and BstxI (R0113S, NEB) were used with buffer number 3. For diagnostic testing of the PB-CAG-mtGFP-SNCA plasmid (Figure 4.2c) the restriction enzymes EcoRV and SalI-HF® (R3138S, NEB) were used with buffer number 3 in the presence of BSA. Reaction mixes were incubated at 37°C for 1-2 hours. The fragments were then loaded onto an agarose gel for analysis of fragments or for gel extraction (Section 2.4.1.4).

2.4.1.3 Gateway Cloning

Gateway Cloning was performed to move the insert from the Entry Clone pENTR2B2-mtGFP-SNCA (Figure 4.1e and 4.2a) into the destination vector PB-CAG (Figure 4.2b). 10 µl reactions were set up using 2 µl Gateway® LR Clonase® II (Life Technologies, 11791), 150 ng PB-CAG, 150 ng pENTR2B2-mtGFP-SNCA and Tris-EDTA buffer solution (4.8 µl). The reaction was allowed to proceed at room temperature for 60 minutes. The reaction was stopped by addition of 2 µg Proteinase K and incubation at 37°C for 10 minutes. The DNA products were transformed into competent DH5α cells (Sections 2.4.1.7).

2.4.1.4 DNA Electrophoresis

DNA electrophoresis was performed after restriction digests (Section 2.4.1.2) for analysis of DNA fragments and for gel extraction. 0.8-1% (w/v) agarose gels containing 1x SyberSafe (Life Technologies, S33102) for DNA band visualisation was prepared in 1x TAE Buffer (40 mM Tris (Sigma), 20 mM Acetic Acid (Fisher), 1 mM EDTA (Sigma)). Samples were loaded with Orange G (Sigma) alongside a 1kb marker (Life Technologies, 15615-016). Gels were run at 100 V for 30-60 minutes. Fragments sizes, from BamHI/EcoRI digestion of pENTR2B2 and the GeneArt construct, for gel extraction are stated in section 2.4.1.5. The EcoRV/BstxI digestion of pENTR2B2-mtGFP-SNCA gave fragments of around 2415 and 1191 base pairs. Whereas the EcoRV/SalI-HF® digest of PB-CAG-mtGFP-SNCA gave fragments of around 4368, 1922 and 1350 base pairs.

2.4.1.5 DNA Extraction from Agarose Gel

The 1323 base pair fragment from the GeneArt Construct BamHI/EcoRI restriction digest (Figure 4.1b) and the 2283 base pair fragment of the pENTR2B2 BamHI/EcoRI restriction digest (Figure 4.1d) were extracted from agarose gel using the QIAquick Gel Extraction kit (QUIAGEN, 28704) according to the manufacturer's instructions.

2.4.1.6 DNA Fragment Ligation

The DNA fragments extracted from the agarose gel (Section 2.4.1.5) were ligated using T4 DNA ligase (Life Technologies, 15224). A molar ratio of 1:4, pENTR2B2 fragment to GeneArt Construct fragment, was added to T4 DNA ligase and T4 DNA ligase buffer. The reaction was incubated at room temperature for 20 minutes before placing on ice. Ligated fragments were transformed into DH5α cells for DNA isolation (Sections 2.4.1.7 and 2.4.1.8).

2.4.1.7 Bacterial Transformation

The ligation products of pENTR2B2-mtGFP-SNCA and the Gateway Cloning products of PB-CAG-mtGFP-SNCA, were transformed into DH5α cells to analyse the products. 5 µl of the ligation mix or 11 µl of the Gateway Cloning mix was added to 100 µl of DH5α competent cells. They were mixed and incubated on ice for 30 minutes. DH5α competent cells were heat shocked at 42°C for 30-45 seconds and placed on ice for 2 minutes. 250 µl LB broth was added to the bacteria and cultures shaken at 37°C with 200 rpm for 1 hour. Cultures were then plated onto Kanamycin (50 µg/ml) selection agar plates for pENTR2B2-mtGFP-SNCA or carbenicillin (50 µg/ml) selection agar plates for

PB-CAG-mtGFP-SNCA and incubated at 37°C overnight. Then DNA isolation was performed on selected colonies (Section 2.4.1.8).

2.4.1.8 DNA Isolation from Bacteria

The colonies produced on the agar plates from the bacterial transformation of pENTR2B2-mtGFP-SNCA and PB-CAG-mtGFP-SNCA (Section 2.4.1.7) were used for DNA isolation from bacteria. A single bacterial colony was picked and used to inoculate 4 ml LB broth containing appropriate antibiotic (As in section 2.4.1.7). Cultures were shaken overnight at 200 rpm at 37°C. The next day DNA was isolated from the cells using the QIAprep™ Spin Miniprep kit (QIAGEN, 27104) according to manufacturer's instructions. The samples containing the correct plasmids were selected after restriction digest diagnostic testing (Section 2.4.1.2).

2.4.2 RNA Extraction

RNA extraction was performed by 2 methods. RNA was extracted from NS-1 cells using the QIAGEN RNeasy Micro Kit (QIAGEN, 74004). Undifferentiated and differentiated SH-SY5Y RNA was extracted using the Epicentre MasterPure™ Complete DNA and RNA Purification Kit (Epicentre, MC85200). Both kits were used according to manufacturer's instructions. RNA concentration was quantified using a Nanodrop spectrophotometer according to manufacturer's instructions.

2.4.3 cDNA Synthesis

Total RNA (1-2 µg) was used for cDNA synthesis. RNase free water was added to the RNA to give a 10 µl sample. The samples were incubated with 1 µl dNTP mix (10 mM, Life Technologies, 10297018) and 1 µl random primers (50 ng/µl, Thermo Fisher, PCR-545-020T) at 65°C for 5 minutes and then chilled on ice. After brief centrifugation, 4µl 5x First strand buffer (Life Technologies, Y02321), 2 µl 0.1M DTT (Life Technologies, Y00147) and 1µl RNAse OUT (40 units/µl, Life Technologies, 10777019) were added. The contents was incubated at 37°C for 2 minutes. Then 1 µl M-MLV reverse transcriptase (200 units/µl, Life Technologies, 28025013) or 1 µl RNase free water for the negative reverse transcriptase sample was added. This was mixed and incubated at room temperature for 10 minutes when it was moved to 37°C for 60 minutes. The reaction was inactivated by incubation at 90°C for 10 minutes. The cDNA mix was placed on ice and 80 µl RNase free water was added. The cDNA samples were then ready for qRT-PCR.

2.4.4 Quantitative Reverse Transcription PCR (qRT-PCR)

qRT-PCR was performed using the Roche LightCycler® 480 System with the Universal Probe Library (UPL) (Roche). The Roche UPL Assay design centre was used to design intron-spanning primers with a specific UPL probe (Table 2.1). Reactions containing primers, UPL Probe, UPL Probe Master Mix (Roche) and PCR water were performed in 386-well plates as described in the manufacturer's instructions. The results were normalised to TATA-binding protein (*TBP*) and the mean of biological replicates with SEM were calculated.

Gene	Primer (5' – 3')	UPL Probe Number
hTBP	F gaacatcatggatcagaacaaca	87
	R atagggattccgggagtcat	
hENO2	F ttgtcagggactatcctgtgg	27
	R ggatccctacattggctgtg	
hMAP2	F ctctcctgtgttaagcggaaa	62
	R aatacactgggagccagagc	
hSYP	F caaggagatgcctgtctgc	17
	R aggttcaggaagccgaaca	
hDBH	F tggctactgcacggacaa	16
	R agctgagaggcgaagatgtg	
hTH	F gtaagcagaacggggaggt	56
	R tctcaggctcctcagacagg	
hVMAT2	F tggcaatcagcaggaagg	67
	R cgggattctgcatcatgttt	
hSLC6A4	F tgtctgaggtggccaaaga	75
	R atgttggctatcgcttctgc	
hSNCA	F gagggagtggtgcatggt	68
	R tgctgtcacacccgtcac	
hCHAT	F catcgtcctggtgcagtg	4
	R gagctcgctgacggagtc	
hNFE2L2/hNrf2	F acacggtccacagctcatc	18
	R tgcctccaaagtatgtcaatca	
hHMOX1	F cagtcaggcagagggtgatag	42
	R agctcctgcaactcctcaaa	
hNQO1	F acgctgccatgtatgacaaa	9
	R ggatcccttgcagagagtaca	
rTBP	F ccctatcactcctgccaca	110
	R ggtcaagtttacagccaagattc	
rBach1	F acagcgagtcctgttctgc	15
	R ttgagcattgaaaggcagttt	
rCKB	F gacctcaacccagacaacct	85
	R gcgagctcagcacgtagtt	
rGAP43	F cggagactgcagaaagcag	63
	R cgggcactttccttaggttt	
rVGF	F agacgggtccggattttc	10
	R ggtacccagtgcctcctg	

Table 2.1 – qRT-PCR primer sequences and UPL probe numbers
F - Forward primer; R- Reverse primer. h -human primers; r -rat primers.

2.4.5 Western Blot

All solutions for the western blot were from Fisher and all powders from Sigma, unless otherwise stated. Cells were lysed using RIPA Buffer (Santa Cruz, sc-24948) with Protease Inhibitor Cocktail (Roche, 05892791001), according to manufacturer's instructions. These were kept on ice for 30 minutes. The samples were then sonicated to break up the DNA and centrifuged to remove debris. To determine sample protein concentration the BioRad DC Protein assay (500-0111) was used, according to manufacturer's instructions using BSA for the standard curve. Samples were prepared for loading into the gel by incubating 10 µg protein with NuPAGE® LDS Sample Buffer (4x, Life Technologies), NuPAGE® Reducing Agent (10x, Life Technologies) and deionised water (to 10 µl) at 75°C for 10 minutes. The gel (4-12% Bis-Tris NuPAGE® gel, Life Technologies, NP0322BOX) was loaded into the tank with running buffer (20x NuPAGE® MOPS SDS Running Buffer in deionised water, Life Technologies, NP0001). Protein samples were loaded along with the SeeBlue Plus 2 protein marker (LC5925, Life Technologies). The gel was run at 200 V for 70 minutes at room temperature.

Nitrocellulose membranes (Amersham Hybond ECL, GE Healthcare Life Science, RPN68D) were soaked in distilled water for 30 seconds and then incubated with transfer buffer (3.02 g Tris, 14.4 g glycine, 800 ml water and 200 ml methanol). The gel was removed and prepared for transfer to the nitrocellulose membrane. The transfer apparatus was assembled with the sponge, two pieces of Whatman paper, the gel, then the nitrocellulose membrane, two pieces of Whatman paper and another sponge, being careful to avoid bubbles. It was then loaded into the transfer tank, transfer buffer was added and the blot was run at 395 mA for 70 minutes at 4°C.

The membrane was removed and incubated in blocking solution (10% non-fat powdered milk in 0.05% TBS-N buffer (8.775 g NaCl, 1.22 g Tris base, 0.74 ml concentrated hydrochloric acid in 1 L distilled water) with 0.05% NP-40) overnight at 4°C. After removal of blocking solution the membrane was incubated with primary antibody (α-synuclein 1:1000, BD Biosciences, 610787 or GFP, 1:1000, Life Technologies, A11122) in blocking solution (5% non-fat powdered milk in 0.15% TBS-N (as 0.05% TBS-N but with 0.15% NP-40)) at room temperature for 2 hours. The membrane was washed 3 times for 15 minutes in wash buffer (TBS, 0.5M NaCl and 0.3% Triton X-100) and then incubated with secondary antibody (anti-mouse HRP; 1:7000, Promega, W402B or anti-rabbit; 1:7000; Promega, W401B) in blocking buffer for 1 hour at room temperature. Subsequently, the membrane was washed in wash buffer 3 times for 15 minutes before HRP was detected using the Pierce ECL Western Blot substrate kit (Thermo Scientific, 32109), according to

manufacturer's instructions. Then the membrane was wrapped in cling film, exposed to autoradiographic film and the film was developed using an automated autoradiograph developer. Images were scanned and band intensities were analysed using ImageJ.

2.4.6 Histochemical Techniques

2.4.6.1 Immunocytochemistry

Cells were fixed by the addition 4% PFA (Sigma) for 20 minutes, unless otherwise stated. They were then washed three times with PBS. Immunocytochemistry was performed by the addition of blocking buffer (0.1% Triton X-100 or 0.3% Triton-X100 for nuclear staining, 2% goat serum, PBS) for 0.5 to 1 hour. Primary antibodies (Table 2.2) in blocking buffer were added to cells for 16 hours at 4°C, when they were washed 3 times in PBS with 0.1% Triton X-100. Secondary antibodies (Table 2.3) in blocking buffer were incubated with cells for 2 to 2.5 hours at room temperature in foil, when they were washed 3 times in PBS with 0.1% Triton X-100. DAPI (10-50 μg/ml, Life Technologies, D1306) in PBS was added for 5 to 10 minutes. Cells were imaged using Olympus IX51 inverted fluorescence microscope unless otherwise stated.

Antigen	Clone/Cat No.	Isotype	Concentration	Supplier
Class III β-tubulin (TUBB3)	TuJ-1/ MAB1195	Mouse IgG2a	1:1000	R&D Systems
Tyrosine hydroxylase (TH)	AB152	Rabbit	1:1000	Chemicon (Millipore)
Microtubule associated protein-2 (MAP2)	ab32454	Rabbit	1:500	Abcam
Synapsin I	AB1543	Rabbit	1:1000	Millipore
α-Synuclein	610787	Mouse IgG1	1:500	BD Transduction Laboratories
Nrf2	C-20/ sc-722	Rabbit	1:800	Santa Cruz
8-OHdG	15A3/ ab62623	Mouse IgG2b	1:1000	Abcam

Table 2.2 – Primary antibodies used for immunocytochemistry

Antigen	Isotype	Conjugate	Concentration	Supplier
Mouse IgG2a	Goat IgG	AlexaFluor 488	1:1000	Molecular Probes
Rabbit IgG	Goat IgG	AlexaFluor 555	1:1000	Molecular Probes
Mouse IgG2a	Goat IgG	AlexaFluor 594	1:1000	Molecular Probes
Rabbit IgG	Goat IgG	AlexaFluor 488	1:1000	Molecular Probes
Mouse IgG1	Goat IgG	AlexaFluor 488	1:1000	Molecular Probes
Mouse IgG1	Goat IgG	AlexaFluor 555	1:1000	Molecular Probes
Rabbit IgG	Goat IgG	AlexaFluor 647	1:1000	Molecular Probes
Mouse IgG2b	Goat IgG	Alexa Fluor 488	1:1000	Molecular Probes

Table 2.3 – Secondary antibodies used for immunocytochemistry

2.4.6.2 Colourimetric Immunohistochemistry

Envision+ System-HRP DAB kit (DAKO, K4006) was used with the α-synuclein primary antibody, according to manufacturer's instructions.

2.4.7 FACS Analysis

Cells were lifted using trypsin, washed in PBS with 2% FBS and resuspended in 100 µl PBS with 2% FBS. The cell solution was filtered and incubated with PI (1 µg/ml) at room temperature for 10 minutes or put directly on ice. 300 µl PBS with 2% FBS was added. Cells were kept on ice until fluorescence was analysed using the FACS Calibur. FlowJo X was used to perform post-acquisition analysis.

2.5 Other Methods

2.5.1 Antioxidant Fluorescence

1 mM solutions of AO-1-530, myricetin and quercetin in DMSO were added to a 96-well plate in triplicate. The fluorescence was read using a FLUOstar OMEGA (BMG LabTech) plate reader with excitation 485 nm and emission 520 nm. DMSO background fluorescence was subtracted.

2.5.2 Galvinoxyl Absorbance

Gavinoxyl (8 µM, Sigma, G307) in DMSO with the appropriate antioxidant concentrations were added to a 96-well plate. The absorbance change at 428 nm over time was measured using FLUOstar OMEGA (BMG LabTech) plate reader. DMSO absorbance was subtracted to give the galvinoxyl absorbance. The difference between galvinoxyl alone and galvinoxyl

with the antioxidants was calculated to give a change in absorbance. This was then plotted against antioxidant concentration. The slope of the change in absorbance was also calculated.

2.5.3 Galvinoxyl Electron Paramagnetic Resonance (EPR) Spectroscopy Experiments

The EPR experiments were performed with the help of Dr. Tilo Kunath, Dr. Janet Lovett (Centre of Magnetic Resonance, University of St. Andrews) and Dr. Mark Miller (BHF Centre for Cardiovascular Science, Queens Medical Research Institute (QMRI), University of Edinburgh). Galvinoxyl (182 μM) was mixed with 5 μM or 10 μM antioxidants in DMSO. These were then loaded into capillaries. The capillary was loaded into the Tech Miniscope MS200 ESR Machine at the QMRI and measurements were taken. Measurements were taken 2, 4 and 6 minutes after addition of antioxidant to galvinoxyl. EPR Settings: BO= 3364.05 G; Sweep= 69.59 G; Sweep Time= 20 s; Smooth= 0 s; Steps= 4096; Number of passes= 1 pass; Modulation= 1500 G; Mw atten= 7dB; Gain= 1E2; Phase= 180.

2.6 Statistical Analysis

Statistical Analysis was performed in Minitab using the Analysis of Variance (ANOVA) statistical test with a Tukey's post-hoc test.

Chapter 3 – Neuronal Cell Models

3.1 Introduction

The symptoms experienced in α-synucleinopathies are caused by the loss of neurons in the brain. For example, the Parkinsonism motor symptoms, including tremor and slow movement, are caused by the loss of SNpc dopaminergic neurons (Parent & Parent, 2010). In addition, the loss of serotonergic and noradrenergic neurons in the brain stem result in sleep disturbances (Boeve *et al*, 2007). Therefore to model α-synucleinopathies a neuronal cell model was needed.

3.2 Neuronal Cell Lines

3.2.1 Clonal Variability of SH-SY5Y Cell Lines

The SK-N-SH cell line was derived from a bone marrow aspiration of a female patient who had a neuroblastoma in the upper chest, which spread to the bone marrow. This cell line contained both epithelial and neuroblast-like cells (Biedler *et al*, 1973). Repeated subcloning of this cell line to remove the epithelial cells produced a number of cell lines, including the thrice-subcloned SH-SY5Y cell line (Biedler *et al*, 1978). Originally, the SH-SY5Y cell line appeared to be a homogeneous neuroblast-like population (Biedler *et al*, 1978). However, longer-term culture showed the presence of both epithelial and neuroblast-like cells (Ross *et al*, 1983). The neuroblast-like cells are thought to be of sympathetic nervous system origin, with fetal sympathetic neuron morphology (Ross *et al*, 1983). Further analysis of the SK-N-SH and SH-SY5Y cell lines suggests they have properties of catecholaminergic and cholinergic neurons (Biedler *et al*, 1978; Ciccarone *et al*, 1989).

SH-SY5Y cells are used extensively in the literature, especially as a cell model of PD, and are referred to as a dopaminergic cell line. However, few groups assess whether the cell line has dopaminergic or even catecholaminergic characteristics. This is necessary since long-term culture of this cell line is known to cause loss of their neuronal character. Therefore, the presence of catecholaminergic and neuronal proteins was assessed in three SH-SY5Y cell lines from different sources – London, Greece and Edinburgh (Figure 3.1). Immunocytochemistry for the catecholaminergic marker TH and the neuronal marker TuJ-1 in the undifferentiated state showed the three SH-SY5Y cell lines were all different (Figure 3.1a). The cell line from London contained only a few TuJ-1 positive cells and no TH staining, suggesting it had lost its neuronal character. In contrast, the cell line from Greece stained positive for TuJ-1 and weakly positive for TH, suggesting it is capable of

catecholamine synthesis. Finally, the cell line from Edinburgh stained positive for TuJ-1 but was negative for TH.

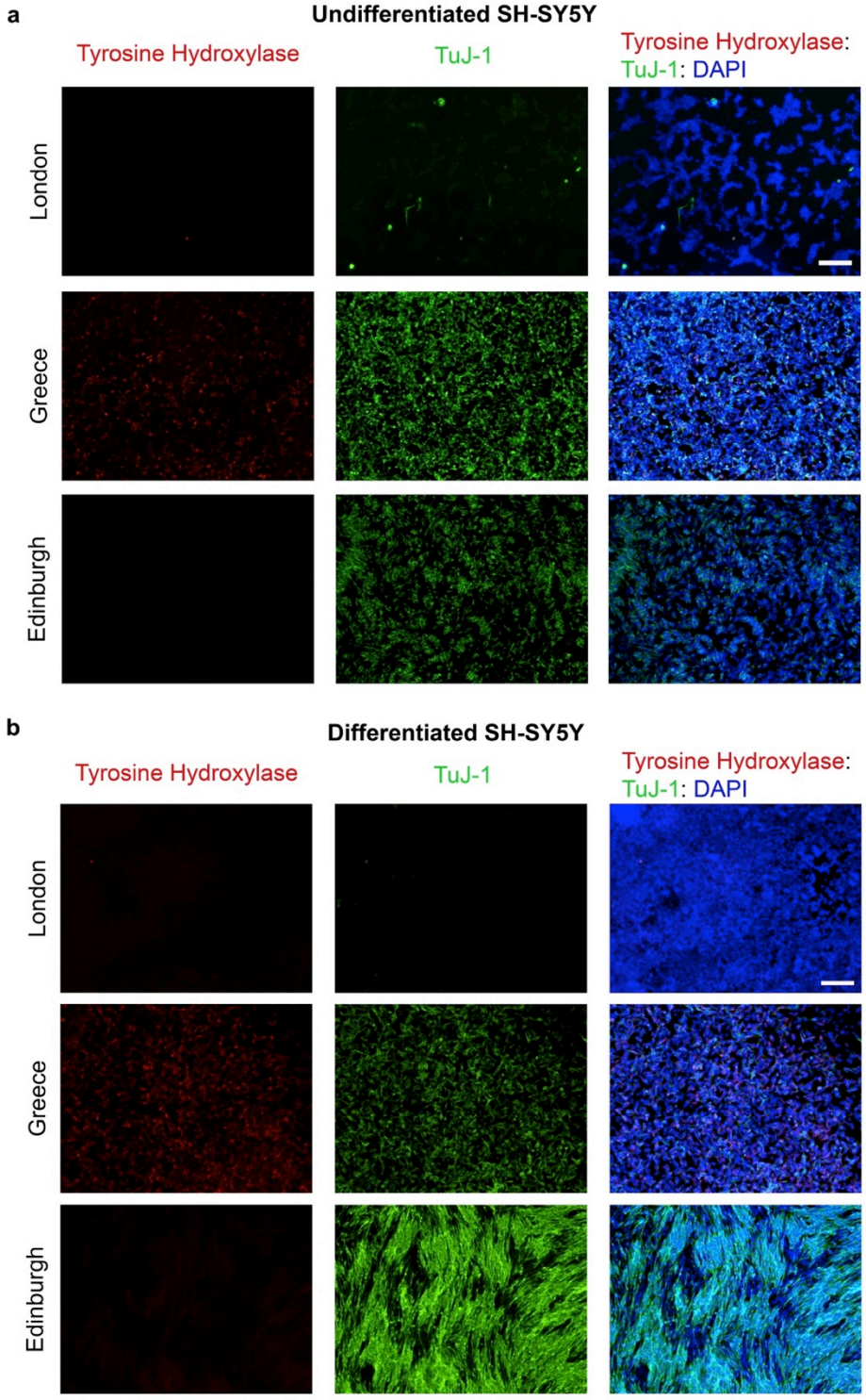

Figure 3.1 - SH-SY5Y cell lines from different sources express different markers and have varied differentiation potential. Immunocytochemistry for the neuronal marker TuJ-1 (green) and the catechloaminergic marker TH (red) was performed on fixed undifferentiated (a) and 6-day differentiated (b) SH-SY5Y cell lines from three different labs, London, Greece and Edinburgh. Cell lines were differentiated by the addition of 10% FBS medium with 10 μM retinoic acid. DAPI staining (blue) was used to mark cell nuclei; scale bar: 160 μm.

SH-SY5Y cells can be differentiated by the addition of retinoic acid to cell culture media. These three SH-SY5Y cell lines were differentiated in 10% FBS containing cell culture medium with the addition of 10 μM retinoic acid for 6 days (Figure 3.1b). The London cell line continued to proliferate and the cells did not elongate. These cells were negative for both TH and TuJ-1, confirming they had lost their neuronal properties. In contrast, the line from Greece showed most of the cells halted or reduced proliferation and the cells elongated. These cells stained positive for TH and TuJ-1. The cell line from Edinburgh showed elongation of the cells and extension of neurites but they also continued to proliferate. These cells were positive for TuJ-1 but were negative for TH, indicating they are neuronal but not catecholaminergic. This shows the clonal variability of SH-SY5Y cells, highlighting the importance of investigating the characteristics of different SH-SY5Y subclones.

From this data the most appropriate cell line to choose, as a model for α-synucleinopathies would be the one from Greece. However, this cell line had been transduced with ectopic transgenes, therefore the cell line from Edinburgh was chosen due to its neuronal characteristics.

3.2.2 Edinburgh SH-SY5Y Cell Line

The SH-SY5Y cell line referred to from here onwards in this thesis is the Edinburgh SH-SY5Y cell line. This SH-SY5Y cell line was found to continue to proliferate after retinoic acid addition to serum containing medium; therefore a literature search was performed to find an alternative differentiation method. Forsby, 2011 used the neuronal medium N2 with the addition of retinoic acid (Forsby, 2011). This produced cells with a neuronal morphology, with small cell bodies and extended neurites. Therefore, the SH-SY5Y cell line was differentiated using this method (Figure 3.2).

Replacing the basal FBS containing medium with N2 medium reduced the proliferation rate of the cells. Cells began to extend neurites as early as day 3 and the number of neurites increased over time. To confirm their neuronal character cells were fixed and immunocytochemistry was performed for TuJ-1, and the catecholaminergic marker TH (Figure 3.3). As the morphology suggested the cells were neuronal shown by TuJ-1 staining. The cells project neurites within 7 days and develop extensive neuronal networks by day 14. In addition, by day 14 clusters of cell bodies can be seen with neurites projecting out from them. As was found in the serum containing medium the cells did not express high levels of TH, suggesting they are not catecholaminergic.

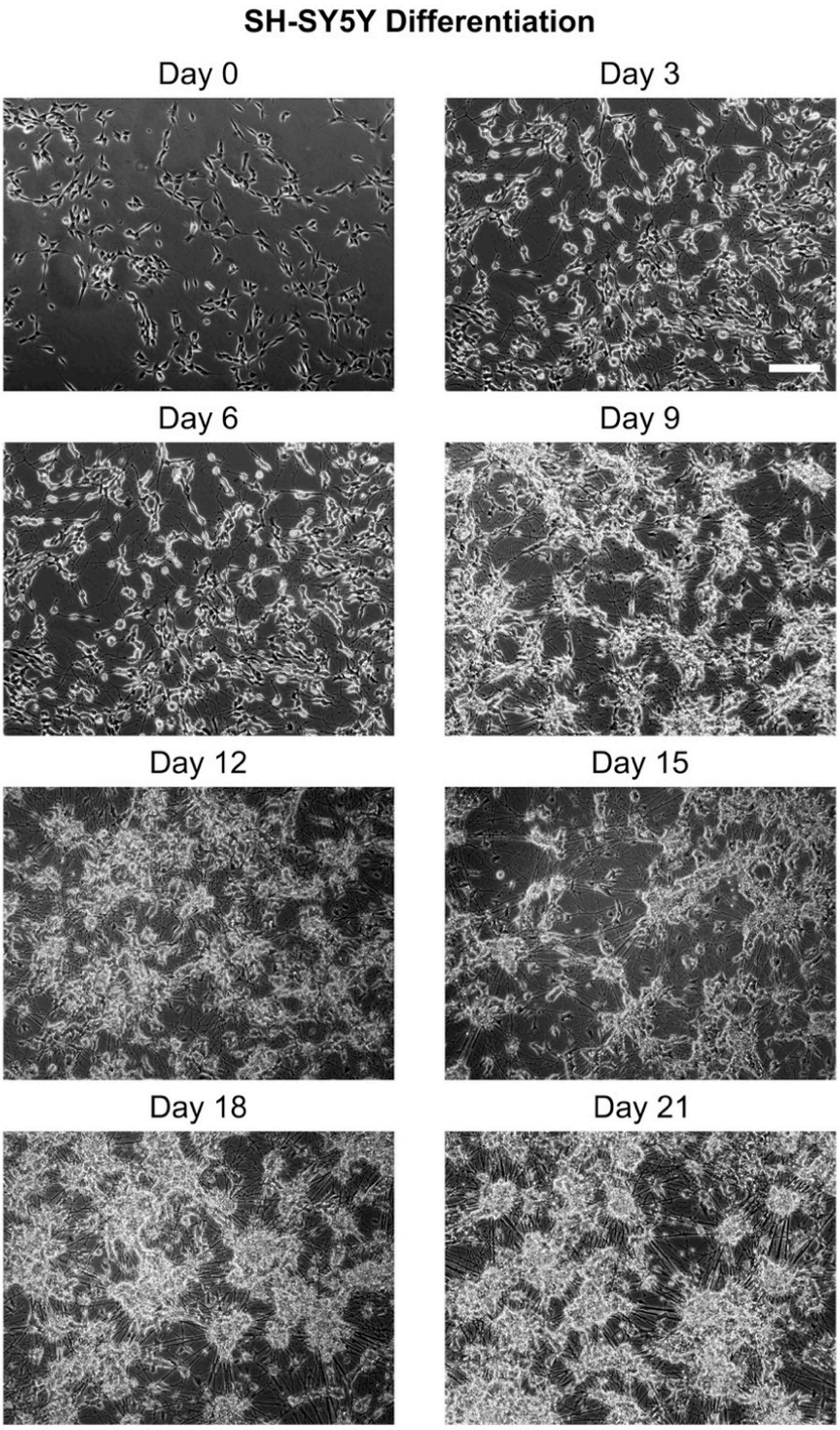

Figure 3.2 - Morphological changes during the differentiation of SH-SY5Y cells in the presence of N2 medium with 10 µM retinoic acid. SH-SY5Y cells were cultured for 48 hours before differentiation was started, by the addition of N2 medium with 10 µM retinoic acid. Images of live cells were taken every 3 days; scale bar: 160 µm.

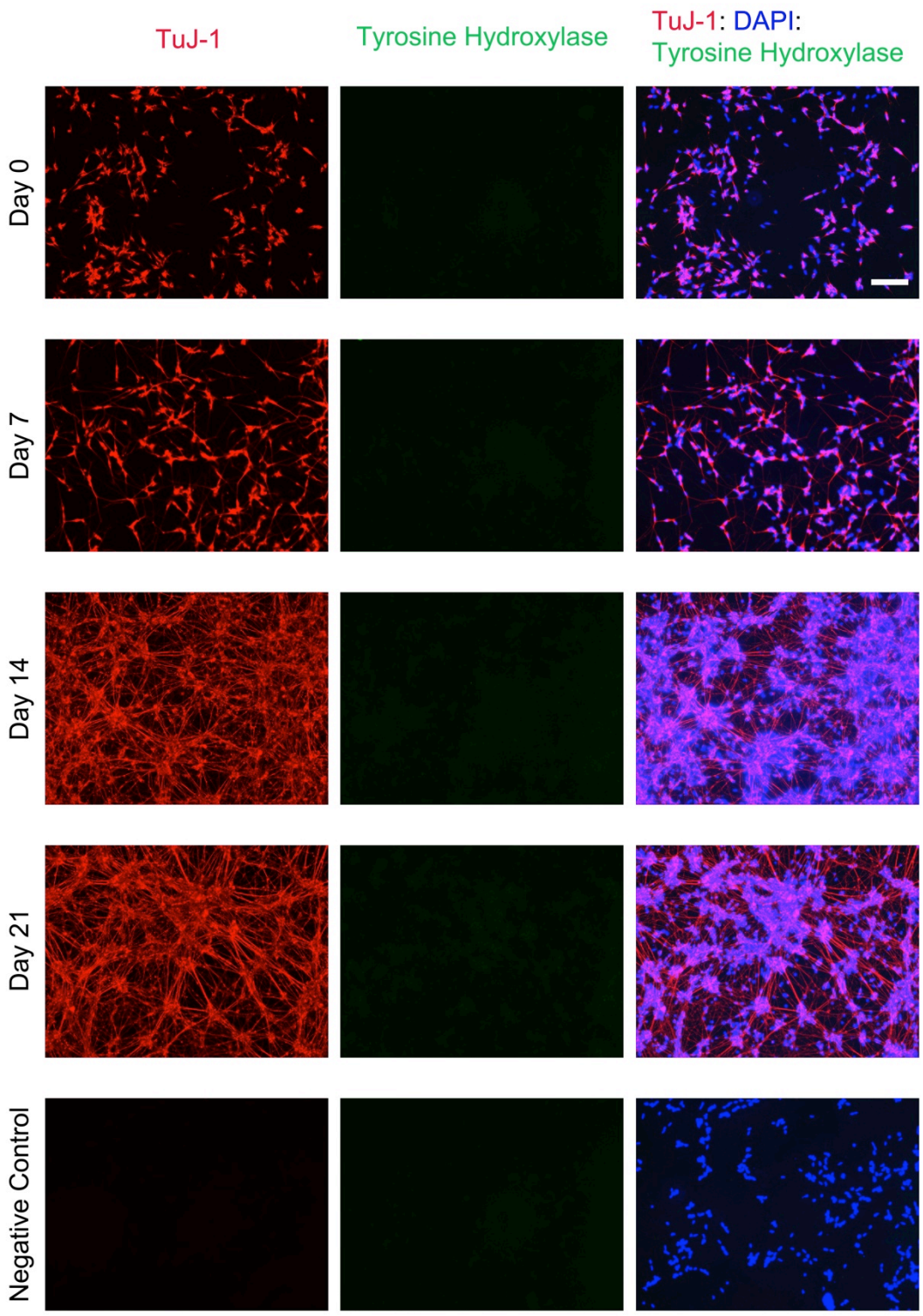

Figure 3.3 - Time-course of neuronal marker expression in the differentiated SH-SY5Y cells. SH-SY5Y cells were differentiated in the presence of N2 medium with 10 μM retinoic acid. Cells were fixed at day 0, 7, 14 and 21 of differentiation, when immunocytochemistry was performed for TuJ-1 (red) and TH (green). The negative control samples were incubated without primary antibodies but in the presence of secondary antibodies. Cells were then counterstained with DAPI (blue) to label cell nuclei; scale bar: 160 μm.

TuJ-1 is a marker for both mature and immature neurons. Therefore to assess the maturity of the neuronal cells produced more mature neuronal markers were used. SH-SY5Y cells differentiated for 28 days were fixed and immunocytochemistry for MAP2, Synapsin I and α-synuclein was performed (Figure 3.4).

Originally, MAP2 was thought to be a specific marker for neurons but has since been found in some other tissues (Loveland *et al*, 1999). In neurons MAP2 is expressed in dendrites. During neuronal differentiation different MAP2 isoforms are expressed. The antibody used here recognises all isoforms. MAP2 can be seen in some neurites of the differentiated SH-SY5Y cells (Figure 3.4a). However, in the undifferentiated and some of the differentiated SH-SY5Y cells MAP2 was nuclear. Nuclear staining has been found in the testis, due to the nuclear localisation signal in exon 10 of MAP2 (Loveland *et al*, 1999). The MAP2 neurite staining suggests the cells are neuronal.

Synapsin I is a neuronal specific protein, which is found in synaptic vesicles at the presynaptic terminal of synapses in most neurons (De Camilli *et al*, 1979; Huttner *et al*, 1983). Synapsin I was present in both the undifferentiated and differentiated SH-SY5Y cells (Figure 3.4b). Undifferentiated SH-SY5Y cells had cytoplasmic staining, whereas differentiated cells showed the typical punctate staining along the neurites as seen in neurons. This suggests neuronal synapses have been formed.

α-Synuclein protein is strongly expressed in neurons in the nucleus, cytoplasm and in the presynaptic terminal of synapses (Zhong *et al*, 2009). However, it is not neural specific as it has also been found in other tissues (Scherzer *et al*, 2008). The presynaptic α-synuclein expression is at a number of neuronal synapses, including catecholaminegic and glutamatergic neurons, but not in all (Totterdell & Meredith, 2005; Totterdell *et al*, 2004; Li *et al*, 2002). In the SH-SY5Y cells α-synuclein was found to increase in differentiated cells compared to undifferentiated cells and showed both nuclear and cytoplasmic staining. However, punctate presynaptic staining was not observed (Figure 3.4c). The expression of these three proteins confirms SH-SY5Y cells become more mature neurons and form synapses when exposed to N2 medium with retinoic acid.

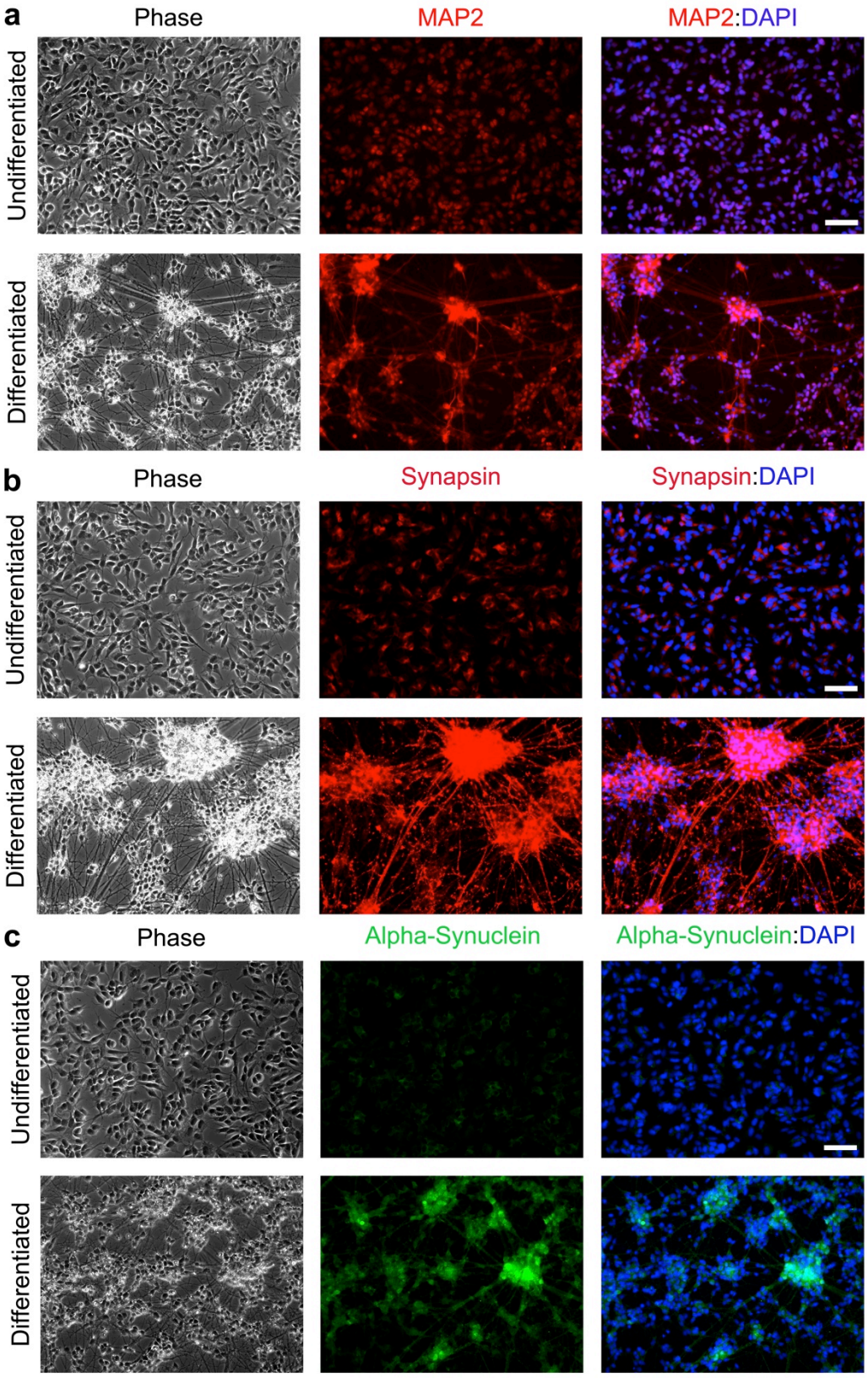

Figure 3.4 - Neuronal maturation marker expression in the differentiated SH-SY5Y cells. SH-SY5Y cells were differentiated in the presence of N2 medium and retinoic acid for 28 days. Cells were fixed and immunocytochemistry was performed for (a) MAP2 (red), (b) Synapsin I (red) and (c) α-synuclein (green). Immunocytochemistry was also performed on undifferentiated cells for comparison. Cells were counterstained with DAPI (blue) to mark cell nuclei; scale bar: 76 μm.

In order to further characterise SH-SY5Y neuronal differentiation, gene expression during differentiation was assessed. qRT-PCR was performed for genes related to neuronal maturation and neuronal subtype (Figure 3.5). The expression of genes that increase as neurons mature (ENO2 and MAP2) and synaptic markers (Synaptobrevin, *SYP* and α-synuclein, *SNCA*) was examined. These markers appear to reach a maximum at day 14 and either plateau or reduce in expression after this day (Figure 3.5). This suggests by day 14 the cells are as mature as they will become. Therefore experiments should be performed at day 14.

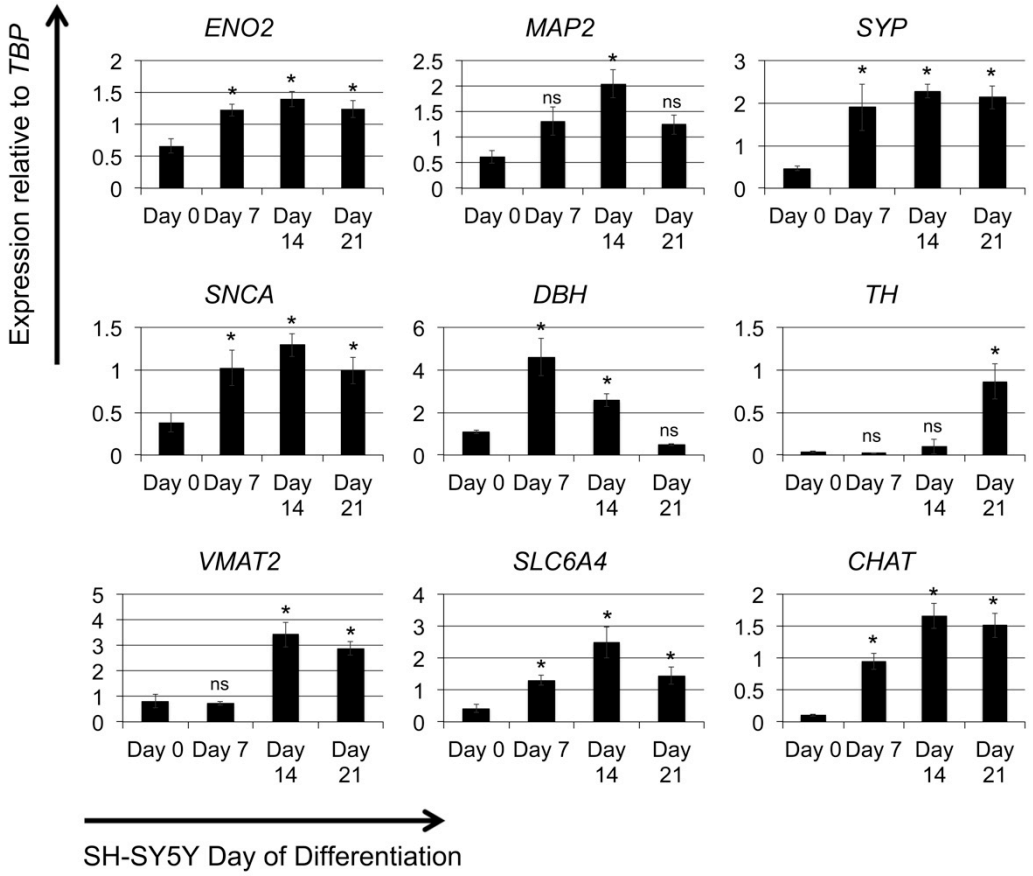

Figure 3.5 - Neuronal maturation and neuronal subtype gene expression during differentiation of SH-SY5Y cells. SH-SY5Y cells were differentiated in the presence of N2 medium and retinoic acid. RNA was extracted from the cells at the stated time points and qRT-PCR was performed. The results were normalised to TATA binding box protein (*TBP*) gene expression. Bars represent the average from 2-3 separate differentiation experiments that contained single or duplicate wells (*ENO2*, *MAP2*, *SNCA*, *TH* and *CHAT* show the average from 3 experiments; *SYP*, *DBH*, *VMAT2* and *SLC6A4* show the average from 2 experiments). The error bars represent the SEM. ANOVA with a Tukey post-hoc test was performed to assess the significant difference between gene expression on day 7, 14 or 21 relative to gene expression on day 0; * $p<0.05$; ns, not significant, $p>0.05$.

The literature suggests that SH-SY5Y cells have the potential to become both catechloaminergic and cholinergic neurons (Biedler *et al*, 1978). TH and Dopamine-β- hydroxylase (DBH) are required for the synthesis of catechloamines. *TH* gene

expression is low until day 21 of differentiation, whereas *DBH* gene expression decreases after day 7 of differentiation (Figure 3.5). Therefore the neurons produced are unlikely to be catecholaminergic. Vesicular monoamine transporter 2 (VMAT2) is required for neurotransmitter loading into synaptic vesicles of serotonin, catecholamines and histamine. *VMAT2* gene expression was found to increase by day 14 (Figure 3.5). SLC6A4 is a serotonin transporter required to recycle serotonin into presynaptic neurons. As with the neuronal maturation markers its RNA levels increase to day 14 and reduce thereafter (Figure 3.5). Therefore the neurons may be serotonergic. Choline acetyltransferase (CHAT) is required for the synthesis of the cholinergic neuron neurotransmitter acetylcholine. Its gene expression increased during differentiation suggesting cholinergic neurons may be produced (Figure 3.5).

Undifferentiated SH-SY5Y cells express a number of neuronal markers, highlighting their neuronal character. Differentiation of these cells in the presence of N2 medium and retinoic acid causes an increase in the expression of neuronal genes, suggesting neuronal differentiation and maturation occurs. However, the markers of all neuronal subtypes appear to increase. The qRT-PCR and immunocytochemistry data suggest catecholaminergic neurons are not produced from SH-SY5Y differentiation. The neurons may be serotonergic or cholinergic. However, further analysis of the presence of proteins rather than just RNA is needed. In addition, analysis of the neurotransmitters that are synthesised would allow the neuronal subtype to be confirmed.

3.2.3 Neuroscreen™-1 Cell Line

Another cell line used extensively as a model for PD is the rat noradrenergic cell line, PC-12. The PC-12 cell line was subclonally derived from a neuroendocrine tumour in the adrenal gland of a rat, known as rat adrenal pheochromocytoma. The cell line was found to contain both dopamine and noradrenaline synthesising enzymes and neurotransmitters (Greene & Tischler, 1976). In addition, the cell line showed termination of cell proliferation and extension of processes 7 days after NGFβ addition (Greene & Tischler, 1976). Neurotransmitter presence reduced after NGFβ treatment. The PC-12 line had a number of disadvantages for high throughput screening so the Ramer lab derived a subclonal line from the PC-12 cell line, NS-1. The NS-1 cell line is reported to proliferate more quickly, does not form aggregates and extends processes within 2 days of NGFβ addition (Radio *et al*, 2008; Dijkmans *et al*, 2008). Therefore this cell line was also assessed for its use as a neuronal cell model.

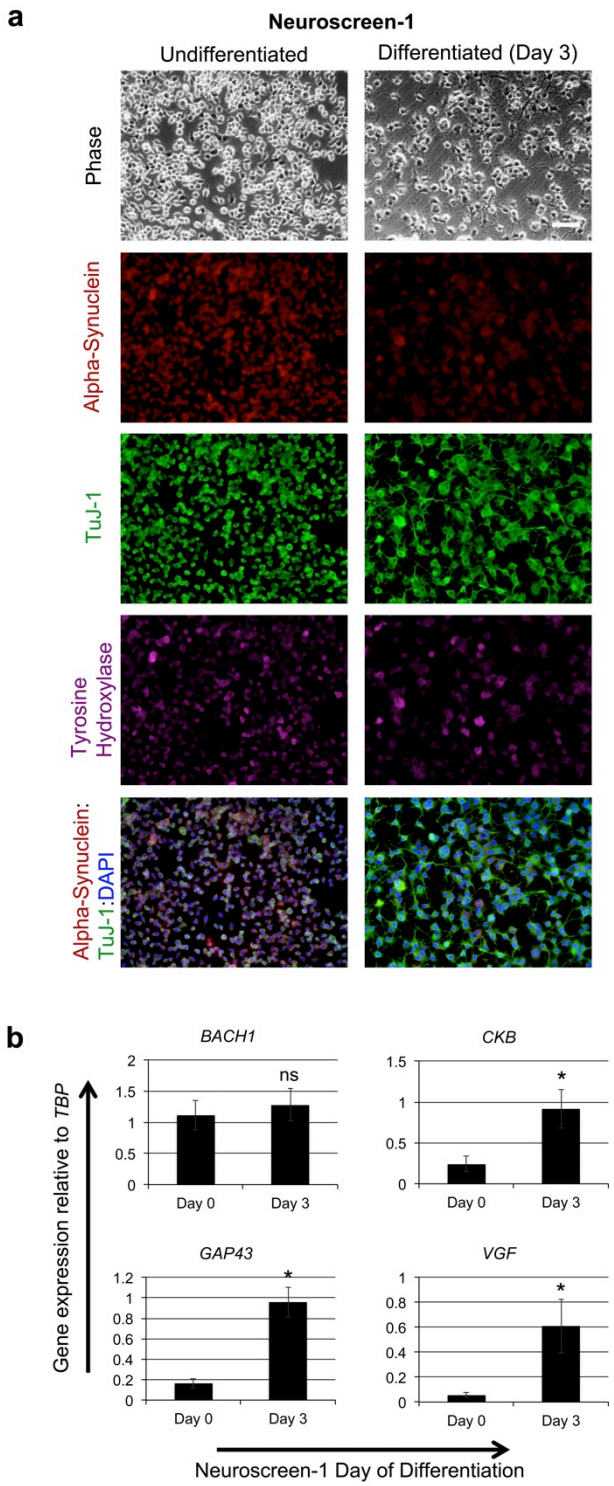

Figure 3.6 - Gene and protein expression in undifferentiated and NGFβ differentiated NS-1 cells. NS-1 cells were differentiated for 3 days by the reduction of serum and the addition of NGFβ. After 3 days cells were fixed to perform immunocytochemistry (a) or RNA was extracted to perform qRT-PCR (b). (a) Immunocytochemistry was performed for α-synuclein (red), TuJ-1 (green) and TH (magenta) and cells were counterstained with the nuclear marker DAPI (blue); scale bar: 76 µm. (b) Bars represent the mean gene expression from 2 independent experiments each with duplicate or triplicate wells. Error bars represent the SEM. Expression was normalised to *TBP* expression. ANOVA with a Tukey post-hoc test was performed to assess the significant difference between gene expression on day 0 and on day 3; * $p<0.05$; ns, not significant, $p>0.05$.

The gene and protein expression in undifferentiated and NGFβ differentiated NS-1 cells was examined (Figure 3.6). Differentiation for 3 days was chosen for two reasons. Firstly studies suggest the extension of neurites plateau at this day (Dijkmans *et al*, 2008). Secondly, during NS-1 differentiation cells still appeared to proliferate and they detached around day 6. The phase images show that by day 3 the cells have extended processes. TuJ-1 is expressed in both undifferentiated and differentiated NS-1 cells, suggesting they are neuronal (Figure 3.6a). In addition, α-synuclein and TH were both present in undifferentiated NS-1 cells. Their levels appear to decrease after differentiation, as was found in PC-12 cells (Greene & Tischler, 1976).

The gene expression before and after NS-1 differentiation was assessed to confirm the differentiation was similar to that reported in the literature (Dijkmans *et al*, 2008). Dijkmans *et al.* reported an increase in *GAP43*, *CKB*, *VGF* and *BACH1* gene expression within 3 days of differentiation. In agreement with this study *GAP43*, *VGF* and *CKB* all increased after 3 days (Figure 3.6b). However, *BACH1* did not show an increase. This was the gene that showed the lowest fold change in their studies and had not been reported in other studies. The difference may be due to slight differences in the differentiation protocol or may be due to subclonal variability of the cell line. These results suggest NS-1 cells are neuronal and that the NGFβ differentiation is similar to that seen in the literature for PC-12 and NS-1 cells.

3.3 Discussion and Future Directions

The SH-SY5Y and the NS-1 cell lines investigated here are both neuronal cell lines. It was found that SH-SY5Y cell lines from different sources had variable protein expression and differentiation potential. Nonetheless, the SH-SY5Y cell line chosen for further investigation had neuronal protein and gene expression in the undifferentiated state that increased after their differentiation in the presence of N2 medium with retinoic acid. The neuronal subtype produced by differentiation requires further investigation. The NS-1 cell line was found to have catecholaminergic neuronal protein expression in the undifferentiated state, which reduced after differentiation. However, their neuronal protein expression remained the same and their neuronal gene expression increased. Therefore both of these neuronal cell lines are suitable to use as a model for α-synucleinopathies and were used in chapter 4 and chapter 5 of this thesis.

Chapter 4 - α-Synuclein-Induced Neuronal Cell Toxicity

4.1 Introduction

The α-synuclein protein, encoded by the *SNCA* gene, is expressed highly in the nervous system and has been found in presynaptic termini and nuclei of neurons (Maroteaux *et al*, 1988). However, its expression level is not the same in all neurons; different neuronal subtypes show variable levels of nuclear and presynaptic expression (Li *et al*, 2002; Iwai *et al*, 1995). This presynaptic localisation and synuclein knockout mice suggest synucleins are involved in presynaptic function and neurotransmission (Greten-Harrison *et al*, 2010; Anwar *et al*, 2011).

α-Synuclein first became implicated in neural cell toxicity when it was found to be the main component of protein inclusions in some neurodegenerative diseases, including PD and DLB (Spillantini *et al*, 1997; Wakabayashi *et al*, 1998). These diseases are now known as α-synucleinopathies. α-Synuclein was further implicated in neurodegeneration when a mutation in the α-synuclein protein, A53T, was found in families displaying Parkinsonism symptoms (Polymeropoulos *et al*, 1997). Further missense mutations in the α-synuclein protein have since been linked to other familial Parkinsonism patients (Kiely *et al*, 2013; Lesage *et al*, 2013; Krüger *et al*, 1998). In addition, triplication or duplication of the *SNCA* gene has been identified to cause early onset Parkinson's. α-Synuclein triplication patients have 4 copies of the *SNCA* gene and this results in twice as much α-synuclein protein than control patients (Singleton, AB *et al*, 2003; Farrer *et al*, 2004). Whereas, duplication patients have 3 copies of the *SNCA* gene and from this gene dosage they are likely to have 1.5 times more α-synuclein protein than controls (Chartier-Harlin *et al*, 2004). This difference in protein level affects the average age of onset of the disease and the severity of symptoms experienced, with triplication patients having an earlier age of onset and symptoms including hallucinations and dementia (Nishioka *et al*, 2006; Chartier-Harlin *et al*, 2004; Gwinn *et al*, 2011; Ahn *et al*, 2008). This led to the theory that the levels of α-synuclein may be fundamental in the development of α-synucleinopathies. However, mutations and multiplications of the *SNCA* gene are not common. Variations in the *SNCA* gene sequence might affect its level of protein expression (Edwards *et al*, 2010; Farrer *et al*, 2001b; Chiba-Falek & Nussbaum, 2001). Alternatively, there may be a deficit in α-synuclein protein degradation, for example due to heterozygous β-glucosidase (*GBA)* mutations (Murphy *et al*, 2014).

A number of labs have performed wild-type α-synuclein overexpression studies with varying results. Some studies have shown slight toxicity in catecholaminergic neurons or neuroblastoma cells but others have shown no toxicity (Zhou *et al*, 2002; Bisaglia *et al*,

2010; Zhou *et al*, 2000). However, these studies all suggest cells overexpressing α-synuclein are more susceptible to oxidative insults (Zhou *et al*, 2000; Bisaglia *et al*, 2010). Further evidence that α-synuclein is toxic comes from rat *in vivo* experiments that resulted in progressive neurodegeneration from 3 weeks after α-synuclein adeno-associated viral overexpression (Kirik *et al*, 2002). These results are conflicting and; therefore the aim was to determine whether an increase in wild-type α-synuclein protein could cause neuronal cell toxicity. This would further provide a model of α-synucleinopathies to allow investigation of the involvement of mitochondrial dysfunction and oxidative stress in neurodegeneration.

4.2 BacMam – Construct Design

There are a number of viral and non-viral methods that can be used to overexpress a protein. It was chosen to use the baculovirus method to overexpress α-synuclein for a number of reasons. Firstly, baculoviruses are capable of transducing neuroblastoma cells and primary neurons with high efficiency (Sarkis *et al*, 2000). Secondly, they can be used at high concentrations with limited toxicity and a dose-dependent increase in the level of protein expression can be achieved (Kost & Condreay, 2002; Boyce & Bucher, 1996). Thirdly, they are mostly non-integrating and therefore should not cause alterations to endogenous genes (Condreay *et al*, 1999). Fourthly, they have been found to be safe and non-replicating in mammalian cells (Tjia *et al*, 1983). Finally, using a baculovirus system to overexpress α-synuclein makes it easily amenable to use in different cell types by the simple addition of the virus to the culture media. A baculovirus that contains a gene whose expression is controlled by a mammalian promoter is known as BacMam.

Life Technologies have a commercially available BacMam with a mitochondrial targeted GFP (mtGFP). In this virus they report the use of emerald GFP with the pyruvate dehydrogenase- E1α leader sequence to target it to the mitochondria (Dahl *et al*, 1987). Since this BacMam would be used as a control these DNA sequences were chosen for use in the α-synuclein overexpression construct. In addition, the presence of mtGFP would allow the transduction efficiency to be assessed easily in live cells. In order to include more than one gene in the same construct a 2A peptide was used. 2A peptides can produce separate proteins from the same mRNA construct by translational skipping (Szymczak *et al*, 2004). This is because the ribosome is not capable of forming a peptide bond, resulting in two separate proteins from one mRNA transcript (Donnelly *et al*, 2001b). 2A peptides have the advantage over internal ribosome entry sequences (IRES) because the two proteins are produced at similar levels, while the coding sequence downstream of the IRES is often poorly translated. However, a small part of the 2A peptide is left on the protein upstream of the 2A peptide, which may affect its function. There are a number of 2A peptides with

varying efficiency in different cell types. In human 293T cells P2A was reported to be the most efficient, followed by T2A and E2A (Kim *et al*, 2011). However, previous reports *in vitro* suggested T2A had the highest cleavage efficiency (Donnelly *et al*, 2001a). Therefore, the T2A sequence was used to separate mt*GFP* and *SNCA*. The *SNCA* gene encoding the full-length human wild-type α-synuclein protein was used since previous studies suggest the full-length protein had potential to cause toxicity, and the triplication and duplication *SNCA* patients do not have any coding mutations.

The *SNCA* sequence was codon optimised for more efficient translation and the final sequence encoding mtGFP and the α-synuclein protein (mtGFP-SNCA) was sent to Life Technologies GeneArt Gene Synthesis service; the construct received is shown in Figure 4.1a. To produce the BacMam Life Technologies required the sequence in a Gateway Entry Clone. Therefore, BamHI and EcoRI were used to isolate the mtGFP-SNCA sequence and the pENTR2B2 vector backbone (Figure 4.1a-d). The fragments were then isolated from agarose gels and ligated. The ligation products were transfected into competent DH5α cells and colonies were assessed for the correct fragment ligation. The plasmid produced is shown in Figure 4.1e. This is a Gateway Entry Clone containing the mtGFP-SNCA sequence, which can be used with Gateway LR Clonase II to easily move the mtGFP-SNCA sequence into a Gateway Destination Vector.

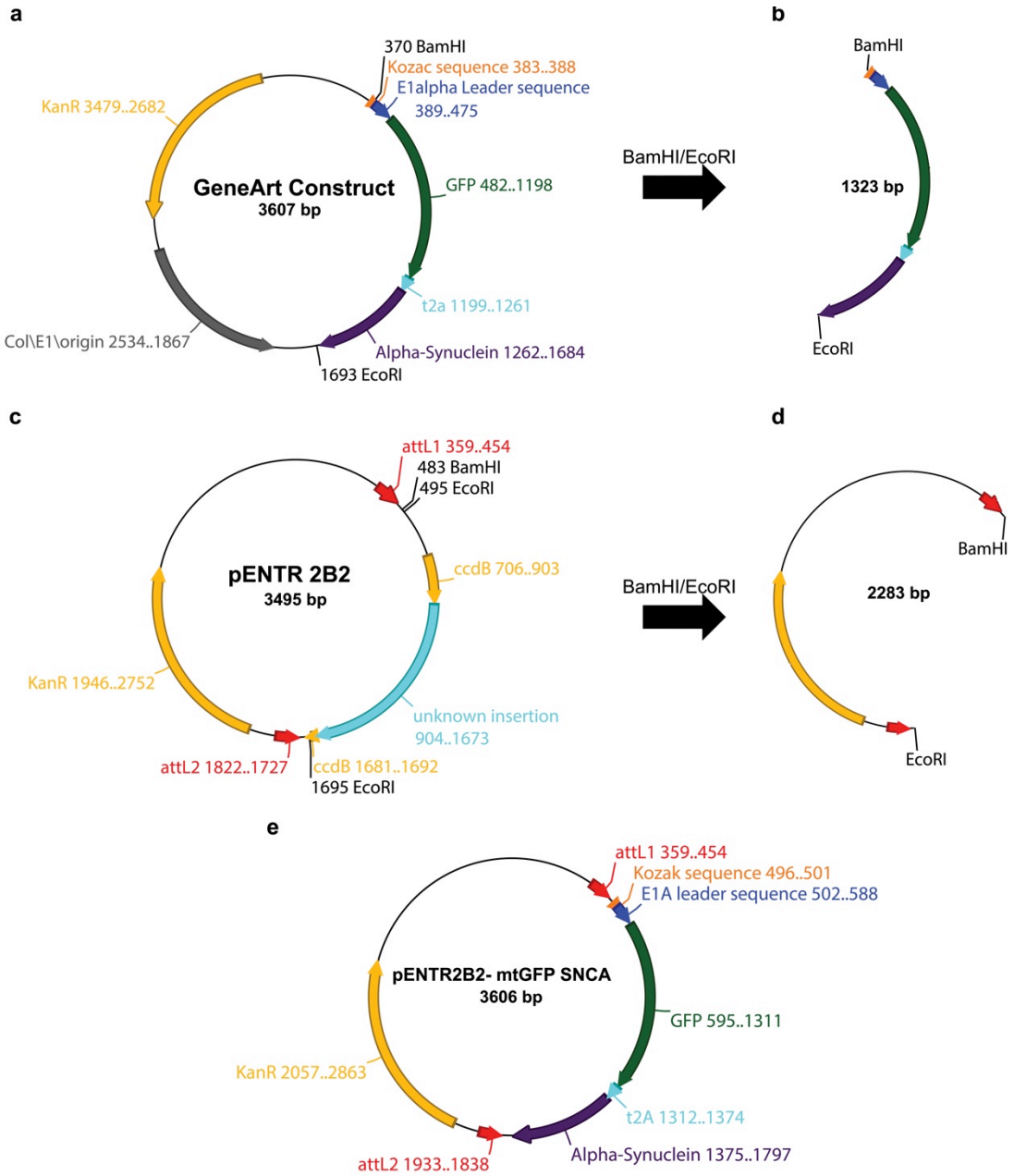

Figure 4.1 – mtGFP-SNCA Gateway Entry Clone preparation for BacMam generation. (a) The plasmid received from Life Technologies GeneArt Gene Synthesis service. (b) Restriction enzyme digestion of (a) with BamHI and EcoRI isolates the mtGFP-SNCA sequence. (c) Life Technologies pENTR2B2 Gateway Entry Vector. (d) Restriction digestion of (c) with BamHI and EcoRI isolates the backbone of the Gateway Entry Vector. (e) Ligation of (b) and (d) produced the Gateway Entry Clone ready to send to Life Technologies for baculovirus generation. KanR: Kanamycin resistance; T2A: Translational skipping peptide; Col/E1/origin: Origin of replication; attL1/attL2: Phage attachment sites for site-specific recombination; ccdB: Cytotoxic protein CcdB**.**

4.3 mtGFP-SNCA Construct Testing

The Gateway Entry Clone in Figure 4.1e was ready to send to Life Technologies to produce the BacMam. However, it was first necessary to confirm the mtGFP-SNCA insert sequence

gave the appropriate protein expression in cells. To do this Gateway Cloning with Gateway LR Clonase II was used to clone the mtGFP-SNCA sequence insert into the PB-CAG Destination Vector (Figure 4.2b). PB-CAG has a constitutively active promoter, pCAG (Niwa *et al*, 1991). The Expression Clone produced is shown in Figure 4.2c. This construct also contains piggyBac (PB) Long Terminal Repeat (LTR) sequences. In the presence of piggyBac transposase the contents between these PB-LTRs is integrated into the target cell genome (Ding *et al*, 2005).

In order to assess the presence of α-synuclein, an antibody specific to α-synuclein was required. Therefore, the specificity of a commercially available α-synuclein antibody from BD Transduction Laboratories™ was determined (Figure 4.3). A strain of C57BL/6 mice from Harlan has been reported in the literature to lose the α-synuclein gene through inbreeding (Specht & Schoepfer, 2001). This C57BL/6 strain can be used to assess the specificity of the α-synuclein antibody. Immunohistochemistry was performed on *ex vivo* mouse brain stem slices from the inbred C57BL/6 strain and an outbred mouse strain using the BD Transduction Laboratories™ α-synuclein antibody. The C57BL/6 mice showed no α-synuclein staining, whereas the positive control had widespread α-synuclein staining (Figure 4.3a). In addition, *ex vivo* mouse brain stem slices were used for immunocytochemistry to detect the localisation of α-synuclein. Co-staining of α-synuclein with the neural marker TuJ-1, the synaptic marker Synapsin I and the nuclear stain DAPI showed the typical α-synuclein localisation, in the nucleus and at synapses of neurons (Figure 4.3b). The co-localisation of α-synuclein with DAPI shows α-synuclein nuclear localisation, whereas the Synapsin I and α-synuclein co-localisation show α-synuclein synaptic localisation. Therefore, this antibody is specific for α-synuclein.

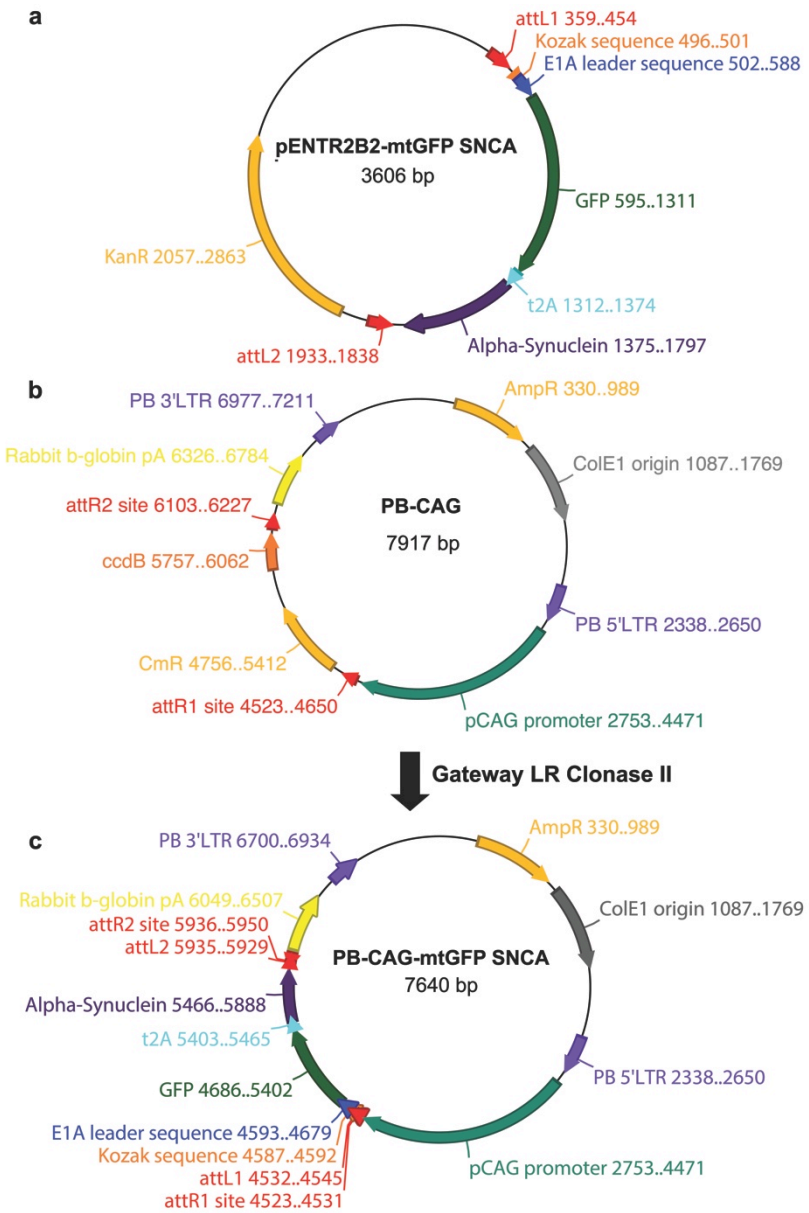

Figure 4.2 – Gateway Cloning to produce a mtGFP-SNCA Expression Clone for use in cells. (a) The pENTR2B2 Entry Clone containing the mtGFP-SNCA sequence between the attL sites. (b) PB-CAG is a Destination Vector with attR sites. It was a kind gift from Keisuke Kaji. (c) The Expression Clone produced using Gateway LR Clonase II and plasmids (a) and (b). This Expression Clone was used to test the protein expression in cells with mtGFP-SNCA under the control of the pCAG constitutive promoter. KanR: Kanamycin resistance; AmpR: Ampicillin resistance; CmR: Chloramphenicol resistance; T2A: Translational skipping peptide; ColE1 origin: Origin of replication; attL1/attL2 and attR1/attR2: Phage attachment sites for site-specific recombination; ccdB: Cytotoxic protein CcdB; Rabbit b-globulin pA: rabbit β-globulin polyadenylation signal; PB 3' LTR and PB 5' LTR: piggyBac Long Terminal Repeat 3' and 5' respectively.

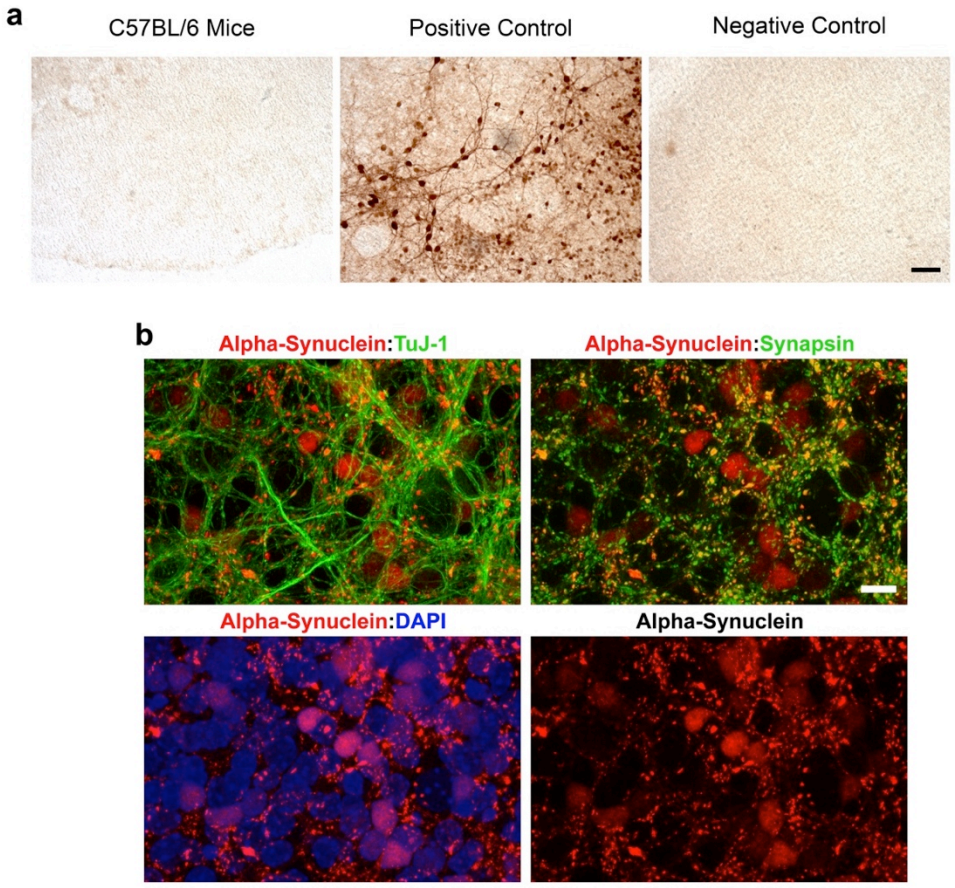

Figure 4.3 - α-Synuclein antibody testing. Hindbrain slices from mice were cultured for 8 days. They were then fixed and immunohistochemistry was performed. (a) Immunohistochemistry was performed for α-synuclein using an HRP secondary antibody and DAB to assess the specificity of the α-synuclein antibody. The negative control is in the absence of primary antibody; scale bar: 68 μM. (b) Immunocytochemistry was performed to assess the localisation of α-synuclein (red) relative to TuJ-1, Synapsin I (green) and DAPI (blue). TuJ-1 positive neurons (green) contain α-synuclein (red). α-Synuclein (red) co-localisation with Synapsin (green) show α-synuclein is found synaptically and α-synuclein (red) co-localisation with DAPI (blue) indicates it localises to the nucleus; scale bar: 11 μM.

The construct in Figure 4.2c, with mtGFP-SNCA under the control of a constitutively active promoter, was introduced into SH-SY5Y cells by lipofection. 24 hours later the cells were fixed and immunocytochemistry was performed for α-synuclein. Proteins encoded by the construct are expressed as expected (Figure 4.4). The GFP is present and localises to the mitochondria. In addition, the GFP is found in cells that also express a higher level of α-synuclein protein. In Figure 4.4 the white arrow highlights a cell with high GFP and α-synuclein expression, the white arrowhead indicates a cell with weak GFP and α-synuclein expression and the blue arrow highlights a cell with no GFP fluorescence and weak endogenous α-synuclein expression. Finally, the α-synuclein protein is not restricted to the mitochondria indicating that the T2A peptide is working. The construct in Figure 4.1e was therefore sent to Life Technologies to produce the BacMam.

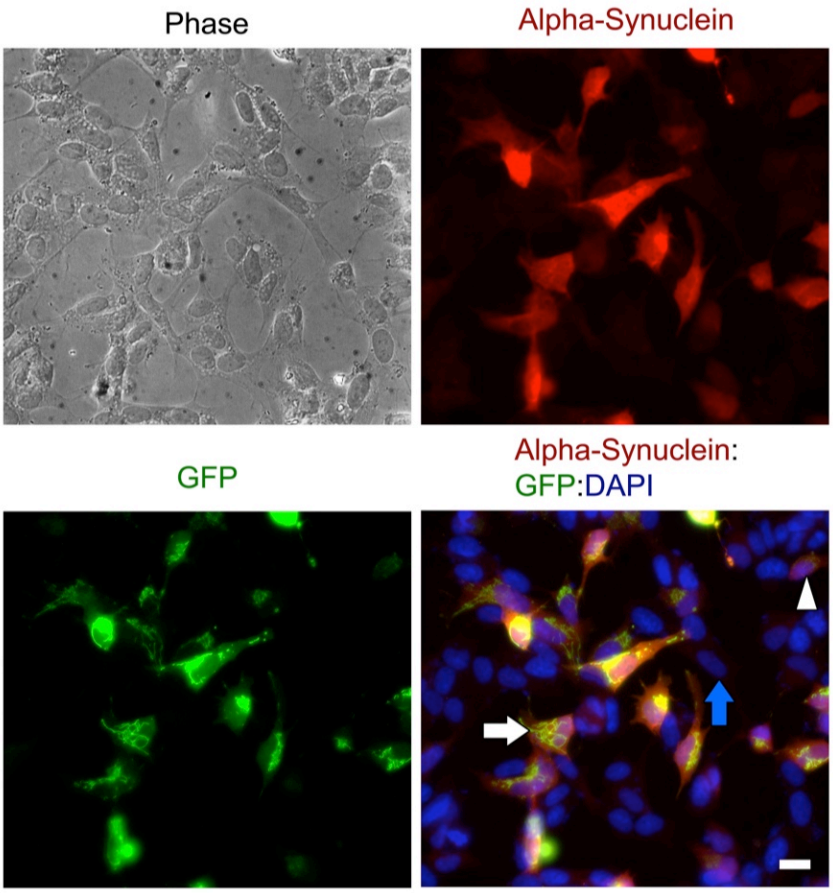

Figure 4.4 – mtGFP-SNCA construct protein expression in SH-SY5Y cells. SH-SY5Y cells were transfected with the plasmid in Figure 4.2c using Lipofectamine. Cells were cultured for 24 hours when they were fixed and immunocytochemistry was performed for α-synuclein (red), GFP (green) was present and cells were counterstained with DAPI (blue). White arrow indicates a cell with high GFP and α-synuclein expression. The blue arrow highlights a cell with no GFP and weak endogenous α-synuclein expression and the white arrowhead indicates a cell with weak GFP expression and weak α-synuclein expression; scale bar: 17 μM.

4.4 BacMam Testing and Optimisation

BacMam generation requires cloning of the sequence of interest into a vector containing a pCMV promoter and the baculovirus viral genome. This construct is then transfected into Sf9 insect cells and cells are cultured until they show signs of viral infection. At this point media is collected and centrifuged to remove cells and debris, to produce a P1 stock. To amplify the virus, the P1 stock can be used to infect Sf9 insect cells again. These are then incubated until cells show signs of infection when the media is collected, centrifuged to remove debris to give a P2 BacMam virus stock (Fornwald *et al*, 2007). Life Technologies performed this as a service and we received 200 ml of P2 viral stock, which is stored at 4^{o}C.

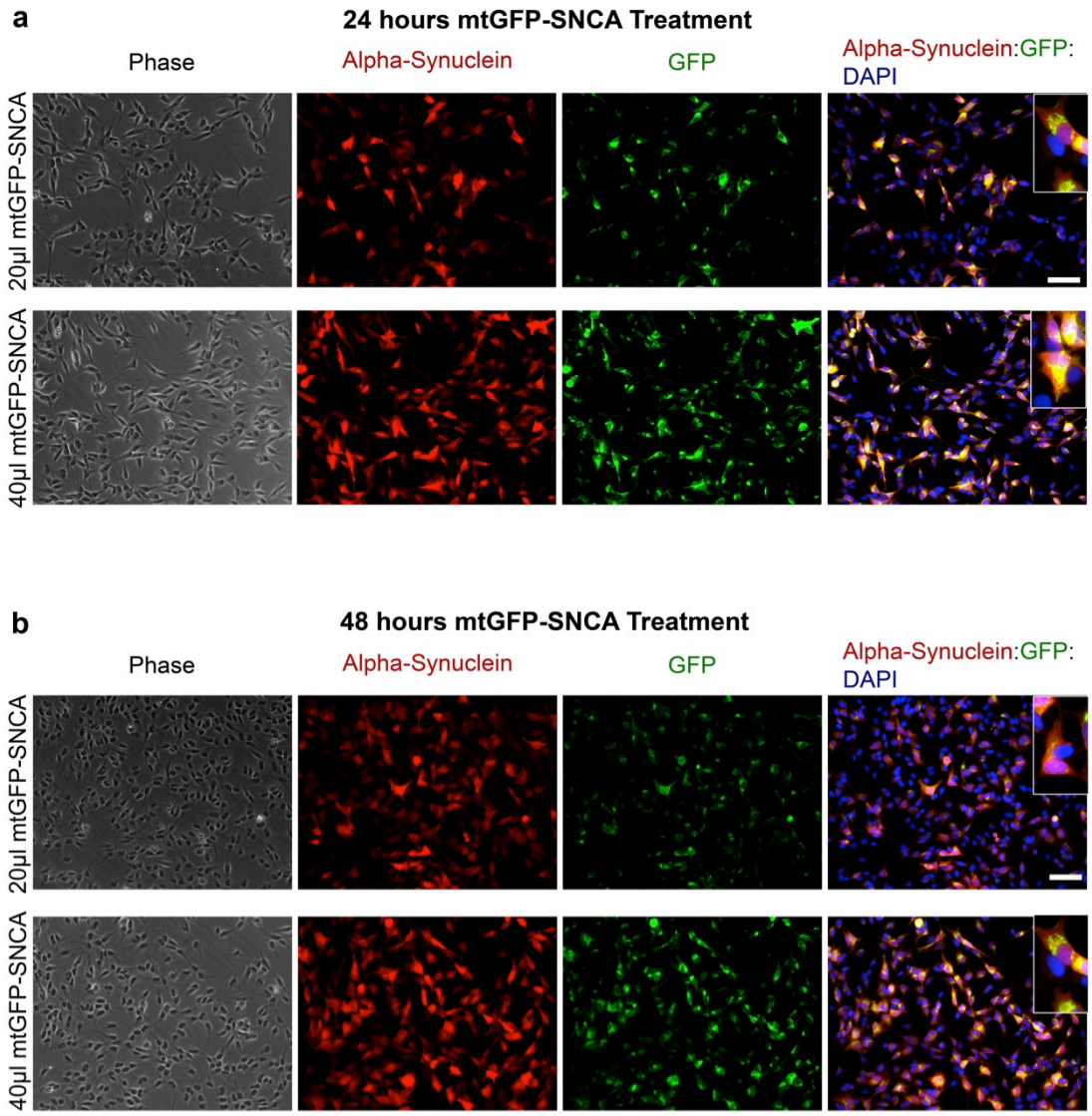

Figure 4.5 - mtGFP-SNCA BacMam protein expression in SH-SY5Y cells. SH-SY5Y cells were incubated with 20 µl or 40 µl mtGFP-SNCA BacMam per $1x10^5$ cells. They were fixed after 24 hours (a) or 48 hours (b) and immunocytochemistry was performed for α-synuclein (red). Cells expressed GFP (green) and were counterstained for DAPI (blue) to mark nuclei; scale bar: 76 µM. Insets show magnified images of α-synuclein (red) and mitochondrial targeted GFP co-localisation.

The mtGFP-SNCA BacMam's ability to transduce undifferentiated SH-SY5Y cells was tested. Two volumes of BacMam virus, 20 µl and 40 µl and two time points, 24 hours and 48 hours were examined (Figure 4.5). In all conditions the proteins were expressed as expected: GFP was present and located to the mitochondria; cells that expressed GFP had a higher level of α-synuclein, shown by yellow in the overlay and the α-synuclein was dispersed in the cell cytoplasm. At both time-points the higher volume of BacMam showed greater transduction efficiency, with more cells expressing α-synuclein at a higher level than the lower volume. The GFP and α-synuclein proteins could be detected at 24 hours and were

still present at 48 hours, with similar expression levels at both time-points (Figure 4.5a and b).

To quantify the transduction efficiency of different volumes of mtGFP-SNCA BacMam virus, FACS analysis was performed 24 hours after viral addition (Figure 4.6a). As a comparison the transduction efficiency of the control mtGFP BacMam virus was also tested (Figure 4.6b). The percentage of cells positive for GFP increased with the volume of BacMam added for both viruses, indicating increased transduction (Figure 4.6a and b). In addition, there is a dose dependent increase in the mean GFP fluorescence (Figure 4.6a and b). This data was plotted to give the volume of virus added on the x-axis and the mean GFP fluorescence on the y-axis (Figure 4.6c and d). Linear regression was performed on the data for mtGFP-SNCA and mtGFP viruses, and the equation of these lines was calculated. It was then calculated that we would need 5-fold more mtGFP-SNCA BacMam to achieve the same level of GFP fluorescence from the mtGFP BacMam virus (Figure 4.6e). For example, 1 µl of mtGFP BacMam virus gives the same level of GFP fluorescence as 5 µl of mtGFP-SNCA BacMam virus.

The BacMam is capable of increasing the GFP protein level but this does not provide information about the α-synuclein protein levels or the T2A cleavage. To determine the cleaving efficiency of the T2A and the α-synuclein protein levels, Dr. Fella Hammachi performed a western blot, with protein samples from transduced SH-SY5Y cells (Figure 4.7a and c). This showed that the T2A was capable of cleaving the proteins with only a small percentage that was not cleaved around 42 kDa, approximately 5% when 20 µl of mtGFP-SNCA BacMam was used (Figure 4.7a). α-Synuclein in its monomeric form is around 14 kDa (Figure 4.7a). Quantification of the 14 kDa α-synuclein bands showed an increase in relative protein levels with increasing volume of virus added (Figure 4.7b). An upper band positive for α-synuclein was also present, around the 49 kDa marker. This band appeared specific for α-synuclein as it increased as more baculovirus was added and may be an oligomer. However, the specificity of the band for α-synuclein would need to be confirmed using an additional α-synuclein antibody, for example the C-20 antibody from Santa Cruz. If this band is specific for α-synuclein, then mass spectrometry could be performed on the isolated band to identify the protein composition. Previous studies have reported a 45 kDa band that is thought to be an azo bond between α-synuclein monomers, similar to a dityrosine bond (Leng *et al*, 2001). The GFP blot also shows a very small proportion of the proteins are not cleaved at the T2A site (Figure 4.7c). Emerald GFP has a molecular weight around 26.9 kDa, in this blot it can be seen at around the 28 kDa marker (Figure 4.7c). Quantification of this band using ImageJ showed the GFP protein increased

with increasing volumes of virus (Figure 4.7d). In addition, it appears that 5 µl mtGFP may be equivalent to 25 µl mtGFP-SNCA, as the FACS plot suggested. There is a faint band that is likely to be a weak, uncleaved dimer around 56 kDa. The lower band around 17 kDa is likely to be a degradation product (Figure 4.7c). There is no β-actin blot here but the protein levels were quantified using Bio-Rad DC Protein assay to load equal volumes of protein samples.

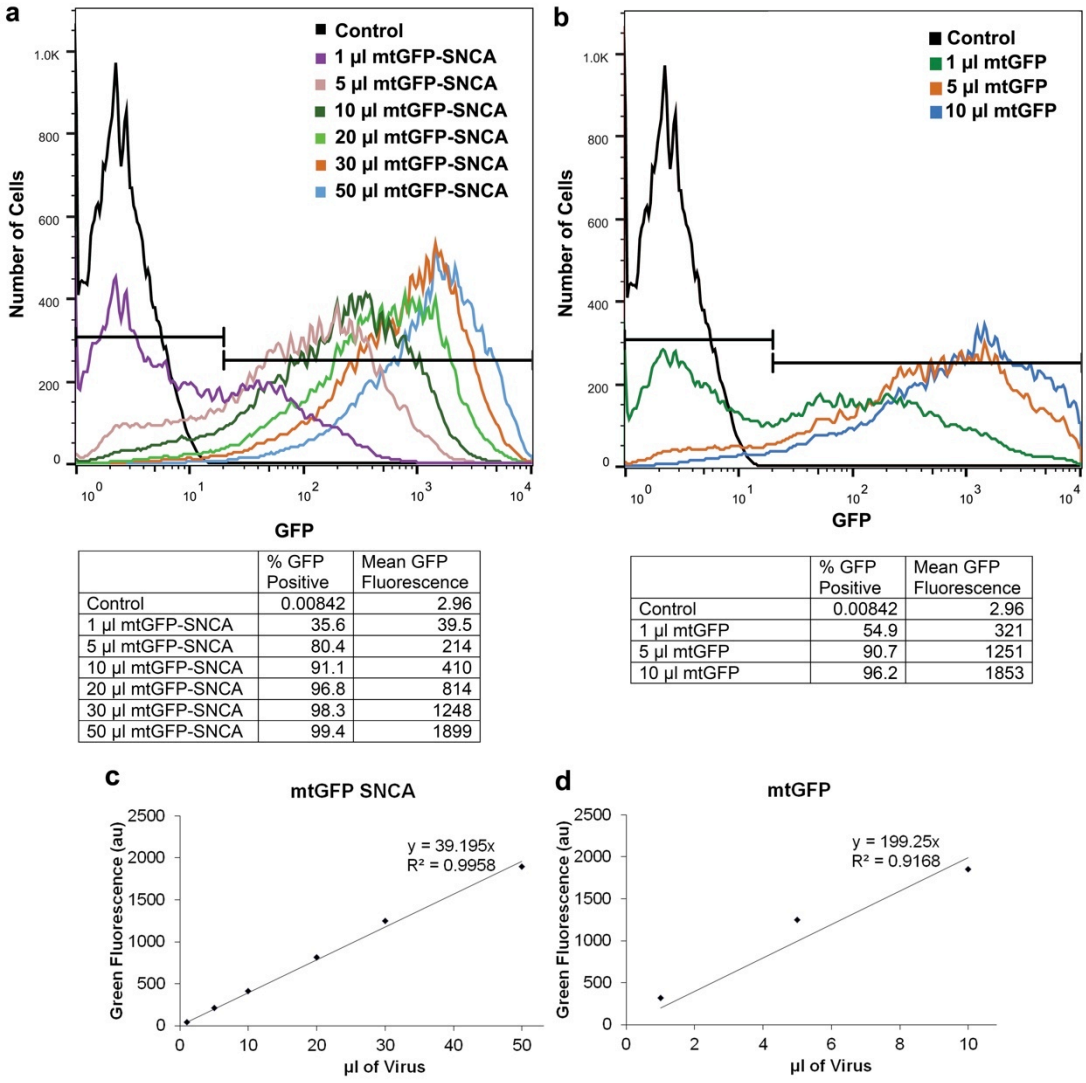

	% GFP Positive	Mean GFP Fluorescence
Control	0.00842	2.96
1 µl mtGFP-SNCA	35.6	39.5
5 µl mtGFP-SNCA	80.4	214
10 µl mtGFP-SNCA	91.1	410
20 µl mtGFP-SNCA	96.8	814
30 µl mtGFP-SNCA	98.3	1248
50 µl mtGFP-SNCA	99.4	1899

	% GFP Positive	Mean GFP Fluorescence
Control	0.00842	2.96
1 µl mtGFP	54.9	321
5 µl mtGFP	90.7	1251
10 µl mtGFP	96.2	1853

e

From the equation of the line (d) y=199.25x; 1 µl of mtGFP (x) gives a GFP fluorescence (y) of 199.25 au; 199.25 au of GFP (y) from the equation of the line (c) y=39.295x; gives a volume of 5.08 µl of mtGFP-SNCA (x). Therefore, 1 µl mtGFP is the equivalent of ~5 µl mtGFP-SNCA.

Figure 4.6– mtGFP-SNCA and mtGFP BacMam transduction efficiencies. SH-SY5Y cells were incubated with mtGFP-SNCA (a) or mtGFP (b) BacMam. The volume stated is per $1x10^5$ cells. After 24 hours cells were lifted for FACS analysis to determine the number of GFP positive cells and the mean GFP fluorescence. At least 30,000 cells were counted for each condition. The mean GFP fluorescence was then plotted against the volume of (c) mtGFP-SNCA BacMam or (d) mtGFP BacMam added. Then the relative volume of mtGFP-SNCA and mtGFP BacMam needed to give the same GFP fluorescence was calculated (e).

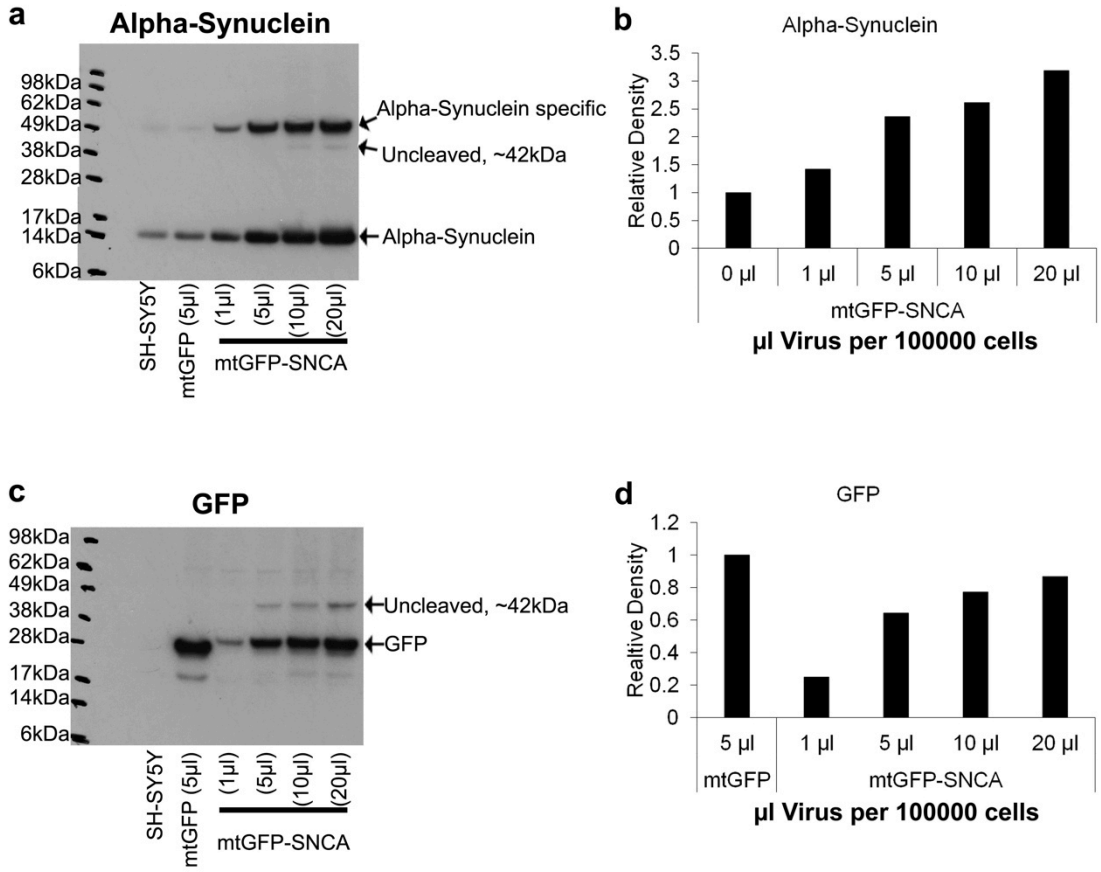

Figure 4.7 – α-Synuclein and GFP protein expression levels after BacMam transduction and T2A cleavage efficiency. SH-SY5Y cells were incubated with mtGFP or mtGFP-SNCA for 24 hours when cells were lifted and western blots were performed to assess the level of α-synuclein (a) and GFP (c) protein expression. The volumes stated are per $1x10^5$ cells (data from Dr. Fella Hammachi). The 14 kDa α-synuclein band in (a) and the 28 kDa GFP band in (c) were quantified for each condition using ImageJ; n=1 (b and d, respectively).

GFP and α-synuclein proteins increase after viral transduction, but BacMam expression is known to be transient. To assess how long the protein expression is maintained, differentiated SH-SY5Y cells were used. Differentiated SH-SY5Y cells would undergo fewer divisions and therefore may maintain expression for longer than undifferentiated SH-SY5Y cells. mtGFP-SNCA BacMam (50 µl) was added at day 7 of differentiation. The GFP expression levels were analysed using FACS analysis after 24 hours and every 3 days thereafter (Figure 4.8). The percentage of GFP positive cells begins to decrease between day 7 and day 10. In addition, the mean GFP fluorescence decreases over time but drops significantly between day 7 and day 10. Therefore, it was decided that to keep the protein expression levels high in differentiated cells the virus should be topped up every 7 days.

a

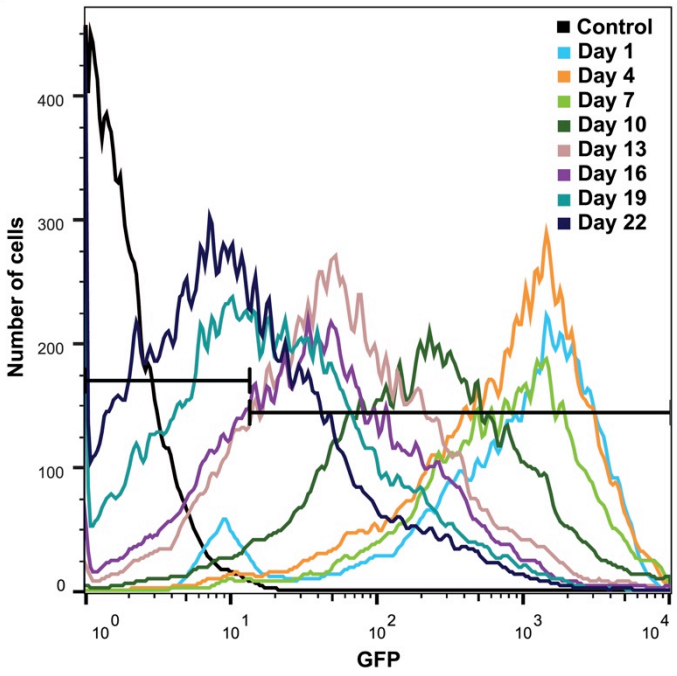

b

	% GFP Positive	Mean GFP Fluorescence
Control	0.048	1.62
Day 1	96.5	1522
Day 4	97	1331
Day 7	98.4	1276
Day 10	92.7	553
Day 13	77.4	209
Day 16	68.5	167
Day 19	47.6	88.1
Day 22	33.1	59.5

Figure 4.8 – Time-course of GFP expression after mtGFP-SNCA transduction in differentiated SH-SY5Y cells. SH-SY5Y cells were differentiated for 7 days in N2 medium with retinoic acid when 50 µl mtGFP-SNCA BacMam was added per well of a 24-well plate. Cells were lifted after 24 hours and every 3 days thereafter to assess the percentage of GFP positive cells and the mean GFP fluorescence using FACS analysis (a and b). At least 10,000 cells were counted per time-point.

4.5 BacMam Toxicity

The optimisation experiments provided important information about the mtGFP-SNCA BacMam. Firstly, α-synuclein protein levels can be increased with increasing volume of BacMam. Secondly, in order to achieve the same level of GFP fluorescence 1 µl of the control mtGFP BacMam equals 5 µl of the α-synuclein overexpression mtGFP-SNCA BacMam. Thirdly, the T2A allows separation of most of the proteins. Finally, in differentiated SH-SY5Y cells the GFP protein starts to show a significant decrease in expression from day 7. From this knowledge experiments were designed to assess the toxicity of α-synuclein overexpression in undifferentiated SH-SY5Y cells. Preliminary experiments performed by Dr. Fella Hammachi indicated that the virus was not toxic over 5 days at a volume of 50 µl mtGFP-SNCA per $1x10^5$ cells. Therefore, the toxicity of an even

greater concentration of α-synuclein was assessed using the MTS assay. The MTS assay gives an absorbance reading, which is relative to the cellular metabolic activity (Figure 4.9a). The MTS assay involves the addition of membrane impermeable MTS and the electron carrier PMS to cells. PMS is taken up into cells and is reduced by the cells. It is thought NADH/NADPH, which are involved in metabolism, are the most abundant compounds that can reduce PMS. Hence, it is a measure of metabolic activity. The reduced PMS is membrane permeable and can then move out of the cell and donate the gained hydrogen to MTS. The reduction of MTS to formazan results in a colour change from yellow to brown, which can be quantified by measuring the absorbance at 490 nm. If the cells used are of the same type and cultured in the same medium they will have similar metabolic activity, therefore the absorbance will correlate with the number of cells. Cells were cultured in the presence of BacMam for 4 days when the MTS assay was performed to assess toxicity. Incubation was performed for 4 days because beyond that cells became over confluent. The volumes of mtGFP and mtGFP-SNCA used here were based on a previous calculation looking at the percentage of cells positive for GFP, therefore 1 µl mtGFP was used as an equivalent to 2 µl mtGFP-SNCA. Although this is an incorrect way of calculating the equivalent, these results still show that mtGFP-SNCA is not toxic at an equivalent volume of mtGFP. That is, the toxicity at 25 µl mtGFP is not statistically different from 100 µl or 200 µl of mtGFP-SNCA even though it shows a difference to control (Figure 4.9b). Therefore, the toxicity detected is not due to the overexpression of α-synuclein but rather due to the baculovirus or the presence of mtGFP. In undifferentiated SH-SY5Y cells α-synuclein overexpression is not toxic to cells up to 4 days of culture. Beyond 4 days of culture was not assessed.

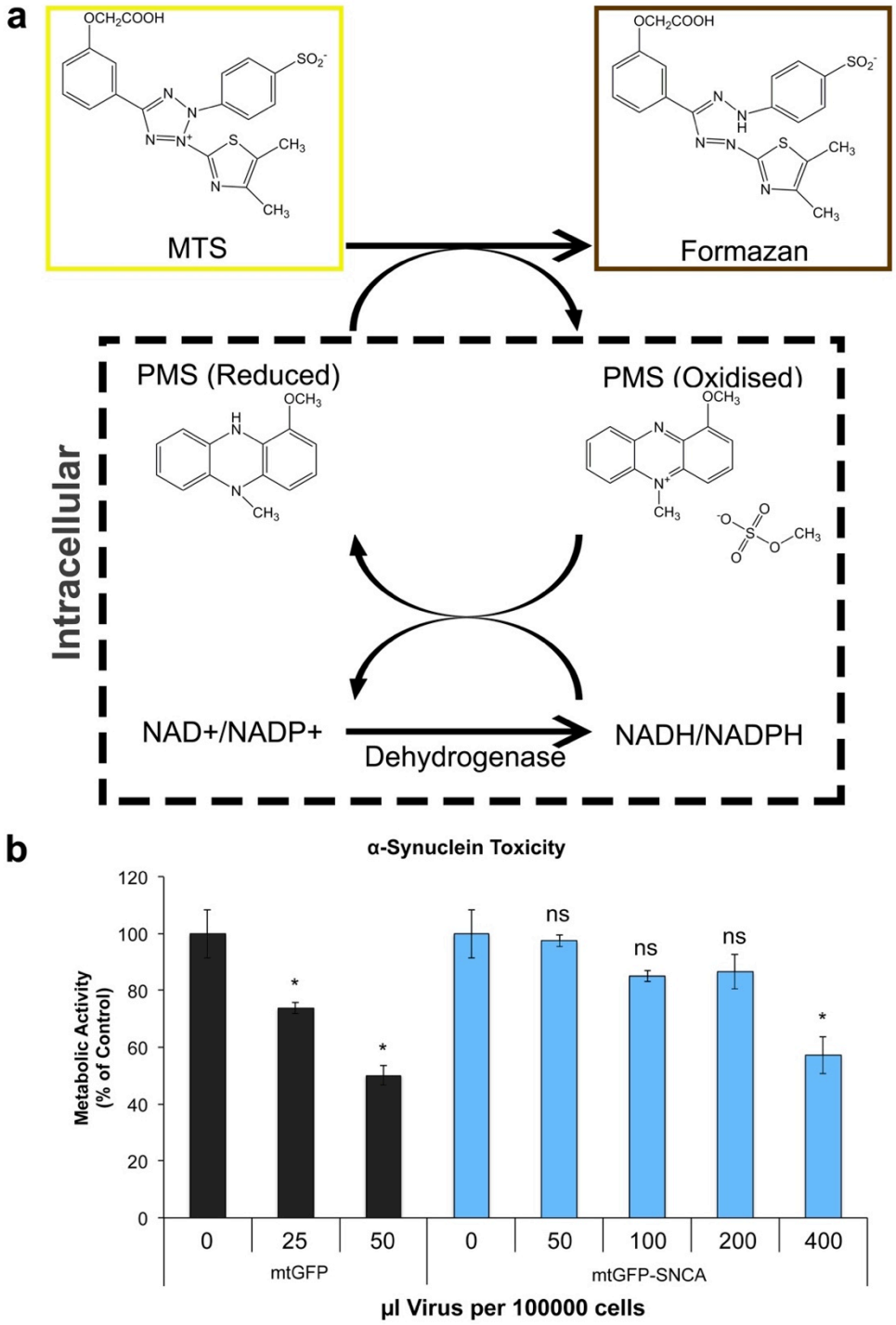

Figure 4.9 – MTS assay chemistry and α-synuclein toxicity in undifferentiated SH-SY5Y cells. (a) The MTS assay chemistry. MTS, which is yellow in colour, is added to cells in the presence of PMS, an electron coupler. MTS is membrane impermeable therefore the electron coupler is required to enter the cell and carry electrons to the MTS. The reduction of MTS by reduced PMS produces formazan that is brown in colour. The absorbance at 490 nm is a read-out of the relative formazan production. (b**)** SH-SY5Y cells were transduced with mtGFP or mtGFP-SNCA BacMam virus for 4 days when the MTS assay was performed. The volumes stated are per $1x10^5$ cells. The experiment was performed three times (n=3) with triplicate wells on each occasion. ANOVA with the post-hoc Tukey test was performed to assess statistical significance of the difference between samples and controls; * $p<0.05$; ns is not significant.

Since the overexpression of α-synuclein did not cause toxicity in undifferentiated SH-SY5Y cells, the ability to cause toxicity with the addition of an inducer of oxidative stress was assessed (Figure 4.10). Rotenone is a mitochondrial complex I inhibitor, which also inhibits microtubule formation (Earley & Ragan, 1984; Srivastava & Panda, 2007). It was chosen as an inducer of oxidative stress because previous studies have suggested links between rotenone, α-synuclein aggregation and neuronal toxicity. Rotenone can cause oxidative modifications to α-synuclein that may enhance its aggregation (Mirzaei *et al*, 2006; Souza *et al*, 2000). In addition, chronic rotenone exposure increases the levels of insoluble α-synuclein with an increase in toxicity (Betarbet *et al*, 2000; Sherer *et al*, 2002). mtGFP-SNCA BacMam (50 µl) was added to SH-SY5Y cells for 24 hours before addition of rotenone. Cells were then cultured for a further 4 days when the MTS assay was performed. Rotenone caused a dose dependent decrease in SH-SY5Y cell number where no BacMam virus was added. However, the overexpression of α-synuclein did not increase this toxicity (Figure 4.10).

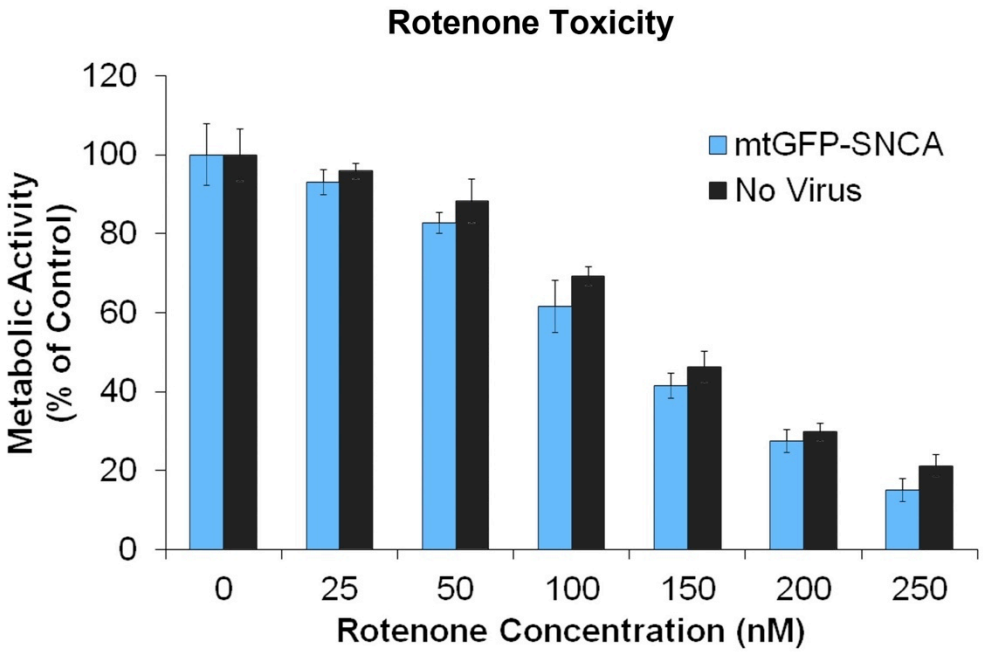

Figure 4.10- Rotenone toxicity in the presence of α-synuclein overexpression. Undifferentiated SH-SY5Y cells were incubated with 50 µl mtGFP-SNCA per $1x10^5$ cells or no virus for 24 hours. Then various rotenone concentrations were added for 4 days when the MTS assay was performed (n=1).

One other study showed α-synuclein overexpression was not toxic to undifferentiated SH-SY5Y cells for up to 10 days. However, when SH-SY5Y cells were differentiated with retinoic acid the presence of α-synuclein was toxic after 6-8 days

(Vekrellis *et al*, 2009). Therefore α-synuclein toxicity in differentiated SH-SY5Y cells was assessed. The FACS experiment performed in Figure 4.8 indicated α-synuclein was not toxic in differentiated SH-SY5Y cells. However, GFP was lost between day 7 and 10. So the toxicity of α-synuclein overexpression for 2 and 4 weeks was assessed using the MTS assay, with the virus topped up every 7 days (Figure 4.11a and 4.12a). α-Synuclein overexpression showed no significant toxicity at 2 or 4 weeks (Figure 4.11a and 4.12a). However, immunocytochemistry performed for α-synuclein at 2 weeks and 4 weeks showed unexpectedly weak immunofluorescence for α-synuclein compared to the robust GFP expression. The merged images showed very little α-synuclein staining in GFP positive cells (Figure 4.11b and 4.12b). Since the differentiated cells formed clumps, these clumps may be inaccessible to the α-synuclein antibody preventing their staining. Therefore the α-synuclein protein level after differentiation should be quantified by western blot. If the α-synuclein protein level decreases quicker than the GFP this may be due to the degradation of α-synuclein being more efficient than GFP. α-Synuclein is degraded by the proteasome and autophagy, and its half-life in SH-SY5Y cells could be shorter than GFP (Webb *et al*, 2003). The half-life of GFP is reported to be approximately 26 hours in mammalian cells but amino acid modifications made to turn it into emerald GFP may enhance its stability (Corish & Tyler-Smith, 1999). In addition, the mitochondrial localisation may delay its degradation. The half-life reported for α-synuclein varies depending on the cell type it is expressed in; in HEK 293 cells the half-life is over 48 hours; in mouse primary cortical neurons it is 26-160 hours depending on the maturity of neurons; in undifferentiated SH-SY5Y cells it is about 13 hours and in differentiated SH-SY5Y it is about 50 hours (Paxinou *et al*, 2001; Li *et al*, 2004). This suggests the half-lfe for α-synuclein is longer than GFP in some cell lines. However, the mitochondrial localisation of GFP may increase its half-life compared to the cytosolic α-synuclein protein. Therefore to determine if the half-life is influential in lack of α-synuclein-induced toxicity, the half-lives of both the α-synuclein protein and the mitochondrial targeted GFP protein should be determined.

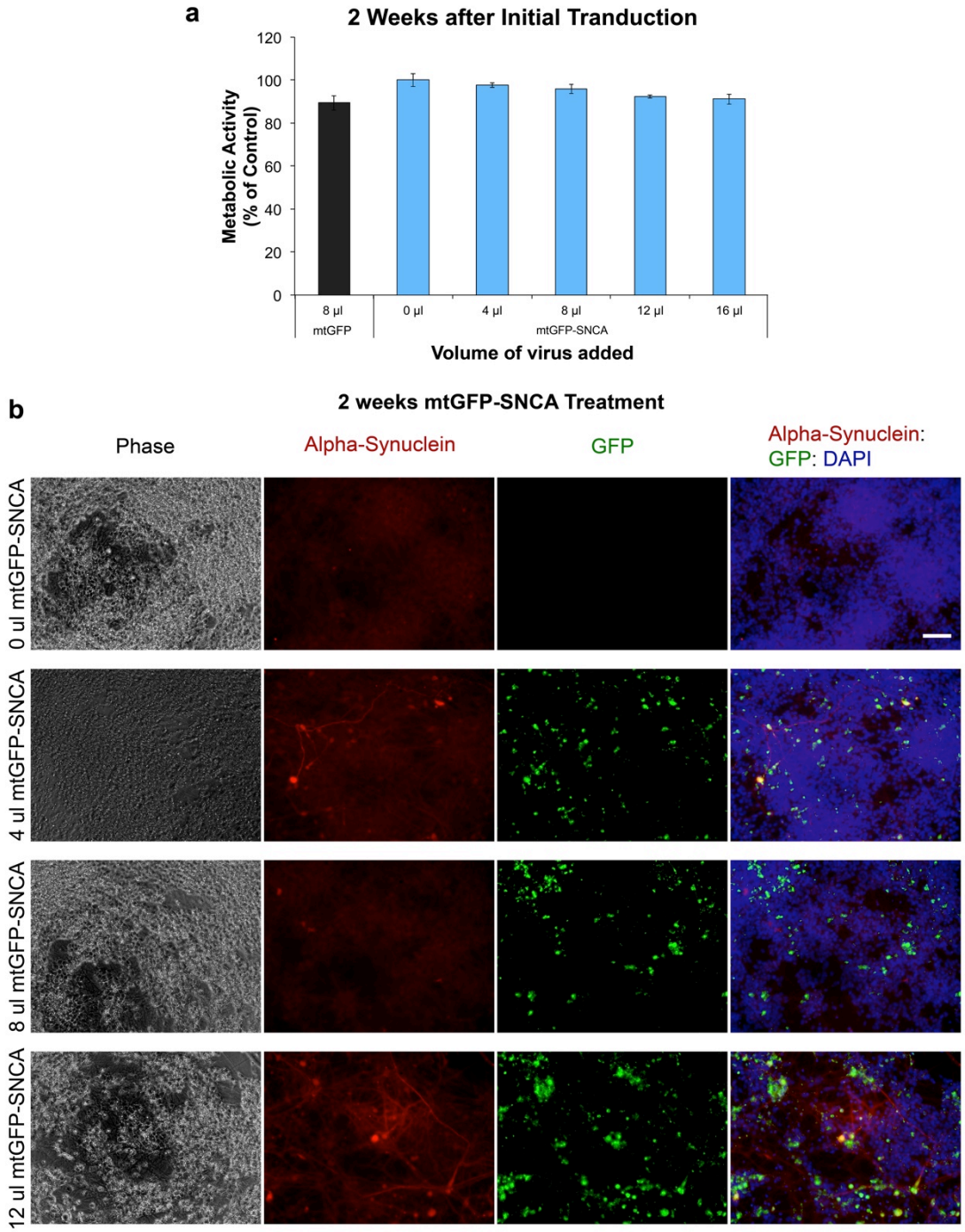

Figure 4.11 – α-Synuclein toxicity in differentiated SH-SY5Y cells after 2 weeks. SH-SY5Y cells were differentiated in the presence of N2 medium and retinoic acid for 12 days. Then various volumes of mtGFP or mtGFP-SNCA were added to the 96-well plates. Note 50 µl added in Figure 4.8 is equivalent to 8 µl added to a 96-well plate here. Cells were then cultured for a further 2 weeks, with a virus top up every 7 days, when the MTS assay was performed (a) (n=1). At 2 weeks cells were fixed and immunocytochemistry for α-synuclein (red) was performed (b). Cells expressed GFP (green) and were counterstained with DAPI (blue); scale bar: 76 µM.

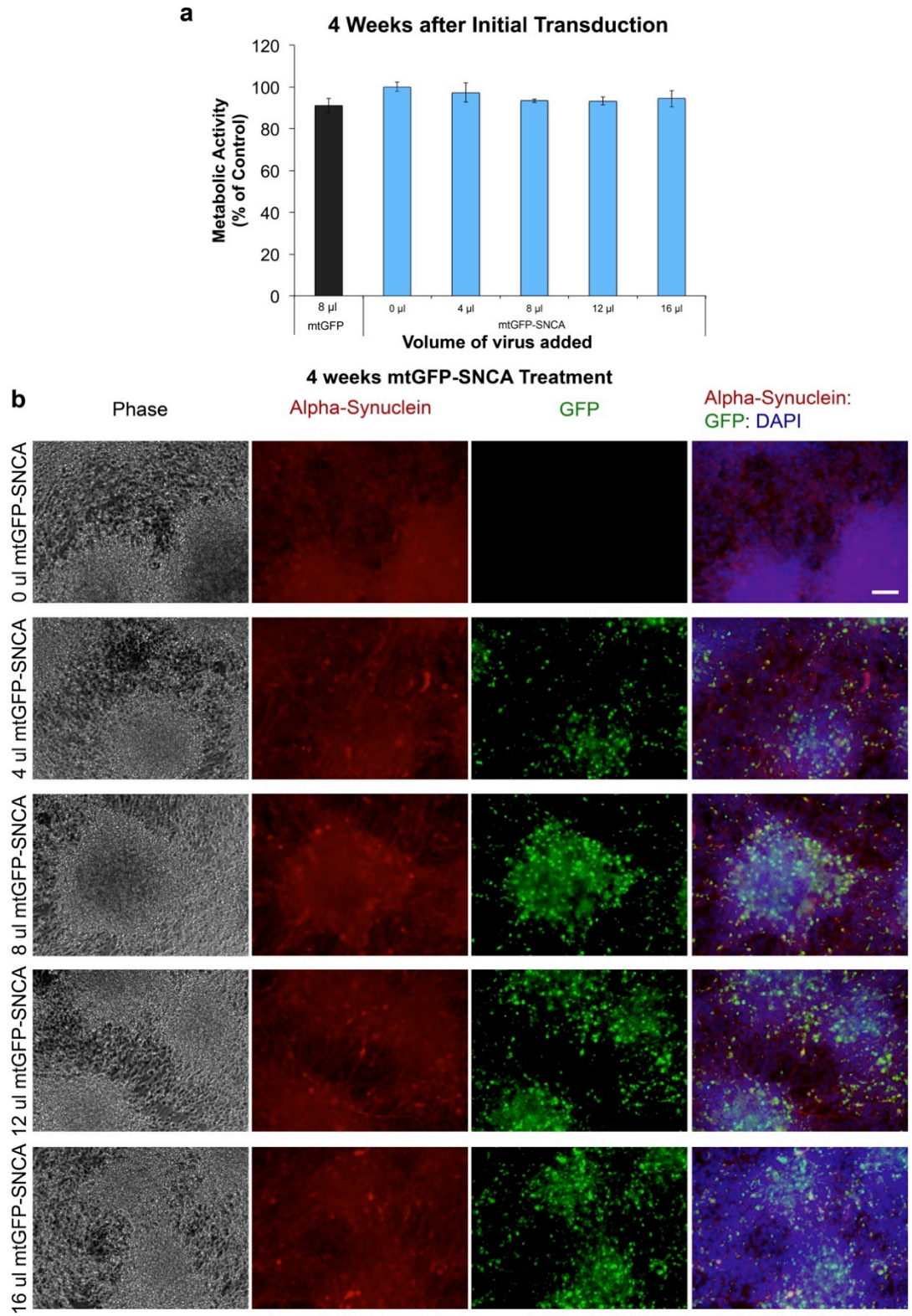

Figure 4.12 - α-Synuclein toxicity in differentiated SH-SY5Y cells after 4 weeks. SH-SY5Y cells were differentiated in the presence of N2 medium and retinoic acid for 12 days. Then various volumes of mtGFP or mtGFP-SNCA were added to the 96-well plates. Note 50 µl added in Figure 4.8 is equivalent to 8 µl added to a 96-well plate here. Cells were then cultured for a further 4 weeks, with a virus top up every 7 days, when the MTS assay was performed (a) (n=1). At 4 weeks cells were fixed and immunocytochemistry for α-synuclein (red) was performed (b). Cells expressed GFP (green) and were counterstained with DAPI (blue); scale bar: 76 µM.

4.6 Effect of α-Synuclein Overexpression on Mitochondrial Morphology

Both undifferentiated and differentiated SH-SY5Y cells did not show α-synuclein-induced toxicity, so more subtle differences were examined. In 2011 Nakamura *et al.* showed that transient overexpression of α-synuclein can result in mitochondrial fragmentation after 48 hours (Nakamura *et al*, 2011). They found no change in mitochondrial function at 24 hours but by 48 hours there was a reduction in respiration and by 96 hours a very small increase in cell death was detected. Therefore, Xing Zheng, a Masters student, and Dr. Fella Hammachi assessed the effect of BacMam α-synuclein overexpression on mitochondrial morphology (Figure 4.13). Confocal images were taken 24, 48 and 72 hours after transduction of undifferentiated SH-SY5Y cells. The images were then randomised and mitochondrial morphology of each cell was classified blind using ImageJ. Each cell in the images was classified as having tubular, fragmented or intermediate mitochondrial morphologies, depending on the length divided by the width (axis) of their mitochondria. Cells that contained mitochondria with an axis of >10 μm were classified as tubular. Those with an axis of <3 μm were classified as fragmented and cells that contained both types of mitochondria were classified as intermediate (Figure 4.13a). The percentage of cells with each type of mitochondrial morphology in each condition was calculated (Figure 4.13b). After 24 hours the majority of cells had tubular mitochondria. This changed by 48 hours when there was an increase in the number of cells containing fragmented mitochondria at the highest level of α-synuclein overexpression, 50 μl mtGFP-SNCA. The lower level of α-synuclein overexpression, 20 μl mtGFP-SNCA, and the control, mtGFP treated cells showed much fewer cells with fragmented mitochondria. The increase in mitochondrial fragmentation at the higher level of α-synuclein overexpression was maintained at 72 hours. However, the lower volume of mtGFP-SNCA and control mtGFP still showed no increase in mitochondrial fragmentation. In parallel, the same doses of virus used in the mitochondrial fragmentation assay were used to assess toxicity in undifferentiated SH-SY5Y cells using the MTS assay (Figure 4.13c). In this assay there was no toxicity detected up to 5 days after transduction, therefore the mitochondrial fragmentation does not appear to increase cellular toxicity.

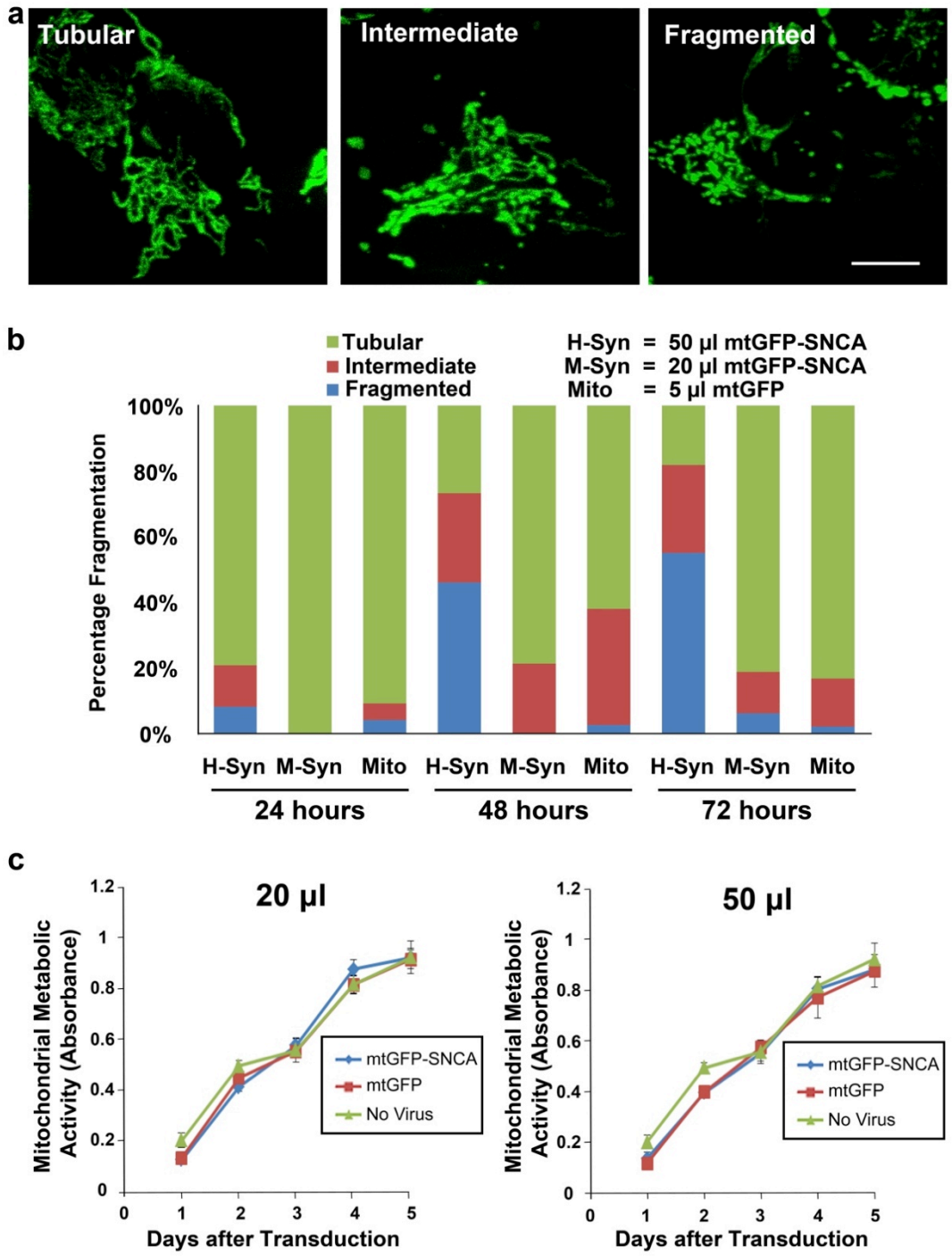

Figure 4.13 – Effect of α-synuclein overexpression on mitochondrial morphology.
Undifferentiated SH-SY5Y cells were incubated with mtGFP-SNCA or the control mtGFP for 24, 48 or 72 hours, when live confocal images were taken (data from Dr. Fella Hammachi). The mitochondrial morphology was assessed and each cell was classified as tubular, fragmented or intermediate, if they contained both tubular and fragmented mitochondria (a); scale bar: 10 µM. The percentage of cells with each type of morphology for each condition was calculated (b) (n=1). In addition, the toxicity of mtGFP-SNCA and mtGFP was assessed using the MTS assay over 5 days (c).

Mitochondrial morphology is reliant on the balance between mitochondrial fission and fusion. If there is fragmentation this may be due to an increase in mitochondrial fission or a reduction in mitochondrial fusion. Dyanmin-related protein 1 (Drp1) is a major regulator of mitochondrial fission that moves from the cytosol to the mitochondria to induce fission (Smirnova *et al*, 1998). Therefore the protein levels of Drp1 and the subcellular localisation of Drp1 could determine whether there is an increase in mitochondrial fission. Mitofusin and OPA1 are involved in mitochondrial fusion (Chen *et al*, 2003; Olichon *et al*, 2002). The levels of these could determine whether there is a reduction in mitochondrial fusion. An increase in mitochdondrial fission could also be a sign of early apoptosis therefore whether cytochrome c has been released from the mitochondria or whether the proapoptotic protein BAX has increased should be assessed. Nakamura *et al* show that knock-out of Drp1 does not prevent α-synuclein induced fragmentation and instead α-synuclein directly interacts with cardiolipin in the mitochondrial membrane. Therefore this too should be assessed in the SH-SY5Y cell line.

4.7 Effect of α-Synuclein Overexpression on Oxidative Stress

High overexpression of α-synuclein increased the number of cells with fragmented mitochondria, possibly due to an increase in mitochondrial fission. Since the mitochondria may be a major source of ROS production in cells, this change in fragmentation may be associated with an increase in ROS production. Previous studies found aggregation of α-synuclein increases ROS production. In addition, oligomeric or sonicated α-synuclein fibrils are taken up into cells and increase ROS production, whereas fibrils or monomers do not (Cremades *et al*, 2012; Dryanovski *et al*, 2013).

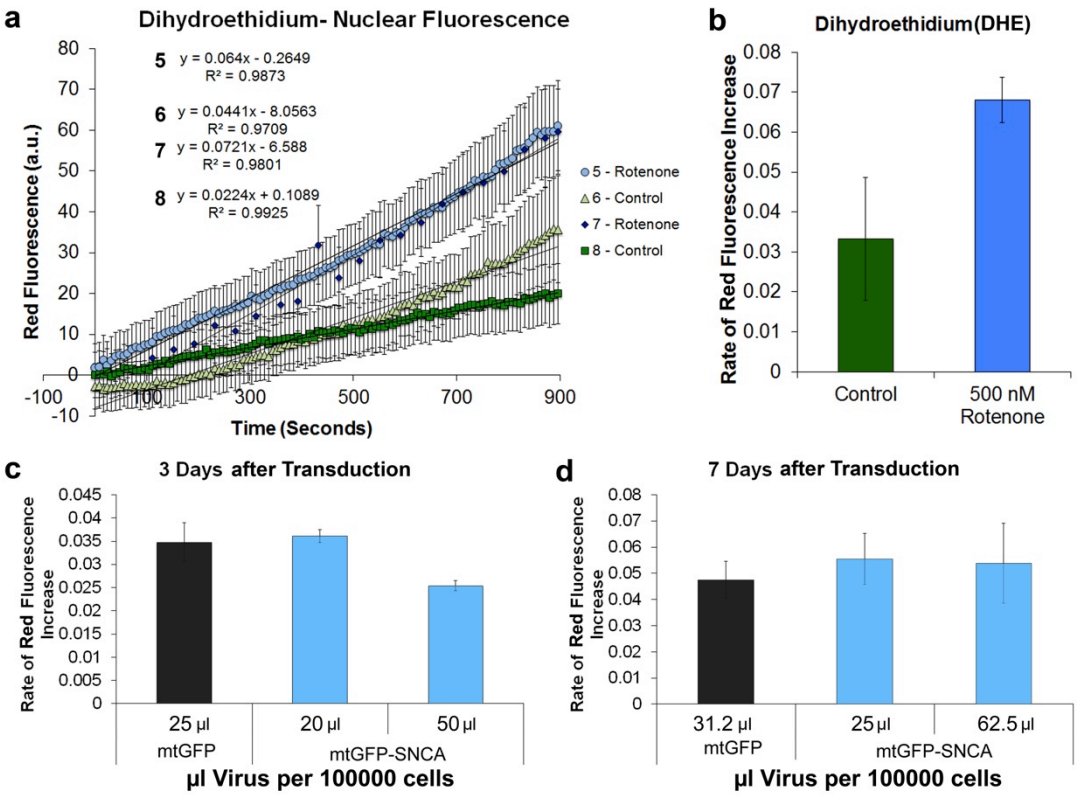

Figure 4.14 – Effect of α-synuclein overexpression on ROS production. Undifferentiated SH-SY5Y cells on coverslips were cultured in the presence of 500 nM rotenone or vehicle, in duplicate, for 2 hours. Coverslips were loaded into coverslip holders and DHE was added. Images were taken every 8 seconds for 15 minutes. The nuclear red fluorescence intensity was measured using Volocity. This red fluorescence was plotted against time (a). The slope of the red fluorescence increase was calculated, as a measure of rate of ROS production, for both control and 500 nM rotenone (b). Undifferentiated SH-SY5Y cells were seeded on coverslips and mtGFP or mtGFP-SNCA was added for 3 days (c) or 7 days (d) when DHE was added and the rate of red fluorescence increase was calculated. Coverslip samples for each condition were in duplicate or triplicate with n=1.

The rate of ROS production in cells was assessed with a DHE live-imaging assay. When DHE is oxidised to ethidium or 2-hydroxyethidium in cells it binds to genomic DNA resulting in an increase of nuclear red fluorescence over time. The rate of this increase is directly correlated to the rate of ROS production (Bindokas *et al*, 1996; Zhao *et al*, 2003). Initially the assay was optimised using rotenone as a positive control (Figure 4.14a and b). Cells were incubated with 500 nM rotenone or DMSO vehicle for 2 hours. They were then loaded into a coverslip holder and an area was selected for imaging. DHE (5 µM) in HBSS was added to cells on the microscope and images were taken every 8 seconds for 15 minutes. Subsequently, areas in the nuclei of each cell were selected using Volocity and the red fluorescence intensity was measured at each time point (Figure 4.14a). The slope of the red fluorescence increase was calculated as a measure of the rate of DHE oxidation, which is directly related to rate of ROS production. This showed that 500 nM rotenone had a greater increase of ROS production than the control treated cells; therefore the assay is capable of

detecting an increase in ROS production (Figure 4.14b). This DHE assay was used to assess the effect of α-synuclein overexpression on ROS production. In this assay, as previously, the volumes of the control mtGFP and mtGFP-SNCA used were based on a previous calculation where the percentage of GFP positive cells were compared, therefore 1 µl mtGFP was used as an equivalent to 2 µl mtGFP-SNCA. Even though this is an incorrect way of calculating the equivalent it resulted in a much higher volume of mtGFP being used than needed. The results show neither of the mtGFP treated cell samples had an increased ROS production. Therefore neither the baculovirus, nor the mtGFP have an effect on ROS production. α-Synuclein overexpression for 3 and 7 days at 20-25 µl per 100,000 cells also failed to show an increase in ROS production (Figure 4.14 c and d). However, 50 µl per 100,000 cells for 3 days appeared to show a decrease in ROS production but this was only from one experiment with duplicate coverslips. This experiment needs repeating to determine whether there is a significant reduction. Since 62.5 µl per 100,000 cells for 7 days did not show a decrease in ROS production it is possible that the reduction is not reproducible. If there is a reduction in ROS production then α-synuclein may be capable of preventing oxidative stress and therefore may be protective rather than toxic. However, this would require further investigation.

4.8 Discussion and Future Directions

α-Synuclein overexpression showed no toxicity in undifferentiated or differentiated SH-SY5Y cells, despite inducing mitochondrial fragmentation at high levels of overexpression.

Overexpression was achieved using a BacMam construct that encoded α-synuclein and mtGFP. The transduction resulted in an increase in α-synuclein protein and GFP in a dose dependent manner after 24 hours. Increasing the α-synuclein levels for up to 5 days did not cause toxicity in undifferentiated SH-SY5Y cells. In addition, in the presence of rotenone, an initiator of oxidative stress, α-synuclein overexpression failed to show an increase in toxicity. In differentiated SH-SY5Y cells the increase in mtGFP was maintained at a high level for 7 days after which it was reduced. How this relates to α-synuclein protein expression is unknown but immunocytochemistry at 2 and 4 weeks suggested α-synuclein might be degraded more quickly than mitochondrially targeted GFP. However, this is in contrast to the published half-lives of α-synuclein, which is 50 hours in differentiated SH-SY5Y cells and cytosolic GFP, which is around 26 hours in mammalian cells (Corish & Tyler-Smith, 1999; Li *et al*, 2004). Therefore clarification of the α-synuclein protein level relative to the GFP protein level over time by western blot is needed to see how quickly the α-synuclein is degraded. If α-synuclein is degraded more quickly than mitochondrial GFP

then it could be why toxicity was not seen, and may mean the BacMam needs to be topped up more often than every 7 days. There are a number of possible reasons why no toxicity was found. The α-synuclein protein levels may not have been at a high enough level for long enough to cause toxicity. An inducible increase of longer-lasting and higher levels of α-synuclein could be achieved by creating cell lines with inducible α-synuclein gene expression. Alternatively toxic oligomeric α-synuclein may not have been produced. Another reason may be due to the cell type that was used. SH-SY5Y cells are a cancer cell line that is likely to be more robust than neurons. The use of a different cell line or primary neurons with catecholaminergic properties may be needed. In addition, cells or neurons with a greater level of endogenous α-synuclein expression and with presynaptic localisation could be required.

No lethal toxicity was found in either undifferentiated or differentiated SH-SY5Y cells but there may be more subtle defects in cell function. α-Synuclein has been shown to be capable of preventing protein degradation therefore its ability to inhibit proteasomal function could be assessed. This could be assessed by analysis of the ubiquitination of proteins over time by western blotting in α-synuclein overexpressing cell lines and control cell lines. If there is a build up of ubiquitinated protein in the α-synuclein overexpressing cell lines compared to the control cell lines then it would suggest the proteasome function is inhibited. In addition, since there is an increase in mitochondrial fragmentation this could be investigated further to determine what causes the fragmentation. The levels of mitophagy could be assessed using a lysotracker dye. If the lysotracker dye co-locates with the mitochondrial targeted GFP then it would suggest mitophagy is occurring.

Chapter 5 – *tert*-Butyl hydroperoxide-Induced Oxidative Stress Cell Model

5.1 Introduction

Antoxis Limited have developed a number of novel compounds based on natural antioxidants. They showed AO-1-530 was one of their lead compounds at protecting against microsome lipid peroxidation (Bennett *et al*, 2004). This antioxidant property makes it an exciting compound to test in models of α-synucleinopathies, where oxidative stress has been implicated (Dryanovski *et al*, 2013; Cremades *et al*, 2012). However, since an α-synuclein-induced toxicity model could not be produced, a toxin-based neuronal model was established. This model was used to assess the protective potential of AO-1-530 compared to other natural antioxidants and allowed investigation into its mechanism of protection.

5.2 Antioxidants

Antoxis' lead compound AO-1-530 is a flavonol. Flavonols are a subgroup of flavonoid antoxidants the structures of which is shown in Figure 5.1a. They have a hydroxyl group attached to position 3 of the C ring, which is a pyran-4-one. These ring structures with hydroxyl groups attached make them good hydrogen donators to free radicals due to the delocalisation of electrons. There is significant literature comparing flavonoid antioxidants to determine the functional groups important for optimal antioxidant action. The best antioxidants have a catechol group (a benzene ring with 2 hydroxyl groups attached) at the B ring, a double bond in the C ring between carbon 2 and 3 and a 4-oxo group in the C ring surrounded by hydroxyl groups at carbon 3 and 5 (van Acker *et al*, 1996; Bors *et al*, 1990). Myricetin and quercetin have these groups (Figure 5.1b) and are some of the best flavonol antioxidants. Comparing flavonoids to ascorbic acid and Trolox, a water-soluble derivative of vitamin E, showed flavonols are more potent free radical scavengers (Oliveira *et al*, 2014; Rice-Evans *et al*, 1997). However, flavonoids do not have the same absorption through the diet as vitamin E (Duthie & Morrice, 2012). Therefore, combining the radical scavenging potential of flavonols, like myricetin, and the bioavailability of vitamin E may produce a more effective antioxidant. Antoxis Limited develop novel compounds, combining antioxidant properties of flavonoids with improved bioavailability. They synthesised a variety of compounds with a myricetin head groups and varying chain length, chain position and chain branching (Bennett *et al*, 2004). This showed the 8-carbon chain length with methyl groups attached like vitamin E and the straight 10-carbon chain were the best protectors against lipid peroxidation. The 10-carbon chain antioxidant is Antoxis' lead compound AO-1-530. AO-1-530 was compared to the three other natural antioxidants in Figure 5.1b for their ability to protect against oxidative stress.

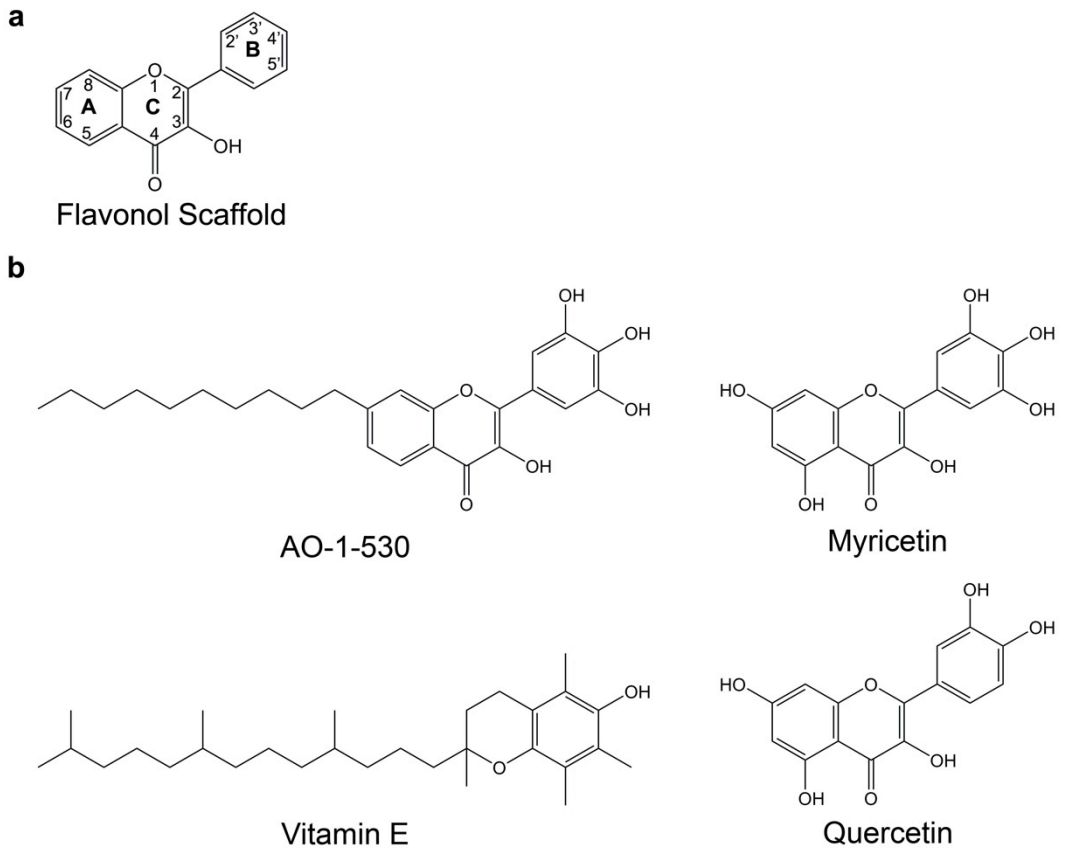

Figure 5.1 - Antioxidant chemical structures. (a) This shows the structure of the subgroup of flavonoids known as flavonols. (b) The natural antioxidants myricetin and quercetin and the synthetic antioxidant AO-1-530 contain the flavonol scaffold. AO-1-530 has a similar head group to myricetin with a lipophilic tail that was based on that of vitamin E. These four antioxidants were compared for their ability to protect cells against oxidative stress.

Flavonols, which have a carbonyl group next to the hydroxyl group at position 3 on ring C naturally fluoresce (Mukai *et al*, 2011; McMorrow & Kasha, 1984). The fluorescence of the antioxidants in DMSO was confirmed using a fluorescence plate reader with excitation 485 nm and emission 520 nm (Figure 5.2). All three flavonoid antioxidants showed green fluorescence to varying degrees. AO-1-530 was highly fluorescent, whereas myricetin and quercetin showed a similar lower fluorescence.

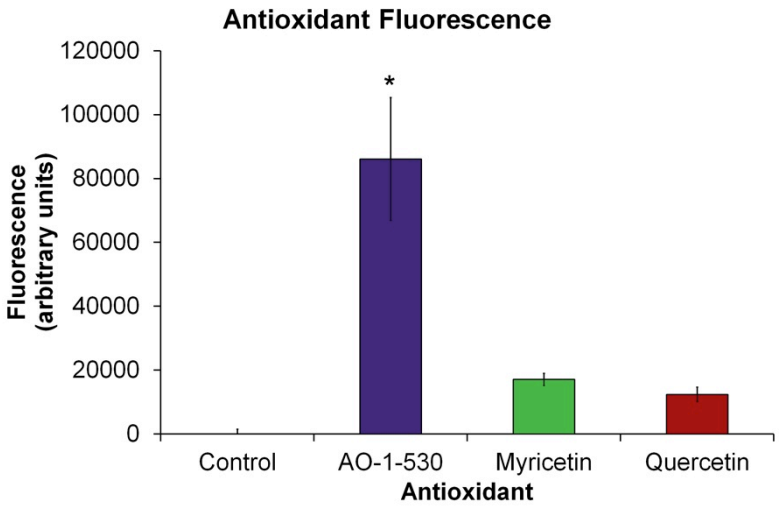

Figure 5.2 - Flavonol antioxidants naturally fluoresce green. 1 mM antioxidant solutions in DMSO were loaded into a 96-well plate in triplicate. The fluorescence level was assessed in a plate reader with excitation 485 nm and emission 520 nm. Each bar represents the mean of four separate experiments and the error bars represent the SEM. ANOVA with a Tukey post-hoc test was performed to assess the significant difference between samples and the control; * $p<0.05$.

The flavonoid antioxidants fluoresce green so their uptake and localisation within cells can be examined (Figures 5.3-5.5). A 10-fold lower concentration of AO-1-530 than myricetin or quercetin was used because AO-1-530 is toxic at 100 µM. This toxicity could be due to auto-oxidation of AO-1-530 producing H_2O_2, which has also been found for myricetin (Mukai *et al*, 2011; Kajiya *et al*, 2001). Confocal microscopy showed AO-1-530 was taken up into cells, excluded from the nucleus and enriched in filamentous structures, which looked mitochondrial (Figure 5.3). Therefore, the co-localisation of AO-1-530 with Mitotracker Deep Red was assessed (Figure 5.4). The overlay shows AO-1-530 was enriched in the mitochondria and was found elsewhere in the cytoplasm. Quercetin was also taken up into cells, but in contrast to AO-1-530, quercetin showed strong nuclear localisation (Figure 5.3). The cells incubated with myricetin showed no green fluorescence, indicating it was not taken up into cells. This may be due to myricetin's lower lipophilicity (Kajiya *et al*, 2001) or due to its instability at neutral pH (Yao *et al*, 2014).

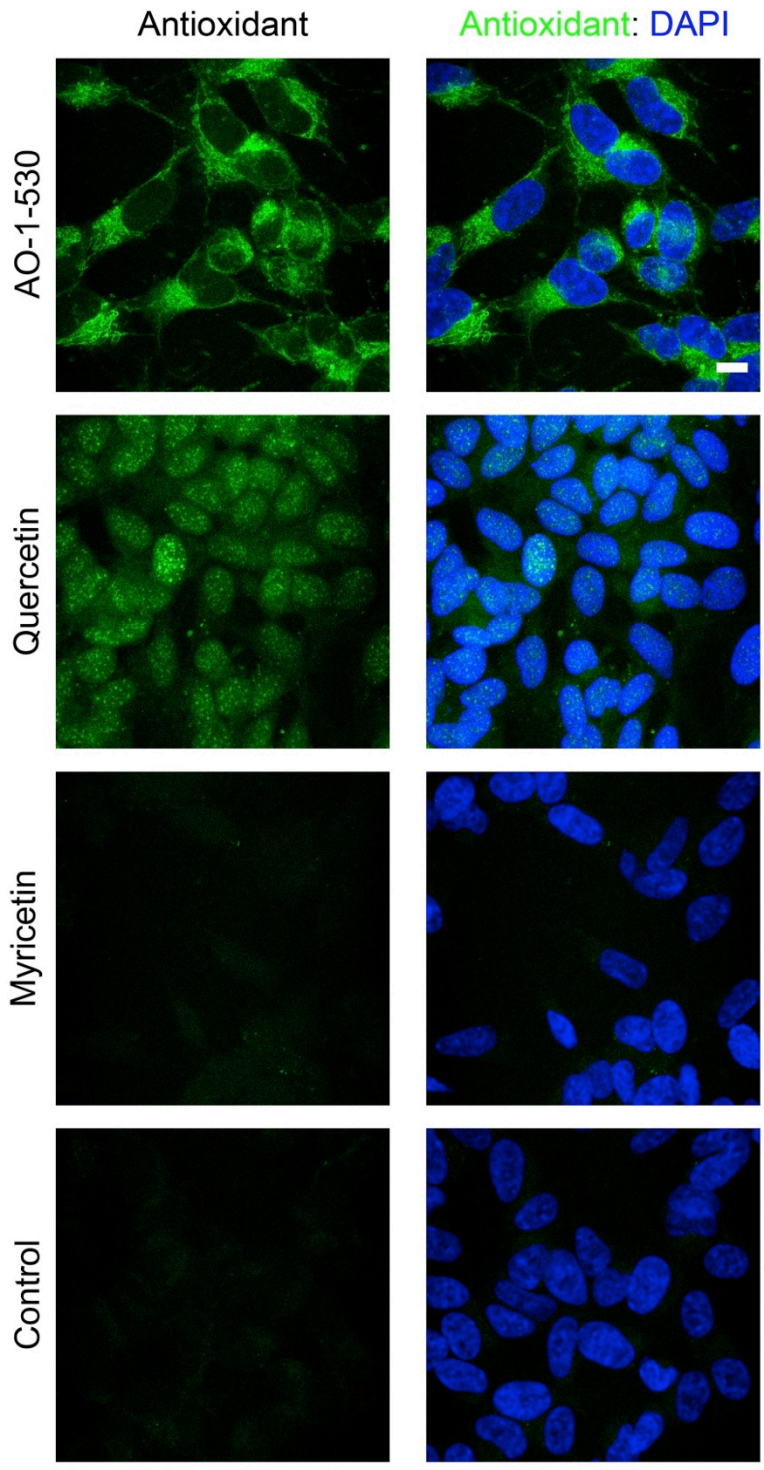

Figure 5.3 - Flavonol antioxidant localisation in SH-SY5Y cells. SH-SY5Y cells were incubated with antioxidants (myricetin, 100 µM; quercetin, 100 µM; AO-1-530, 10 µM) for 2 hours, fixed, counterstained with DAPI (blue) and mounted with Vectashield onto slides. They were then imaged using the 63x objective of the Leica TCS SPE confocal microscope; scale bar: 11 µm.

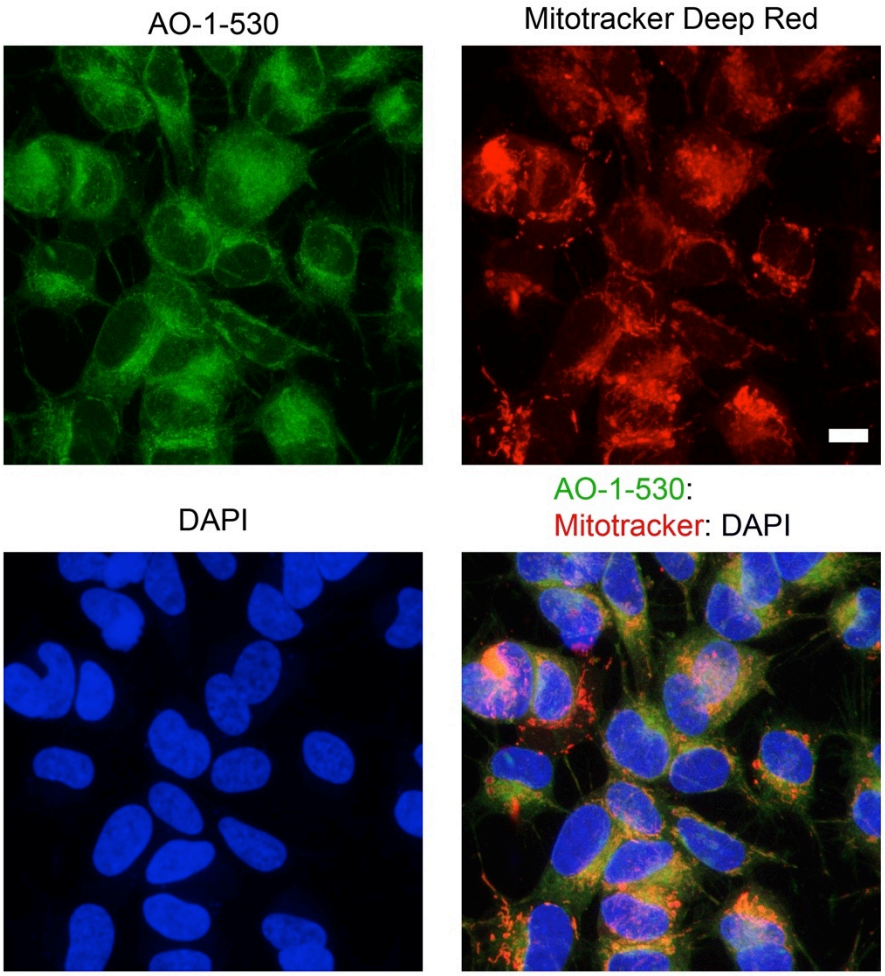

Figure 5.4 - AO-1-530 localisation in SH-SY5Y cells. SH-SY5Y cells were incubated with Mitotracker Deep Red (100 nM) for 20 minutes. Then AO-1-530 (10 µM) was added for 2 hours. Cells were fixed, counterstained with DAPI (blue), mounted with Vectashield onto slides and imaged using the 63x objective of the Leica TCS SPE confocal microscope; scale bar: 11 µm.

FACS analysis was performed to get a quantitative measure of the number of cells that had taken up the antioxidant (Figure 5.5). The FACS plot in Figure 5.5a shows that, as with confocal microscopy, AO-1-530 and quercetin were inside the cells but myricetin was not. All cells have taken up some AO-1-530 or quercetin. FACS analysis was performed twice with triplicate samples; the mean fluorescence and SEM are shown in Figure 5.5b. This confirms the antioxidants that were taken up into cells. However, it is important to note the fluorescence intensity varies with antioxidant (Figure 5.2), so just because AO-1-530 incubated cells have a higher level of fluorescence it does not mean more AO-1-530 has been taken up into cells than quercetin.

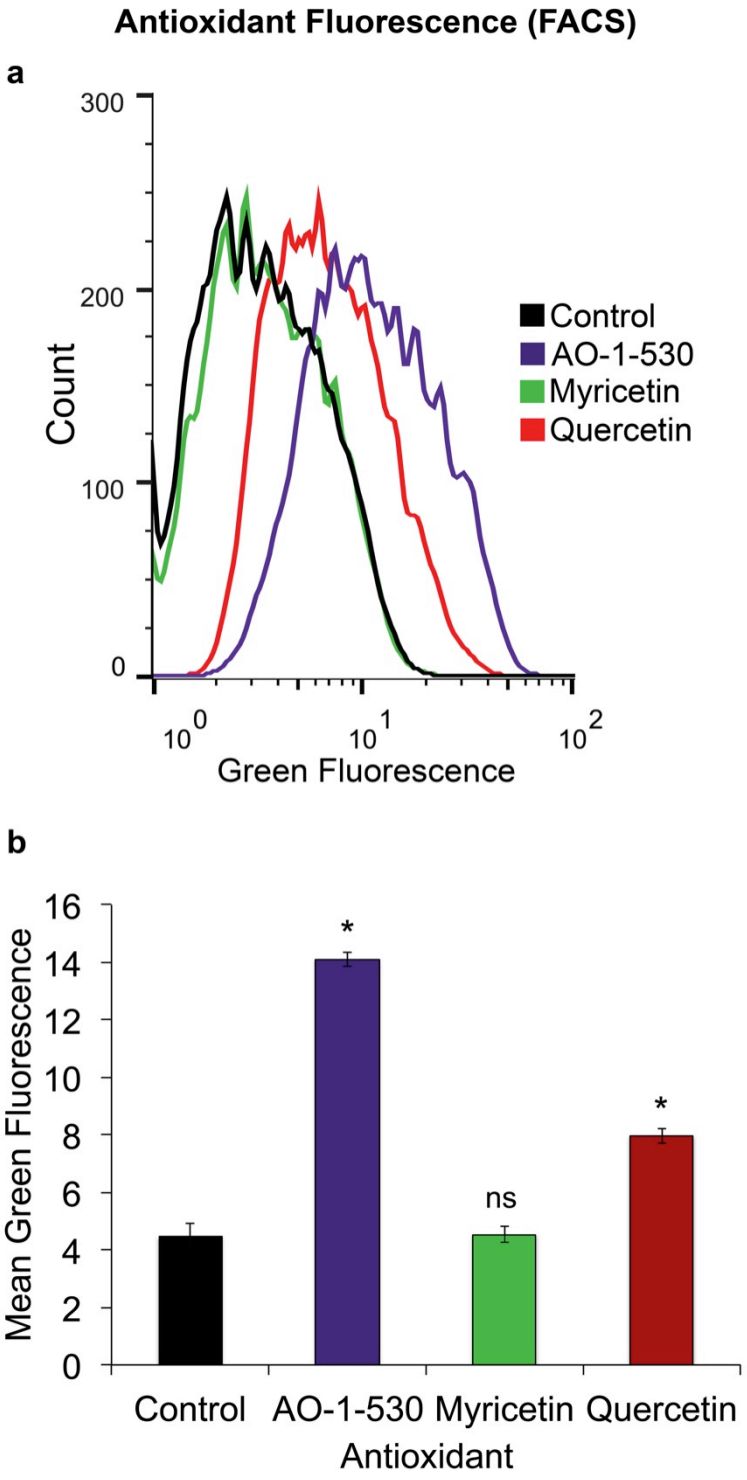

Figure 5.5 - Flavonol antioxidant uptake into cells determined using FACS analysis. Antioxidants (myricetin 100 µM; quercetin 100 µM and AO-1-530 10 µM) were added to SH-SY5Y cells for 2 hours. Cells were then lifted using trypsin, washed and incubated with PI, to exclude dead cells. The level of green fluorescence from each cell was analysed using the FACS Calibur (a). (b) Bars represent the mean green fluorescence from two separate FACS experiments each with triplicate samples and error bars represent the SEM**.** ANOVA with a Tukey post-hoc test was performed to assess the significant difference between samples and the control; * $p<0.05$; ns, not significant, $p>0.05$.

5.3 Protection against tBHP-Induced Toxicity

In order to compare the antioxidant capabilities of AO-1-530 and the natural antioxidants an oxidative stress cell model was needed. Undifferentiated SH-SY5Y cells and NS-1 cells were used with the toxin tBHP. tBHP is an organic peroxide, easily taken up by cells. Once inside cells tBHP is a substrate for the enzyme GPx, which enzymatically reduces it to *tert*-butyl alcohol (Flohe, 1982). However, not all of the tBHP is removed in this way. When tBHP comes into contact with transition metal ions, free radicals are produced, initially alkoxyl ($RO^{\bullet}$) and subsequently peroxyl ($ROO^{\bullet}$) radicals. These free radicals are capable of damaging cellular components (Van der Zee *et al*, 1996). tBHP was chosen as an inducer of oxidative stress for a number of reasons. Firstly, tBHP is known on reaction with iron (II) to produce the alkoxyl radical ($RO^{\bullet}$) which can induce a lipid peroxidation chain reaction in cellular membranes (Van der Zee *et al*, 1996). The lipophilic tail attached to AO-1-530 may embed it in the membrane, like vitamin E, inhibiting lipid peroxidation. Secondly, tBHP rather than H_2O_2 was chosen as cells have a more effective antioxidant response to H_2O_2. Therefore the induction of oxidative stress is more consistent with tBHP (Alía *et al*, 2005). Thirdly, a number of studies have evaluated the effect of tBHP on isolated mitochondria. This has shown tBHP is capable of inducing lipid peroxidation of the mitochondrial membrane (Radi *et al*, 1993). Finally, addition of tBHP to hepatocytes has shown that the mitochondrial NADPH is reduced and the mitochondrial and cytosolic oxidative stress increases. Therefore, tBHP addition to intact cells damages the mitochondria (Nieminen *et al*, 1997).

In order to quantify the toxicity of tBHP and the protection of antioxidants a number of cell viability assays were used. One of these was the MTS assay (Figure 4.9a). To optimise undifferentiated SH-SY5Y cells for use with the MTS assay, cells were seeded at different densities into 96-well plates and cultured for 24 hours when the MTS assay was performed (Figure 5.6). The cells show a linear correlation of cell number to absorbance up to 40,000 cells per well. In this case the assay was being optimised for use as a measure of toxicity therefore a point at the higher end of the linear slope was chosen, 40,000 cells per well for further experiments (Figure 5.6).

Based on a time-course of tBHP addition, the toxin, should be added to cells for 5 hours. It was then necessary to determine the appropriate concentration of tBHP to use (Figure 5.7a). 100 μM tBHP or below was not significantly toxic but concentrations above 200 μM were toxic. The toxicity plateaued at 400 μM, therefore this concentration was chosen to induce a significant reduction in metabolic activity, allowing the antioxidant protective potential to be assessed.

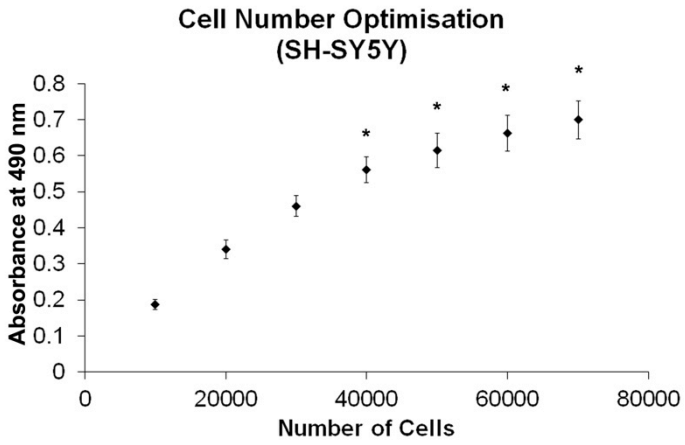

Figure 5.6 - Optimisation of SH-SY5Y cell number. The MTS assay was performed on SH-SY5Y cells seeded at different densities. MTS and PMS were incubated with cells for 1 hour when the absorbance at 490 nm and reference wavelength 650 nm were recorded. Each point represents the average absorbance from three separate experiments each with triplicate samples and the error bars show the SEM. ANOVA with a Tukey post-hoc test was performed to assess the significant difference between samples and 10,000 cells absorbance * $p<0.05$.

In addition, the antioxidant toxicity was assessed (Figure 5.7b and c). Discussion with Antoxis Limited and preliminary experiments were used to choose an appropriate concentration range for each antioxidant. AO-1-530 would be used at up to 10 μM. Since it was also shown to be significantly toxic at 40 μM and above (Figure 5.7c). Myricetin and quercetin would be used at up to 100 μM and vitamin E at up to 300 μM. Cells treated for 16 hours with antioxidants showed most antioxidant concentrations were not significantly toxic, except for 100 μM quercetin (Figure 5.7b).

These optimisation experiments led to the following experimental design; SH-SY5Y cells were pre-incubated for 30 minutes with the vehicle or antioxidants before addition of 400 μM tBHP. The cells were then incubated for 5 hours or 16 hours when the cell viability was assessed by examining cellular morphology (Figure 5.8) and using the MTS assay (Figure 5.9), LDH assay (Figure 5.11) and PI with FACS analysis (Figure 5.12).

The cell morphology 5 hours after tBHP addition appeared rounded and the short processes were retracted (Figure 5.8). Pre-incubation with 10 μM AO-1-530 or 100 μM quercetin protected the cells from rounding up; cells were attached and spread out similar to control treated cells. In contrast, pre-incubation with 100 μM myricetin or 300 μM vitamin E failed to prevent the cells rounding up. Similar protection results can be seen in the videos on the enclosed CD, which were imaged every 30 minutes for 12 hours after tBHP addition.

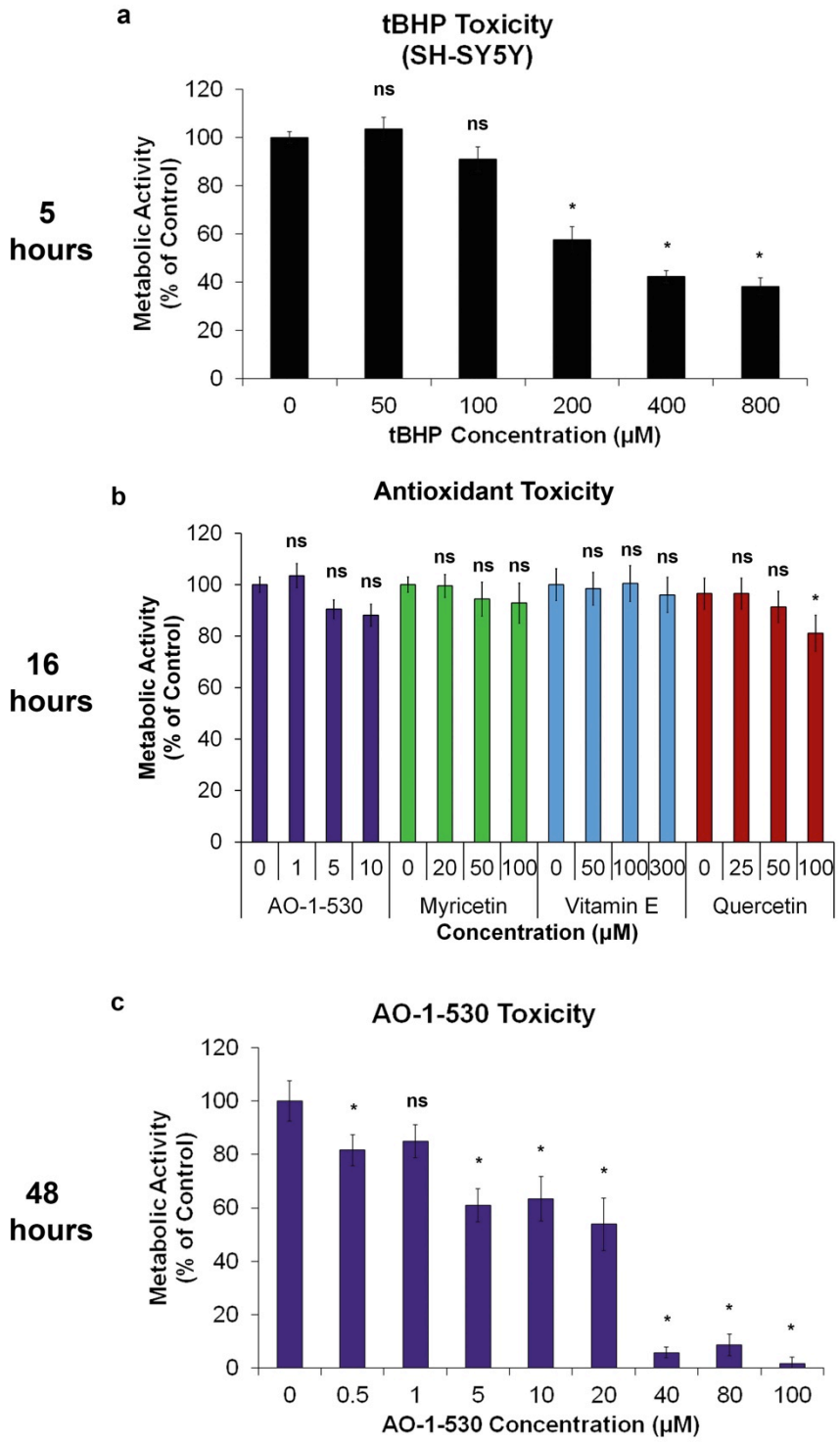

Figure 5.7 - tBHP and antioxidant toxicity in SH-SY5Y cells. tBHP was added to SH-SY5Y cells for 5 hours (a), antioxidants were added for 16 hours (b) or AO-1-530 was added for 48 hours (c). The MTS assay was then performed in the last hour when the absorbance was read. Each bar represents the average absorbance relative to untreated control cells from three separate experiments; each with triplicate wells. Error bars represent the SEM. ANOVA with a Tukey post-hoc test was performed to assess the significant difference between samples and the control; * $p<0.05$; ns, not significant, $p>0.05$.

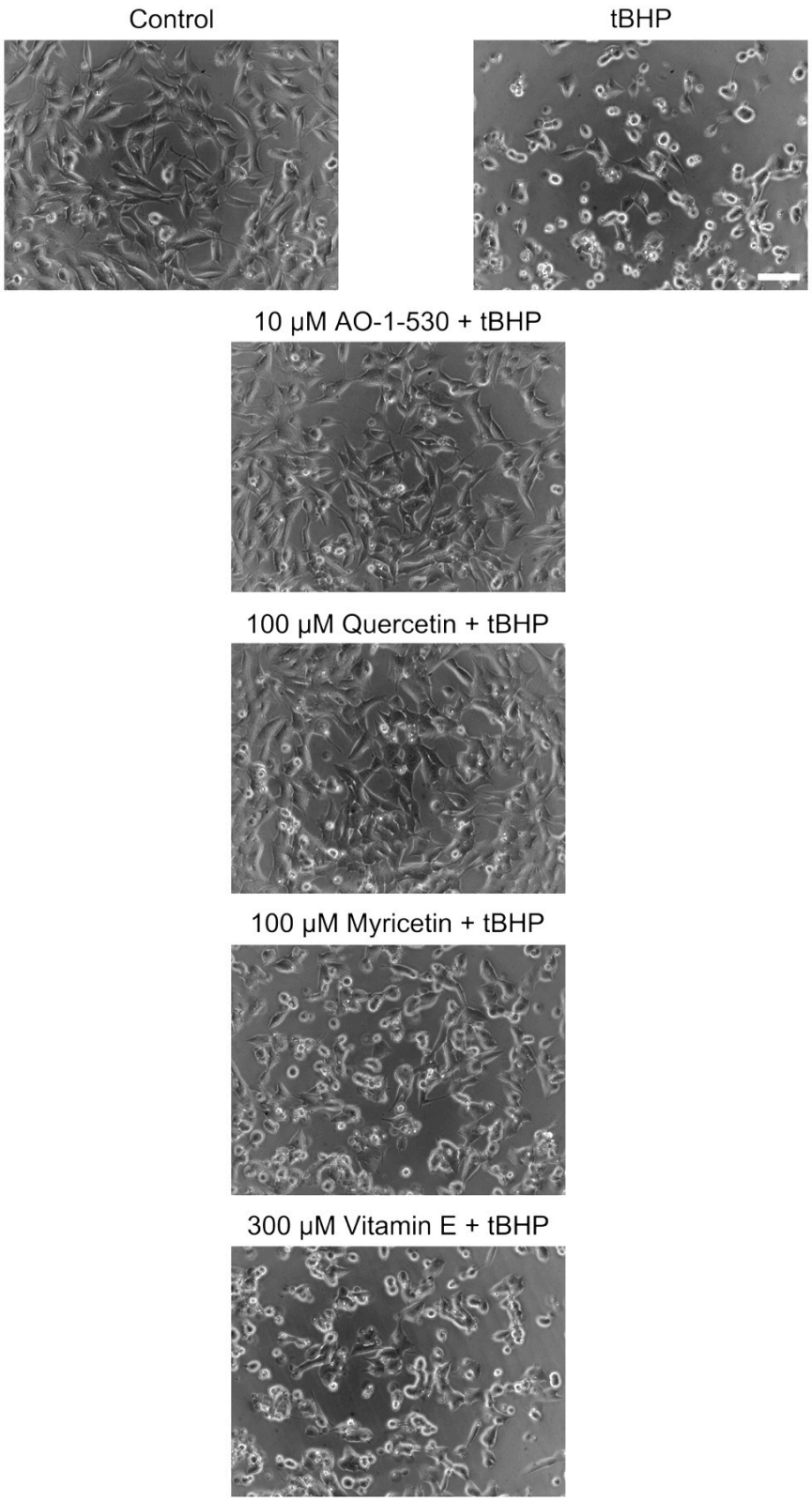

Figure 5.8 – Antioxidant protection against tBHP-induced toxicity assessed by cell morphology. SH-SY5Y cells were pre-incubated with the stated antioxidants or vehicle for 30 minutes, when 400 µM tBHP was added. 5 hours later live images were taken; scale bar: 76 µm.

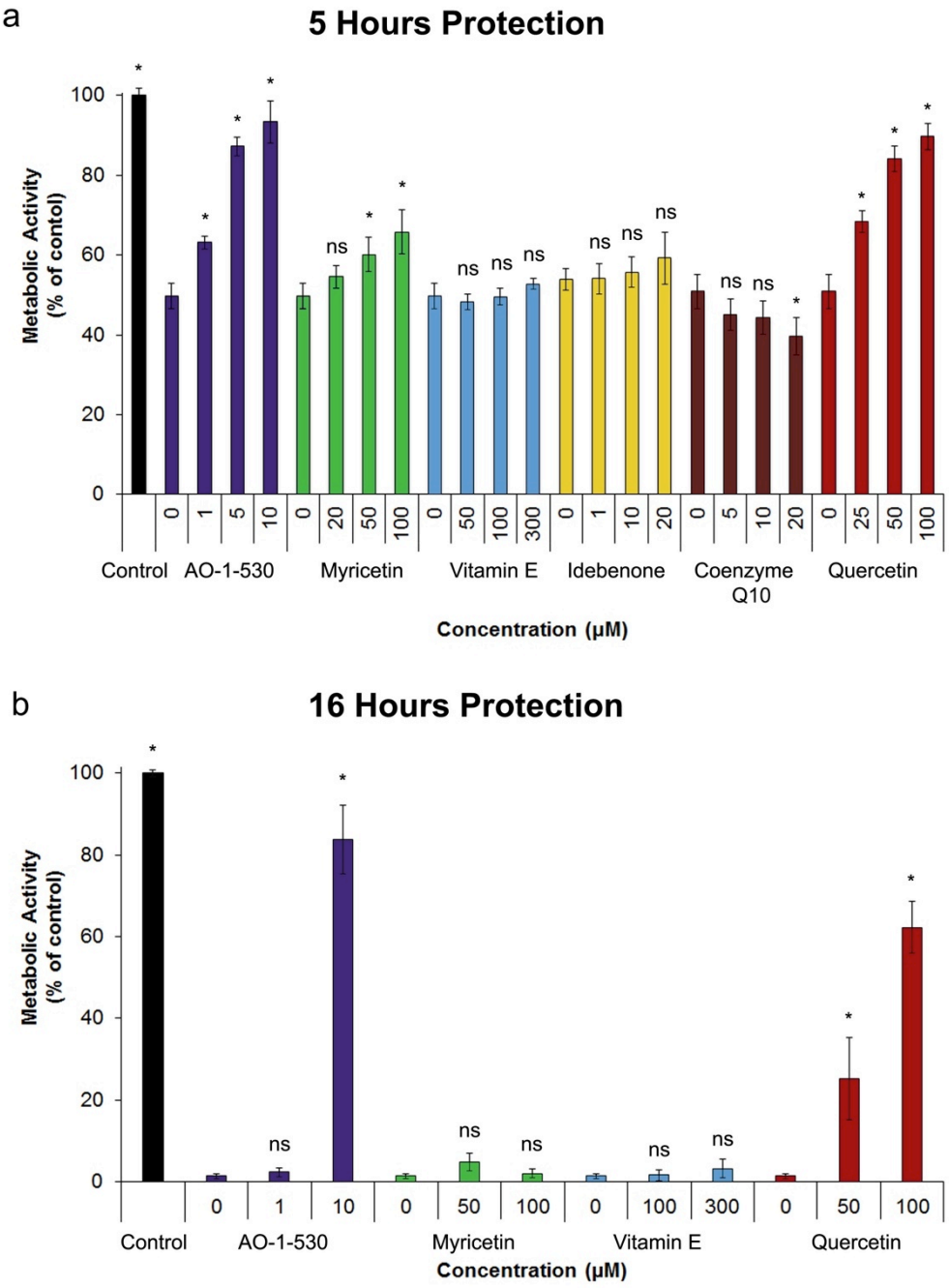

Figure 5.9 - Antioxidant protection against tBHP-induced toxicity assessed using the MTS assay. SH-SY5Y cells were pre-incubated with antioxidants or vehicle for 30 minutes, when tBHP was added for 5 hours (a) or 16 hours (b). In the last hour MTS was added and the absorbance was read. Each bar represents the average absorbance relative to untreated control cells (black bar) from three separate experiments each with triplicate wells, error bars represent the SEM. ANOVA with a Tukey post-hoc test was performed to assess the significant difference between samples and the tBHP treated cells; * $p<0.05$; ns, not significant.

Figure 5.9a shows the antioxidant protection against tBHP-induced toxicity assessed by the MTS assay. 400 μM tBHP caused a 50% reduction in metabolic activity 5 hours after its addition. If cells were pre-incubated with AO-1-530, there was a concentration dependent

protection against toxicity. 10 µM AO-1-530 was the only treatment that was not significantly different from the control, making it the most effective antioxidant treatment tested. A 10-fold higher concentration of quercetin was needed to show a similar level of protection. The flavonol which AO-1-530 is based, myricetin showed limited protection against tBHP-induced cell death. In addition, vitamin E, Idebenone and coenzyme Q10 showed no protection against tBHP. Coenzyme Q10 is a natural antioxidant found in the mitochondria and Idebenone is a synthetic drug based on coenzyme Q10. tBHP treatment for 16 hours (Figure 5.9b) produced an even greater reduction in metabolic activity to less than 2%. Only pre-incubation with 10 µM AO-1-530 or 50-100 µM quercetin showed significant protection. Vitamin E and myricetin showed no protection.

The antioxidant protection revealed using MTS was also assessed in 14 day differentiated SH-SY5Y cells. The neurons were pre-incubated with antioxidant for 30 minutes before the addition of tBHP. They were incubated for a further 8 hours when the MTS assay was performed for 1 hour (Figure 5.10). 400 µM tBHP was found to reduce metabolic activity to 30%. As with undifferentiated SH-SY5Y cells, AO-1-530 and quercetin showed protection, whereas myricetin did not. In this assay 10 µM AO-1-530 and both concentrations of quercetin were not statistically different from control treated cells.

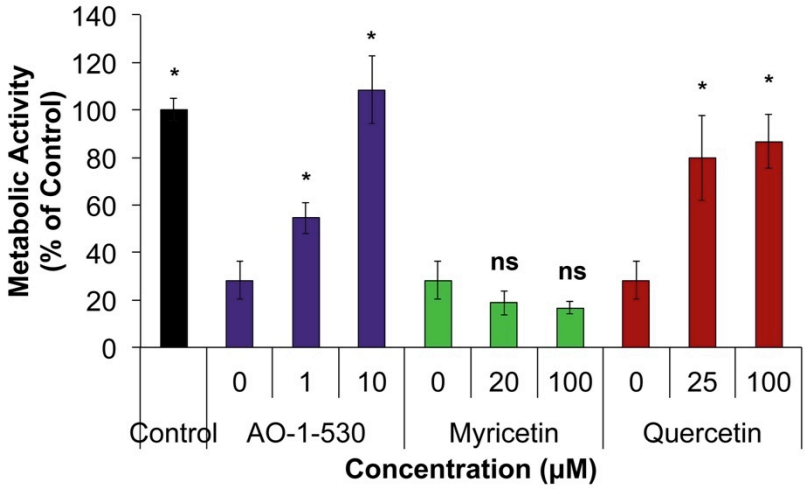

Figure 5.10 - Antioxidant protection against tBHP-induced toxicity assessed using the MTS assay in differentiated SH-SY5Y cells. 14 day differentiated SH-SY5Y cells were pre-incubated with antioxidants or vehicle for 30 minutes, when 400 µM tBHP was added for 9 hours. In the last hour the MTS assay was performed. Each bar represents the average absorbance relative to untreated control cells (black bar) from four experiments (Three of which were performed at the same time) each with triplicate or quadruplicate wells, error bars represent the SEM. ANOVA with a Tukey post-hoc test was performed to assess the significant difference between samples and the tBHP treated cells; * $p<0.05$, ns not significant.

Antioxidant protection in undifferentiated SH-SY5Y cells was confirmed using another assay, the LDH assay at 5 hours and 16 hours after tBHP addition (Figure 5.11). LDH is an intracellular enzyme. When the cell membrane integrity is lost, LDH is released into the culture medium. This assay measures the levels of LDH in the medium and is therefore a measure of the number of cells that have lost their cell membrane integrity. Figure 5.11a shows 5 hours after tBHP addition, AO-1-530 and quercetin are the only antioxidants tested that show significant protection of the cell membrane. Myricetin does not protect the cell membrane but vitamin E does show a trend towards protection that was not significant. The negative quercetin cytotoxicity at 6 hours may be due to quercetin absorbing at the 650 nm reference wavelengths. 16 hours after tBHP addition AO-1-530 and quercetin still showed protection (Figure 5.11b). As with the MTS assay 10 μM AO-1-530 was the only antioxidant condition that showed no significant difference statistically from the control. Quercetin showed protection but a 10-fold higher concentration than AO-1-530 was needed.

PI is a nuclear stain, which is only taken up into cells that have lost their cell membrane integrity. Therefore, PI can be used to assess cell viability. 6 hours after tBHP addition there is not a significant increase in PI staining (Figure 5.12a), preventing AO-1-530 protection from being assessed. If the cells were left for a further 10 hours there was a significant increase in PI positive cells. This allowed the protective affect of pre-incubation with 1 μM and 10 μM AO-1-530 to be examined. 1 μM AO-1-530 showed significant but limited protection. 10 μM AO-1-530 significantly protected cells against tBHP-induced toxicity and was not significantly different from control treated cells. In addition, AO-1-530 was not toxic in this assay as there was no increase in the number of PI positive cells. These experiments clearly show that pre-incubation with AO-1-530 is capable of preventing or delaying tBHP-induced toxicity.

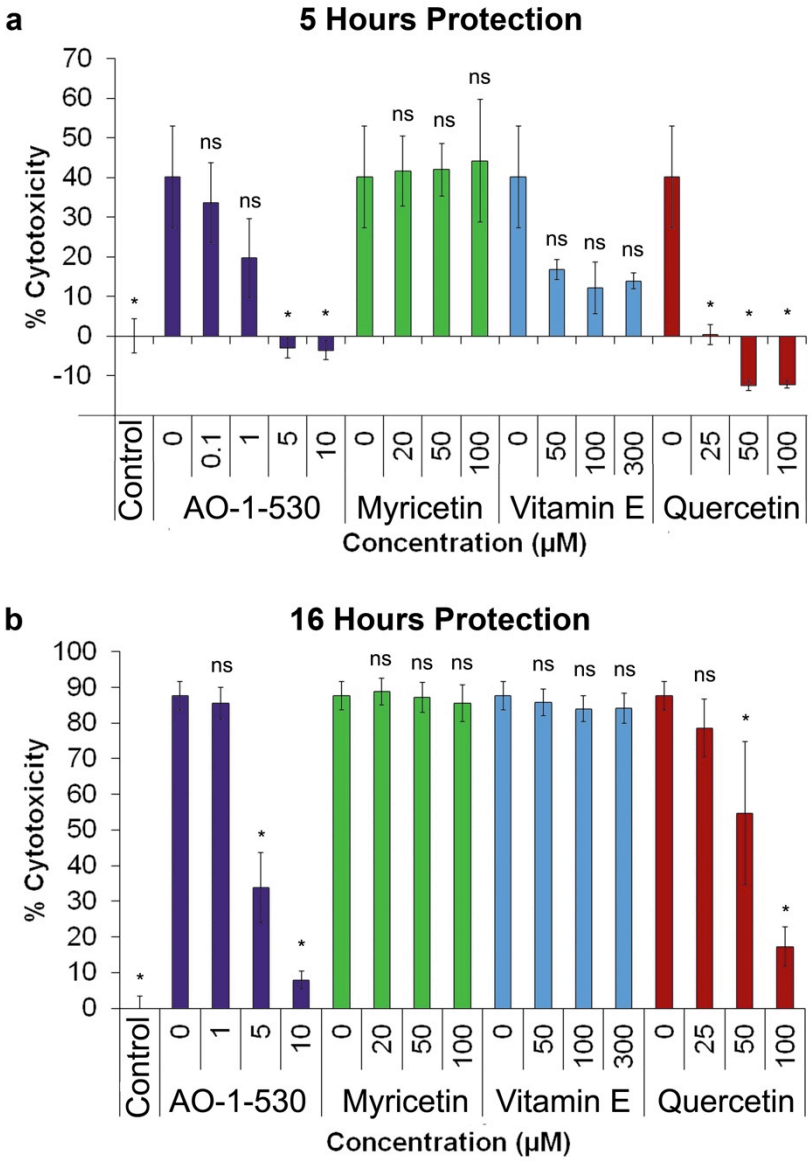

Figure 5.11 – Antioxidant protection against tBHP-induced toxicity assessed using the LDH assay. SH-SY5Y cells were pre-incubated with antioxidants or vehicle for 30 minutes, when tBHP was added for 5 hours (a) or 16 hours (b). Media was collected from each well and the LDH assay was performed to determine the amount of LDH released from cells. Each bar represents the average absorbance relative to untreated control cells and from fully lysed cells from three separate experiments each with triplicate wells. Error bars represent the SEM. ANOVA with a Tukey post-hoc test was performed to assess the significant difference between samples and the tBHP treated cells; * $p<0.05$; ns, not significant.

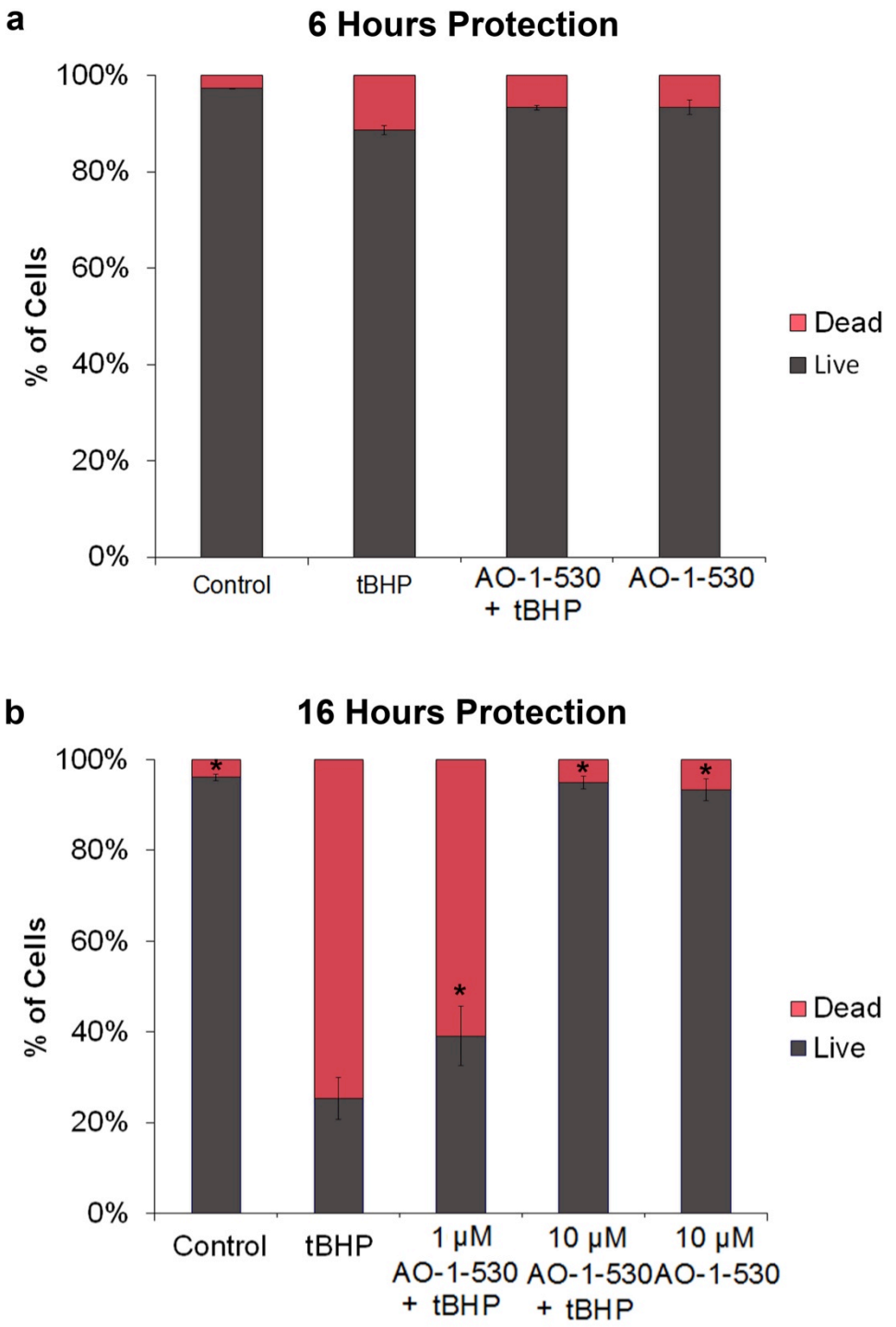

Figure 5.12 – Antioxidant protection against tBHP-induced toxicity assessed using PI staining with FACS analysis. SH-SY5Y cells were pre-incubated with AO-1-530 or vehicle for 30 minutes, when tBHP was added for 6 hours (a) or 16 hours (b). Cells were lifted, incubated with PI and analysed using the FACS Calibur. The bars represent the average number of cells positive or negative for PI from (a) one experiment with triplicate samples or (b) two experiments with triplicate samples; error bars represent the SEM. ANOVA with a Tukey post-hoc test was performed to assess the significant difference between samples and the tBHP treated cells; * $p<0.05$; ns, not significant.

5.3.1 Intracellular AO-1-530 Protection

In all of the protection experiments mentioned so far the antioxidants were present in the media when tBHP was added so the antioxidant and tBHP may be interacting outside the cell. To try to assess the intracellular AO-1-530 protection SH-SY5Y cells were incubated with AO-1-530 for 30 minutes. It was then removed and tBHP was added to the cells. Cells were then cultured for a further 5 hours with the MTS assay being performed in the last hour (Figure 5.13). AO-1-530 was found to be significantly protective at all concentrations added but higher concentrations were needed to obtain the same level of protection as when it was present in the media. This proves a significant portion of the protection is due to the intracellular activity of AO-1-530.

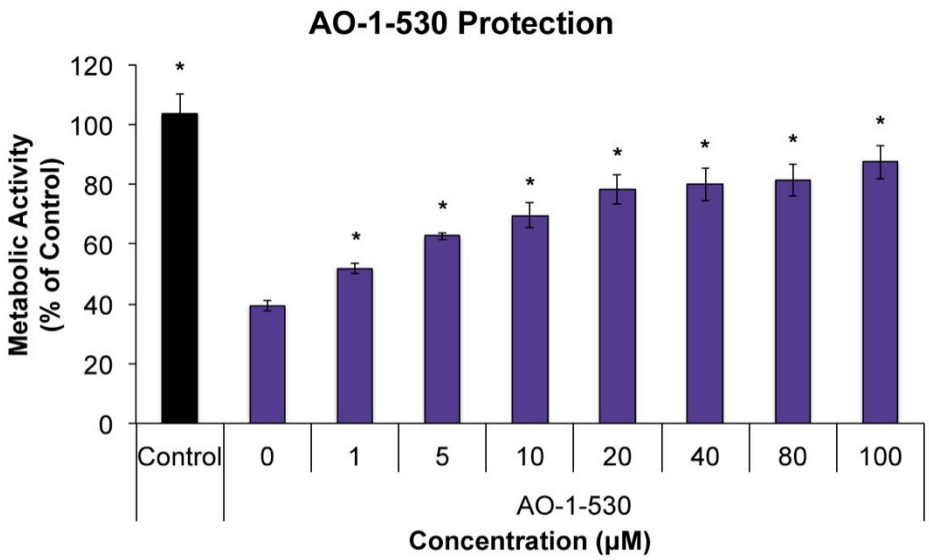

Figure 5.13 - Intracellular AO-1-530 protection. SH-SY5Y cells were pre-incubated with AO-1-530 for 30 minutes. Then AO-1-530 was removed and 400 μM tBHP was added. Cells were cultured for a further 5 hours when the MTS assay was performed. Each bar represents the average absorbance relative to untreated control cells from three separate experiments each with triplicate wells, error bars represent the SEM. ANOVA with a Tukey post-hoc test was performed to assess the significant difference between samples and the tBHP treated cells; * $p<0.05$; ns, not significant.

5.3.2 Antioxidant Protection of Cells after tBHP Addition

Another question is whether AO-1-530 and quercetin can protect cells that are already in a state of oxidative stress (Figure 5.14). Cells were either pre-incubated with antioxidant (-0.5 hour), co-treated with antioxidant and tBHP (0 hour) or post-tBHP treated with antioxidant (1 hour and 1.5 hour). 10 μM AO-1-530 was significantly protective when added after tBHP, even at 1.5 hours after tBHP addition. Quercetin also showed protection post-tBHP addition at a 10-fold higher concentration but was only protective up to 1 hour after tBHP treatment addition.

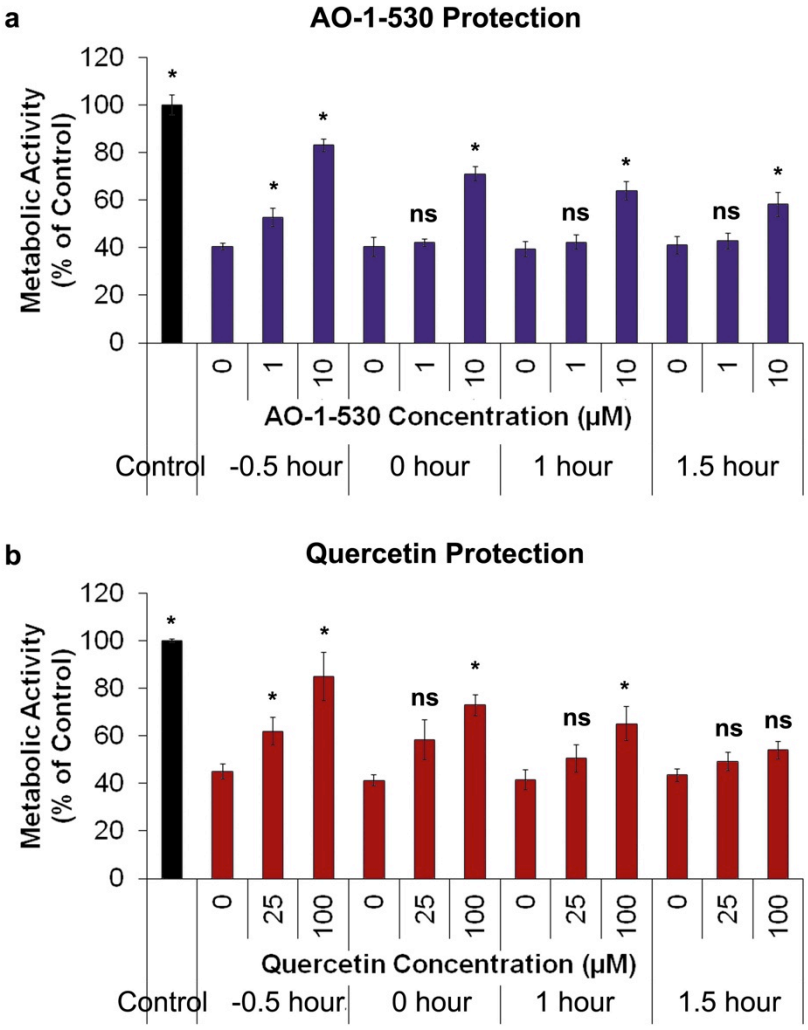

Figure 5.14 – Antioxidant protection in cells already in a state of oxidative stress. SH-SY5Y cells were either: pre-incubated with antioxidant for 30 minutes before tBHP addition, co-incubated with antioxidant and tBHP or post-incubated with antioxidant after tBHP addition. Antioxidants AO-1-530 (a) and quercetin (b) were used. Cells were cultured for 5.5 hours in total with the MTS assay performed in the last hour. Each bar represents the average absorbance relative to untreated control cells from three separate experiments each with triplicate wells, error bars represent the SEM. ANOVA with a Tukey post-hoc test was performed to assess the significant difference between samples and the tBHP treated cells; * $p<0.05$; ns, not significant.

5.3.3 Antioxidant Protection against tBHP in Neuroscreen™-1 Cells

To observe the antioxidant protection in another cell line, NS-1 was used. Initially, the cell density was optimised for the use of 3 day NGFβ differentiated NS-1 cells with the MTS assay. Seeding at 10,000 cells per well was chosen as this gave a strong absorbance to allow toxicity to be detected, and was in the linear range where absorbance is relative to cell number (Figure 5.15a). The tBHP concentration was also optimised for this number of cells at 16 hours after addition (Figure 5.15b). Significant toxicity was found at 100 μM tBHP and

above, therefore 200 μM tBHP was chosen to give an 80% reduction in metabolic activity. In addition, the toxicity of antioxidants was examined and showed AO-1-530 and myricetin were not toxic at the concentrations used but quercetin was significantly toxic (Figure 5.15c). As mentioned previously toxicity may be due to auto-oxidation of the flavonols producing toxic H_2O_2. Alternativey it coud be due to the reduction of ROS levels that are required for cell signalling. These experiments led to the following experimental design to assess the protection of antioxidants against tBHP-induced toxicity: NS-1 cells were differentiated for 3 days, then pre-incubated with antioxidants or vehicle for 30 minutes before the addition of 200 μM tBHP. Cells were then cultured for 15 hours before the MTS assay was performed for 1 hour (Figure 5.16). As with the SH-SY5Y cell line, AO-1-530 and quercetin showed significant protection, whereas myricetin showed no protection. This confirmed that the AO-1-530 protection could also be seen in differentiated NS-1 cells.

AO-1-530 is significantly protective against tBHP-induced oxidative stress. Myricetin shows limited protection. A 10-fold higher concentration of quercetin compared to AO-1-530 is needed to provide a similar level of protection. These results may be due to their uptake into cells, their localisation in cells relative to the location of free radical production or their radical scavenging potency. Further experiments were performed to investigate the mechanism by which AO-1-530 protects cells.

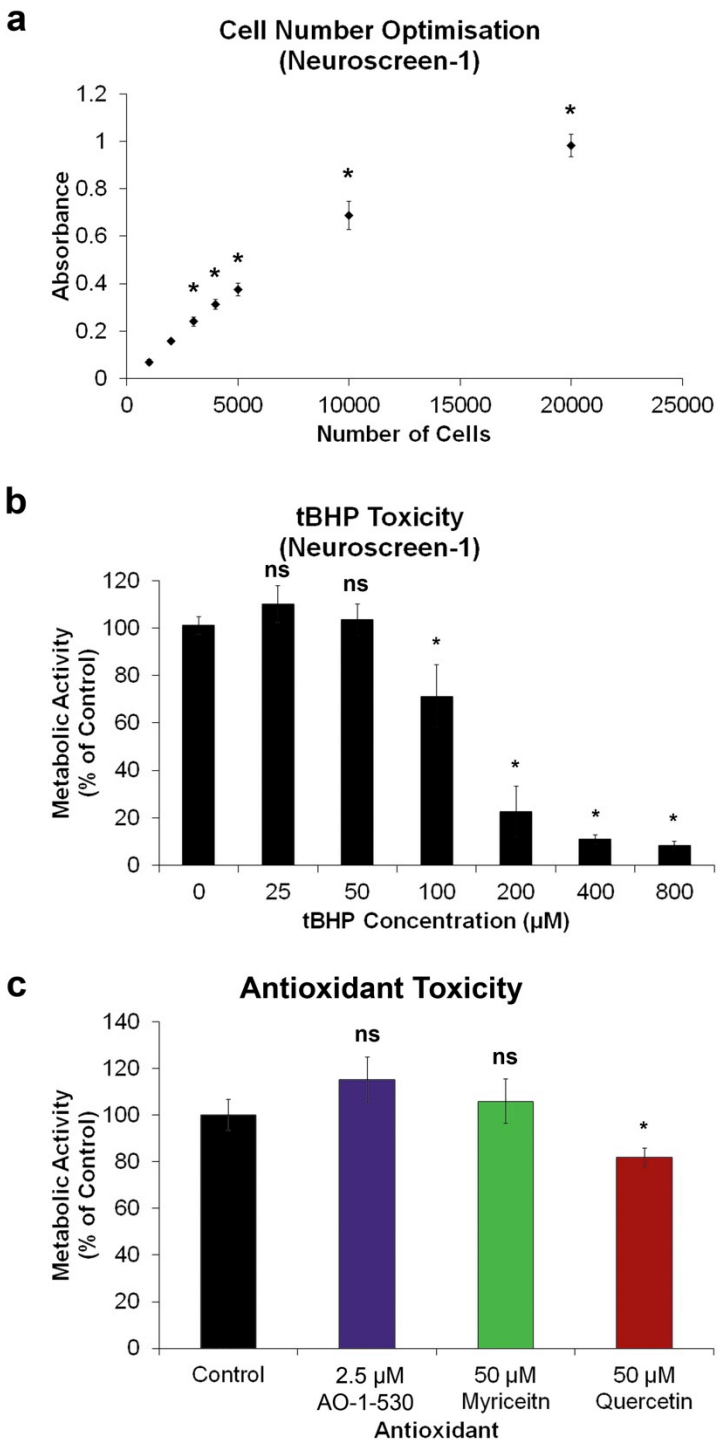

Figure 5.15 - tBHP-induced toxicity in differentiated NS-1 assay optimisation. (a) Differentiated NS-1 cell number optimisation. Cells were differentiated for 3 days when the MTS assay was performed. (b) Optimisation of tBHP concentration toxicity in 3 day differentiated NS-1 cells. tBHP was added for 15 hours when the MTS assay was performed for 1 hour. (c) Assessment of antioxidant toxicity in 3 day differentiated NS-1 cells after 16-hour exposure using the MTS assay. Each bar represents the average absorbance relative to untreated control cells from three separate experiments each with triplicate wells, error bars represent the SEM. ANOVA with a Tukey post-hoc test was performed to assess the significant difference between samples and the control treated cells; * $p<0.05$; ns, not significant. In (a) significant difference between NS-1 cell number and 1000 NS-1 cells absorbance, * $p<0.05$.

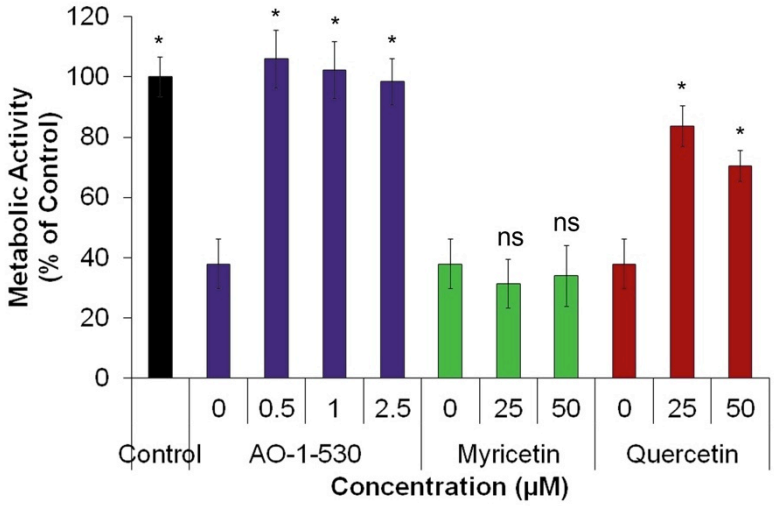

Figure 5.16 – Antioxidant protection against tBHP-induced toxicity in differentiated NS-1 cells. 3 day differentiated NS-1 cells were pre-incubated with vehicle or antioxidant for 30 minutes, and then they were exposed to 200 µM tBHP. 15 hours later MTS was added for 1 hour, when the absorbance was read. Bars represent the mean from three independent experiments with triplicate wells. Error bars show the SEM. ANOVA with a Tukey post-hoc test was performed to assess the significant difference between samples and the tBHP treated cells; * $p<0.05$; ns not significant.

5.4 Radical Scavenging Potential of Antioxidants

5.4.1 Galvinoxyl Radical Scavenging

Galvinoxyl is a known stable free radical. It has one unpaired electron making it a free radical. There are two reasons why it shows slow reactivity with oxygen and is therefore stable (Coppinger, 1957). Firstly, the unpaired electron is delocalised across the molecule. Secondly, the presence of the *tert*-butyl groups provides steric hindrance, protecting the unpaired electron and preventing dimerization. The presence of this unpaired electron gives galvinoxyl a strong absorbance at 428 nm (Shi *et al*, 2001). The loss of this unpaired electron by donation of a hydrogen atom from another molecule results in a reduction in absorbance at 428 nm. Therefore, galvinoxyl can be used to examine the hydrogen donating ability or scavenging potential of antioxidants. Shi *et al.* used this method to assess the hydrogen donating ability of myricetin, quercetin and vitamin E. In these conditions myricetin donated the most hydrogen atoms and it was the most reactive with galvinoxyl. Quercetin was capable of donating more hydrogen atoms than vitamin E but the rate of the donation of each hydrogen atom was slower. To compare the hydrogen donating ability of AO-1-530 to myricetin and quercetin the change in absorbance at 428 nm at different antioxidant concentrations was assessed (Figure 5.17a). The slope of the change in absorbance of each of the antioxidants was calculated (Figure 5.17b). This slope is correlated with the hydrogen donating ability. AO-1-530 has a similar scavenging potential as myricetin, both of which

are better hydrogen donators than quercetin. In these experiments the rate of hydrogen donation was not determined.

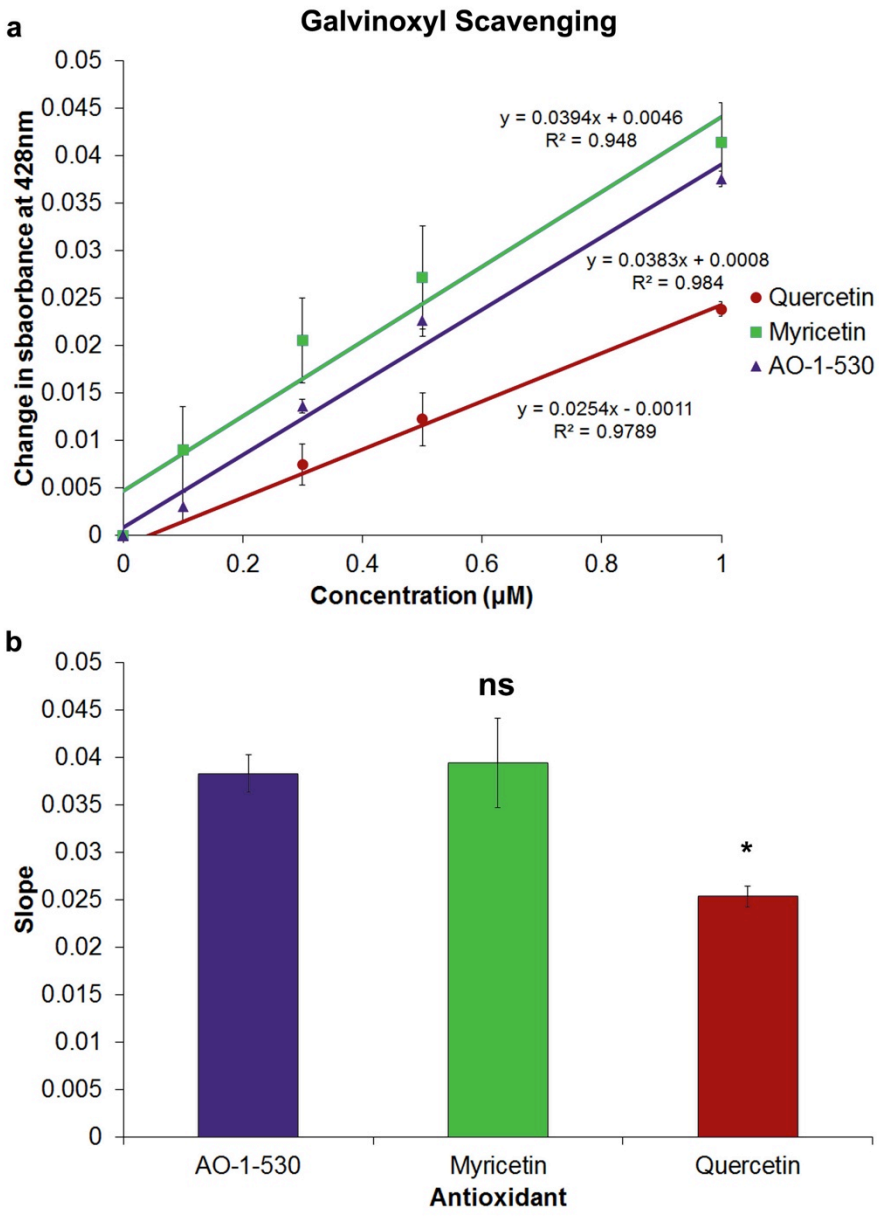

Figure 5.17 - Radical scavenging ability of flavonol antioxidants assessed using galvinoxyl absorbance. Galvinoxyl and antioxidants were mixed at the appropriate concentrations, 6 minutes later the absorbance at 428 nm was measured. The change in absorbance was plotted against the antioxidant concentration (a). The slope was calculated, as this is a measure of scavenging potency (b). Points represent the average of four independent experiments with duplicate or triplicate wells. ANOVA with the post-hoc Tukey test was performed to assess statistical significance; * $p<0.05$, ns not significant.

The unpaired electron in galvinoxyl also makes it possible to measure the relative concentration using EPR spectroscopy. The unpaired electron is like a magnet that can align

parallel or antiparallel to an external magnetic field, with two energy levels. This electron can move from the lower energy level to the upper energy level by absorbing energy, if a specific energy in the form of electromagnetic radiation is present. The absorbance is measured and presented as the rate of change in absorbance. An unpaired electron's absorbance will be affected by the atoms, which surround it, as these too have charges. Galvinoxyl shows a signal using EPR. When mixed with antioxidants that can donate hydrogen to the unpaired electron, the unpaired electron is lost resulting in a reduction in the signal intensity (Figure 5.18). EPR has been used to study hydrogen donating ability and rate of reaction of galvinoxyl with antioxidants, including myricetin, quercetin and vitamin E (McPhail *et al*, 2003). When comparing these three antioxidants the order was the same for hydrogen donating ability and rate of reaction with myricetin the best followed by quercetin and then vitamin E. To compare the hydrogen donating ability of AO-1-530 with myricetin and quercetin EPR experiments were performed. It was found the ability of antioxidants to donate hydrogen atoms to galvinoxyl was time dependent. The reaction reached the maximum by 6 minutes, similar to the time point used by McPhail *et al*. (Figure 5.18a). The scavenging potential of AO-1-530, myricetin and quercetin is concentration dependent with 10 μM scavenging more radicals than 5 μM (Figure 5.18b). The overlay of 10 μM scavenging of each antioxidant shows AO-1-530 and myricetin have similar scavenging ability with quercetin showing a lower ability, as was found in the plate reader experiment (Figure 5.18b and 5.17). The kinetics of the reaction for AO-1-530 scavenging galvinoxyl was not measured here. However, the time-course radical scavenging experiments (Figure 5.18a) indicate at 2 minutes and 4 minutes after antioxidant addition AO-1-530 was slightly slower in scavenging than myricetin.

These galvinoxyl experiments show AO-1-530 is capable of donating the same number of hydrogen atoms as myricetin, which is more than quercetin. Therefore, AO-1-530 and myricetin are more potent antioxidants in solution. However, this measure of scavenging ability does not take into account the cellular uptake of these compounds.

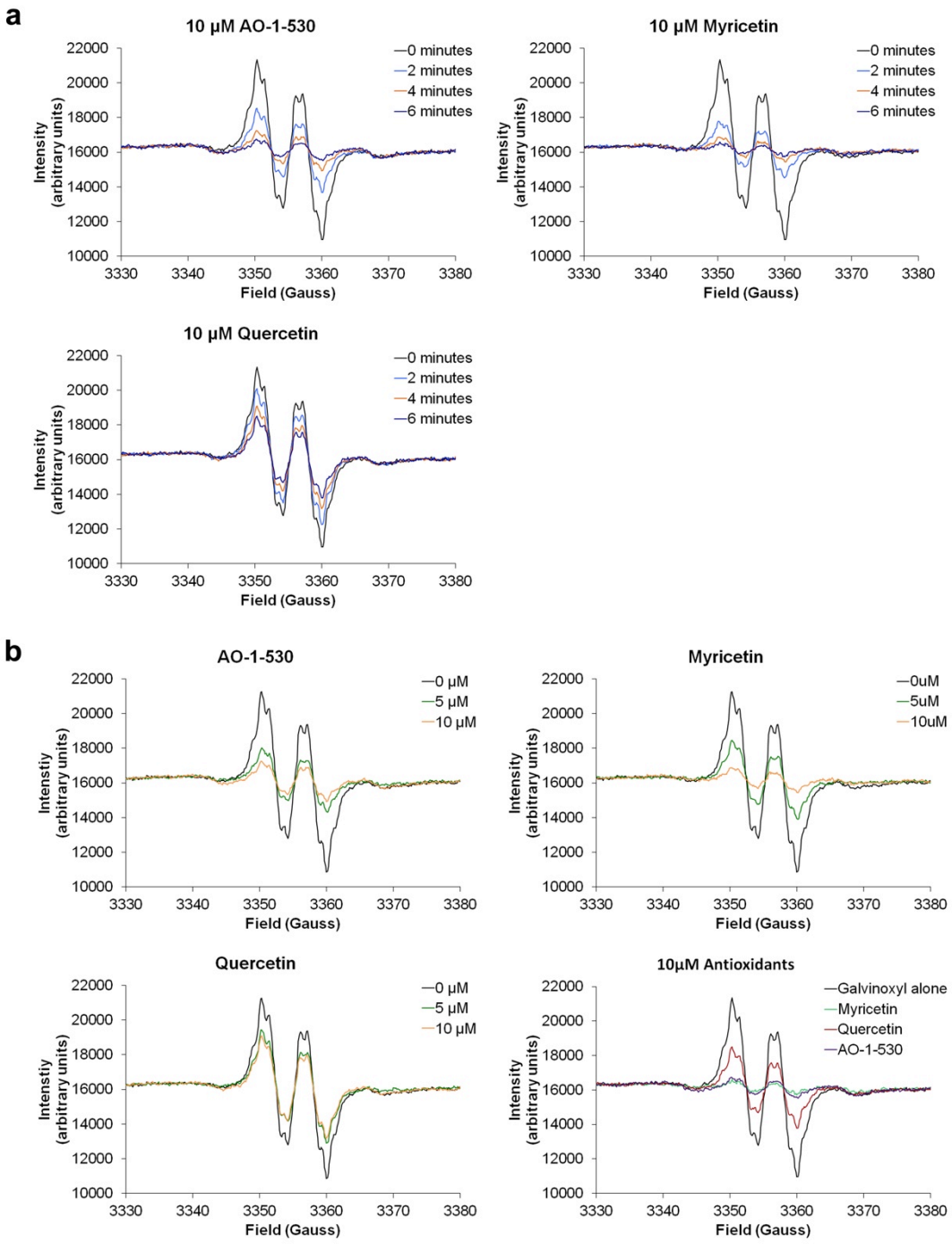

Figure 5.18 - Radical scavenging ability of flavonol antioxidants assessed using galvinoxyl EPR spectroscopy. The EPR signal of galvinoxyl represents the presence of an unpaired electron. When antioxidants donate a hydrogen atom to the galvinoxyl radical the signal is lost. Galvinoxyl was mixed with the stated concentration of antioxidants and loaded into a capillary for EPR spectroscopy. The times stated are the times after initial mixing of galvinoxyl and antioxidants. The speed at which the radical is lost represents the antioxidant reactivity towards galvinoxyl (a). The scavenging potential at 6 minutes is relative to the concentration that was added (b). These are results from one experiment, but are representative of a number of experiments.

5.4.2 Intracellular Radical Scavenging - CellROX® Deep Red

In order to investigate the intracellular antioxidant radical scavenging potency of these flavonol antioxidants, the commercially available dye from Life Technologies, CellROX® Deep Red was used. This dye is membrane permeable and in the reduced state is non-fluorescent. Once inside cells it can become oxidised by ROS to produce a fluorescent compound (emission, 665 nm). This can be quantified as a measure of cellular ROS production (Figure 5.19).

Initially, it was necessary to optimise the CellROX® dye for use with the SH-SY5Y cell line and tBHP. In these optimisation experiments, the dye appeared to show uneven fluorescence after fixation, therefore it was chosen to image the cells live. In addition, there appeared to be no difference if the CellROX® was incubated in the presence of complete media or HBSS therefore complete media was chosen for future experiments. It was also necessary to pre-incubate the cells with 10 μM CellROX®. Addition of CellROX® after removal of tBHP showed no difference in fluorescence and addition in the presence of tBHP resulted in tBHP directly oxidising the dye.

These optimisation experiments led to the following experimental plan. 10 μM CellROX® Deep Red and 2.8 μg/ml Hoechst 33342 were added to SH-SY5Y cells for 30 minutes, the cells were then washed 3 times with cell culture medium. The antioxidants were added for 30 minutes before the addition of 400 μM tBHP for one hour. The cells were then washed once in HBSS and imaged live in HBSS. Images were taken with the appropriate filters for CellROX® (emission, 665 nm) and Hoechst 33342 (emission, 461 nm), as well as phase contrast images (Figure 5.19a). The far-red fluorescence intensity in a small area of each cell was quantified for each image using Volocity. The mean and SEM relative to the mean number of cells counted from a number of experiments was calculated (Figure 5.19b).

The addition of tBHP in the presence of vehicle increased the levels of ROS in SH-SY5Y cells (Figure 5.19b). Myricetin pre-incubation significantly reduced the ROS production compared to tBHP treated cells but the reduction was not to control levels. AO-1-530 and quercetin were both capable of reducing ROS production to control levels, with quercetin being added at a 10-fold higher concentration than AO-1-530. Incubation with AO-1-530 alone was not significantly different from control treated cells so at 10 μM AO-1-530 is incapable of significantly reducing basal intracellular ROS.

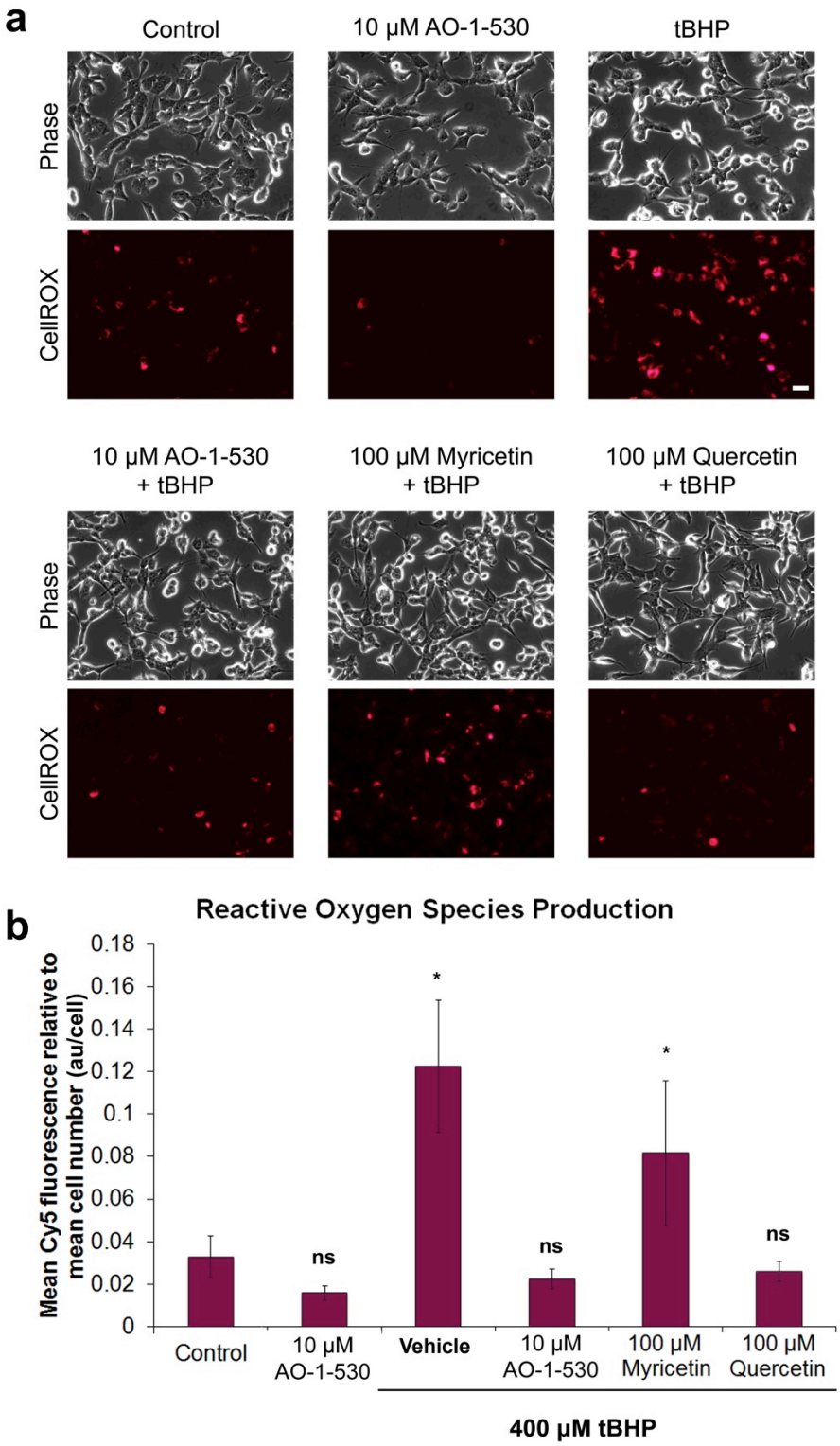

Figure 5.19 - Intracellular flavonol antioxidant scavenging potential using CellROX® Deep Red. SH-SY5Y cells were incubated with CellROX® Deep Red and Hoechst 33342 for 30 minutes when they were washed. Antioxidants were then added for 30 minutes, when 400 μM tBHP was added for one hour. Cells were washed and phase, CellROX® and Hoechst 33342 images were taken (a). The mean CellROX® Deep Red fluorescence was quantified (b). Bars represent the mean from four independent experiments for AO-1-530, two for myricetin and one for quercetin with duplicate coverslips. Error bars represent the SEM. ANOVA with the post-hoc Tukey test was performed to assess statistically significant difference to control treated cells; * $p<0.05$; ns, not significant.

Unlike the galvinoxyl experiments the CellROX® assay takes into account the cellular uptake of antioxidants. For this reason myricetin, which is poorly taken up into cells, shows less scavenging potency than AO-1-530 and quercetin. This data suggests the ability of AO-1-530 and quercetin to prevent tBHP-induced toxicity may be through their ability to scavenge the radicals produced by tBHP. To further investigate the antioxidant scavenging effect of AO-1-530 on tBHP-induced oxidative stress, oxidative stress responses were examined.

5.5 Cellular Oxidative Stress Responses

5.5.1 Cellular Redox Status – Ratio of Oxidised to Reduced Glutathione

GSH is an antioxidant synthesised in cells and is present at high concentrations. Its direct antioxidant function as a free radical scavenger comes from the presence of a thiol group, allowing it to act as an electron donor. In addition, GSH acts as a cofactor for GPx and GST that act to remove peroxides and xenobiotics, respectively. GSSG is then reduced by glutathione reductase. The presence of oxidative stress increases the levels of GSSG. Therefore the ratio of GSSG to GSH is a read-out of the redox status of the cells.

As mentioned previously tBHP is taken up into cells and the main detoxification method the cells have is through GPx degradation. GPx uses GSH as a cofactor to convert tBHP to *tert*-butyl alcohol. This seems to be a separate pathway than the reaction of tBHP with metal ions to produce alkoxyl radicals ($RO^{\bullet}$).

tBHP significantly increased the levels of GSSG after 2 hours treatment (Figure 5.20). This could be due to the actions of GPx and/or through GSH acting as a direct radical scavenger of tBHP radicals. AO-1-530 pre-incubation was incapable of preventing this tBHP oxidation of GSH. This can be explained if AO-1-530 is acting as a direct radical scavenger of the alkoxyl radicals produced, then it is unlikely to have any effect on the GPx oxidation of GSH. This has been found with other antioxidants (Masaki *et al*, 1989). Alternatively, if the increase in GSSG were due to GSH acting as a direct radical scavenger then AO-1-530 would be expected to reduce the levels of GSSG. However, AO-1-530 does not reduce the GSSG and therefore could be acting in conjunction with the natural antioxidant defence, GSH with GPx, to improve cell survival. Another possible reason AO-1-530 protection against tBHP induced GSSG is not detected may be due to the low sensitivity of the assay as two wells of a 6-well plate were needed to detect the tBHP induced increase. It is not possible from this experiment to separate these two pathways but this data suggests AO-1-530 and GSH work independently to remove tBHP from the cell and prevent its toxicity. These two pathways could be separated by inhibiting GPx with mercaptosuccinic

acid at the same time as addition of tBHP. In the absence of GPx activity if there is still a tBHP induced increase in GSSG, then GSH is acting as a direct antioxidant rather than a GPx cofactor. If there is no GSSG increase in the presence of tBHP then GSH acts mainly as a GPx cofactor.

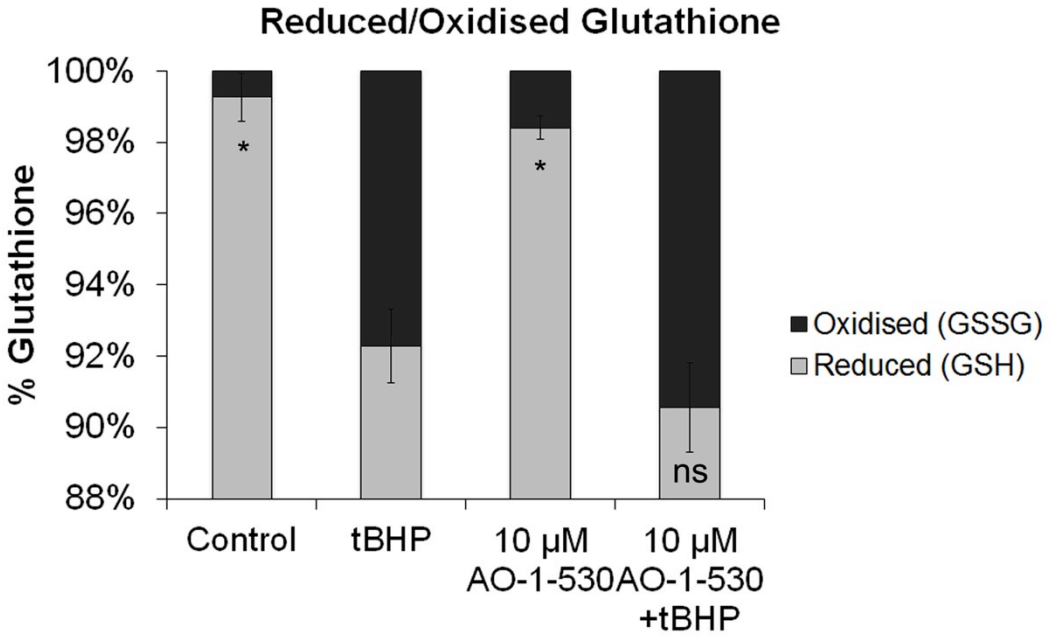

Figure 5.20 – Measurement of oxidised and reduced glutathione. SH-SY5Y cells were pre-incubated with antioxidant or vehicle for 30 minutes, when 400 µM tBHP was added for 2 hours. Cells were then scraped to lift and lysed. The level of GSH and GSSG was measured using GSH/GSSG Ratio assay kit from Calbiochem. Bars represent the ratio of GSSG to GSH from three independent experiments. Error bars represent the SEM. ANOVA with the post-hoc Tukey test was performed to assess statistical significance relative to tBHP treated cells; * $p<0.05$; ns, not significant.

5.5.2 Oxidative Stress Response - Nrf2 Nuclear Localisation

Nrf2 is a transcription factor found in most cells. In cellular stress conditions Nrf2 activates transcription of detoxification and antioxidant genes, to combat the stress and prevent cell death (Figure 1.6). In the absence of stressors, the Nrf2 protein binds to the Keap1 protein, which targets Nrf2 for degradation by the ubiquitin-proteosome degradation system (Kobayashi *et al*, 2004). However, in the presence of oxidative stress cysteine residues in the Keap1 protein are altered preventing its degradation of Nrf2, allowing Nrf2 to locate to the nucleus (Yamamoto *et al*, 2008). Once inside the nucleus Nrf2 can heterodimerise with small Maf proteins and activate transcription of ARE containing genes, including *HMOX1* and *NQO1* (Itoh *et al*, 1997). Therefore, the nuclear localisation of Nrf2 in cells and the activation of ARE containing genes can be a measure of cellular oxidative stress.

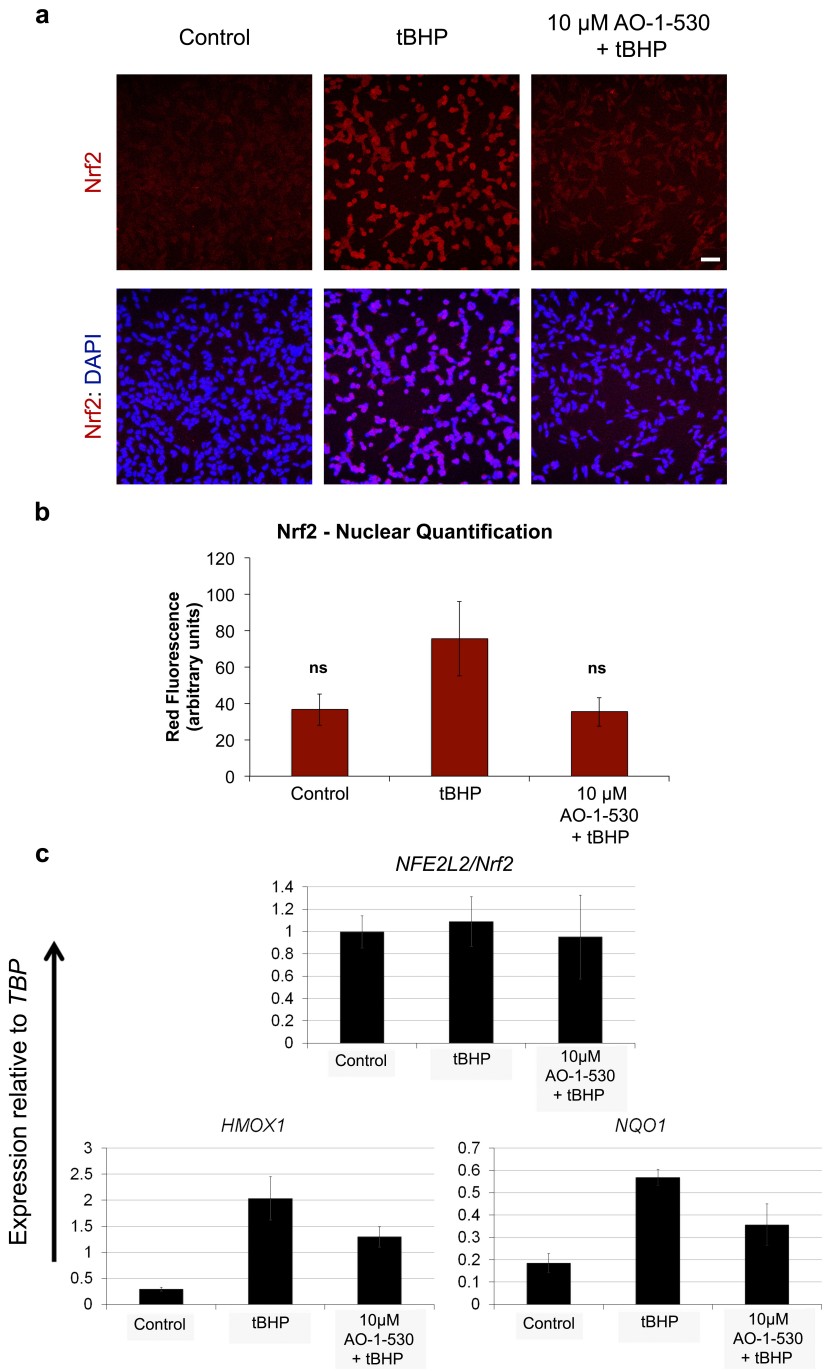

Figure 5.21 - AO-1-530 protection against tBHP-induced Nrf2 nuclear localisation and ARE gene activation. AO-1-530 or vehicle was added to cells for 30 minutes before the addition of 400 µM tBHP. Cells were incubated for 4.5 hours when they were fixed and immunocytochemistry was performed for Nrf2 (red) and nuclei were stained by DAPI (blue) (a), scale bar 54 µm. The intensity of nuclear fluorescence was quantified using ImageJ. The p-values for control to tBHP was 0.155 and tBHP to AO-1-530 and tBHP was 0.09. (b). Bars represent the mean from three individual coverslips with 2-4 images per coverslip. Error bars represent the SEM. ANOVA with the post-hoc Tukey test was performed to assess statistical significance relative to tBHP treated cells; ns, not significant $p>0.05$. Alternatively, 4.5 hours after tBHP addition cells were lifted and RNA was extracted for qRT-PCR of *Nrf2* also known as *NFE2L2*, *HMOX1* and *NQO1* (c). Bars represent the mean from one experiment with duplicate or triplicate wells. Error bars represent the standard deviation.

Immunocytochemistry was performed to assess the localisation of Nrf2 4.5 hours after tBHP treatment with AO-1-530 or vehicle pre-incubation (Figure 5.21a). The nuclear Nrf2 levels were quantified using ImageJ (Figure 5.21b). SH-SY5Y cells treated with tBHP showed a trend towards an increase in Nrf2 nuclear localisation compared to control treated cells (Figure 5.21a and b). AO-1-530 pre-incubation reduced the nuclear levels of Nrf2 to control levels. In all experiments tBHP had a higher Nrf2 nuclear staining intensity than control treated cells and 2 of the 3 experiments the difference was significant. However, when the results from 3 experiments were merged the differences were not statistically significant due to variability in Nrf2 staining intensity between coverslips. This may be due to underrepresentation and therefore if the number of experiments were increased there may be a significant difference.

To confirm the ability of AO-1-530 to reduce Nrf2 nuclear localisation and ARE gene transcription, the gene expression of two ARE containing genes was assessed, *NQO1* and *HMOX1* (Figure 5.21c). The presence of tBHP for 4.5 hours increased the transcription of *HMOX1* and *NQO1* compared to control treated cells. AO-1-530 pre-incubation reduced the gene expression compared to tBHP with vehicle but did not reduce it to control levels. As found in other studies the presence of oxidative stress has no effect on the transcriptional level of *Nrf2* itself (Figure 5.21c) (Purdom-Dickinson *et al*, 2007).

These experiments suggest that AO-1-530 can reduce Nrf2 nuclear translocation. Since Nrf2 nuclear localisation occurs due to the presence of oxidative stress, this suggests that AO-1-530 can reduce the levels of oxidative stress. AO-1-530 is not capable of completely preventing Nrf2 activated ARE gene expression but it does reduce it. This reduction may be enough to allow the cell to cope with the tBHP-induced stress. Therefore, AO-1-530 may act in conjunction with ARE response genes to reduce oxidative stress and protect the cell from death.

5.6 Oxidative DNA Damage

Another method to assess oxidative stress in cells is to quantify the damage produced by ROS. These are known as biomarkers or fingerprints of oxidative stress. Oxidative damage is usually an end product of oxidative stress and is therefore present in the cell for longer than ROS. However, it is important to take into account that there are also repair mechanisms for oxidative damage. If these repair mechanisms are overwhelmed with damage, they are incapable of repairing it all and this can be detected.

A major product of DNA oxidative damage is 8-OHdG (Figure 1.4) (Gajewski *et al*, 1990; Kasai *et al*, 1986; Dizdaroglu *et al*, 1991). It is formed from oxidation of the nucleic acid guanosine and can therefore be found in damaged RNA and DNA. Cells have been

found to have a natural repair mechanism to 8-OHdG damage, indicating it is normally produced in cells at sufficient levels to require repair. Other bases are also damaged by oxidation but 8-OHdG is the most studied.

To characterise the potency of AO-1-530 to protect against RNA and DNA oxidative damage anti- 8-OHdG immunocytochemistry was performed (Figure 5.22a). The majority of the staining did not appear to be nuclear; instead it was around the edges of the nuclei and in the cytoplasm. The intensity of fluorescence in and around the nuclei was quantified using ImageJ (Figure 5.22b). tBHP significantly increased the level of 8-OHdG oxidative damage compared to control treated cells. Whereas AO-1-530 pre-incubation before tBHP addition significantly reduced the intensity of 8-OHdG immunocytochemistry to control levels. Therefore, AO-1-530 is capable of preventing tBHP-induced 8-OHdG oxidative DNA and RNA damage.

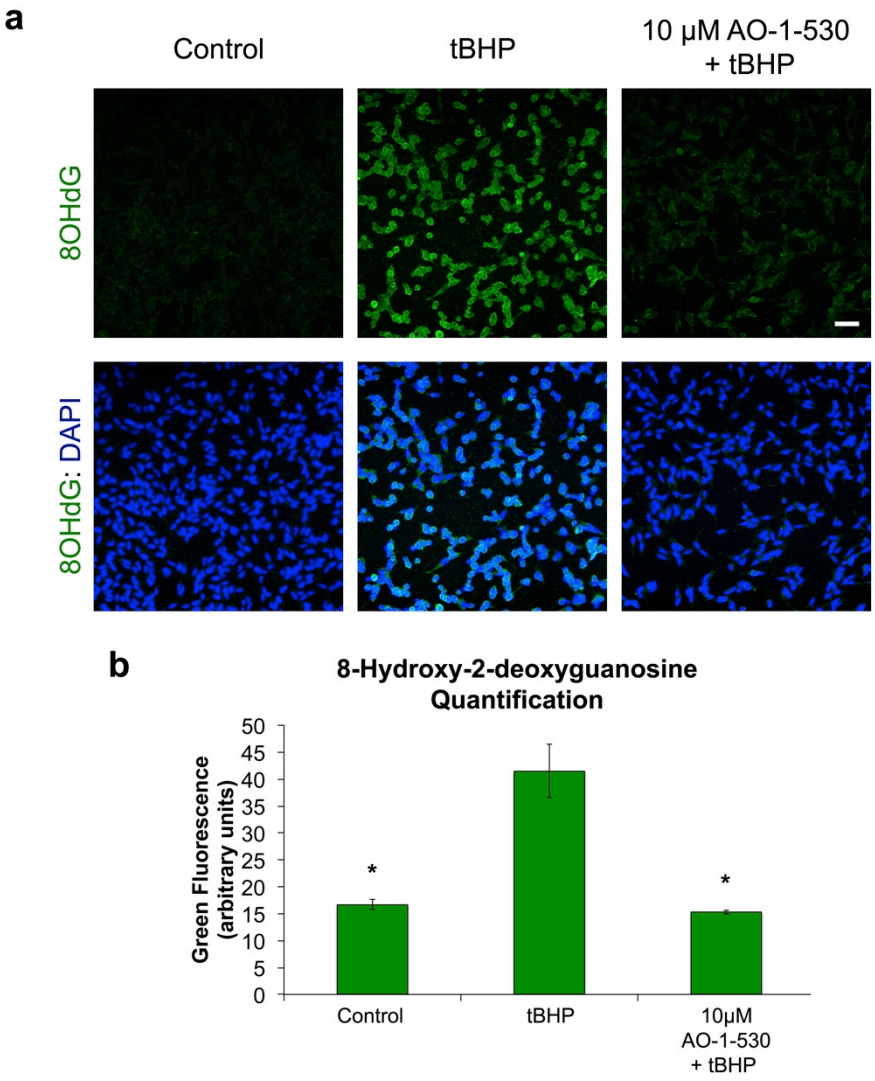

Figure 5.22 - AO-1-530 protection against 8-OHdG oxidative DNA damage. SH-SY5Y cells were pre-incubated with AO-1-530 or vehicle for 30 minutes before the addition of 400 µM tBHP. Cells were incubated for 4.5 hours when they were fixed and immunocytochemistry was performed for 8-OHdG (green) and nuclei were stained with DAPI (blue) (a), scale bar 54 µm. The intensity of fluorescence in and around the nuclei was quantified using ImageJ (b). Bars represent the mean from three coverslips from three independent experiments with 2-4 images per coverslip. Error bars represent the SEM. ANOVA with the post-hoc Tukey test was performed to assess statistical significance relative to tBHP treated cells; * $p<0.05$.

5.7 Discussion and Future Directions

AO-1-530 is a potent mitochondrial-targeted antioxidant. Cell viability assays showed AO-1-530 was protective against tBHP-induced oxidative stress at a 10-fold lower concentration than quercetin, whereas myricetin had limited protection. However, from the galvinoxyl assay AO-1-530 and myricetin are both potent radical scavengers. Since myricetin is unstable and poorly taken up into cells it cannot scavenge intracellular radicals. This was confirmed using the CellROX® assay to assess intracellular scavenging capability. The lipophilic tail of AO-1-530 enhanced its uptake, mitochondrial location in cells and may

improve its stability. Quercetin is a less potent antioxidant scavenger and locates to the nucleus. These two characteristics could be why a 10-fold higher concentration of quercetin is needed than AO-1-530 to protect against tBHP-induced toxicity. However, the intracellular concentration of antioxidants was not determined so this too may be influential.

AO-1-530 was found to scavenge intracellular ROS using the CellROX® assay. This antioxidant capability was further assessed for downstream effects of oxidative stress. These results show AO-1-530 works with the cells natural antioxidant defences, GSH and Nrf2 mediated transcription to prevent DNA oxidative damage caused by tBHP. To confirm this AO-1-530's ability to prevent other biomarkers of oxidative stress could be assessed, for example protein carbonyls and lipid peroxidation. The Nrf2 results are slightly inconsistent with the CellROX® data, which suggested AO-1-530 is capable of scavenging all ROS produced. However, it is not clear which tBHP-induced ROS are capable of reacting with CellROX® to increase fluorescence and the sensitivity of the fluorescent dye is not known. Therefore, AO-1-530 appears to act in conjunction with other cellular responses to tBHP-induced oxidative stress to promote cell survival.

It is important to note, flavonoid antioxidants are capable of scavenging metal ions as well as radicals. Since iron is required for tBHP radical production, AO-1-530 could prevent radical production or scavenge the radicals produced or both. To distinguish between these two antioxidant mechanisms, free radical producing toxins that do not require iron could be used.

The potency of AO-1-530 may be due to the AO-1-530 radicals produced being recycled by other antioxidants in the cell, back to AO-1-530, as happens with vitamin E. This could be assessed in solution using EPR.

MitoQ is another mitochondrial-targeted antioxidant but its uptake into the mitochondria appears to be reliant on mitochondrial membrane potential. The data here suggests AO-1-530 does not rely on the membrane potential at least for maintenance of its localisation, since it is still present after fixation. In addition, AO-1-530 can protect in cells already exposed to oxidative stress. However, the direct assessment could be done using the uncoupler trifluorocarbonylcyanide phenylhydrazone (FCCP) to depolarise the mitochondria and then assess if AO-1-530 can still be found in the mitochondria.

Antoxis Limited have now synthesised AO-1-530 without one of the hydroxyl groups on the B-ring, so with a quercetin head group. Preliminary experiments suggest it does not locate to the nucleus and may locate to the mitochondria. However, this needs further assessment. If this derivative does locate to the mitochondria, then the lipophilic tail is responsible for the mitochondrial localisation. The ability of this antioxidant to scavenge

radicals is expected to be similar to quercetin and this could be confirmed using the galvinoxyl assay. If this is the case, then comparing the ability of AO-1-530 and this new compound to protect against tBHP-induced oxidative stress could distinguish between the importance of radical scavenging potential and mitochondrial localisation. In addition, mitochondiral ROS probes, for example MitoSOX or MitoHR, could be used to assess whether there is an increase in mitochondrial ROS and whether AO-1-530 could prevent this.

This mitochondrial-targeted antioxidant, AO-1-530, can be used as a tool to assess the involvement of mitochondrial oxidative stress in disease models, like α-synucleinopathy models. This would improve understanding of the disease processes and help with development of treatments. In addition, AO-1-530 could be used during cell transplantation, for example during dopaminergic neuron transplantations in PD patients where oxidative stress has been implicated in the poor cell survival. This would involve incubation of midbrain cells with AO-1-530 after isolation from aborted fetuses. These cells would then be transplanted into PD patients. AO-1-530 may prove protective due to its radical scavenging ability. However, AO-1-530 was found to be toxic at high concentrations and it is not capable of preventing all of the Nrf2 ARE gene activation. Therefore, further experiments are needed to determine the appropriate concentration and timing to incubate cells with AO-1-530 to prevent toxicity but to allow a reduction in oxidative stress. In addition, experiments to determine how quickly AO-1-530 is metabolised are also needed.

Chapter 6 – Discussion and Summary

The aim of this project was to examine whether reducing oxidative stress could prevent neuronal cell toxicity in a α-synucleinopathy model. To do this a neuronal model of α-synucleinopathy needed to be developed. However, the attempts to create this model by overexpression of α-synuclein failed to show any toxicity in the cell types used. Therefore a toxin-induced oxidative stress cell model was established. Using this system the protective ability of the synthetic flavonoid, AO-1-530, was shown to be very potent. The localisation of AO-1-530 to the mitochondria may be responsible for some of its potent activity. Other possible properties responsible for AO-1-530's potent protective activity can be speculated upon by its comparison with natural flavonoid antioxidants.

6.1 SH-SY5Y Subclonal Variation

Since neurons die in α-synucleinopathies, neuronal cell lines were needed to model the disease. SH-SY5Y and NS-1 cell lines are commonly used in the literature as PD models and are reported to be neuronal and catecholaminergic (Biedler *et al*, 1978; Greene & Tischler, 1976; Radio *et al*, 2008). However, when a number of SH-SY5Y cell lines from different sources were examined differences were found in their neuronal and catecholaminegic properties. In addition, they had varied differentiation capabilities (Figure 3.1). The parental SH-SY5Y cell line was thrice subcloned from the original neuroblastoma cell line SK-N-SH (Biedler *et al*, 1978; Cohen *et al*, 2003). Therefore the differences between cell lines from different sources may be due to further subcloning of the parental SH-SY5Y cell line. This subcloning may be the result of genetic modifications caused when the cells are stressed, for example by cell passaging or cell freezing. These cells are not known to be modified and therefore retain the name of the parental cell line, SH-SY5Y. This highlights the importance of confirming the cell lines characteristics before their use. The genetic alterations that occur in different subclones could be distinguished using whole genome sequencing or whole genome SNP analysis. Whole genome SNP analysis has been used to compare the SH-SY5Y cell line and its parental cell line SK-N-SH, which showed genetic changes in the SH-SY5Y subclone that were not present in the parental cell line (Kryh *et al*, 2011). The NS-1 cell line expressed neuronal and catecholaminergic markers as expected. In addition, they were capable of differentiation by the addition of NGFβ (Figure 3.6). Therefore the neuronal SH-SY5Y and NS-1 cell lines were used to try to produce a model of α-synucleinopathies.

6.2 Inability of BacMam Transient α-Synuclein Overexpression to Induce Toxicity

The neuronal SH-SY5Y cell line from Edinburgh was used to determine the toxicity of α-synuclein overexpression. This overexpression was achieved using a BacMam construct encoding the *SNCA* gene and the *GFP* gene with a mitochondrial-targeting sequence separated by a translational skipping site. This GFP expression allowed confirmation of transduced cells and the relative levels of expression to be determined. The control BacMam construct only contained the mitochondrial-targeted *GFP* construct. Using this system α-synuclein overexpression for up to 5 days showed no toxicity in undifferentiated SH-SY5Y cells (Figure 4.9 and 4.13). This is similar to a previous study that found no α-synuclein toxicity up to 10 days in undifferentiated SH-SY5Y cells, using a doxycycline controlled α-synuclein overexpression system (Vekrellis *et al*, 2009). In addition another study using a different dopaminergic neuroblastoma cell line, BE(2)-M17, that had stable α-synuclein overexpression found no toxicity using the LDH assay (Ostrerova-Golts *et al*, 2000). However, these cells were shown to have a greater susceptibility to oxidative insults, including addition of dopamine, L-DOPA and the Fenton reaction substrates, iron chloride ($FeCl_2$) and H_2O_2 (Ostrerova-Golts *et al*, 2000; Bisaglia *et al*, 2010). Therefore the ability of rotenone, an inducer of superoxide production, in combination with α-synuclein overexpression to induce toxicity was examined. However, this too failed to show an increase in toxicity in the presence of α-synuclein overexpression (Figure 4.10). This could be due to the type of ROS that is induced and the location of the ROS production. Since rotenone will increase superoxide production in the mitochondria but dopamine would induce H_2O_2 production at various sites in the cell. Alternatively, the lack of toxicity may be due to the lack of dopaminergic cell line characteristics, since dopamine itself is known to produce oxidative stress (Klegeris *et al*, 1995; Rosenberg, 1988). Finally, since the models are cancer cell lines, they may possess highly robust characteristics making them less amenable to toxicity due to α-synuclein overproduction.

The Vekrellis *et al*, 2009 study showed even though there was no toxicity in the undifferentiated state there was toxicity after 6 days when α-synuclein was overexpressed during SH-SY5Y differentiation. This is in contrast to the results presented in this thesis, as there was no toxicity in differentiated SH-SY5Y cells after up to 4 weeks of overexpression (Figure 4.11 and 4.12). There are several possible reasons why there are differences in toxicity. The systems used to achieve α-synuclein overexpression were different. The BacMam system for overexpression used in this thesis is transient and from the immunocytochemistry of differentiated SH-SY5Y cells it suggests the α-synuclein may be

degraded more quickly than the GFP (Figure 4.11 and 4.12). However, this requires further analysis, as the published half-life for the α-synuclein is relatively long. If, α-synuclein is degraded more quickly than mitochondrial GFP then overexpression may require top-up of the virus more often than every 7 days to maintain high protein levels. In addition, the SH-SY5Y subclones and the differentiation method used were different. The Vekrellis *et al*, 2009 study used an SH-SY5Y cell line that expressed both neuronal and catecholaminergic proteins, which were differentiated by the addition of retinoic acid to FBS containing cell culture medium; whereas in this thesis the SH-SY5Y cell line was neuronal but not catecholaminergic and the cells were differentiated in N2 medium with retinoic acid. Other studies have shown α-synuclein overexpression for 5 days in human primary neurons may induce toxicity in dopaminergic neurons but not other neuronal subtypes (Zhou *et al*, 2002). In addition, this overexpression in primary catecholaminergic neurons results in increased susceptibility to oxidative insult induced cell death (Zhou *et al*, 2000). This importance of neuronal cell type is also highlighted in α-synucleinopathy disease patients where some neuronal subtypes, especially the SNpc neurons, are more susceptible to toxicity than others. Therefore the differentiated SH-SY5Y cells used here may not show toxicity, as they are not catecholaminergic. Whether the differentiated SH-SY5Y cells overexpressing α-synuclein are more susceptible to oxidative insults than control treated cells was not assessed in this thesis. Another possible reason for the lack of toxicity may be because the toxic α-synuclein oligomers have not formed. Native western blots could be performed to assess whether α-synuclein oligomers have formed and determine if this is the reason for the lack of toxicity.

One other study has used a BacMam system to overexpress α-synuclein. They used the LUHMES cell line, which is a human embryonic mesencephalic cell line containing v-myc expression, which is tetracycline controlled (Zhang *et al*, 2014). Therefore these cells differentiate by the addition of tetracycline. In this study BacMam α-synuclein overexpression during differentiation induces significant toxicity shown by a reduction in ATP and an increase in caspase 3/7 after just one day. However, there are a number of experiments missing from this paper. There is no indication as to the efficiency of BacMam transduction for α-synuclein and the GFP control. In addition, there are no images of the cells before use in the assays to show cellular morphology and no quantification of the number of live cells after one day to give a better indication of the percentage of cells that died. These pieces of data should be used to confirm the toxicity. The toxicity found in this paper was not found in this thesis for a number of possible reasons. Firstly, the cell line used was different. Secondly, the BacMam construct was different, as it does not contain a

mitochondrial-targeted GFP with the α-synuclein protein, whereas the control construct only contains GFP. Thirdly, the assays used to assess toxicity are different from those used in this thesis.

Even though high levels of α-synuclein overexpression used in this thesis failed to induce toxicity these levels did appear to induce mitochondrial fragmentation (Figure 4.13). This fragmentation of the mitochondria has been reported previously where α-synuclein was overexpressed in HeLa cells, COS cells and primary rat hippocampal neurons. The increase in fragmentation was detected within 48 hours in HeLa cells similar to that found in this thesis. However, in the Nakamura *et al*, 2011 study these HeLa cells had more intermediate mitochondria whereas in this thesis most of the cells had tubular mitochondria. This may be due to a difference in cell types. The fragmentation of the mitochondria in the Nakamura *et al*, 2011 study preceded a small increase in the number of dead cells and a reduction in mitochondrial respiration in COS cells and rat hippocampal neurons. However, no toxicity was found in this thesis. This may be due to the cell type that was used, as undifferentiated SH-SY5Y cells are a cancer cell line that produces most of their ATP through glycolysis rather than mitochondrial oxidative phosphorylation (Schneider *et al*, 2011; Xun *et al*, 2012). Alternatively it may be due to the MTS assay used for detection, as it may not be able to detect a small decrease in cell number. The Nakamura *et al*, 2011 study showed selective fragmentation of mitochondria rather than other subcellular compartments was due to the high cardiolipin content found in the mitochondria. Whether other subcellular compartments show fragmentation in the SH-SY5Y cells was not tested but could be assessed at the same time as the mitochondrial fragmentation.

The BacMam α-synuclein overexpression failed to show an increase in ROS production after up to 7 days (Figure 4.14). This is consistent with the Nakamura paper that showed no increase in superoxide production even though the mitochondria fragment. In addition, a previous study showed oligomeric forms of α-synuclein were capable of increasing ROS production using the DHE assay but the monomeric form had no effect on ROS levels (Cremades *et al*, 2012). Therefore the overexpression of α-synuclein using the BacMam system may increase monomeric α-synuclein and not induce the formation of oligomers, thus showing no increase in ROS production. Western blotting could be used to assess the absence of α-synuclein oligomers.

This thesis shows the transient overexpression of α-synuclein using the BacMam system does not cause SH-SY5Y neuronal cell toxicity in the undifferentiated or differentiated state. The reason for this lack of toxicity may be due to the length of time α-synuclein expression is maintained for, the level and consistency of α-synuclein

overexpression that is achieved or the robustness of the SH-SY5Y cancer cell line that is used.

6.3 AO-1-530 Protection against Acute Oxidative Stress

The inability of α-synuclein overexpression to induce toxicity meant the antioxidant ability of the novel flavonoid AO-1-530 needed to be assessed in a toxin-induced oxidative stress neuronal cell model. The toxin tBHP was used as an oxidative stress inducer as it is known to increase the production of ROS that can induce lipid peroxidation, resulting in cell death (Van der Zee *et al*, 1996).

AO-1-530 was shown to fluoresce like other flavonoids myricetin and quercetin but its emission was greater (Figure 5.2). This difference in levels of fluorescence emission by AO-1-530, quercetin and myricetin prevent the relative intracellular levels of antioxidants from being determined. However, this fluorescence did allow assessment of the localisation of flavonoid antioxidants. AO-1-530 was enriched in the mitochondria and was found elsewhere in the cytoplasm but was excluded from the nucleus (Figure 5.4). Quercetin was enriched in the nucleus and myricetin was not readily taken up into cells (Figure 5.3). This is consistent with reports in the literature that show quercetin is nuclear, although this was dependent on the cell line (Mukai *et al*, 2011). In addition, myricetin has a lower lipophilicity than quercetin and is unstable at neutral pH likely preventing its uptake into cells (Kajiya *et al*, 2001; Yao *et al*, 2014; Yokomizo & Moriwaki, 2006). This difference in intracellular antioxidant levels and subcellular localisation may be influential in their ability to protect against tBHP.

The poor cellular uptake of myricetin likely explains its limited protection against tBHP-induced oxidative stress, whereas AO-1-530 and quercetin, which are taken up into cells easily, were both highly protective (Figure 5.9 and 5.11). AO-1-530 was more potent than quercetin as it showed similar or more significant protection at a 10-fold lower concentration than quercetin. These results agree with published reports where quercetin is more protective than myricetin against H_2O_2 induced oxidative stress (Yokomizo & Moriwaki, 2006; Aherne & O'Brien, 1999). Other antioxidants, vitamin E, Idebenone and coenzyme Q10, which were tested, showed limited protection against tBHP induced oxidative stress. Vitamin E's limited protection could be due to its inefficient uptake into cells in the presence of FBS, its poor solubility in media or its inability to scavenge radicals produced by such an acute high dose of tBHP (Anwar *et al*, 2006; Nowak *et al*, 2012). Coenzyme Q10 and its analogue Idebenone have been shown to protect against lipid peroxidation but the direct radical scavenging ability of coenzyme Q10 is lower than Trolox, the water-soluble form of vitamin E (McDaniel *et al*, 2005; Choi *et al*, 2009).

AO-1-530 treatment alone was toxic at high concentrations (Figure 5.7c). This may be due to its auto-oxidation, since auto-oxidation of myricetin produces H_2O_2, which is toxic to cells (Mukai *et al*, 2011; Kajiya *et al*, 2001). Therefore the protective concentration range may be limited by its toxicity and this requires further investigation.

The AO-1-530 protection was shown to be at least partly due to its intracellular mechanism of action (Figure 5.13). In addition, AO-1-530 and a 10-fold higher concentration of quercetin were found to be protective when added after tBHP, indicating their potent scavenging ability (Figure 5.14).

To further assess the mechanism behind the differences between AO-1-530, myricetin and quercetin protection, their scavenging potencies were examined using the stable free radical galvinoxyl. In addition, their intracellular scavenging potential was examined using CellROX® Deep Red. As found in previous studies using galvinoxyl, myricetin was a more potent radical scavenger than quercetin since it has more hydrogen atoms to donate (Figure 5.17 and 5.18) (Shi *et al*, 2001; McPhail *et al*, 2003). AO-1-530 was shown to have similar scavenging potency to myricetin, although the kinetics of the hydrogen donation was not determined. The CellROX® Deep Red assay, which examined intracellular scavenging potency, showed both AO-1-530 and a 10-fold higher concentration of quercetin were capable of scavenging the tBHP radicals produced to control levels (Figure 5.19). However, myricetin, which has a similar scavenging potency to AO-1-530, was incapable of reducing the intracellular ROS levels to control levels likely due to its lack of uptake into cells. AO-1-530 was shown to be more protective than quercetin against tBHP toxicity. This difference in toxicity at 5 hours after tBHP addition may still be due to different ROS levels but the CellROX® assay was performed 1 hour after tBHP addition, therefore a longer incubation with tBHP could result in an increase in ROS. Alternatively, the CellROX® dye may not be sensitive enough to detect small differences in ROS levels. In addition to scavenging the ROS produced, flavonoids can also scavenge metal ions preventing tBHP radical production (Fernandez *et al*, 2002). The CellROX® assay should also detect these differences, as it would result in overall lower levels of ROS.

Further investigation into the protective mechanism of AO-1-530 showed it is not capable of preventing the oxidation of GSH caused by tBHP (Figure 5.20). This tBHP-induced oxidation of GSH could be the result of direct radical scavenging of the tBHP radicals or the result of its action as a cofactor for the enzyme GPx, which breaks down the tBHP into *tert*-butyl alcohol. The inability of AO-1-530 to prevent GSH oxidation may be because GSH is acting as a cofactor for the GPx removal of tBHP rather than directly scavenging the tBHP radicals. This is consistent with other reports that suggest GSH acts

more as a cofactor for enzymes rather than a direct radical scavenger (Masaki *et al*, 1989; Jones *et al*, 2003). However, this requires further investigation using an inhibitor of the GPx enzyme to see wheter tBHP can still increase the GSSG levels. This would allow separation of the direct radical scavenging ability of GSH and its GPx cofactor function.

AO-1-530 was capable of preventing tBHP-induced nuclear localisation of Nrf2 (Figure 5.21). This was not due to an increase in *Nrf2* gene expression, which agrees with previously published data (Purdom-Dickinson *et al*, 2007). The tBHP-induced increase in nuclear Nrf2 resulted in an increase in the gene expression of two known ARE genes, *HMOX1* and *NQO1* (Alam *et al*, 2000; Nioi *et al*, 2003). The ability of AO-1-530 pre-incubation to reduce nuclear Nrf2 also resulted in a reduction in the gene expression of *HMOX1* and *NQO1* (Alam *et al*, 2000; Nioi *et al*, 2003). However, the reduction was not to control levels. This is slightly contradictory to the Nrf2 immunocytochemistry, which suggests Nrf2 nuclear levels are the same as control levels when pre-incubated with AO-1-530. This may be because imunocytochemistry is not sensitive enough to detect small changes in protein levels, whereas qRT-PCR can detect small changes in gene expression. These results suggest that AO-1-530, the Nrf2 response and GSH act together to prevent tBHP-induced toxicity in cells.

AO-1-530 is also capable of preventing tBHP-induced 8-OHdG DNA oxidative damage (Figure 5.22). Immunocytochemistry performed 4.5 hours after tBHP addition using an 8-OHdG antibody showed pre-incubation with AO-1-530 reduced 8-OHdG levels to control levels. This is consistent with other studies that show flavonoids, including quercetin, are capable of reducing ROS induced DNA oxidative damage (Kanupriya *et al*, 2006; Aherne & O'Brien, 1999).

AO-1-530 is a potent flavonoid antioxidant that can protect against oxidative stress induced death at a 10-fold lower concentration than the natural flavonoid quercetin. This greater ability to protect against tBHP-induced cell death may be due to the higher intracellular level of antioxidant, the mitochondrial rather than nuclear subcellular localisation or the greater scavenging potency.

MitoQ and SS-31 are two published mitochondrial-targeted compounds. MitoQ is based on coenzyme Q10, but the isoprenoid side chain has been changed to a carbon side chain and the TPP lipophilic cation is attached to attract it to the mitochondria (Figure 1.8). SS-31 contains 4 amino acids, D-arginine, Dmt, lysine and phenylalanine (Figure 1.8). It is difficult to know how AO-1-530 compares to SS-31 and MitoQ in its antioxidant potential as they have each been used in different models. From stable free radical experiments coenzyme Q10 is a weaker scavenger than Trolox and the flavonols, myricetin and

quercetin, are stronger scavengers than vitamin E (Choi *et al*, 2009; McPhail *et al*, 2003). This would suggest AO-1-530 would be a more potent radical scavenger than MitoQ. However, MitoQ is also recycled back to its antioxidant state after it has scavenged a radical. This would increase its scavenging potential. The quercetin oxidation product can be recycled back to the antioxidant form by ascorbate (Boots *et al*, 2003; Skaper *et al*, 1997). Since AO-1-530 has a similar head group to quercetin it is likely it too can be recycled back to its antioxidant state by ascorbate. MitoQ protection against tBHP has not been assessed. SS-31 has been used in tBHP-induced oxidative stress cell models and was shown to protect at nanomolar concentrations. However, the concentrations of tBHP used were much lower. In addition SS-31 reduced ROS but was incapable of removing all ROS produced by 50 μM tBHP when assessed using the 2',7'-dichlorofluorescein (DCF) fluorescence, an indicator of ROS levels (Zhao *et al*, 2005). The scavenging potency of SS-31 with a stable free radical has not been reported. Therefore the differences in scavenging potency are unknown. The other influential characteristic in their protective potential is their mitochondrial localisation. MitoQ shows a 50% uptake into the mitochondria, whereas SS-31 shows 30% (Kelso *et al*, 2001; Zhao *et al*, 2005). The percentage of AO-1-530 located to the mitochondria is unknown. The localisation of each of these antioxidants within the mitochondria may be different for example in the inner or outer membrane or the matrix. In addition, the reliability on the mitochondrial membrane potential differs. MitoQ requires the mitochondrial membrane potential to be protective, whereas SS-31 does not. Whether AO-1-530 requires an intact mitochondrial membrane potential is unknown. In order to objectively compare these antioxidants they would need to be assessed in the same assay and in the same cell type.

6.4 Future Work

Future work would include determining the properties of AO-1-530 that locate it to the mitochondria and assessing the most important properties of AO-1-530 that allow protection against tBHP. In addition, comparison of AO-1-530 to MitoQ and SS-31 in the same assay would allow the most potent antioxidant to be determined. Further modifications can also be made to try to produce a α-synuclein overexpression model of toxicity to assess oxidative stress involvement in α-synucleinopathies. In addition, another use of AO-1-530 is in cell transplantation to improve cell survival.

Other mitochondrial-targeted antioxidants rely on their charge and lipophilicity to locate them to the mitochondria; therefore the importance of these in AO-1-530's mitochondrial localisation should be determined. To assess the importance of mitochondrial membrane potential the localisation of AO-1-530 in FCCP treated cells should be assessed.

FCCP causes the depolarisation of the mitochondria. In order to determine whether the lipophilic tail is important for mitochondrial localisation, another compound synthesised by Antoxis Limited can be used that has a head group like quercetin and a lipophilic tail like AO-1-530. If this new compound also locates to the mitochondria, it will show the lipophilic tail is required for mitochondrial localisation. In addition, if the scavenging potential of this new compound is the same as quercetin but less than AO-1-530, then the importance of the mitochondrial localisation and scavenging potential can be compared. It would also be useful to get an idea of the relative intracellular levels of AO-1-530 and quercetin from the fluorescence levels. By examining the fluorescence intensity at a number of different concentrations of AO-1-530 and quercetin, it would be possible to determine the fluorescence relative to the concentration. This would allow the relative concentration to be determined from the intracellular FACS fluorescence. Whether there is a difference in the intracellular concentration of AO-1-530 and quercetin can be determined and the relevance of this in the differences in their protective ability against tBHP can be assessed. Since tBHP is known to induce lipid peroxidation it is necessary to determine AO-1-530's ability to prevent lipid peroxidation. There are a number of methods available, to assess lipid peroxidation, including the Click-iT® Lipid Peroxidation imaging kit from Life Technologies. In addition, if it is possible to get MitoQ and SS-31, which are not commercially available it would be interesting to directly compare them to AO-1-530 in their ability to protect in this tBHP-induced oxidative stress toxicity model.

Flavonoids are known to have anti-inflammatory, anti-allergic, anti-viral and anti-carcinogenic properties (Reviewed by Nijveldt *et al*, 2001). Therefore, whether AO-1-530 has other protective properties as well as its antioxidant action remain to be determined. If it does, these may complicate its use as a tool to determine the involvement of oxidative stress in a α-synucleinopathy disease model.

In order to develop an α-synucleinopathy model by α-synuclein overexpression it would be interesting to use a different cell line, for example primary catecholaminergic neurons or human embryonic stem cell derived catecholaminergic neurons. These cells are likely to have endogenous α-synuclein expression that is cytoplasmic, nuclear and presynaptic and they are likely to be less robust than SH-SY5Y cells. In addition, it is important to determine the length of time α-synuclein is overexpressed for using the BacMam system. This can be done using western blots to determine how the α-synuclein levels change over time to see how quickly the overexpression is lost. If the expression is too transient it may be necessary to create stable α-synuclein overexpressing cell lines. In

addition, it is necessary to perform native western blots to determine whether oligomeric α-synuclein has been produced, since this is thought to be the toxic form.

AO-1-530 could also be used to increase cell survival after transplantation. It is known after cell transplantation there is significant death of transplanted cells, which can prevent an improvement in symptoms. A possible reason for this death is oxidative stress that may occur during the transplantation procedure. Further evidence of the importance of oxidative stress was shown when lazaroids, which prevent lipid peroxidation and reduce brain trauma injury, were shown to improve catecholaminergic cell survival after transplantation into rats (Nakao *et al*, 1994; Othberg *et al*, 1997). Lazaroids have also been used in a PD patient cell transplantation study, but in this study all patients received lazaroid treated mesencephalic tissue therefore there was no lazaroid untreated control. Instead results are compared to a previous study, which is inadequate as the number of cells transplanted was different. The authors suggest that even though less tissue was transplanted into the patients they showed the same graft survival and improved symptoms therefore lazaroids increase cell survival after transplantation (Brundin *et al*, 2000). The other mitochondrial targeted compound SS-31 has been shown to improve islet cell survival after isolation from the donor. In addition, transplantation of these islet cells into diabetic mice caused a reduction in blood glucose levels in half of the mice, whereas islet cells isolated and cultured in the absence of SS-31 could not reduce blood glucose levels (Thomas *et al*, 2006). Therefore, AO-1-530 may also be capable of improving cell survival after transplantation. However, further experiments are required to determine the best dose of AO-1-530 to use, as it is toxic at high concentrations and how long cells should be exposed to AO-1-530 for.

6.5 Conclusion

AO-1-530 is a potent mitochondrial-targeted antioxidant that is capable of protecting against acute oxidative stress. Further research will determine how important the mitochondrial localisation and scavenging potency are in its protective ability. The use of this antioxidant in combination with other tools available to measure oxidative stress will allow the involvement of oxidative stress in cell based disease models, including α-synucleinopathies, to be assessed. This would help in understanding the disease process and could help in the development of treatments. In addition, AO-1-530 could be used as a tool to increase cell survival in situations where cells are exposed to higher levels of oxidative stress than normal, for example in cell culture or during cell transplantation. This would require further experiments to determine the appropriate concentrations of AO-1-530 to use and how long AO-1-530 incubation should be, as there is a balance between protection and toxicity. In

addition, the metabolism and distribution of AO-1-530 in tissue should be determined before use *in vivo*.

References

Aherne SA & O'Brien NM (1999) Protection by the Flavonoids Myricetin, Quercetin, and Rutin Against Hydrogen Peroxide-Induced DNA Damage in Caco-2 and Hep G2 Cells. *Nutrition and Cancer* **34:** 160–166

Ahn TB, Kim SY, Kim JY, Park SS, Lee DS, Min HJ, Kim YK, Kim SE, Kim JM, Kim HJ, Cho J & Jeon BS (2008) alpha-Synuclein gene duplication is present in sporadic Parkinson disease. *Neurology* **70:** 43–49

Aikawa J, Chen WW, Kelley RI, Tada K, Moser HW & Chen GL (1991) Low-density particles (W-particles) containing catalase in Zellweger syndrome and normal fibroblasts. *Proc. Natl. Acad. Sci. U.S.A.* **88:** 10084–10088

Akasaka M, Mizoguchi J & Takahashi K (1990) A human cDNA sequence of a novel glutathione peroxidase-related protein. *Nucleic Acids Research* **18:** 4619

Alam J, Wicks C, Stewart D, Gong P, Touchard C, Otterbein S, Choi AM, Burow ME & Tou J (2000) Mechanism of heme oxygenase-1 gene activation by cadmium in MCF-7 mammary epithelial cells. Role of p38 kinase and Nrf2 transcription factor. *J. Biol. Chem.* **275:** 27694–27702

Alam ZI, Jenner A, Daniel SE, Lees AJ, Cairns N, Marsden CD, Jenner P & Halliwell B (1997) Oxidative DNA damage in the parkinsonian brain: an apparent selective increase in 8-hydroxyguanine levels in substantia nigra. *Journal of Neurochemistry* **69:** 1196–1203

Alía M, Ramos S, Mateos R, Bravo L & Goya L (2005) Response of the antioxidant defense system to tert-butyl hydroperoxide and hydrogen peroxide in a human hepatoma cell line (HepG2). *J. Biochem. Mol. Toxicol.* **19:** 119–128

Aller P, Rould MA, Hogg M, Wallace SS & Doublié S (2007) A structural rationale for stalling of a replicative DNA polymerase at the most common oxidative thymine lesion, thymine glycol. *Proc. Natl. Acad. Sci. U.S.A.* **104:** 814–818

Alvarez B, Ferrer-Sueta G, Freeman BA & Radi R (1999) Kinetics of Peroxynitrite Reaction with Amino Acids and Human Serum Albumin. *Journal of Biological Chemistry* **274:** 842–848

Andres-Mateos E, Perier C, Zhang L, Blanchard-Fillion B, Greco TM, Thomas B, Ko HS, Sasaki M, Ischiropoulos H, Przedborski S, Dawson TM & Dawson VL (2007) DJ-1 gene deletion reveals that DJ-1 is an atypical peroxiredoxin-like peroxidase. *Proc. Natl. Acad. Sci. U.S.A.* **104:** 14807–14812

Antunes F & Cadenas E (2001) Cellular titration of apoptosis with steady state concentrations of H(2)O(2): submicromolar levels of H(2)O(2) induce apoptosis through Fenton chemistry independent of the cellular thiol state. *Free Radical Biology and Medicine* **30:** 1008–1018

Anwar K, Kayden HJ & Hussain MM (2006) Transport of vitamin E by differentiated Caco-2 cells. *J. Lipid Res.* **47:** 1261–1273

Anwar S, Peters O, Millership S, Ninkina N, Doig N, Connor-Robson N, Threlfell S, Kooner G, Deacon RM, Bannerman DM, Bolam JP, Chandra SS, Cragg SJ, Wade-Martins R & Buchman VL (2011) Functional Alterations to the Nigrostriatal System in Mice Lacking All Three Members of the Synuclein Family. *Journal of Neuroscience* **31:** 7264–7274

Appel-Cresswell S, Vilarino-Guell C, Encarnacion M, Sherman H, Yu I, Shah B, Weir D, Thompson C, Szu-Tu C, Trinh J, Aasly JO, Rajput A, Rajput AH, Jon Stoessl A & Farrer MJ (2013) Alpha-synuclein p.H50Q, a novel pathogenic mutation for Parkinson's disease. *Mov. Disord.* **28:** 811–813

Arora A, Nair MG & Strasburg GM (1998) Structure-activity relationships for antioxidant activities of a series of flavonoids in a liposomal system. *Free Radical Biology and Medicine* **24:** 1355–1363

Asin-Cayuela J, Manas A-RB, James AM, Smith RAJ & Murphy MP (2004) Fine-tuning the hydrophobicity of a mitochondria-targeted antioxidant. *FEBS Letters* **571:** 9–16

Babior BM, Kipnes RS & Curnutte JT (1973) Biological defense mechanisms. The production by leukocytes of superoxide, a potential bactericidal agent. *J. Clin. Invest.* **52:** 741–744

Babior BM, Curnutte JT & Kipnes BS (1975) Pyridine nucleotide-dependent superoxide production by a cell-free system from human granulocytes. *J. Clin. Invest.* **56:** 1035–1042

Bae E-J, Ho D-H, Park E, Jung JW, Cho K, Hong JH, Lee H-J, Kim KP & Lee S-J (2013) Lipid Peroxidation Product 4-Hydroxy-2-Nonenal Promotes Seeding-Capable Oligomer Formation and Cell-to-Cell Transfer of α-Synuclein. *Antioxidants & Redox Signaling* **18:** 770–783

Baez S, Segura-Aguilar J, Widersten M, Johansson AS & Mannervik B (1997) Glutathione transferases catalyse the detoxication of oxidized metabolites (o-quinones) of catecholamines and may serve as an antioxidant system preventing degenerative cellular processes. *Biochem. J.* **324 (Pt 1):** 25–28

Baier WE (1955) Chemistry of bioflavonoids. *Ann. N. Y. Acad. Sci.* **61:** 639–645

Balasubramanian B, Pogozelski WK & Tullius TD (1998) DNA strand breaking by the hydroxyl radical is governed by the accessible surface areas of the hydrogen atoms of the DNA backbone. *Proc. Natl. Acad. Sci. U.S.A.* **95:** 9738–9743

Barnes MM, James SP & Wood PB (1959) The formation of mercapturic acids. 1. Formation of mercapturic acid and the levels of glutathione in tissues. *Biochem. J.* **71:** 680–690

Barron ESG, Ambrose J & Johnson P (1955) Studies on the mechanism of action of ionizing radiations. XIII. The effect of x-irradiation on some physico-chemical properties of amino acids and proteins. *Radiat. Res.* **2:** 145–158

Bateman L (1954) Olefin oxidation. *Q. Rev., Chem. Soc.* **8:** 147–167

Bennett CJ, Caldwell ST, McPhail DB, Morrice PC, Duthie GG & Hartley RC (2004) Potential therapeutic antioxidants that combine the radical scavenging ability of myricetin and the lipophilic chain of vitamin E to effectively inhibit microsomal lipid peroxidation. **12:** 2079–2098

Benov L, Sztejnberg L & Fridovich I (1998) Critical evaluation of the use of hydroethidine as a measure of superoxide anion radical. *Free Radical Biology and Medicine* **25:** 826–831

Berg D, Niwar M, Maass S, Zimprich A, Möller JC, Wuellner U, Schmitz-Hübsch T, Klein C, Tan E-K, Schöls L, Marsh L, Dawson TM, Janetzky B, Müller T, Woitalla D, Kostic V, Pramstaller PP, Oertel WH, Bauer P, Krueger R, et al (2005) Alpha-synuclein and Parkinson's disease: implications from the screening of more than 1,900 patients. *Mov. Disord.* **20:** 1191–1194

Betarbet R, Sherer TB, MacKenzie G, Garcia-Osuna M, Panov AV & Greenamyre JT (2000) Chronic systemic pesticide exposure reproduces features of Parkinson's disease. *Nature Neuroscience* **3:** 1301–1306

Bhagwat S, Haytowitz DB & Holden JM (2014) USDA Database for the flavonoid content of selected foods. **:** 1–176

Biedler JL, Helson L & Spengler BA (1973) Morphology and growth, tumorigenicity, and cytogenetics of human neuroblastoma cells in continuous culture. *Cancer Res.* **33:** 2643–2652

Biedler JL, Roffler-Tarlov S, Schachner M & Freedman LS (1978) Multiple neurotransmitter synthesis by human neuroblastoma cell lines and clones. *Cancer Res.* **38:** 3751–3757

Bindokas VP, Jordán J, Lee CC & Miller RJ (1996) Superoxide production in rat hippocampal neurons: selective imaging with hydroethidine. *J. Neurosci.* **16:** 1324–1336

Bisaglia M, Greggio E, Maric D, Miller DW, Cookson MR & Bubacco L (2010) α-Synuclein overexpression increases dopamine toxicity in BE (2)-M17 cells. *BMC Neurosci* **11:** 41

Boeve BF, Silber MH, Saper CB, Ferman TJ, Dickson DW, Parisi JE, Benarroch EE, Ahlskog JE, Smith GE, Caselli RC, Tippman-Peikert M, Olson EJ, Lin SC, Young T, Wszolek Z, Schenck CH, Mahowald MW, Castillo PR, Del Tredici K & Braak H (2007) Pathophysiology of REM sleep behaviour disorder and relevance to neurodegenerative disease. *Brain* **130:** 2770–2788

Bolland JL (1949) Kinetics of olefin oxidation. *Q. Rev., Chem. Soc.* **3:** 1–21

Bonifati V, Rizzu P, van Baren MJ, Schaap O, Breedveld GJ, Krieger E, Dekker MCJ, Squitieri F, Ibanez P, Joosse M, van Dongen JW, Vanacore N, van Swieten JC, Brice A, Meco G, van Duijn CM, Oostra BA & Heutink P (2003) Mutations in the DJ-1 gene associated with autosomal recessive early-onset parkinsonism. *Science* **299:** 256–259

Booth J, Boyland E & Sims P (1961) An enzyme from rat liver catalysing conjugations with glutathione. *Biochem. J.* **79:** 516–524

Boots AW, Kubben N, Haenen GRMM & Bast A (2003) Oxidized quercetin reacts with thiols rather than with ascorbate: implication for quercetin supplementation. *Biochem. Biophys. Res. Commun.* **308:** 560–565

Bors W, Heller W, Michel C & Saran M (1990) Flavonoids as antioxidants: determination of radical-scavenging efficiencies. *Meth. Enzymol.* **186:** 343–355

Bostantjopoulou S, Katsarou Z, Papadimitriou A, Veletza V, Hatzigeorgiou G & Lees A (2001) Clinical features of parkinsonian patients with the alpha-synuclein (G209A) mutation. *Mov. Disord.* **16:** 1007–1013

Boveris A, Oshino N & Chance B (1972) The cellular production of hydrogen peroxide. *Biochem. J.* **128:** 617–630

Boyce FM & Bucher NL (1996) Baculovirus-mediated gene transfer into mammalian cells. *Proc. Natl. Acad. Sci. U.S.A.* **93:** 2348–2352

Braak H, Del Tredici K, Rüb U, de Vos RAI, Jansen Steur ENH & Braak E (2003) Staging of brain pathology related to sporadic Parkinson's disease. *NBA* **24:** 197–211

Braak H, Ghebremedhin E, Rüb U, Bratzke H & Del Tredici K (2004) Stages in the development of Parkinson's disease-related pathology. *Cell Tissue Res* **318:** 121–134

Brouillard R, Wigand M-C & Cheminat A (1990) Loss of colour, a prerequisite to plant pigmentation by flavonoids. *Phytochemistry* **29:** 3457–3460

Brueggemann N, Odin P, Gruenewald A, Tadic V, Hagenah J, Seidel G, Lohmann K, Klein C & Djarmati A (2008) Re: Alpha-synuclein gene duplication is present in sporadic Parkinson disease. *Neurology* **71:** 1294

Brundin P, Pogarell O, Hagell P, Piccini P, Widner H, Schrag A, Kupsch A, Crabb L, Odin P, Gustavii B, Björklund A, Brooks DJ, Marsden CD, Oertel WH, Quinn NP, Rehncrona S & Lindvall O (2000) Bilateral caudate and putamen grafts of embryonic mesencephalic tissue treated with lazaroids in Parkinson's disease. *Brain* **123 (Pt 7):** 1380–1390

Carballal S, Radi R, Kirk MC, Barnes S, Freeman BA & Alvarez B (2003) Sulfenic acid formation in human serum albumin by hydrogen peroxide and peroxynitrite. *Biochemistry* **42:** 9906–9914

Catalá A (2010) A synopsis of the process of lipid peroxidation since the discovery of the essential fatty acids. *Biochem. Biophys. Res. Commun.* **399:** 318–323

Chae HZ, Kim IH, Kim K & Rhee SG (1993) Cloning, sequencing, and mutation of thiol-specific antioxidant gene of Saccharomyces cerevisiae. *J. Biol. Chem.* **268:** 16815–16821

Chae HZ, Chung SJ & Rhee SG (1994a) Thioredoxin-dependent peroxide reductase from yeast. *J. Biol. Chem.* **269:** 27670–27678

Chae HZ, Uhm TB & Rhee SG (1994b) Dimerization of thiol-specific antioxidant and the essential role of cysteine 47. *Proc. Natl. Acad. Sci. U.S.A.* **91:** 7022–7026

Chakrabarti AK, Feeney K, Abueg C, Brown DA, Czyz E, Tendera M, Janosi A, Giugliano RP, Kloner RA, Weaver WD, Bode C, Godlewski J, Merkely B & Gibson CM (2013) Rationale and design of the EMBRACE STEMI study: a phase 2a, randomized, double-blind, placebo-controlled trial to evaluate the safety, tolerability and efficacy of intravenous Bendavia on reperfusion injury in patients treated with standard therapy including primary percutaneous coronary intervention and stenting for ST-segment elevation myocardial infarction. *Am. Heart J.* **165:** 509–514.e7

Chartier-Harlin M-C, Kachergus J, Roumier C, Mouroux V, Douay X, Lincoln S, Levecque C, Larvor L, Andrieux J, Hulihan M, Waucquier N, Defebvre L, Amouyel P, Farrer M & Destée A (2004) α-synuclein locus duplication as a cause of familial Parkinson's disease. *The Lancet* **364:** 1167–1169

Chen H, Detmer SA, Ewald AJ, Griffin EE, Fraser SE & Chan DC (2003) Mitofusins Mfn1 and Mfn2 coordinately regulate mitochondrial fusion and are essential for embryonic development. *J. Cell Biol.* **160:** 189–200

Chen K, Kirber MT, Xiao H, Yang Y & Keaney JF (2008) Regulation of ROS signal transduction by NADPH oxidase 4 localization. *J. Cell Biol.* **181:** 1129–1139

Chen Y & Dorn GW (2013) PINK1-phosphorylated mitofusin 2 is a Parkin receptor for culling damaged mitochondria. *Science* **340:** 471–475

Cheng JZ, Sharma R, Yang Y, Singhal SS, Sharma A, Saini MK, Singh SV, Zimniak P, Awasthi S & Awasthi YC (2001) Accelerated metabolism and exclusion of 4-hydroxynonenal through induction of RLIP76 and hGST5.8 is an early adaptive response of cells to heat and oxidative stress. *J. Biol. Chem.* **276:** 41213–41223

Cheng KC, Cahill DS, Kasai H, Nishimura S & Loeb LA (1992) 8-Hydroxyguanine, an abundant form of oxidative DNA damage, causes G----T and A----C substitutions. *J. Biol. Chem.* **267:** 166–172

Chiba-Falek O & Nussbaum RL (2001) Effect of allelic variation at the NACP-Rep1 repeat upstream of the alpha-synuclein gene (SNCA) on transcription in a cell culture luciferase reporter system. *Human Molecular Genetics* **10:** 3101–3109

Cho J, Won K, Wu D, Soong Y, Liu S, Szeto HH & Hong MK (2007) Potent mitochondria-targeted peptides reduce myocardial infarction in rats. *Coron. Artery Dis.* **18:** 215–220

Choi BS, Song HS, Kim HR, Park TW, Kim TD, Cho BJ, Kim CJ & Sim SS (2009) Effect of coenzyme Q10 on cutaneous healing in skin-incised mice. *Arch. Pharm. Res.* **32:** 907–913

Christophersen BO (1969) Reduction of linolenic acid hydroperoxide by a glutathione peroxidase. *Biochim. Biophys. Acta* **176:** 463–470

Chu FF, Doroshow JH & Esworthy RS (1993) Expression, characterization, and tissue distribution of a new cellular selenium-dependent glutathione peroxidase, GSHPx-GI. *J. Biol. Chem.* **268:** 2571–2576

Chu Y & Kordower JH (2010) Lewy body pathology in fetal grafts. *Ann. N. Y. Acad. Sci.* **1184:** 55–67

Ciccarone V, Spengler BA, Meyers MB, Biedler JL & Ross RA (1989) Phenotypic diversification in human neuroblastoma cells: expression of distinct neural crest lineages. *Cancer Res.* **49:** 219–225

Ciorba MA, Heinemann SH, Weissbach H, Brot N & Hoshi T (1997) Modulation of potassium channel function by methionine oxidation and reduction. *Proc. Natl. Acad. Sci. U.S.A.* **94:** 9932–9937

Clark RA, Volpp BD, Leidal KG & Nauseef WM (1990) Two cytosolic components of the human neutrophil respiratory burst oxidase translocate to the plasma membrane during cell activation. *J. Clin. Invest.* **85:** 714–721

Cohen N, Betts DR, Rechavi G, Amariglio N & Trakhtenbrot L (2003) Clonal expansion and not cell interconversion is the basis for the neuroblast and nonneuronal types of the SK-N-SH neuroblastoma cell line. *Cancer Genetics and Cytogenetics* **143:** 80–84

Combes B & Stakelum GS (1961) A liver enzyme that conjugates sulfobromophthalein sodium with glutathione. *J. Clin. Invest.* **40:** 981–988

Condreay JP, Witherspoon SM, Clay WC & Kost TA (1999) Transient and stable gene expression in mammalian cells transduced with a recombinant baculovirus vector. *Proc. Natl. Acad. Sci. U.S.A.* **96:** 127–132

Coppinger GM (1957) A stable phenoxy radical inert to oxygen. *J. Am. Chem. Soc.* **79:** 501–502

Corish P & Tyler-Smith C (1999) Attenuation of green fluorescent protein half-life in mammalian cells. *Protein engineering* **12:** 1035–1040

Crapo JD, Oury T, Rabouille C, Slot JW & Chang LY (1992) Copper,zinc superoxide dismutase is primarily a cytosolic protein in human cells. *Proc. Natl. Acad. Sci. U.S.A.* **89:** 10405–10409

Cremades N, Cohen SIA, Deas E, Abramov AY, Chen AY, Orte A, Sandal M, Clarke RW, Dunne P, Aprile FA, Bertoncini CW, Wood NW, Knowles TPJ, Dobson CM & Klenerman D (2012) Direct observation of the interconversion of normal and toxic forms of α-synuclein. *Cell* **149:** 1048–1059

Cullinan SB, Gordan JD, Jin J, Harper JW & Diehl JA (2004) The Keap1-BTB Protein Is an Adaptor That Bridges Nrf2 to a Cul3-Based E3 Ligase: Oxidative Stress Sensing by a Cul3-Keap1 Ligase. *Molecular and Cellular Biology* **24:** 8477–8486

Curnutte JT, Whitten DM & Babior BM (1974) Defective superoxide production by granulocytes from patients with chronic granulomatous disease. *N. Engl. J. Med.* **290:** 593–597

Curnutte JT, Kipnes RS & Babior BM (1975) Defect in pyridine nucleotide dependent superoxide production by a particulate fraction from the granulocytes of patients with chronic granulomatous disease. *N. Engl. J. Med.* **293:** 628–632

Dahl HH, Hunt SM, Hutchison WM & Brown GK (1987) The human pyruvate dehydrogenase complex. Isolation of cDNA clones for the E1 alpha subunit, sequence analysis, and characterization of the mRNA. *Journal of Biological Chemistry* **262:** 7398–7403

Darios F, Corti O, Lücking CB, Hampe C, Muriel M-P, Abbas N, Gu W-J, Hirsch EC, Rooney T & Ruberg M (2003) Parkin prevents mitochondrial swelling and cytochrome c release in mitochondria-dependent cell death. *Human Molecular Genetics* **12:** 517–526

Darvish H, Movafagh A, Omrani MD, Firouzabadi SG, Azargashb E, Jamshidi J, Khaligh A, Haghnejad L, Naeini NS, Talebi A, Heidari-Rostami HR, Noorollahi-Moghaddam H, Karkheiran S, Shahidi G-A, Paknejad SMH, Ashrafian H, Abdi S, Kayyal M, Akbari M, Pedram N, et al (2013) Detection of copy number changes in genes associated with Parkinson's disease in Iranian patients. *Neuroscience Letters* **551:** 75–78

Davies KJ, Delsignore ME & Lin SW (1987) Protein damage and degradation by oxygen radicals. II. Modification of amino acids. *J. Biol. Chem.* **262:** 9902–9907

De Camilli P, Ueda T, Bloom FE, Battenberg E & Greengard P (1979) Widespread distribution of protein I in the central and peripheral nervous systems. *Proc. Natl. Acad. Sci. U.S.A.* **76:** 5977–5981

de Vries JH, Hollman PC, Meyboom S, Buysman MN, Zock PL, van Staveren WA & Katan MB (1998) Plasma concentrations and urinary excretion of the antioxidant flavonols quercetin and kaempferol as biomarkers for dietary intake. *Am. J. Clin. Nutr.* **68:** 60–65

Dexter DT, Carter CJ, Wells FR, Javoy-Agid F, Agid Y, Lees A, Jenner P & Marsden CD (1989) Basal lipid peroxidation in substantia nigra is increased in Parkinson's disease. *Journal of Neurochemistry* **52:** 381–389

Dijkmans TF, van Hooijdonk LWA, Schouten TG, Kamphorst JT, Vellinga ACA, Meerman JHN, Fitzsimons CP, de Kloet ER & Vreugdenhil E (2008) Temporal and functional dynamics of the transcriptome during nerve growth factor-induced differentiation. *Journal of Neurochemistry* **105:** 2388–2403

Ding S, Wu X, Li G, Han M, Zhuang Y & Xu T (2005) Efficient Transposition of the piggyBac (PB) Transposon in Mammalian Cells and Mice. *Cell* **122:** 473–483

Dizdaroglu M, Nackerdien Z, Chao BC, Gajewski E & Rao G (1991) Chemical nature of in vivo DNA base damage in hydrogen peroxide-treated mammalian cells. *Archives of Biochemistry and Biophysics* **285:** 388–390

Donnelly ML, Hughes LE, Luke G, Mendoza H, Dam ten E, Gani D & Ryan MD (2001a) The 'cleavage' activities of foot-and-mouth disease virus 2A site-directed mutants and naturally occurring '2A-like' sequences. *J. Gen. Virol.* **82:** 1027–1041

Donnelly ML, Luke G, Mehrotra A, Li X, Hughes LE, Gani D & Ryan MD (2001b) Analysis of the aphthovirus 2A/2B polyprotein 'cleavage'mechanism indicates not a proteolytic reaction, but a novel translational effect: a putative ribosomal "skip". *J. Gen. Virol.* **82:** 1013–1025

Douki T, Ravanat J-L, Pouget J-P, Testard I & Cadet J (2006) Minor contribution of direct ionization to DNA base damage inducedby heavy ions. *Int J Radiat Biol* **82:** 119–127

Drake MP, Giffee JW, Johnson DA & Koenig VL (1957) Chemical Effects of Ionizing Radiation on Proteins. 1, 2 I. Effects of γ-Radiation on the Amino Acid Content of Insulin. *J. Am. Chem. Soc.* **79:** 1395–1401

Dryanovski DI, Guzman JN, Xie Z, Galteri DJ, Volpicelli-Daley LA, Lee VM-Y, Miller RJ, Schumacker PT & Surmeier DJ (2013) Calcium entry and α-synuclein inclusions elevate dendritic mitochondrial oxidant stress in dopaminergic neurons. *Journal of Neuroscience* **33:** 10154–10164

Dubuisson M, Vander Stricht D, Clippe A, Etienne F, Nauser T, Kissner R, Koppenol WH, Rees J-F & Knoops B (2004) Human peroxiredoxin 5 is a peroxynitrite reductase. *FEBS Letters* **571:** 161–165

Duthie G & Morrice P (2012) Antioxidant Capacity of Flavonoids in Hepatic Microsomes Is not Reflected by Antioxidant Effects In Vivo. *Oxidative Medicine and Cellular Longevity* **2012:** 1–6

Earley FG & Ragan CI (1984) Photoaffinity labelling of mitochondrial NADH dehydrogenase with arylazidoamorphigenin, an analogue of rotenone. *Biochem. J.* **224:** 525–534

Edwards TL, Scott WK, Almonte C, Burt A, Powell EH, Beecham GW, Wang L, Züchner S, Konidari I, Wang G, Singer C, Nahab F, Scott B, Stajich JM, Pericak-Vance M, Haines J, Vance JM & Martin ER (2010) Genome-wide association study confirms SNPs in SNCA and the MAPT region as common risk factors for Parkinson disease. *Ann. Hum. Genet.* **74:** 97–109

Eggler AL, Liu G, Pezzuto JM, van Breemen RB & Mesecar AD (2005) Modifying specific cysteines of the electrophile-sensing human Keap1 protein is insufficient to disrupt binding to the Nrf2 domain Neh2. *Proc. Natl. Acad. Sci. U.S.A.* **102:** 10070–10075

Elchuri S, Oberley TD, Qi W, Eisenstein RS, Jackson Roberts L, Van Remmen H, Epstein CJ & Huang T-T (2005) CuZnSOD deficiency leads to persistent and widespread oxidative damage and hepatocarcinogenesis later in life. *Oncogene* **24:** 367–380

Elia AE, Petrucci S, Fasano A, Guidi M, Valbonesi S, Bernardini L, Consoli F, Ferraris A, Albanese A & Valente EM (2013) Alpha-synuclein gene duplication: Marked intrafamilial variability in two novel pedigrees. *Mov. Disord.* **28:** 813–817

Enomoto A, Itoh K, Nagayoshi E, Haruta J, Kimura T, O'Connor T, Harada T & Yamamoto M (2001) High sensitivity of Nrf2 knockout mice to acetaminophen hepatotoxicity associated with decreased expression of ARE-regulated drug metabolizing enzymes and antioxidant genes. *Toxicological Sciences* **59:** 169–177

Eriksen TE & Fransson G (1988) Formation of reducing radicals on radiolysis of glutathione and some related compounds in aqueous solution. *Journal of the Chemical Society, Perkin Transactions 2***:** 1117–1122

Farrer M, Chan P, Chen R, Tan L, Lincoln S, Hernandez D, Forno L, Gwinn-Hardy K, Petrucelli L, Hussey J, Singleton A, Tanner C, Hardy J & Langston JW (2001a) Lewy bodies and parkinsonism in families with parkin mutations. *Ann Neurol.* **50:** 293–300

Farrer M, Maraganore DM, Lockhart P, Singleton A, Lesnick TG, de Andrade M, West A, de Silva R, Hardy J & Hernandez D (2001b) alpha-Synuclein gene haplotypes are associated with Parkinson's disease. *Human Molecular Genetics* **10:** 1847–1851

Farrer M, Kachergus J, Forno L, Lincoln S, Wang D-S, Hulihan M, Maraganore D, Gwinn-Hardy K, Wszolek Z, Dickson D & Langston JW (2004) Comparison of kindreds with parkinsonism and alpha-synuclein genomic multiplications. *Ann Neurol.* **55:** 174–179

Fenton H (1894) LXXIII.—Oxidation of tartaric acid in presence of iron. *J. Chem. Soc., Trans.* **65:** 899–910

Fernandez MT, Mira ML, Florêncio MH & Jennings KR (2002) Iron and copper chelation by flavonoids: an electrospray mass spectrometry study. *J. Inorg. Biochem.* **92:** 105–111

Finkel T & Holbrook NJ (2000) Oxidants, oxidative stress and the biology of ageing. *Nature* **408:** 239–247

Finkel T (2011) Signal transduction by reactive oxygen species. *J. Cell Biol.* **194:** 7–15

Firuzi O, Lacanna A, Petrucci R, Marrosu G & Saso L (2005) Evaluation of the antioxidant activity of flavonoids by 'ferric reducing antioxidant power' assay and cyclic voltammetry. *Biochimica et Biophysica Acta (BBA) - General Subjects* **1721:** 174–184

Flohe L, Günzler WA & Schock HH (1973) Glutathione peroxidase: a selenoenzyme. *FEBS Letters* **32:** 132–134

Flohe L (1982) Glutathione peroxidase brought into focus. In *Glutathione peroxidase brought into focus*. Academic Pr pp 223–253

Fong KL, McCay PB, Poyer JL, Keele BB & Misra H (1973) Evidence that peroxidation of lysosomal membranes is initiated by hydroxyl free radicals produced during flavin enzyme activity. *J. Biol. Chem.* **248:** 7792–7797

Fornwald JA, Lu Q, Wang D & Ames RS (2007) Gene Expression in Mammalian Cells Using BacMam, a Modified Baculovirus System. *In Gene Expression in Mammalian Cells Using BacMam, a Modified Baculovirus System.* Humana Press pp 95–116.

Forsby A (2011) Neurite Degeneration in Human Neuronal SH-SY5Y Cells as an Indicator of Axonopathy. **56:** 255–268

Frelon S, Douki T, Ravanat J-L, Pouget J-P, Tornabene C & Cadet J (2000) High-Performance Liquid Chromatography−Tandem Mass Spectrometry Measurement of Radiation-Induced Base Damage to Isolated and Cellular DNA. *Chem. Res. Toxicol.* **13:** 1002–1010

Fridovich SE & Porter NA (1981) Oxidation of arachidonic acid in micelles by superoxide and hydrogen peroxide. *J. Biol. Chem.* **256:** 260–265

Friguet B, Stadtman ER & Szweda LI (1994) Modification of glucose-6-phosphate dehydrogenase by 4-hydroxy-2-nonenal. Formation of cross-linked protein that inhibits the multicatalytic protease. *J. Biol. Chem.* **269:** 21639–21643

Fuchs J, Nilsson C, Kachergus J, Munz M, Larsson E-M, Schule B, Langston JW, Middleton FA, Ross OA & Hulihan M (2007) Phenotypic variation in a large Swedish pedigree due to SNCA duplication and triplication. *Neurology* **68:** 916–922

Furukawa M & Xiong Y (2005) BTB protein Keap1 targets antioxidant transcription factor Nrf2 for ubiquitination by the Cullin 3-Roc1 ligase. *Molecular and Cellular Biology* **25:** 162–171

Gajewski E, Rao G, Nackerdien Z & Dizdaroglu M (1990) Modification of DNA bases in mammalian chromatin by radiation-generated free radicals. *Biochemistry* **29:** 7876–7882

Galano A & Alvarez-Idaboy JR (2011) Glutathione: mechanism and kinetics of its non-enzymatic defense action against free radicals. *RSC Advances* **1:** 1763–1771

Garraux G, Caberg J-H, Vanbellinghen J-F, Jamar M, Bours V, Moonen G & Dive D (2012) Partial trisomy 4q associated with young-onset dopa-responsive parkinsonism. *Arch. Neurol.* **69:** 398–400

Garrison WM, Bennett W & Jayko ME (1962) Radiation-Induced Oxidation of Protein in Aqueous Solution. *Radiat. Res.* **16:** 483–502

Geisler S, Holmström KM, Skujat D, Fiesel FC, Rothfuss OC, Kahle PJ & Springer W (2010) PINK1/Parkin-mediated mitophagy is dependent on VDAC1 and p62/SQSTM1. *Nat. Cell Biol.* **12:** 119–131

Gemelli C, Dongmo BM, Ferrarini F, Grande A & Corsi L (2014) Cytotoxic effect of hemin in colonic epithelial cell line: Involvement of 18kDa translocator protein (TSPO). *Life Sci.* **107:** 14–20

Gerschman R, Gilbert DL, Nye SW, Dwyer P & Fenn WO (1954) Oxygen poisoning and x-irradiation: a mechanism in common. *Science* **119:** 623–626

Giasson BI, Duda JE, Murray IV, Chen Q, Souza JM, Hurtig HI, Ischiropoulos H, Trojanowski JQ & Lee VM-Y (2000) Oxidative damage linked to neurodegeneration by selective α-synuclein nitration in synucleinopathy lesions. *Science* **290:** 985–989

Gilman S, Wenning GK, Low PA, Brooks DJ, Mathias CJ, Trojanowski JQ, Wood NW, Colosimo C, Dürr A, Fowler CJ, Kaufmann H, Klockgether T, Lees A, Poewe W, Quinn N, Revesz T, Robertson D, Sandroni P, Seppi K & Vidailhet M (2008) Second consensus statement on the diagnosis of multiple system atrophy. *Neurology* **71**: 670–676.

Girotti AW (1985) Mechanisms of lipid peroxidation. *J Free Radic Biol Med* **1:** 87–95

Golbe LI, Di Iorio G, Bonavita V, Miller DC & Duvoisin RC (1990) A large kindred with autosomal dominant Parkinson's disease. *Ann Neurol.* **27:** 276–282

Goldberg JA, Guzman JN, Estep CM, Ilijic E, Kondapalli J, Sanchez-Padilla J & Surmeier DJ (2012) Calcium entry induces mitochondrial oxidant stress in vagal neurons at risk in Parkinson's disease. *Nature Neuroscience* **15:** 1414–1421

Goldberg MS, Fleming SM, Palacino JJ, Cepeda C, Lam HA, Bhatnagar A, Meloni EG, Wu N, Ackerson LC, Klapstein GJ, Gajendiran M, Roth BL, Chesselet MF, Maidment NT, Levine MS & Shen J (2003) Parkin-deficient Mice Exhibit Nigrostriatal Deficits but Not Loss of Dopaminergic Neurons. *Journal of Biological Chemistry* **278:** 43628–43635

Goldstein S & Czapski G (1995) The reaction of NO. with O2.- and HO2.: a pulse radiolysis study. *Free Radical Biology and Medicine* **19:** 505–510

Gorsky LD, Koop DR & Coon MJ (1984) On the stoichiometry of the oxidase and monooxygenase reactions catalyzed by liver microsomal cytochrome P-450. Products of oxygen reduction. *J. Biol. Chem.* **259:** 6812–6817

Gorter E & Grendel F (1925) ON BIMOLECULAR LAYERS OF LIPOIDS ON THE CHROMOCYTES OF THE BLOOD. *J. Exp. Med.* **41:** 439–443

Greene LA & Tischler AS (1976) Establishment of a noradrenergic clonal line of rat adrenal pheochromocytoma cells which respond to nerve growth factor. *Proc. Natl. Acad. Sci. U.S.A.* **73:** 2424–2428

Greten-Harrison B, Polydoro M, Morimoto-Tomita M, Diao L, Williams AM, Nie EH, Makani S, Tian N, Castillo PE, Buchman VL & Chandra SS (2010) αβγ-Synuclein triple knockout mice reveal age-dependent neuronal dysfunction. *Proc. Natl. Acad. Sci. U.S.A.* **107:** 19573–19578

Gross E, Sevier CS, Heldman N, Vitu E, Bentzur M, Kaiser CA, Thorpe C & Fass D (2006) Generating disulfides enzymatically: reaction products and electron acceptors of the endoplasmic reticulum thiol oxidase Ero1p. *Proc. Natl. Acad. Sci. U.S.A.* **103:** 299–304

Guzman JN, Sanchez-Padilla J, Wokosin D, Kondapalli J, Ilijic E, Schumacker PT & Surmeier DJ (2010) Oxidant stress evoked by pacemaking in dopaminergic neurons is attenuated by DJ-1. *Nature* **468:** 696–700

Gwinn K, Devine MJ, Jin L-W, Johnson J, Bird T, Muenter M, Waters C, Adler CH, Caselli R & Houlden H (2011) Clinical features, with video documentation, of the original familial lewy body Parkinsonism caused by α-synuclein triplication (Iowa kindred). *Movement disorders: official journal of the Movement Disorder Society* **26:** 2134

Halliwell B & Gutteridge JM (1984) Oxygen toxicity, oxygen radicals, transition metals and disease. *Biochem. J.* **219:** 1–14

Harrison R (2002) Structure and function of xanthine oxidoreductase: where are we now? *Free Radical Biology and Medicine* **33:** 774–797

Harwood J, Tachibana A & Meuth M (1991) Multiple dispersed spontaneous mutations: a novel pathway of mutation in a malignant human cell line. *Molecular and Cellular Biology* **11:** 3163–3170

Hawkins CL & Davies MJ (2014) Detection and characterisation of radicals in biological materials using EPR methodology. *Biochim. Biophys. Acta* **1840:** 708–721

Hazra TK, Izumi T, Maidt L, Floyd RA & Mitra S (1998) The presence of two distinct 8-oxoguanine repair enzymes in human cells: their potential complementary roles in preventing mutation. *Nucleic Acids Research* **26:** 5116–5122

Heck DE, Vetrano AM, Mariano TM & Laskin JD (2003) UVB Light Stimulates Production of Reactive Oxygen Species: Unexpected role for catalase. *Journal of Biological Chemistry* **278:** 22432–22436

Heinecke JW, LI W, Daehnke HL & Goldstein JA (1993) Dityrosine, a specific marker of oxidation, is synthesized by the myeloperoxidase-hydrogen peroxide system of human neutrophils and macrophages. *J. Biol. Chem.* **268:** 4069–4077

Herrmann K (1988) On the occurrence of flavonol and flavone glycosides in vegetables. *Zeitschrift für Lebensmittel-Untersuchung und Forschung* **186:** 1–5

Herzberg L & Herzberg G (1947) Fine Structure of the Infrared Atmospheric Oxygen Bands. *The Astrophysical Journal* **105:** 353–359

Ho Y-S, Gargano M, Cao J, Bronson RT, Heimler I & Hutz RJ (1998) Reduced fertility in female mice lacking copper-zinc superoxide dismutase. *J. Biol. Chem.* **273:** 7765–7769

Ho YS, Xiong Y, Ma W, Spector A & Ho DS (2004) Mice Lacking Catalase Develop Normally but Show Differential Sensitivity to Oxidant Tissue Injury. *Journal of Biological Chemistry* **279:** 32804–32812

Hodara R, Norris EH, Giasson BI, Mishizen-Eberz AJ, Lynch DR, Lee VM-Y & Ischiropoulos H (2004) Functional consequences of alpha-synuclein tyrosine nitration: diminished binding to lipid vesicles and increased fibril formation. *J. Biol. Chem.* **279:** 47746–47753

Hollman PC, de Vries JH, van Leeuwen SD, Mengelers MJ & Katan MB (1995) Absorption of dietary quercetin glycosides and quercetin in healthy ileostomy volunteers. *Am. J. Clin. Nutr.* **62:** 1276–1282

Hollman PCH & Arts ICW (2000) Flavonols, flavones and flavanols–nature, occurrence and dietary burden. *Journal of the Science of Food and Agriculture* **80:** 1081–1093

Holmström KM & Finkel T (2014) Cellular mechanisms and physiological consequences of redox-dependent signalling. *Nature Rev Mol Cell Biol* **15:** 411–421

Hopkins FG (1929) On glutathione : A reinvestigation. *J. Biol. Chem.* **84:** 269–320

Horton KL, Stewart KM, Fonseca SB, Guo Q & Kelley SO (2008) Mitochondria-Penetrating Peptides. *Chemistry & Biology* **15:** 375–382

Huttner WB, Schiebler W, Greengard P & De Camilli P (1983) Synapsin I (protein I), a nerve terminal-specific phosphoprotein. III. Its association with synaptic vesicles studied in a highly purified synaptic vesicle preparation. *J. Cell Biol.* **96:** 1374–1388

Ibáñez P, Bonnet A-M, Débarges B, Lohmann E, Tison F, Agid Y, Dürr A, Brice A & Pollak P (2004) Causal relation between α-synuclein locus duplication as a cause of familial Parkinson's disease. *The Lancet* **364:** 1169–1171

Ikeuchi T, Kakita A, Shiga A, Kasuga K, Kaneko H, Tan C-F, Idezuka J, Wakabayashi K, Onodera O, Iwatsubo T, Nishizawa M, Takahashi H & Ishikawa A (2008) Patients homozygous and heterozygous for SNCA duplication in a family with parkinsonism and dementia. *Arch. Neurol.* **65:** 514–519

Ishiyama A, Atarashi K, Minami M, Takagi M, Kimura K, Goto A & Omata M (1999) Role of free radicals in the pathogenesis of lipid-induced glomerulosclerosis in rats. *Kidney Int.* **55:** 1348–1358

Itoh K, Chiba T, Takahashi S, Ishii T, Igarashi K, Katoh Y, Oyake T, Hayashi N, Satoh K, Hatayama I, Yamamoto M & Nabeshima Y (1997) An Nrf2/small Maf heterodimer mediates the induction of phase II detoxifying enzyme genes through antioxidant response elements. *Biochem. Biophys. Res. Commun.* **236:** 313–322

Itokawa K, Sekine T, Funayama M, Tomiyama H, Fukui M, Yamamoto T, Tamura N, Matsuda H, Hattori N & Araki N (2012) A case of α- synucleingene duplication presenting with head-shaking movements. *Mov. Disord.* **28:** 384–387

Iwai A, Masliah E, Yoshimoto M, Ge N, Flanagan L, de Silva HA, Kittel A & Saitoh T (1995) The precursor protein of non-A beta component of Alzheimer's disease amyloid is a presynaptic protein of the central nervous system. *Neuron* **14:** 467–475

Iwashina T (2003) Flavonoid function and activity to plants and other organisms. *Biol. Sci. Space* **17:** 24–44

Jakobson I, Warholm M & Mannervik B (1979) The binding of substrates and a product of the enzymatic reaction to glutathione S-transferase A. *J. Biol. Chem.* **254:** 7085–7089

James AM, Smith RAJ & Murphy MP (2004) Antioxidant and prooxidant properties of mitochondrial Coenzyme Q. *Archives of Biochemistry and Biophysics* **423:** 47–56

James AM, Cocheme HM, Smith RAJ & Murphy MP (2005) Interactions of Mitochondria-targeted and Untargeted Ubiquinones with the Mitochondrial Respiratory Chain and Reactive Oxygen Species: IMPLICATIONS FOR THE USE OF EXOGENOUS UBIQUINONES AS THERAPIES AND EXPERIMENTAL TOOLS. *Journal of Biological Chemistry* **280:** 21295–21312

Jaruga P & Dizdaroglu M (1996) Repair of products of oxidative DNA base damage in human cells. *Nucleic Acids Research* **24:** 1389–1394

Javitch JA, D'Amato RJ, Strittmatter SM & Snyder SH (1985) Parkinsonism-inducing neurotoxin, N-methyl-4-phenyl-1,2,3,6 -tetrahydropyridine: uptake of the metabolite N-methyl-4-phenylpyridine by dopamine neurons explains selective toxicity. *Proc. Natl. Acad. Sci. U.S.A.* **82:** 2173–2177

Jenner P, Dexter DT, Sian J, Schapira AH & Marsden CD (1992) Oxidative stress as a cause of nigral cell death in Parkinson‘s disease and incidental Lewy body disease. The Royal Kings and Queens Parkinson’s Disease Research Group. *Ann Neurol.* **32 Suppl:** S82–7

Jones CM, Lawrence A, Wardman P & Burkitt MJ (2003) Kinetics of superoxide scavenging by glutathione: an evaluation of its role in the removal of mitochondrial superoxide. *Biochem. Soc. Trans* **31:** 1337–1339

Kajiya K, Ichiba M, Kuwabara M, Kumazawa S & Nakayama T (2001) Role of lipophilicity and hydrogen peroxide formation in the cytotoxicity of flavonols. *Bioscience, Biotechnology and Biochemistry* **65:** 1227–1229

Kang SW, Baines IC & Rhee SG (1998) Characterization of a mammalian peroxiredoxin that contains one conserved cysteine. *J. Biol. Chem.* **273:** 6303–6311

Kanupriya, Dipti P, Sharma SK, Sairam M, Ilavazhagan G, Sawhney RC & Banerjee PK (2006) Flavonoids protect U-937 macrophages against tert-butylhydroperoxide induced oxidative injury. *Food and Chemical Toxicology* **44:** 1024–1030

Kasai H, Crain PF, Kuchino Y, Nishimura S, Ootsuyama A & Tanooka H (1986) Formation of 8-hydroxyguanine moiety in cellular DNA by agents producing oxygen radicals and evidence for its repair. *Carcinogenesis* **7:** 1849–1851

Kasap M, Akpinar G, Sazci A, Idrisoglu HA & Vahaboğlu H (2009) Evidence for the presence of full-length PARK2 mRNA and Parkin protein in human blood. *Neuroscience Letters* **460:** 196–200

Keele BB, McCord JM & Fridovich I (1970) Superoxide dismutase from escherichia coli B. A new manganese-containing enzyme. *J. Biol. Chem.* **245:** 6176–6181

Keeney PM, Xie J, Capaldi RA & Bennett JP (2006) Parkinson's disease brain mitochondrial complex I has oxidatively damaged subunits and is functionally impaired and misassembled. *Journal of Neuroscience* **26:** 5256–5264

Kellogg EW & Fridovich I (1975) Superoxide, hydrogen peroxide, and singlet oxygen in lipid peroxidation by a xanthine oxidase system. *J. Biol. Chem.* **250:** 8812–8817

Kelso GF, Porteous CM, Coulter CV, Hughes G, Porteous WK, Ledgerwood EC, Smith RAJ & Murphy MP (2001) Selective Targeting of a Redox-active Ubiquinone to Mitochondria within Cells: ANTIOXIDANT AND ANTIAPOPTOTIC PROPERTIES. *Journal of Biological Chemistry* **276:** 4588–4596

Keyser RJ, Lombard D, Veikondis R, Carr J & Bardien S (2009) Analysis of exon dosage using MLPA in South African Parkinson's disease patients. *Neurogenetics* **11:** 305–312

Ki CS, Stavrou EF, Davanos N, Lee WY, Chung EJ, Kim JY & Athanassiadou A (2007) The Ala53Thr mutation in the α-synuclein gene in a Korean family with Parkinson disease. *Clinical genetics* **71:** 471–473

Kiely AP, Asi YT, Kara E, Limousin P, Ling H, Lewis P, Proukakis C, Quinn N, Lees AJ, Hardy J, Revesz T, Houlden H & Holton JL (2013) α-Synucleinopathy associated with G51D SNCA mutation: a link between Parkinson's disease and multiple system atrophy? *Acta Neuropathol* **125:** 753–769

Kikugawa K, Kato T & Okamoto Y (1994) Damage of amino acids and proteins induced by nitrogen dioxide, a free radical toxin, in air. *Free Radical Biology and Medicine* **16:** 373–382

Kim JH, Lee S-R, Li L-H, Park H-J, Park J-H, Lee KY, Kim M-K, Shin BA & Choi S-Y (2011) High Cleavage Efficiency of a 2A Peptide Derived from Porcine Teschovirus-1 in Human Cell Lines, Zebrafish and Mice. *PLoS ONE* **6:** e18556

Kim RH, Peters M, Jang Y, Shi W, Pintilie M, Fletcher GC, DeLuca C, Liepa J, Zhou L, Snow B, Binari RC, Manoukian AS, Bray MR, Liu F-F, Tsao M-S & Mak TW (2005) DJ-1, a novel regulator of the tumor suppressor PTEN. *Cancer Cell* **7:** 263–273

Kirik D, Rosenblad C, Burger C, Lundberg C, Johansen TE, Muzyczka N, Mandel RJ & Björklund A (2002) Parkinson-like neurodegeneration induced by targeted overexpression of alpha-synuclein in the nigrostriatal system. *Journal of Neuroscience* **22:** 2780–2791

Kirkman HN & Gaetani GF (1984) Catalase: a tetrameric enzyme with four tightly bound molecules of NADPH. *Proc. Natl. Acad. Sci. U.S.A.* **81:** 4343–4347

Kitada T, Asakawa S, Hattori N, Matsumine H, Yamamura Y, Minoshima S, Yokochi M, Mizuno Y & Shimizu N (1998) Mutations in the parkin gene cause autosomal recessive juvenile parkinsonism. *Nature* **392:** 605–608

Klegeris A, Korkina LG & Greenfield SA (1995) Autoxidation of dopamine: a comparison of luminescent and spectrophotometric detection in basic solutions. *Free Radical Biology and Medicine* **18:** 215–222

Kobayashi A, Kang MI, Okawa H, Ohtsuji M, Zenke Y, Chiba T, Igarashi K & Yamamoto M (2004) Oxidative Stress Sensor Keap1 Functions as an Adaptor for Cul3-Based E3 Ligase To Regulate Proteasomal Degradation of Nrf2. *Molecular and Cellular Biology* **24:** 7130–7139

Kobayashi A, Kang M-I, Watai Y, Tong KI, Shibata T, Uchida K & Yamamoto M (2006) Oxidative and electrophilic stresses activate Nrf2 through inhibition of ubiquitination activity of Keap1. *Molecular and Cellular Biology* **26:** 221–229

Kojovic M, Sheerin U-M, Rubio-Agusti I, Saha A, Bras J, Gibbons V, Palmer R, Houlden H, Hardy J, Wood NW & Bhatia KP (2013) Young-onset parkinsonism due to homozygous duplication of α-synuclein in a consanguineous family. *Mov. Disord.* **27:** 1827–1829

Kordower JH, Chu Y, Hauser RA, Freeman TB & Olanow CW (2008) Lewy body–like pathology in long-term embryonic nigral transplants in Parkinson's disease. *Nat. Med.* **14:** 504–506

Kosower NS & Kosower EM (1978) The glutathione status of cells. *Int. Rev. Cytol.* **54:** 109–160

Kost TA & Condreay JP (2002) Recombinant baculoviruses as mammalian cell gene-delivery vectors. *Trends Biotechnol.* **20:** 173–180

Krüger R, Kuhn W, Müller T, Woitalla D, Graeber M, Kösel S, Przuntek H, Epplen JT, Schöls L & Riess O (1998) Ala30Pro mutation in the gene encoding alpha-synuclein in Parkinson's disease. *Nat. Genet.* **18:** 106–108

Kryh H, Carén H, Erichsen J, Sjöberg R-M, Abrahamsson J, Kogner P & Martinsson T (2011) Comprehensive SNP array study of frequently used neuroblastoma cell lines; copy neutral loss of heterozygosity is common in the cell lines but uncommon in primary tumors. *BMC Genomics* **12:** 443

Kryukov GV (2003) Characterization of Mammalian Selenoproteomes. *Science* **300:** 1439–1443

Kudin AP, Bimpong-Buta NY-B, Vielhaber S, Elger CE & Kunz WS (2004) Characterization of superoxide-producing sites in isolated brain mitochondria. *J. Biol. Chem.* **279:** 4127–4135

Kussmaul L & Hirst J (2006) The mechanism of superoxide production by NADH: ubiquinone oxidoreductase (complex I) from bovine heart mitochondria. *Proc. Natl. Acad. Sci. U.S.A.* **103:** 7607–7612

Langston JW, Irwin I, Langston EB & Forno LS (1984) 1-Methyl-4-phenylpyridinium ion (MPP+): identification of a metabolite of MPTP, a toxin selective to the substantia nigra. *Neuroscience Letters* **48:** 87–92

Langston JW, Forno LS, Tetrud J, Reeves AG, Kaplan JA & Karluk D (1999) Evidence of active nerve cell degeneration in the substantia nigra of humans years after 1-methyl-4-phenyl-1,2,3,6-tetrahydropyridine exposure. *Ann Neurol.* **46:** 598–605

Lawrence A, Jones CM, Wardman P & Burkitt MJ (2003) Evidence for the Role of a Peroxidase Compound I-type Intermediate in the Oxidation of Glutathione, NADH, Ascorbate, and Dichlorofluorescin by Cytochrome c/H2O2: IMPLICATIONS FOR OXIDATIVE STRESS DURING APOPTOSIS. *Journal of Biological Chemistry* **278:** 29410–29419

Leng Y, Chase TN & Bennett MC (2001) Muscarinic receptor stimulation induces translocation of an alpha-synuclein oligomer from plasma membrane to a light vesicle fraction in cytoplasm. *J. Biol. Chem.* **276:** 28212–28218

Leong SL, Pham CLL, Galatis D, Fodero-Tavoletti MT, Perez K, Hill AF, Masters CL, Ali FE, Barnham KJ & Cappai R (2009) Formation of dopamine-mediated α-synuclein-soluble oligomers requires methionine oxidation. *Free Radical Biology and Medicine* **46:** 1328–1337

Lesage S, Anheim M, Letournel F, Bousset L, Honoré A, Rozas N, Pieri L, Madiona K, Dürr A, Melki R, Verny C, Brice Afor the French Parkinson's Disease Genetics Study Group (2013) G51D α-synuclein mutation causes a novel Parkinsonian-pyramidal syndrome. *Ann Neurol.* **73:** 459–471

Lesage S & Brice A (2009) Parkinson's disease: from monogenic forms to genetic susceptibility factors. *Human Molecular Genetics* **18:** R48–R59

Li J-Y, Englund E, Holton JL, Soulet D, Hagell P, Lees AJ, Lashley T, Quinn NP, Rehncrona S, Björklund A, Widner H, Revesz T, Lindvall O & Brundin P (2008) Lewy bodies in grafted neurons in subjects with Parkinson's disease suggest host-to-graft disease propagation. *Nat. Med.* **14:** 501–503

Li JY, Henning Jensen P & Dahlström A (2002) Differential localization of alpha-, beta- and gamma-synucleins in the rat CNS. *Neuroscience* **113:** 463–478

Li W, Lesuisse C, Xu Y, Troncoso JC, Price DL & Lee MK (2004) Stabilization of alpha-synuclein protein with aging and familial parkinson's disease-linked A53T mutation. *Journal of Neuroscience* **24:** 7400–7409

Li Y, Huang TT, Carlson EJ, Melov S, Ursell PC, Olson JL, Noble LJ, Yoshimura MP, Berger C, Chan PH, Wallace DC & Epstein CJ (1995) Dilated cardiomyopathy and neonatal lethality in mutant mice lacking manganese superoxide dismutase. *Nat. Genet.* **11:** 376–381

Life Technologies (2014) The Molecular Probes Handbook 11 ed.; Table 18.1 and Section 18.2

Lindahl PE & Oberg KE (1960) Mechanism of the physiological action of rotenone. *Nature* **187:** 784

Little C & O'Brien PJ (1968) An intracellular GSH-peroxidase with a lipid peroxide substrate. *Biochem. Biophys. Res. Commun.* **31:** 145–150

Liu F, Hindupur J, Nguyen JL, Ruf KJ, Zhu J, Schieler JL, Bonham CC, Wood KV, Davisson VJ & Rochet J-C (2008) Methionine sulfoxide reductase A protects dopaminergic cells from Parkinson's disease-related insults. *Free Radical Biology and Medicine* **45:** 242–255

Loew O (1900) A NEW ENZYME OF GENERAL OCCURRENCE IN ORGANISMIS. *Science* **11:** 701–702

Loschen G, Azzi A, Richter C & Flohe L (1974) Superoxide radicals as precursors of mitochondrial hydrogen peroxide. *FEBS Letters* **42:** 68–72

Lötscher HR, Winterhalter KH, Carafoli E & Richter C (1979) Hydroperoxides can modulate the redox state of pyridine nucleotides and the calcium balance in rat liver mitochondria. *Proc. Natl. Acad. Sci. U.S.A.* **76:** 4340–4344

Loveland KL, Herszfeld D, Chu B, Rames E, Christy E, Briggs LJ, Shakri R, de Kretser DM & Jans DA (1999) Novel Low Molecular Weight Microtubule-associated Protein-2 Isoforms Contain a Functional Nuclear Localization Sequence. *Journal of Biological Chemistry* **274:** 19261–19268

Luk KC, Kehm V, Carroll J, Zhang B, O'Brien P, Trojanowski JQ & Lee VM-Y (2012) Pathological α-synuclein transmission initiates Parkinson-like neurodegeneration in nontransgenic mice. *Science* **338:** 949–953

Maddipati KR & Marnett LJ (1987) Characterization of the major hydroperoxide-reducing activity of human plasma. Purification and properties of a selenium-dependent glutathione peroxidase. *J. Biol. Chem.* **262:** 17398–17403

Maltsev AS, Chen J, Levine RL & Bax A (2013) Site-Specific Interaction between α-Synuclein and Membranes Probed by NMR-Observed Methionine Oxidation Rates. *J. Am. Chem. Soc.* **135:** 2943–2946

Mannervik B & Jensson H (1982) Binary combinations of four protein subunits with different catalytic specificities explain the relationship between six basic glutathione S-transferases in rat liver cytosol. *J. Biol. Chem.* **257:** 9909–9912

Markey SP, Johannessen JN, Chiueh CC, Burns RS & Herkenham MA (1984) Intraneuronal generation of a pyridinium metabolite may cause drug-induced parkinsonism. *Nature* **311:** 464–467

Marklund SL (1982) Human copper-containing superoxide dismutase of high molecular weight. *Proc. Natl. Acad. Sci. U.S.A.* **79:** 7634–7638

Markopoulou K, Wszolek ZK, Pfeiffer RF & Chase BA (1999) Reduced expression of the G209A alpha-synuclein allele in familial Parkinsonism. *Ann Neurol.* **46:** 374–381

Maroteaux L, Campanelli JT & Scheller RH (1988) Synuclein: a neuron-specific protein localized to the nucleus and presynaptic nerve terminal. *J. Neurosci.* **8:** 2804–2815

Martinez-Vicente M, Talloczy Z, Kaushik S, Massey AC, Mazzulli J, Mosharov EV, Hodara R, Fredenburg R, Wu D-C, Follenzi A, Dauer W, Przedborski S, Ischiropoulos H, Lansbury PT, Sulzer D & Cuervo AM (2008) Dopamine-modified alpha-synuclein blocks chaperone-mediated autophagy. *J. Clin. Invest.* **118:** 777–788

Masaki N, Kyle ME & Farber JL (1989) tert-Butyl hydroperoxide kills cultured hepatocytes by peroxidising membrane lipids. *Archives of Biochemistry and Biophysics* **269:** 390–399

Matsuda W, Furuta T, Nakamura KC, Hioki H, Fujiyama F, Arai R & Kaneko T (2009) Single Nigrostriatal Dopaminergic Neurons Form Widely Spread and Highly Dense Axonal Arborizations in the Neostriatum. *Journal of Neuroscience* **29:** 444–453

McCord JM & Fridovich I (1969) Superoxide dismutase. An enzymic function for erythrocuprein (hemocuprein). *J. Biol. Chem.* **244:** 6049–6055

McCord JM, Keele BB & Fridovich I (1971) An enzyme-based theory of obligate anaerobiosis: the physiological function of superoxide dismutase. *Proc. Natl. Acad. Sci. U.S.A.* **68:** 1024–1027

McDaniel DH, Neudecker BA, DiNardo JC, Lewis JA & Maibach HI (2005) Idebenone: a new antioxidant - Part I. Relative assessment of oxidative stress protection capacity compared to commonly known antioxidants. *J Cosmet Dermatol* **4:** 10–17

McKeith IG, Galasko D, Kosaka K, Perry EK, Dickson DW, Hansen LA, Salmon DP, Lowe J, Mirra SS, Byrne EJ, Lennox G, Quinn NP, Edwardson JA, Ince PG, Bergeron C, Burns A, Miller BL, Lovestone S, Collerton D, Jansen ENH, et al (1996) Consensus guidelines for the clinical and pathologic diagnosis of dementia with Lewy bodies (DLB): Report of the consortium on DLB international workshop. *Neurology* **47:** 1113–1124

McMahon M, Itoh K, Yamamoto M & Hayes JD (2003) Keap1-dependent Proteasomal Degradation of Transcription Factor Nrf2 Contributes to the Negative Regulation of Antioxidant Response Element-driven Gene Expression. *Journal of Biological Chemistry* **278:** 21592–21600

McMorrow D & Kasha M (1984) Proton-transfer spectroscopy of 3-hydroxyflavone in an isolated-site crystal matrix. *Proc. Natl. Acad. Sci. U.S.A.* **81:** 3375–3378

McPhail DB, Hartley RC, Gardner PT & Duthie GG (2003) Kinetic and Stoichiometric Assessment of the Antioxidant Activity of Flavonoids by Electron Spin Resonance Spectroscopy. *J. Agric. Food Chem.* **51:** 1684–1690

Miean KH & Mohamed S (2001) Flavonoid (Myricetin, Quercetin, Kaempferol, Luteolin, and Apigenin) Content of Edible Tropical Plants. *J. Agric. Food Chem.* **49:** 3106–3112

Mirzaei H, Schieler JL, Rochet J-C & Regnier F (2006) Identification of rotenone-induced modifications in alpha-synuclein using affinity pull-down and tandem mass spectrometry. *Anal. Chem.* **78:** 2422–2431

Mlakar A & Spiteller G (1996) Previously unknown aldehydic lipid peroxidation compounds of arachidonic acid. *Chem. Phys. Lipids* **79:** 47–53

Mo JY, Maki H & Sekiguchi M (1992) Hydrolytic elimination of a mutagenic nucleotide, 8-oxodGTP, by human 18-kilodalton protein: sanitization of nucleotide pool. *Proc. Natl. Acad. Sci. U.S.A.* **89:** 11021–11025

Moskovitz J, Bar-Noy S, Williams WM, Requena J, Berlett BS & STADTMAN ER (2001) Methionine sulfoxide reductase (MsrA) is a regulator of antioxidant defense and lifespan in mammals. *Proc. Natl. Acad. Sci. U.S.A.* **98:** 12920–12925

Mueller S, Weber A, Fritz R, Mütze S, Rost D, Walczak H, Völkl A & Stremmel W (2002) Sensitive and real-time determination of H2O2 release from intact peroxisomes. *Biochem. J.* **363:** 483–491

Mukai R, Ashida H, Terao J, Saito N & Shirai Y (2011) Determination of Subcellular Localization of Flavonol in Cultured Cells by Laser Scanning; Laser Scanning, Theory and Applications, Chau-Chang Wang (Ed.), InTech

Murphy KE, Gysbers AM, Abbott SK, Tayebi N, Kim WS, Sidransky E, Cooper A, Garner B & Halliday GM (2014) Reduced glucocerebrosidase is associated with increased α-synuclein in sporadic Parkinson's disease. *Brain* **137:** 834–848

Murphy MP (2009) How mitochondria produce reactive oxygen species. *Biochem. J.* **417:** 1

Nakamura K, Nemani VM, Azarbal F, Skibinski G, Levy JM, Egami K, Munishkina L, Zhang J, Gardner B, Wakabayashi J, Sesaki H, Cheng Y, Finkbeiner S, Nussbaum RL, Masliah E & Edwards RH (2011) Direct membrane association drives mitochondrial fission by the Parkinson disease-associated protein alpha-synuclein. *J. Biol. Chem.* **286:** 20710–20726

Nakao N, Frodl EM, Duan WM, Widner H & Brundin P (1994) Lazaroids improve the survival of grafted rat embryonic dopamine neurons. *Proc. Natl. Acad. Sci. U.S.A.* **91:** 12408–12412

Neuman EW (1934) Potassium Superoxide and the Three-Electron Bond. *The Journal of Chemical Physics* **2:** 31–33

Nieminen AL, Byrne AM, Herman B & Lemasters JJ (1997) Mitochondrial permeability transition in hepatocytes induced by t-BuOOH: NAD(P)H and reactive oxygen species. *Am. J. Physiol.* **272:** C1286–94

Nijveldt RJ, van Nood E, van Hoorn DE, Boelens PG, van Norren K & van Leeuwen PA (2001) Flavonoids: a review of probable mechanisms of action and potential applications. *Am. J. Clin. Nutr.* **74:** 418–425

Nioi P, McMahon M, Itoh K, Yamamoto M & Hayes JD (2003) Identification of a novel Nrf2-regulated antioxidant response element (ARE) in the mouse NAD(P)H:quinone oxidoreductase 1 gene: reassessment of the ARE consensus sequence. *Biochem. J.* **374:** 337–348

Nishioka K, Hayashi S, Farrer MJ, Singleton AB, Yoshino H, Imai H, Kitami T, Sato K, Kuroda R, Tomiyama H, Mizoguchi K, Murata M, Toda T, Imoto I, Inazawa J, Mizuno Y & Hattori N (2006) Clinical heterogeneity of α-synuclein gene duplication in Parkinson's disease. *Ann Neurol.* **59:** 298–309

Nishioka K, Ross OA, Ishii K, Kachergus JM, Ishiwata K, Kitagawa M, Kono S, Obi T, Mizoguchi K, Inoue Y, Imai H, Takanashi M, Mizuno Y, Farrer MJ & Hattori N (2009) Expanding the clinical phenotype of SNCA duplication carriers. *Mov. Disord.* **24:** 1811–1819

Niwa H, Yamamura K & Miyazaki J (1991) Efficient selection for high-expression transfectants with a novel eukaryotic vector. *Gene* **108:** 193–199

Nowak G, Bakajsova D, Hayes C, Hauer-Jensen M & Compadre CM (2012) γ-Tocotrienol protects against mitochondrial dysfunction and renal cell death. *Journal of Pharmacology and Experimental Therapeutics* **340:** 330–338

Nuytemans K, Meeus B, Crosiers D, Brouwers N, Goossens D, Engelborghs S, Pals P, Pickut B, Van den Broeck M, Corsmit E, Cras P, De Deyn PP, Del-Favero J, Van Broeckhoven C & Theuns J (2009) Relative contribution of simple mutations vs. copy number variations in five Parkinson disease genes in the Belgian population. *Hum. Mutat.* **30:** 1054–1061

O'Donnell V & Azzi A (1996) High rates of extracellular superoxide generation by cultured human fibroblasts: involvement of a lipid-metabolizing enzyme. *Biochem. J.* **318:** 805–812

Okado-Matsumoto A, Matsumoto A, Fujii J & Taniguchi N (2000) Peroxiredoxin IV is a secretable protein with heparin-binding properties under reduced conditions. *J. Biochem.* **127:** 493–501

Olichon A, Baricault L, Gas N, Guillou E, Valette A, Belenguer P & Lenaers G (2003) Loss of OPA1 perturbates the mitochondrial inner membrane structure and integrity, leading to cytochrome c release and apoptosis. *J. Biol. Chem.* **278:** 7743–7746

Oliveira S de, Souza GA de, Eckert CR, Silva TA, Sobral ES, Fávero OA, Ferreira MJP, Romoff P & Baader WJ (2014) Evaluation of antiradical assays used in determining the antioxidant capacity of pure compounds and plant extracts. *Química Nova* **37:** 497-503

Ostrerova-Golts N, Petrucelli L, Hardy J, Lee JM, Farer M & Wolozin B (2000) The A53T alpha-synuclein mutation increases iron-dependent aggregation and toxicity. *J. Neurosci.* **20:** 6048–6054

Othberg A, Keep M, Brundin P & Lindvall O (1997) Tirilazad mesylate improves survival of rat and human embryonic mesencephalic neurons in vitro. *Experimental Neurology* **147:** 498–502

Palacino JJ, Sagi D, Goldberg MS, Krauss S, Motz C, Wacker M, Klose J & Shen J (2004) Mitochondrial Dysfunction and Oxidative Damage in parkin-deficient Mice. *Journal of Biological Chemistry* **279:** 18614–18622

Papadimitriou A, Veletza V, Hadjigeorgiou GM, Patrikiou A, Hirano M & Anastasopoulos I (1999) Mutated α-synuclein gene in two Greek kindreds with familial PD: Incomplete penetrance? *Neurology* **52:** 651–651

Parent M & Parent A (2010) Substantia nigra and Parkinson's disease: a brief history of their long and intimate relationship. *Can J Neurol Sci* **37:** 313–319

Pauling L (1931) The nature of the chemical bond. II. The one-electron bond and the three-electron bond. *J. Am. Chem. Soc.* **53:** 3225–3237

Pauling L (1979) The discovery of the superoxide radical. *Trends in Biochemical Sciences* **4:** N270–N271

Paxinou E, Chen Q, Weisse M, Giasson BI, Norris EH, Rueter SM, Trojanowski JQ, Lee VM & Ischiropoulos H (2001) Induction of alpha-synuclein aggregation by intracellular nitrative insult. *Journal of Neuroscience* **21:** 8053–8061

Pemble SE, Wardle AF & Taylor JB (1996) Glutathione S-transferase class Kappa: characterization by the cloning of rat mitochondrial GST and identification of a human homologue. *Biochem. J.* **319 (Pt 3):** 749–754

Petri S, Kiaei M, Damiano M, Hiller A, Wille E, Manfredi G, Calingasan NY, Szeto HH & Beal MF (2006) Cell-permeable peptide antioxidants as a novel therapeutic approach in a mouse model of amyotrophic lateral sclerosis. *Journal of Neurochemistry* **98:** 1141–1148

Polymeropoulos MH, Lavedan C, Leroy E, Ide SE, Dehejia A, Dutra A, Pike B, Root H, Rubenstein J & Boyer R (1997) Mutation in the α-synuclein gene identified in families with Parkinson's disease. *Science* **276:** 2045–2047

Pouget J-P, Frelon S, Ravanat J-L, Testard I, Odin F & Cadet J (2002) Formation of modified DNA bases in cells exposed either to gamma radiation or to high-LET particles. *Radiat. Res.* **157:** 589–595

Pramstaller PP, Schlossmacher MG, Jacques TS, Scaravilli F, Eskelson C, Pepivani I, Hedrich K, Adel S, Gonzales-McNeal M, Hilker R, Kramer PL & Klein C (2005) Lewy body Parkinson's disease in a large pedigree with 77Parkin mutation carriers. *Ann Neurol.* **58:** 411–422

Prat F, Hou C-C & Foote CS (1997) Determination of the quenching rate constants of singlet oxygen by derivatized nucleosides in nonaqueous solution. *J. Am. Chem. Soc.* **119:** 5051–5052

Proctor BE & Bhatia DS (1953) Mode of Action of High-Voltage Cathode Rays on Aqueous Solutions of Amino-Acids. *Biochem. J.* **53:** 1–3

Proukakis C, Dudzik CG, Brier T, MacKay DS, Cooper JM, Millhauser GL, Houlden H & Schapira AH (2013) A novel α-synuclein missense mutation in Parkinson disease. *Neurology* **80:** 1062–1064

Pryor WA, Jin X & Squadrito GL (1994) One- and two-electron oxidations of methionine by peroxynitrite. *Proc. Natl. Acad. Sci. U.S.A.* **91:** 11173–11177

Purdom-Dickinson SE, Sheveleva EV, Sun H & Chen QM (2007) Translational Control of Nrf2 Protein in Activation of Antioxidant Response by Oxidants. *Molecular Pharmacology* **72:** 1074–1081

Puschmann A, Ross OA, Vilarino-Guell C, Lincoln SJ, Kachergus JM, Cobb SA, Lindquist SG, Nielsen JE, Wszolek ZK, Farrer M, Widner H, van Westen D, HAgerstrOm D, Markopoulou K, Chase BA, Nilsson K, Reimer J & Nilsson C (2009) A Swedish family with de novo alpha-synuclein A53T mutation: evidence for early cortical dysfunction. *Parkinsonism Relat. Disord.* **15:** 627–632

Putnam CD, Arvai AS, Bourne Y & Tainer JA (2000) Active and inhibited human catalase structures: ligand and NADPH binding and catalytic mechanism. *Journal of Molecular Biology* **296:** 295–309

Rachakonda G, Xiong Y, Sekhar KR, Stamer SL, Liebler DC & Freeman ML (2008) Covalent Modification at Cys151 Dissociates the Electrophile Sensor Keap1 from the Ubiquitin Ligase CUL3. *Chem. Res. Toxicol.* **21:** 705–710

Radi R, Sims S, Cassina A & Turrens JF (1993) Roles of catalase and cytochrome C in hydroperoxide-dependent lipid peroxidation and chemiluminescence in rat heart and kidney mitochondria. *Free Radical Biology and Medicine* **15:** 653–659

Radio NM, Breier JM, Shafer TJ & Mundy WR (2008) Assessment of Chemical Effects on Neurite Outgrowth in PC12 cells Using High Content Screening. *Toxicological Sciences* **105:** 106–118

Rafat Husain S, Cillard J & Cillard P (1987) Hydroxyl radical scavenging activity of flavonoids. *Phytochemistry* **26:** 2489–2491

Reaume AG, Elliott JL, Hoffman EK, Kowall NW, Ferrante RJ, Siwek DF, Wilcox HM, Flood DG, Beal MF, Brown RH, Scott RW & Snider WD (1996) Motor neurons in Cu/Zn superoxide dismutase-deficient mice develop normally but exhibit enhanced cell death after axonal injury. *Nat. Genet.* **13:** 43–47

Rhee SG, Chae HZ & Kim K (2005) Peroxiredoxins: A historical overview and speculative preview of novel mechanisms and emerging concepts in cell signaling. *Free Radical Biology and Medicine* **38:** 1543–1552

Rice-Evans C, Miller N & Paganga G (1997) Antioxidant properties of phenolic compounds. *Trends in plant science* **2:** 152–159

Richardson JR, Caudle WM, Guillot TS, Watson JL, Nakamaru-Ogiso E, Seo BB, Sherer TB, Greenamyre JT, Yagi T, Matsuno-Yagi A & Miller GW (2007) Obligatory role for complex I inhibition in the dopaminergic neurotoxicity of 1-methyl-4-phenyl-1,2,3,6-tetrahydropyridine (MPTP). *Toxicological Sciences* **95:** 196–204

Robinson KM, Janes MS, Pehar M, Monette JS, Ross MF, Hagen TM, Murphy MP & Beckman JS (2006) Selective fluorescent imaging of superoxide in vivo using ethidium-based probes. *Proc. Natl. Acad. Sci. U.S.A.* **103:** 15038–15043

Ross RA, Spengler BA & Biedler JL (1983) Coordinate morphological and biochemical interconversion of human neuroblastoma cells. *J. Natl. Cancer Inst.* **71:** 741–747

Rosen DR, Siddique T, Patterson D, Figlewicz DA, Sapp P, Hentati A, Donaldson D, Goto J, O'Regan JP & Deng HX (1993) Mutations in Cu/Zn superoxide dismutase gene are associated with familial amyotrophic lateral sclerosis. *Nature* **362:** 59–62

Rosenberg PA (1988) Catecholamine toxicity in cerebral cortex in dissociated cell culture. *J. Neurosci.* **8:** 2887–2894

Samaranch L, Lorenzo-Betancor O, Arbelo JM, Ferrer I, Lorenzo E, Irigoyen J, Pastor MA, Marrero C, Isla C, Herrera-Henriquez J & Pastor P (2010) PINK1-linked parkinsonism is associated with Lewy body pathology. *Brain* **133:** 1128–1142

Sanchez-Padilla J, Guzman JN, Ilijic E, Kondapalli J, Galtieri DJ, Yang B, Schieber S, Oertel W, Wokosin D, Schumacker PT & Surmeier DJ (2014) Mitochondrial oxidant stress in locus coeruleus is regulated by activity and nitric oxide synthase. *Nature Neuroscience* **17:** 832–840

Sanders SA, Eisenthal R & Harrison R (1997) NADH oxidase activity of human xanthine oxidoreductase--generation of superoxide anion. *Eur. J. Biochem.* **245:** 541–548

Sarkis C, Serguera C, Petres S, Buchet D, Ridet JL, Edelman L & Mallet J (2000) Efficient transduction of neural cells in vitro and in vivo by a baculovirus-derived vector. *Proc. Natl. Acad. Sci. U.S.A.* **97:** 14638–14643

Schapira AH, Cooper JM, Dexter D, Clark JB, Jenner P & Marsden CD (1990) Mitochondrial complex I deficiency in Parkinson's disease. *Journal of Neurochemistry* **54:** 823–827

Scherzer CR, Grass JA, Liao Z, Pepivani I, Zheng B, Eklund AC, Ney PA, Ng J, McGoldrick M, Mollenhauer B, Bresnick EH & Schlossmacher MG (2008) GATA transcription factors directly regulate the Parkinson's disease-linked gene alpha-synuclein. *Proc. Natl. Acad. Sci. U.S.A.* **105:** 10907–10912

Schildknecht S, Pape R, Muller N, Robotta M, Marquardt A, Burkle A, Drescher M & Leist M (2011) Neuroprotection by Minocycline Caused by Direct and Specific Scavenging of Peroxynitrite. *Journal of Biological Chemistry* **286:** 4991–5002

Schiller PW, Nguyen TM, Berezowska I, Dupuis S, Weltrowska G, Chung NN & Lemieux C (2000) Synthesis and in vitro opioid activity profiles of DALDA analogues. *Eur J Med Chem* **35:** 895–901

Schneider L, Giordano S, Zelickson BR, Johnson MS, Benavides GA, Ouyang X, Fineberg N, Darley-Usmar VM & Zhang J (2011) Differentiation of SH-SY5Y cells to a neuronal phenotype changes cellular bioenergetics and the response to oxidative stress. *Free Radical Biology and Medicine* **51:** 2007–2017

Seidel K, Schöls L, Nuber S, Petrasch-Parwez E, Gierga K, Wszolek Z, Dickson D, Gai W-P, Bornemann A, Riess O, Rami A, Dunnen den W, Deller T, Rüb U & Krüger R (2010) First appraisal of brain pathology owing to A30P mutant alpha-synuclein. *Ann Neurol.* **67:** 684-689

Sekine T, Kagaya H, Funayama M, Li Y, Yoshino H, Tomiyama H & Hattori N (2010) Clinical course of the first Asian family with Parkinsonism related to SNCA triplication. *Mov. Disord.* **25:** 2871–2875

Seo MS, Kang SW, Kim K, Baines IC, Lee TH & Rhee SG (2000) Identification of a New Type of Mammalian Peroxiredoxin That Forms an Intramolecular Disulfide as a Reaction Intermediate. *Journal of Biological Chemistry* **275:** 20346–20354

Serdaroglu P, Tasli H, Hanagasi H & Emre M (2005) Parkin expression in human skeletal muscle. *Journal of Clinical Neuroscience* **12:** 927–929

Sevcsik E, Trexler AJ, Dunn JM & Rhoades E (2011) Allostery in a Disordered Protein: Oxidative Modifications to α-Synuclein Act Distally To Regulate Membrane Binding. *J. Am. Chem. Soc.* **133:** 7152–7158

Sherer TB, Betarbet R, Stout AK, Lund S, Baptista M, Panov AV, Cookson MR & Greenamyre JT (2002) An in vitro model of Parkinson's disease: linking mitochondrial impairment to altered alpha-synuclein metabolism and oxidative damage. *Journal of Neuroscience* **22:** 7006–7015

Sheu S-S, Nauduri D & Anders MW (2006) Targeting antioxidants to mitochondria: A new therapeutic direction. *Biochimica et Biophysica Acta (BBA) - Molecular Basis of Disease* **1762:** 256–265

Shi H, Noguchi N & Niki E (2001) Galvinoxyl method for standardizing electron and proton donation activity. *Meth. Enzymol.* **335:** 157–166

Shin CW, Kim HJ, Park SS, Kim SY, Kim JY & Jeon BS (2010) Two Parkinson's disease patients with α-synuclein gene duplication and rapid cognitive decline. *Mov. Disord.* **25:** 957–959

Sies H, Gerstenecker C, Menzel H & Flohe L (1972) Oxidation in the NADP system and release of GSSG from hemoglobin-free perfused rat liver during peroxidatic oxidation of glutathione by hydroperoxides. *FEBS Letters* **27:** 171–175

Sies H (1993) Strategies of antioxidant defense. *Eur. J. Biochem.* **215:** 213–219

Singleton, AB, Farrer M, Johnson J, Singleton A, Hague S, Kachergus J, Hulihan M, Peuralinna T, Dutra A & Nussbaum R (2003) α-Synuclein locus triplication causes Parkinson's disease. *Science* **302:** 841–841

Sironi F, Trotta L, Antonini A, Zini M, Ciccone R, Mina Della E, Meucci N, Sacilotto G, Primignani P, Brambilla T, Coviello DA, Pezzoli G & Goldwurm S (2010) alpha-Synuclein multiplication analysis in Italian familial Parkinson disease. *Parkinsonism Relat. Disord.* **16:** 228–231

Sjoberg L, Eriksen TE & Revesz L (1982) The Reaction of the Hydroxyl Radical with Glutathione in Neutral and Alkaline Aqueous-Solution. *Radiat. Res.* **89:** 255–263

Skaltsa H, Verykokidou E, Harvala C, Karabourniotis G & Manetasi Y (1994) UV-B protective potential and flavonoid content of leaf hairs of Quercus ilex. *Phytochemistry* **37:** 987–990

Skaper SD, Fabris M, Ferrari V, Dalle Carbonare M & Leon A (1997) Quercetin protects cutaneous tissue-associated cell types including sensory neurons from oxidative stress induced by glutathione depletion: cooperative effects of ascorbic acid. *Free Radical Biology and Medicine* **22:** 669–678

Smirnova E, Shurland DL, Ryazantsev SN & van der Bliek AM (1998) A human dynamin-related protein controls the distribution of mitochondria. *J. Cell Biol.* **143:** 351–358

Smith AC, Mears AJ, Bunker R, Ahmed A, MacKenzie M, Schwartzentruber JA, Beaulieu CL, Ferretti E, FORGE Canada Consortium, Majewski J, Bulman DE, Celik FC, Boycott KM & Graham GE (2014) Mutations in the enzyme glutathione peroxidase 4 cause Sedaghatian-type spondylometaphyseal dysplasia. *J. Med. Genet.* **51:** 470–474

Smith RA, Porteous CM, Coulter CV & Murphy MP (1999) Selective targeting of an antioxidant to mitochondria. *Eur. J. Biochem.* **263:** 709–716

Snow BJ, Rolfe FL, Lockhart MM, Frampton CM, O'Sullivan JD, Fung V, Smith RAJ, Murphy MP & Taylor KM (2010) A double-blind, placebo-controlled study to assess the mitochondria-targeted antioxidant MitoQ as a disease-modifying therapy in Parkinson's disease. *Mov. Disord.* **25:** 1670–1674

Sofic E, Riederer P, Heinsen H, Beckmann H, Reynolds GP, Hebenstreit G & Youdim MB (1988) Increased iron (III) and total iron content in post mortem substantia nigra of parkinsonian brain. *J. Neural Transm.* **74:** 199–205

Sofic E, Lange KW, Jellinger K & Riederer P (1992) Reduced and oxidized glutathione in the substantia nigra of patients with Parkinson's disease. *Neuroscience Letters* **142:** 128–130

Souza JM, Giasson BI, Chen Q, Lee VM & Ischiropoulos H (2000) Dityrosine cross-linking promotes formation of stable alpha -synuclein polymers. Implication of nitrative and oxidative stress in the pathogenesis of neurodegenerative synucleinopathies. *J. Biol. Chem.* **275:** 18344–18349

Specht CG & Schoepfer R (2001) Deletion of the alpha-synuclein locus in a subpopulation of C57BL/6J inbred mice. *BMC Neurosci* **2:** 11

Spillantini MG, Schmidt ML, Lee VM-Y, Trojanowski JQ, Jakes R & Goedert M (1997) α-Synuclein in Lewy bodies. *Nature* **388:** 839–840

Spira PJ, Sharpe DM, Halliday G, Cavanagh J & Nicholson GA (2001) Clinical and pathological features of a Parkinsonian syndrome in a family with an Ala53Thr alpha-synuclein mutation. *Ann Neurol.* **49:** 313–319

Srivastava P & Panda D (2007) Rotenone inhibits mammalian cell proliferation by inhibiting microtubule assembly through tubulin binding. *FEBS Journal* **274:** 4788–4801

Steenken S & Jovanovic SV (1997) How easily oxidizable is DNA? One-electron reduction potentials of adenosine and guanosine radicals in aqueous solution. *J. Am. Chem. Soc.* **119:** 617–618

Stekol JA (1941) Studies on the mercapturic acid synthesis in animals XII. The synthesis of n-acetyl-S-p-bromobenzyl-l-cysteine in the rat from p- bromobenzyl bromide, S-p-bromobenzyl-l-cysteine, and S-p- bromobenzylglutathione. *J. Biol. Chem.* **138:** 225–229

Stockman PK, Beckett GJ & Hayes JD (1985) Identification of a basic hybrid glutathione S-transferase from human liver. Glutathione S-transferase delta is composed of two distinct subunits (B1 and B2). *Biochem. J.* **227:** 457–465

Sumner JB & Dounce AL (1937) Crystalline catalase. *J. Biol. Chem.* **121:** 417–424

Surmeier DJ, Guzman JN, Sanchez-Padilla J & Schumacker PT (2011) The role of calcium and mitochondrial oxidant stress in the loss of substantia nigra pars compacta dopaminergic neurons in Parkinson's disease. *Neuroscience* **198:** 221–231

Szczesna-Skorupa E & Kemper B (1993) An N-terminal glycosylation signal on cytochrome P450 is restricted to the endoplasmic reticulum in a luminal orientation. *J. Biol. Chem.* **268:** 1757–1762

Szeto HH (2006) Cell-permeable, mitochondrial-targeted, peptide antioxidants. *AAPS J* **8:** E277–83

Szymczak AL, Workman CJ, Wang Y, Vignali KM, Dilioglou S, Vanin EF & Vignali DAA (2004) Correction of multi-gene deficiency in vivo using a single 'self-cleaving' 2A peptide–based retroviral vector. *Nat Biotechnol* **22:** 589–594

Taguchi K, Motohashi H & Yamamoto M (2011) Molecular mechanisms of the Keap1-Nrf2 pathway in stress response and cancer evolution. *Genes to Cells* **16:** 123–140

Takahara S, Hamilton HB, Neel JV, Kobara TY, Ogura Y & Nishimura ET (1960) Hypocatalasemia: a new genetic carrier state. *J. Clin. Invest.* **39:** 610–619

Tan X, Grollman AP & Shibutani S (1999) Comparison of the mutagenic properties of 8-oxo-7,8-dihydro-2'-deoxyadenosine and 8-oxo-7,8-dihydro-2'-deoxyguanosine DNA lesions in mammalian cells. *Carcinogenesis* **20:** 2287–2292

Thomas DA, Stauffer C, Zhao K, Yang H, Sharma VK, Szeto HH & Suthanthiran M (2006) Mitochondrial Targeting with Antioxidant Peptide SS-31 Prevents Mitochondrial Depolarization, Reduces Islet Cell Apoptosis, Increases Islet Cell Yield, and Improves Posttransplantation Function. *Journal of the American Society of Nephrology* **18:** 213–222

Thomas JP, Maiorino M, Ursini F & Girotti AW (1990) Protective action of phospholipid hydroperoxide glutathione peroxidase against membrane-damaging lipid peroxidation. In situ reduction of phospholipid and cholesterol hydroperoxides. *J. Biol. Chem.* **265:** 454–461

Tjia ST, zu Altenschildesche GM & Doerfler W (1983) Autographa californica nuclear polyhedrosis virus (AcNPV) DNA does not persist in mass cultures of mammalian cells. *Virology* **125:** 107–117

Tong KI, Katoh Y, Kusunoki H, Itoh K, Tanaka T & Yamamoto M (2006) Keap1 Recruits Neh2 through Binding to ETGE and DLG Motifs: Characterization of the Two-Site Molecular Recognition Model. *Molecular and Cellular Biology* **26:** 2887–2900

Tong KI, Padmanabhan B, Kobayashi A, Shang C, Hirotsu Y, Yokoyama S & Yamamoto M (2007) Different Electrostatic Potentials Define ETGE and DLG Motifs as Hinge and Latch in Oxidative Stress Response. *Molecular and Cellular Biology* **27:** 7511–7521

Toppo S, Vanin S, Bosello V & Tosatto SCE (2008) Evolutionary and Structural Insights Into the Multifaceted Glutathione Peroxidase (Gpx) Superfamily. *Antioxidants & Redox Signaling* **10:** 1501–1514

Torel J, Cillard J & Cillard P (1986) Antioxidant activity of flavonoids and reactivity with peroxy radical. *Phytochemistry* **25:** 383–385

Totterdell S, Hanger D & Meredith GE (2004) The ultrastructural distribution of alpha-synuclein-like protein in normal mouse brain. *Brain Research* **1004:** 61–72

Totterdell S & Meredith GE (2005) Localization of Alpha-synuclein to identified fibers and synapses in the normal mouse brain. *Neuroscience* **135:** 907–913

Troiano AR, Cazeneuve C, Le Ber I, Bonnet A-M, Lesage S & Brice A (2008) Re: Alpha-synuclein gene duplication is present in sporadic Parkinson disease. *Neurology* **71:** 1295–author reply 1295

Tyurin VA, Tyurina YY, Borisenko GG, Sokolova TV, Ritov VB, Quinn PJ, Rose M, Kochanek P, Graham SH & Kagan VE (2000) Oxidative stress following traumatic brain injury in rats: quantitation of biomarkers and detection of free radical intermediates. *Journal of Neurochemistry* **75:** 2178–2189

Uchida K & Kawakishi S (1993) 2-Oxo-Histidine as a Novel Biological Marker for Oxidatively Modified Proteins. *FEBS Letters* **332:** 208–210

Uchida K & Stadtman ER (1993) Covalent attachment of 4-hydroxynonenal to glyceraldehyde-3-phosphate dehydrogenase. A possible involvement of intra-and intermolecular cross-linking reaction. *J. Biol. Chem.* **268:** 6388–6393

Uchiyama T, Ikeuchi T, Ouchi Y, Sakamoto M, Kasuga K, Shiga A, Suzuki M, Ito M, Atsumi T, Shimizu T & Ohashi T (2008) Prominent psychiatric symptoms and glucose hypometabolism in a family with a SNCA duplication. *Neurology* **71:** 1289–1291

Unoki M & Nakamura Y (2001) Growth-suppressive effects of BPOZ and EGR2, two genes involved in the PTEN signaling pathway. *Oncogene* **20:** 4457–4465

Ursini F, Maiorino M & Gregolin C (1985) The selenoenzyme phospholipid hydroperoxide glutathione peroxidase. *Biochim. Biophys. Acta* **839:** 62–70

Valavanidis A, Vlachogianni T & Fiotakis K (2009) Tobacco Smoke: Involvement of Reactive Oxygen Species and Stable Free Radicals in Mechanisms of Oxidative Damage, Carcinogenesis and Synergistic Effects with Other Respirable Particles. *IJERPH* **6:** 445–462

Valente EM, Abou-Sleiman PM, Caputo V, Muqit MMK, Harvey K, Gispert S, Ali Z, Del Turco D, Bentivoglio AR, Healy DG, Albanese A, Nussbaum R, González-Maldonado R, Deller T, Salvi S, Cortelli P, Gilks WP, Latchman DS, Harvey RJ, Dallapiccola B, et al (2004a) Hereditary early-onset Parkinson's disease caused by mutations in PINK1. *Science* **304:** 1158–1160

Valente EM, Salvi S, Ialongo T, Marongiu R, Elia AE, Caputo V, Romito L, Albanese A, Dallapiccola B & Bentivoglio AR (2004b) PINK1 mutations are associated with sporadic early-onset parkinsonism. *Ann Neurol.* **56:** 336–341

Valentine MR, Rodriguez H & Termini J (1998) Mutagenesis by peroxy radical is dominated by transversions at deoxyguanosine: evidence for the lack of involvement of 8-oxo-dG1 and/or abasic site formation. *Biochemistry* **37:** 7030–7038

van Acker SA, van den Berg DJ, Tromp MN, Griffioen DH, van Bennekom WP, van der Vijgh WJ & Bast A (1996) Structural aspects of antioxidant activity of flavonoids. *Free Radical Biology and Medicine* **20:** 331–342

Van der Zee J, Barr DP & Mason RP (1996) ESR spin trapping investigation of radical formation from the reaction between hematin and tert-Butyl hydroperoxide. *Free Radical Biology and Medicine* **20:** 199–206

Vekrellis K, Xilouri M, Emmanouilidou E & Stefanis L (2009) Inducible over-expression of wild type α-synuclein in human neuronal cells leads to caspase-dependent non-apoptotic death. *Journal of Neurochemistry* **109:** 1348–1362

Volpicelli-Daley LA, Luk KC, Patel TP, Tanik SA, Riddle DM, Stieber A, Meaney DF, Trojanowski JQ & Lee VM-Y (2011) Exogenous α-synuclein fibrils induce Lewy body pathology leading to synaptic dysfunction and neuron death. *Neuron* **72:** 57–71

Wakabayashi K, Yoshimoto M, Tsuji S & Takahashi H (1998) Alpha-synuclein immunoreactivity in glial cytoplasmic inclusions in multiple system atrophy. *Neuroscience Letters* **249:** 180–182

Wakabayashi N, Itoh K, Wakabayashi J, Motohashi H, Noda S, Takahashi S, Imakado S, Kotsuji T, Otsuka F, Roop DR, Harada T, Engel JD & Yamamoto M (2003) Keap1-null mutation leads to postnatal lethality due to constitutive Nrf2 activation. *Nat. Genet.* **35:** 238–245

Webb JL, Ravikumar B, Atkins J, Skepper JN & Rubinsztein DC (2003) Alpha-Synuclein is degraded by both autophagy and the proteasome. *J. Biol. Chem.* **278:** 25009–25013

Wefers H & Sies H (1983) Oxidation of glutathione by the superoxide radical to the disulfide and the sulfonate yielding singlet oxygen. *Eur. J. Biochem.* **137:** 29–36

Weisiger RA & Fridovich I (1973) Mitochondrial superoxide dimutase. Site of synthesis and intramitochondrial localization. *J. Biol. Chem.* **248:** 4793–4796

Wellner VP, Sekura R, Meister A & Larsson A (1974) Glutathione synthetase deficiency, an inborn error of metabolism involving the γ-glutamyl cycle in patients with 5-oxoprolinuria (pyroglutamic aciduria). *Proc. Natl. Acad. Sci. U.S.A.* **71:** 2505–2509

Whitworth AJ, Theodore DA, Greene JC, Benes H, Wes PD & Pallanck LJ (2005) Increased glutathione S-transferase activity rescues dopaminergic neuron loss in a Drosophila model of Parkinson's disease. *Proc. Natl. Acad. Sci. U.S.A.* **102:** 8024–8029

Wu LL, Chiou C-C, Chang P-Y & Wu JT (2004) Urinary 8-OHdG: a marker of oxidative stress to DNA and a risk factor for cancer, atherosclerosis and diabetics. *Clinica Chimica Acta* **339:** 1–9

Xun Z, Lee D-Y, Lim J, Canaria CA, Barnebey A, Yanonne SM & McMurray CT (2012) Retinoic acid-induced differentiation increases the rate of oxygen consumption and enhances the spare respiratory capacity of mitochondria in SH-SY5Y cells. *Mechanisms of Ageing and Development* **133:** 176–185

Yamamoto T, Suzuki T, Kobayashi A, Wakabayashi J, Maher J, Motohashi H & Yamamoto M (2008) Physiological Significance of Reactive Cysteine Residues of Keap1 in Determining Nrf2 Activity. *Molecular and Cellular Biology* **28:** 2758–2770

Yang B, Kotani A, Arai K & Kusu F (2001) Estimation of the antioxidant activities of flavonoids from their oxidation potentials. *Anal Sci* **17:** 599–604

Yang Y, Gehrke S, Imai Y, Huang Z, Ouyang Y, Wang J-W, Yang L, Beal MF, Vogel H & Lu B (2006) Mitochondrial pathology and muscle and dopaminergic neuron degeneration caused by inactivation of Drosophila Pink1 is rescued by Parkin. *Proc. Natl. Acad. Sci. U.S.A.* **103:** 10793–10798

Yant LJ, Ran Q, Rao L, Van Remmen H, Shibatani T, Belter JG, Motta L, Richardson A & Prolla TA (2003) The selenoprotein GPX4 is essential for mouse development and protects from radiation and oxidative damage insults. *Free Radical Biology and Medicine* **34:** 496–502

Yao Y, Lin G, Xie Y, Ma P, Li G, Meng Q & Wu T (2014) Preformulation studies of myricetin: a natural antioxidant flavonoid. *Pharmazie* **69:** 19–26

Yates MS, Tran QT, Dolan PM, Osburn WO, Shin S, McCulloch CC, Silkworth JB, Taguchi K, Yamamoto M, Williams CR, Liby KT, Sporn MB, Sutter TR & Kensler TW (2009) Genetic versus chemoprotective activation of Nrf2 signaling: overlapping yet distinct gene expression profiles between Keap1 knockout and triterpenoid-treated mice. *Carcinogenesis* **30:** 1024–1031

Yoh K, Itoh K, Enomoto A, Hirayama A, Yamaguchi N, Kobayashi M, Morito N, Koyama A, Yamamoto M & Takahashi S (2001) Nrf2-deficient female mice develop lupus-like autoimmune nephritis. *Kidney Int.* **60:** 1343–1353

Yokomizo A & Moriwaki M (2006) Effects of uptake of flavonoids on oxidative stress induced by hydrogen peroxide in human intestinal Caco-2 cells. *Bioscience, Biotechnology and Biochemistry* **70:** 1317–1324

Yoon C-H, Choi Y-E, Koh S-J, Choi J-I, Park Y-B & Kim H-S (2014) High glucose-induced jagged 1 in endothelial cells disturbs notch signaling for angiogenesis: A novel mechanism of diabetic vasculopathy. *Journal of Molecular and Cellular Cardiology* **69:** 52–66

Zarranz JJ, Alegre J, Gómez-Esteban JC, Lezcano E, Ros R, Ampuero I, Vidal L, Hoenicka J, Rodriguez O, Atarés B, Llorens V, Gomez Tortosa E, del Ser T, Muñoz DG & de Yebenes JG (2004) The new mutation, E46K, of alpha-synuclein causes Parkinson and Lewy body dementia. *Ann Neurol.* **55:** 164–173

Zhang DD, Lo SC, Cross JV, Templeton DJ & Hannink M (2004) Keap1 Is a Redox-Regulated Substrate Adaptor Protein for a Cul3-Dependent Ubiquitin Ligase Complex. *Molecular and Cellular Biology* **24:** 10941–10953

Zhang H, Jarjour AA, Boyd A & Williams A (2011) Central nervous system remyelination in culture — A tool for multiple sclerosis research. *Experimental Neurology* **230:** 138–148

Zhang L, Shimoji M, Thomas B, Moore DJ, Yu S-W, Marupudi NI, Torp R, Torgner IA, Ottersen OP, Dawson TM & Dawson VL (2005) Mitochondrial localization of the Parkinson's disease related protein DJ-1: implications for pathogenesis. *Human Molecular Genetics* **14:** 2063–2073

Zhang X, Yin M & Zhang M (2014) Cell-based assays for Parkinson's disease using differentiated human LUHMES cells. *Acta Pharmacologica Sinica* **35:** 945–956

Zhang Y, Gao J, Chung KK, Huang H, Dawson VL & Dawson TM (2000) Parkin functions as an E2-dependent ubiquitin- protein ligase and promotes the degradation of the synaptic vesicle-associated protein, CDCrel-1. *Proc. Natl. Acad. Sci. U.S.A.* **97:** 13354–13359

Zhao H, Kalivendi S, Zhang H, Joseph J, Nithipatikom K, Vásquez-Vivar J & Kalyanaraman B (2003) Superoxide reacts with hydroethidine but forms a fluorescent product that is distinctly different from ethidium: potential implications in intracellular fluorescence detection of superoxide. *Free Radical Biology and Medicine* **34:** 1359–1368

Zhao K, Zhao GM, Wu D, Soong Y, Birk AV, Schiller PW & Szeto HH (2004) Cell-permeable Peptide Antioxidants Targeted to Inner Mitochondrial Membrane inhibit Mitochondrial Swelling, Oxidative Cell Death, and Reperfusion Injury. *Journal of Biological Chemistry* **279:** 34682–34690

Zhao K, Luo G, Giannelli S & Szeto HH (2005) Mitochondria-targeted peptide prevents mitochondrial depolarization and apoptosis induced by tert-butyl hydroperoxide in neuronal cell lines. *Biochemical Pharmacology* **70:** 1796–1806

Zhong S-C, Luo X, Chen X-S, Cai Q-Y, Liu J, Chen X-H & Yao Z-X (2009) Expression and Subcellular Location of Alpha-Synuclein During Mouse-Embryonic Development. *Cell Mol Neurobiol* **30:** 469–482

Zhou W, Hurlbert MS, Schaack J, Prasad KN & Freed CR (2000) Overexpression of human alpha-synuclein causes dopamine neuron death in rat primary culture and immortalized mesencephalon-derived cells. *Brain Research* **866:** 33–43

Zhou W, Schaack J, Zawada WM & Freed CR (2002) Overexpression of human alpha-synuclein causes dopamine neuron death in primary human mesencephalic culture. *Brain Research* **926:** 42–50

Zhou W, Long C, Reaney SH, Di Monte DA, Fink AL & Uversky VN (2010) Methionine oxidation stabilizes non-toxic oligomers of α-synuclein through strengthening the auto-inhibitory intra-molecular long-range interactions. *Biochimica et Biophysica Acta (BBA) - Molecular Basis of Disease* **1802:** 322–330

Zhukov A & Ingelman-Sundberg M (1999) Relationship between cytochrome P450 catalytic cycling and stability: fast degradation of ethanol-inducible cytochrome P450 2E1 (CYP2E1) in hepatoma cells is abolished by inactivation of its electron donor NADPH-cytochrome P450 reductase. *Biochem. J.* **340 (Pt 2):** 453–458

Zielonka J, Sarna T, Roberts JE, Wishart JF & Kalyanaraman B (2006) Pulse radiolysis and steady-state analyses of the reaction between hydroethidine and superoxide and other oxidants. *Archives of Biochemistry and Biophysics* **456:** 39–47

Zielonka J, Hardy M & Kalyanaraman B (2009) HPLC study of oxidation products of hydroethidine in chemical and biological systems: ramifications in superoxide measurements. *Free Radical Biology and Medicine* **46:** 329–338